BIOZENTRUM
Universität Basel

Analysis of the c-di-GMP mediated cell fate determination in *Caulobacter crescentus*

Inauguraldissertation

zur
Erlangung der Würde eines Doktors der Philosophie
vorgelegt der
Philosophisch-Naturwissenschaftlichen Fakultät
der Universität Basel

von

Sören Abel
aus Kiel, Deutschland
Basel 2009

Genehmigt von der Philosopisch-Naturwissenschaftlichen Falkultät auf Antrag von

- Prof. Dr. Urs Jenal
- Prof. Dr. Tilman Schirmer

Basel, den 20. Mai 2008

Prof. Dr. Eberhard Parlow
Dekan

Abstract

Cyclic-di-GMP (c-di-GMP) is a ubiquitous second messenger in bacteria, which has been recognized as a key regulator, antagonistically controlling the transition between motile, planktonic cells and surface attached, multicellular communities. The biosynthesis and degradation of c-di-GMP are mediated by the opposing enzymatic activities of di-guanylate cyclases (DGCs) and phosphodiesterases (PDEs), generally in response to internal and environmental signals. These activities reside in GGDEF and EAL domains respectively, which represent two large families of output domains often found in bacterial one- and two-component systems. In this work, the cell cycle-embedded differentiation from a free-living, motile swarmer cell into a sessile stalked cell in the model organism *Caulobacter crescentus*, and the role of c-di-GMP in this process was investigated. A systematic analysis was used to identify key regulatory enzymes involved in c-di-GMP metabolism that influence this developmental process. The function and regulation of these genes was then examined. One component that has already been implicated in this process, the DGC PleD, was investigated in more detail, with special emphasis on the mechanisms underlying its timed activation and cell cycle specific subcellular localisation.

In the first part of this work, a systematic functional analysis of all GGDEF, EAL and GGDEF/EAL composite proteins from *C. crescentus* with a focus on motility and surface attachment is described. In this screen, the phosphodiesterase PdeA was identified as a gatekeeper that prevents premature paralysis of the flagellum and holdfast synthesis in the *C. crescentus* swarmer cell. It is shown that PdeA, together with its antagonistic DGCs DgcB and PleD, are components of converging pathways and orchestrate polar development during the swarmer-to-stalked cell transition. Furthermore, evidence is presented for a proteolytic regulation mechanism for PdeA.

Secondly, the PleD localisation factor CC1064 is analysed. This transmembrane protein has pleiotropic effects on motility, surface attachment and polar localisation of PleD. It is shown that the motility and PleD localisation phenotypes of a Δ*cc1064* strain are conditional and depend on environmental factors such as oxygen and temperature stress. Moreover, evidence is presented that the impaired motility of a Δ*cc1064* mutant is caused by an assembly defect of the motor proteins MotA and MotB, leading to paralysis of the flagellum. A model is suggested that links altered membrane composition under environmental stress conditions to the Δ*cc1064* phenotypes.

In Paul, Abel et al. (2007), insights were gained into the regulation of PleD. In addition to the well characterised non-competitive feedback inhibition, a second independent layer of activity control via dimerisation was investigated. The response regulator PleD is activated by phosphorylation of the N-terminal receiver domain. Here we show that the phospho-mimetic chemical beryllium fluoride specifically activates the enzymatic activity of PleD *in vitro* and in addition leads to dimerisation. Fractionation experiments showed that the DGC activity exclusively resides within the dimer fraction. Finally, evidence is provided that dimerisation of PleD is not only required for catalytic activity, but also leads to sequestration to the differentiating stalked pole of the *C. crescentus* cell, thereby providing an elegant way of restricting PleD activity to a subcellular region of the cell.

In Paul, Jaeger & Abel et al. (2008), a network of proteins belonging to the two component system that regulates PleD activation and thereby leads to its localisation were investigated in detail. The single domain response regulator DivK is controlled by the phosphatase activity of PleC and the kinase DivJ. It is shown that DivK allosterically activates the kinase activities of PleC and DivJ and thereby switches PleC from a phosphatase into a kinase state. Increased DivJ activity further activates DivK in a feed-forward loop, while PleC and DivJ together stimulate PleD activity and localisation. Evidence is provided that DivJ, PleC, and DivK colocalise in a short time window during the cell cycle, directly prior to PleD activation, suggesting a role for the spatial distribution of these proteins. At last, the wider role of single domain response regulators in the interconnection of two-component signal transduction circuits is discussed.

Finally, in Dürig, Folcher, Abel et al. (2008), a role for c-di-GMP in the cell cycle of *C. crescentus* via regulation of targeted proteolysis of the regulator CtrA is shown. During the swarmer-to-stalked cell transition CtrA is recruited to the incipient stalked pole, where it is degraded by its protease ClpXP. This recruitment and subsequent degradation is dependent on the enzymatically inactive GGDEF domain protein PopA. PopA itself localises to the cell pole and can bind c-di-GMP. It is shown that mutants in the c-di-GMP binding site fail to localise to the developing stalked pole and consequently fail to promote CtrA degradation. Finally, evidence is provided that interconnects PopA with the pathway responsible for substrate inactivation and protease localisation in a cell cycle dependent manner.

Index

1. Introduction

The transition from planktonic to sessile lifestyle is a vital decision for bacteria and highly regulated

Bacteria are subjected to multiple environmental influences. There are two principle options how to react to such changes in the environment; to move away or to persist. The careful control of this vital decision is essential for the fitness and survival of microorganisms. Once made, such a decision cannot be reverted without cost and is sometimes irrevocable, as dramatic physiological and developmental processes must be undertaken to enable the chosen lifestyle [1].

On one hand, motility requires an apparatus that allows locomotion, for example a flagellum, whose energy consuming function must be maintained under all conditions. In return, it allows the bacterium to continuously move towards fresh nutrient sources and away from toxic environments (reviewed in [2]). On the other hand, the generation of sessile communities, so called biofilms, allows bacteria to grow on surfaces, a lifestyle associated with increased persistence in hostile environments and one, which enables the opportunity of acquiring new food resources (reviewed in [1, 3-6]). While the importance of biofilms in industrial processes has been known for several years, with examples including clogging of pipework or aiding water clean-up (reviewed in [1]), the impact on medical treatments has only recently become clear. Biofilms threaten our ability to treat bacterial infections, as they are inherently protected from host defences as well as antibiotics and can become reservoirs for systemic infections (reviewed in [4]). It is therefore important to understand the molecular mechanisms that are used by bacteria to register environmental signals and translate them in appropriate outputs that determine a motile or a sessile lifestyle. Recently, the bacteria-specific second messenger bis-(3`, 5`)-cyclic dimeric guanosine monophosphate (c-di-GMP) was found to be critically involved in the switch from a planktonic to a sessile existence (reviewed in [7-11]).

The mechanisms underlying c-di-GMP turnover

C-di-GMP (Fig. 1) is a ubiquitous bacterial second messenger that has been shown to be involved in the regulation of a growing number of physiological processes.

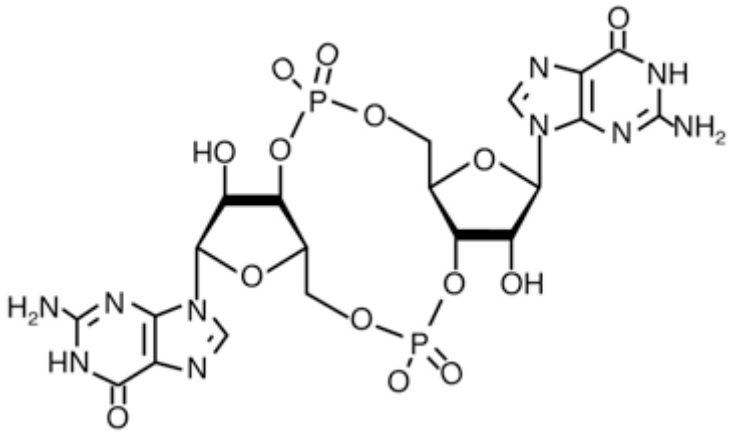

Figure 1: Chemical structure of the bacterial second messenger bis-(3`, 5`)-cyclic dimeric guanosine monophosphate (c-di-GMP).

First identified as an allosteric activator of cellulose synthase in *Gluconacetobacter xylinus*, c-di-GMP is thought to be present in the vast majority of eubacteria [12]. During the pioneering work carried out in *G. xylinus* by the Benziman group, candidate enzymes for the synthesis and degradation of c-di-GMP were identified [13]. These were characterized by the presence of two widely conserved domains, termed GGDEF and EAL, based on conserved amino acid motifes. Later work confined the di-guanylate cyclase (DGC) activity to the GGDEF domain, which catalyses the condensation of two GTP molecules to one molecule of c-di-GMP (Fig. 2) [14]. The confirmation of this finding in various different experimental systems indicates that c-di-GMP is generally produced by these domains [15-26]. The GG(D/E)EF motif itself is an important part of the active site, consequently almost all mutations in the GG(D/E)EF motif abolish enzymatic activity [14-18]. Consequently, this motif is also called the active site (A-site).

Some DGCs have been shown to be subject to feedback inhibition by their product c-di-GMP [19]. The crystal structure of the model DGC PleD from *Caulobacter crescentus* revealed a high-affinity binding site for c-di-GMP within the GGDEF domain, whose core binding motif was identified as RXXD. This motif is positioned five amino acids upstream of the A-site [16, 17, 19]. As binding of c-di-GMP to this site has been shown to be responsible for non-competitive inhibition of DGC activity, it has been designated the inhibitory site (I-site) [16, 17, 19]. The I-site is found in the majority of GGDEF domains with a conserved A-site, indicating that inhibition of DGC activity in response to c-di-GMP is a general regulatory principle of bacterial c-di-GMP signalling [8, 19].

C-di-GMP specific phosphodiesterase activity has been linked to the EAL domain [20-23]. The enzymatic activity of EAL domain-containing proteins hydrolyzes c-di-GMP to the

linear molecule 5`-pGpG. It is believed that this molecule in turn is rapidly hydrolyzed to GMP by other, unknown phosphoesterases in the cell (Fig. 2) [20-22, 24]. Recently another domain family, called HD-GYP, was shown to possess phosphodiesterase activity that is specific for c-di-GMP. This domain family is a member of the metal-dependent phosphohydrolase superfamily, and is able to degrade c-di-GMP directly to GMP (Fig. 2) [25].

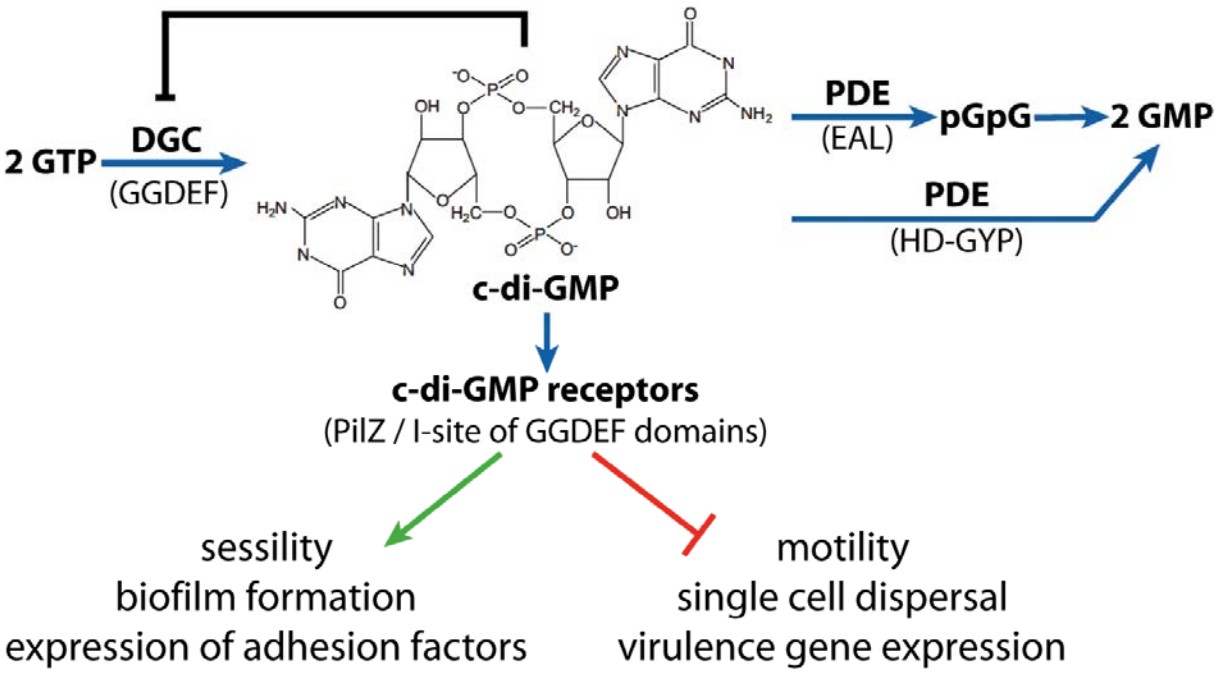

Figure 2: Scheme of the general c-di-GMP signalling pathway.

C-di-GMP is synthesised from two molecules of GTP by proteins harbouring DGC activity. Two alternative degradation pathways are known, either via HD-GYP domain containing proteins to GTP, or by EAL domain containing proteins to pGpG and then further to GMP by other phosphoesterases. The c-di-GMP concentration is detected by c-di-GMP sensors, which then control cellular functions. The black line indicates non-competitive inhibition of DGC activity. This figure was adapted from [10].

C-di-GMP sensory proteins

To translate the cellular concentration of c-di-GMP into a physiological output, binding molecules are required. Two classes of binding proteins have been identified so far (Fig. 2). Firstly, c-di-GMP can bind to the I-site as described above. As not all GGDEF domains harbouring an I-site also contain a conserved A-site, it has been suggested that these molecules can transduce signals upon binding to c-di-GMP [8]. Indeed, the GGDEF domain protein PopA from *C. crescentus* requires an intact I-site but not its degenerate A-site to be correctly sequestered to the cell pole and to maintain its function in cell cycle control [26]. Secondly, the PilZ domain, named after the PilZ protein from *Pseudomonas aeruginosa*, was

implicated in c-di-GMP binding, with several examples of different cellular outputs characterised [27-34]. PilZ domains were identified in glycosyl transferases, like the cellulose synthases of *G. xylinus*, *Escherichia coli* and *Salmonella enterica* [31, 33, 34] and in proteins that are likely to interact with glycosyl transferases like in the alginate and PEL polysaccharide synthase systems of *P. aeruginosa* [35, 36]. This indicates a direct link between c-di-GMP and exopolysaccharid (EPS) production. Furthermore, the *C. crescentus* PilZ domain protein DgrA, which has been shown to bind c-di-GMP *in vitro*, negatively regulates flagellar rotation upon binding [33], suggesting a role for PilZ in the control of motility.

Regulation of c-di-GMP metabolism

In contrast to archea and eukaryotes, which do not employ c-di-GMP signalling, the majority of eubacteria harbour a multitude of GGDEF, EAL or HD-GYP domain proteins [12]. Most bacteria possess an intermediate number, for example *C. crescentus* (14) (Fig. 3) or *E. coli* (36), although a few contain none (e.g. *Haemophilus influenzae*), while others contain up to 98 (e.g. *Shewanella oneidensis*) of these proteins.

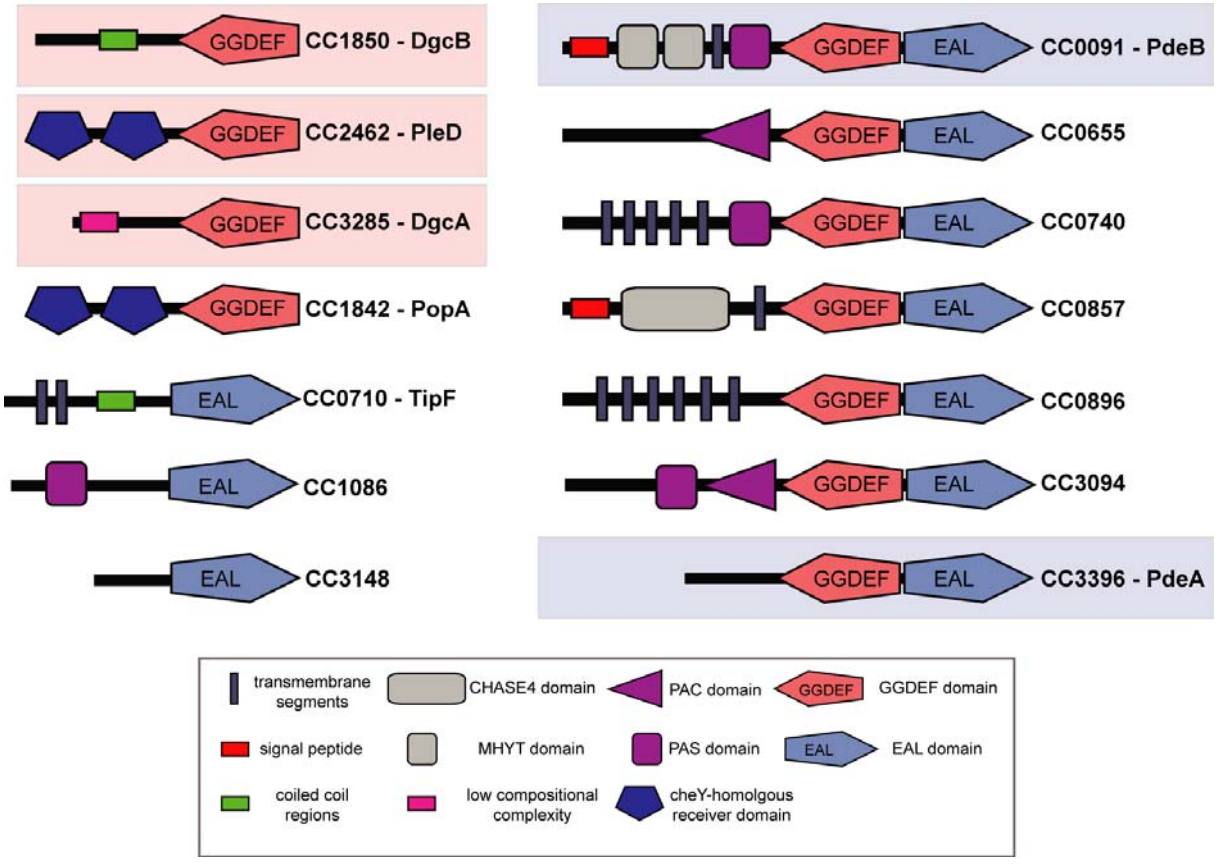

Figure 3: Schematic representation of the domain structure of all known *C. crescentus* GGDEF/EAL domain proteins.

The domain prediction was retrieved from the SMART database [37]. Proteins with biochemically characterised DGC and PDE activities are highlighted in light red and blue, respectively. The annotation for PopA (CC1842) was manually adjusted.

One question arising from this distribution is why such diversity is needed. Do all proteins regulate one global c-di-GMP pool, or does each enzyme act on a separate, local pool? And if so, what are the mechanisms that circumvent cross-talk between different c-di-GMP dependent regulatory pathways?

Strikingly, most GGDEF, EAL, and HD-GYP domains are fused with known or hypothetical signal input domains [7, 12]. Among these are components of the bacterial two-component regulatory system as well as one-component systems, making it likely that these domains regulate the activity of their fused GGDEF, EAL, and/or HD-GYP domains. It was also shown that the c-di-GMP signalling domains themselves can act as regulatory domains. Examples for this are the phosphodiesterases FimX from *P. aeruginosa* and PdeA for *C. crescentus*, where GTP binding to a non-conserved GG(D/E)EF motif was shown to activate the PDE activity of these composite GGDEF/EAL domain proteins [20, 23]. Another example is the GGDEF domain protein PopA, where c-di-GMP binding to its I-site leads to altered subcellular localisation [26]. This variety of different input domains likely allows sensing of a range of (so far largely unknown) environmental and internal signals that can be integrated in a c-di-GMP mediated response, enabling the cell to adapt to diverse environmental niches. This gives a first explanation for the abundance of c-di-GMP metabolising enzymes within each species.

Furthermore, a subcellular localisation was shown for some components of the c-di-GMP regulatory system [14, 26, 30, 38]. Most notable is the localisation of the *C. crescentus* DGC PleD, from a diffuse cytoplasmic distribution to the incipient stalked pole upon the swarmer-to-stalked cell differentiation (Fig. 4) [14]. Another example is the previously mentioned c-di-GMP sensor PopA, which shows a complex localisation pattern in a cell cycle dependent manner and in response to c-di-GMP binding [26]. This localisation of proteins important for c-di-GMP signalling was interpreted as evidence for microcompartmentalisation and reveals a possible mechanism to separate different c-di-GMP dependent pathways that are active at the same time in the cell [7-10, 39].

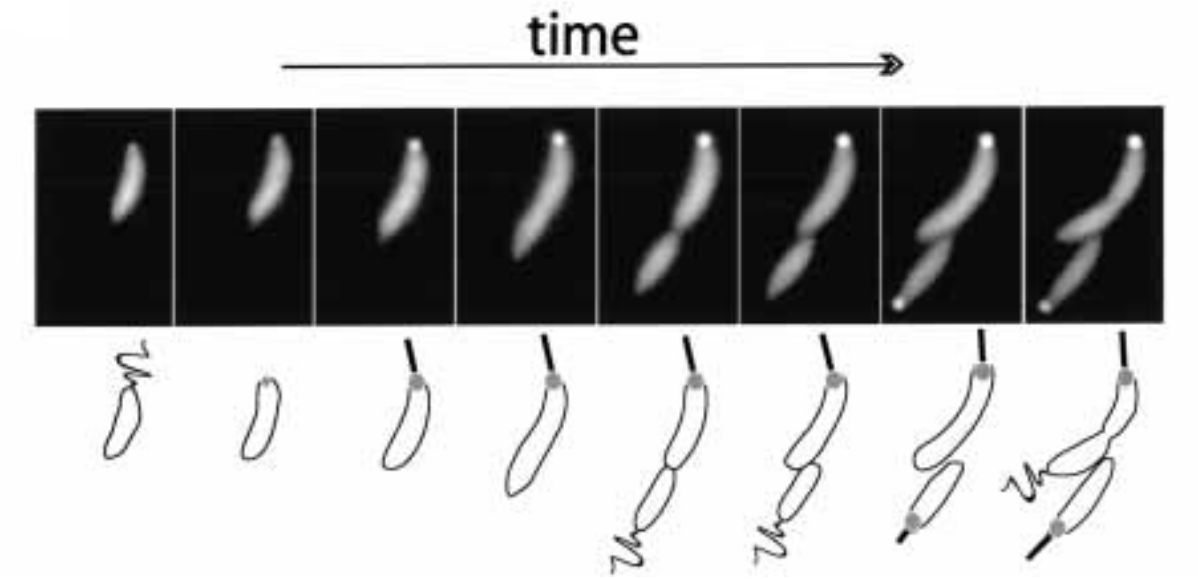

Figure 4: The cell cycle dependent spatial distribution of PleD.

A single cell expressing PleD-GFP was analysed at several timepoints during its growth on a microscope slide. While PleD is delocalised in swarmer cells, in stalked and predivisional cells the majority of the fluorescent signal it is sequestered to the stalked pole of the cell, as illustrated in the schematic drawing. This figure was adopted from [14].

As well as the spatial sequestration of c-di-GMP signalling proteins, different pathways may also be separated in time. Two mechanisms to achieve a temporal segregation have been described so far; differential expression regulated on the transcriptional level and protein stability due to regulated proteolysis. One example of c-di-GMP-related transcriptional regulation is the autoregulatory expression of *vieSAB* in *Vibrio cholerae* [40]. VieA is a dual function protein with independent transcriptional activator and PDE activities. It is coexpressed with its putative cognate sensor histidine kinase VieS. Upon phosphorylation by VieS, VieA is thought to stimulate the expression of *vieSA* and therefore increases PDE activity (see below). An example of proteolytic regulation is HmsT, a putative DGC that is implicated in the regulation of hemin storage (Hms) and biofilm formation in *Yersinia pestis* [41]. Upon a temperature shift to 37 °C, which is associated with transfer from the flea vector to the mammalian host, three Hms proteins including HmsT are degraded by Lon and ClpXP proteases [42], thereby switching the bacterium from a biofilm mode into a lifestyle associated with acute infection. To summarise, there is a wide range of diverse regulatory mechanisms monitoring the activity of PDEs and DGCs including allosteric binding, phosphorylation of other domains in the protein, localisation to microdomains within the cell, and regulation of protein levels by transcription and protein stability. This can be seen as an indication for the need of a tight c-di-GMP metabolism control, which is probably due to the

fact that this second messenger regulates processes critical to many aspects of bacterial survival in diverse and often dynamic environments [10].

From the phenotypes described so far, it was concluded that high cellular levels of c-di-GMP generally activate biofilm formation, while inhibiting motility. Therefore, the paradigm in the field is that c-di-GMP functions as a switch, regulating the transition between sessile and motile lifestyle (Fig. 2) [7-10]. In addition, c-di-GMP has been shown to influence the expression of virulence factors [43-45] and affects the cell cycle [26]. Although the specific target molecules and effector mechanisms involved in c-di-GMP signalling remain largely unknown, c-di-GMP has been demonstrated to control cellular functions at the transcriptional, translational, and posttranslational level [46-50].

Regulation of biofilm formation by c-di-GMP

One major process regulated by c-di-GMP is the promotion of surface adhesion and biofilm formation. Bacteria either exist as free planktonic cell or they form surface-attached communities known as biofilms [51, 52]. The latter lifestyle is associated with persistence in adverse environments, as biofilms have been shown to increase bacterial tolerance against toxic compounds, antibiotics, stress factors and predators [51, 53-55]. The organization of biofilms can vary from a simple monolayer of cells attached to biotic or abiotic surfaces to a sessile microbial community with a complex three-dimensional structure [56]. The generation of biofilms is a multistep process that generally contains three distinct stages (Fig. 5). Initially, motile bacteria move towards surfaces until they are able to overcome surface tension and bind. After this initial attachment, the cells irreversibly attach by the production of an adhesive matrix. The young biofilm eventually matures, building a tight pack with additional cells, finally resulting in microcolonies. The last stage of the biofilm is characterized by the release of new planktonic cells and is therefore termed the detachment state [56-58].

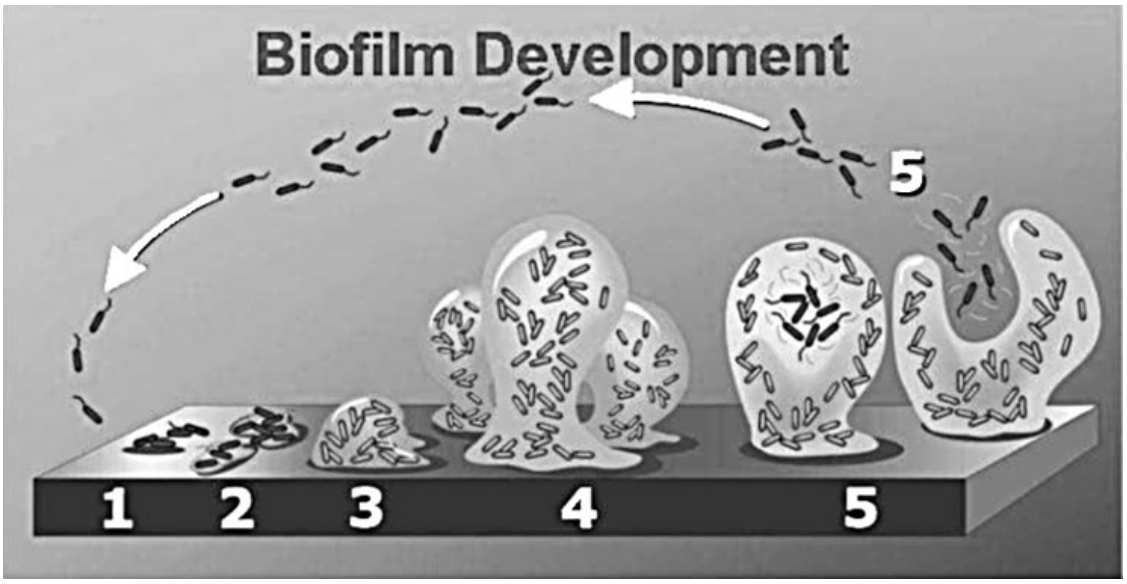

Figure 5: Illustration of the developmental steps of a biofilm.

Motile cells overcome surface tension and make first reversible contact to the surface in stage 1. In stage 2, the cells become irreversibly attached to the surface by synthesising adhesive matrices. In the next steps, microcolonies are formed. The biofilm matures and builds its three dimensional, sometimes complex structures. In the fifth step, single motile cells are released from the biofilm and invade new resources. This figure was adopted from [56].

During biofilm formation, three structures were shown to be of interspecies importance: pili, flagella, and adhesive matrices [6]. One prominent class of adhesive material is known as exopolysaccharides (EPS). These may account for 50 % to 90 % of the total organic carbon of biofilms and are therefore considered to be the main matrix material of the biofilm [59]. The nature of these polymers shows great variability, with a multitude of different chemical and physical properties [60]. Numerous reports have documented the influence of c-di-GMP on biofilm formation [29, 42, 45, 47, 50, 61-72]. In addition to its effect on adhesion factors, for example pili [23, 30] or curli fimbriae [71], the synthesis of EPS components was shown to be increased by high cellular c-di-GMP in various species including *Pseudomonas putida* [73, 74], *Pseudomonas fluorescens* SBW25 [68, 74-76], *Salmonella typhimurium* [67, 71, 77], *Thermotoga maritima* [78], and *Vibrio cholerae* [63, 79, 80].

One example of how EPS production is regulated on a transcriptional level was described in *V. cholerae*. The phosphodiesterase VieA was shown to influence the transcription of *vpsR* and *vpsT* [72, 81]. These two transcriptional activators regulate operons coding for *Vibrio* exopolysaccharide (VPS) biosynthesis enzymes. VPS is an exopoly-saccharide used as a biofilm matrix component in *V. cholerae* [82, 83]. The absence of VieA leads to increased transcription of *vps* genes and therefore an increase in biofilm development [72]. This effect can also be achieved via overexpression of the DGC VCA0956 [81].

A second example linking exopolysaccharide synthesis to increased cellular c-di-GMP levels is the Wsp system in *P. aeruginosa* and *P. fluorescens*. The Wsp system is a chemosensory system with homology to the chemotaxis pathway of *E. coli* [84], but instead of altered flagellar rotation, the output is c-di-GMP production [18, 85, 86]. The current model describes the transmembrane protein WspA as a chemoreceptor that changes conformation upon binding to an unknown molecule. This signal is transduced via either WspB or WspD to the histidine kinase WspE. WspE then phosphorylates the receiver domains of the response regulators WspR as well as WspF. Upon phosphorylation the methylesterase WspF, in concert with the methyltransferase WspC, becomes involved in signal adaptation, while the DGC activity of WspR is activated [18, 68, 85, 86]. Therefore, signalling through the Wsp system leads to the production of c-di-GMP by WspR. It has been suggested that the activation of WspR is mediated by release of its C-terminal GGDEF domain from the inhibitory N-terminal CheY-like receiver domain upon phosphorylation [18, 68]. Among other influences, including inhibition of twitching and swimming motility and regulation of Cup fimbriae [85, 86], signalling through the Wsp system regulates biofilm formation. In *Pseudomonas fluorescens* the production of partially acetylated cellulose is stimulated [75, 76] and in *Pseudomonas aeruginosa* increased expression of the exopolysaccharide operons *pel* and *psl* was shown [87, 88]. These operons encode two sets of genes predicted to be involved in the production of two distinct carbohydrate-rich biofilm matrix components. The *pel* gene cluster is involved in the production of a glucose-rich matrix material, while the *psl* gene cluster is involved in the production of a mannose-rich exopolysaccharide [87]. Both molecules are required for biofilm maturation (reviewed in [89]). In addition to its regulation on the transcriptional level, the production of the PEL exopolysaccharide has been shown to be allosterically regulated by c-di-GMP, via the c-di-GMP binding protein PelD [90]. These examples illustrate how increased levels of c-di-GMP propagate biofilm formation, a process that has been shown in a variety of species. Furthermore, the mechanisms described here demonstrate regulation on a transcriptional level and on a direct allosteric level.

Regulation of motility by c-di-GMP

The ability to move is important for the lifestyle of many bacteria, as it permits the scavenging of nutrient resources, the exploration of new niches and the avoidance of toxic environments. It is therefore not surprising that bacteria employ a multitude of different ways to enable locomotion, including twitching, swarming, and swimming. While twitching

motility involves a cycle of assembly, attachment, and retraction of Type IV pili [91, 92], swarming and swimming are mediated by flagella. In many bacteria one kind of flagella is used for both swimming and swarming, but some species employ distinct flagella for the two modes of motility [93]. All of these types of locomotion have been shown to be regulated by c-di-GMP in various ways (reviewed in [8-10, 94]).

An example how c-di-GMP interferes with twitching motility was characterised in *P. aeruginosa*. FimX is a composite GGDEF/EAL domain protein with a degenerate A-site. It was shown to function as a phosphodiesterase, whose activity can be stimulated by GTP, presumably by binding to the degenerate A-site, as a mutation in this motif abolishes the activation by GTP [23]. The fully functional PDE activity of FimX is needed to enable twitching motility in *P. aeruginosa* [23]. Although the levels of the major subunit of pili, PilA, are unchanged in a *fimX* mutant, these cells fail to efficiently assemble their pili, as almost no PilA is detectable on the outside of the bacteria [23, 30]. Therefore, FimX is believed to regulate the assembly of pili via c-di-GMP.

In *Vibrio parahaemolyticus* it was reported that c-di-GMP, produced by the composite GGDEF/EAL protein ScrC, specifically controls the expression of lateral flagella [50]. These flagella are arranged randomly on the cell surface of *V. parahaemolyticus* and, in contrast to the polar flagella that are only used for swimming motility, permit the cell to migrate across hydrated, viscous semisolid surfaces, a process called swarming [2, 95]. Another composite protein was recently identified to also play a role in lateral flagella expression. ScrG is a composite protein like ScrC, but with a degenerate GG(D/E)EF motif [96]. Mutation analysis as well as biochemical evidence suggest that ScrG has PDE, but no DGC activity [96]. Both systems are believed to react to different stimuli and were shown to inversely regulate lateral flagella expression. This activity is cumulative and operates on the level of transcription via a yet uncharacterised mechanism.

The final example given here is the effect of c-di-GMP on swimming; the best understood form of motility in bacteria. Swimming allows movement through a liquid environment with low viscosity by rotation of flagella, which generate thrust and propel the bacteria forward. Upon artificially increasing the cellular c-di-GMP level, several studies have shown that bacteria stop rotating their flagella [14, 19, 33, 61, 97]. In *C. crescentus* this paralysis can be mediated by the PilZ domain proteins DgrA and DgrB [33]. In *E. coli* as well as in *S. enterica* serovar Typhimurium the PilZ domain protein YcgR and the PDE YhjH are suggested to function in the same pathway, regulating flagellar rotation on a functional level [29, 34, 98]. These publications suggest a model in which YhjH, together with a yet unknown

DGC, inversely regulates c-di-GMP levels. The concentration of c-di-GMP is sensed by YcgR, which transduces the signal further to the flagellum. Initial evidence suggests that the YhjH/YcgR system may control the interaction between the flagellar motor protein MotA and its stator counterpart FliG (reviewed in [94]). Taken together, these examples show that low concentrations of c-di-GMP are associated with locomotion of cells by flagellar motors or retracting pili. Furthermore, they show that this regulation can acts on different levels, including assembly, transcription, and function.

Caulobacter crescentus is a model organism for cell cycle control and bacterial development

Understanding the inverse regulation of motility and biofilm formation by c-di-GMP is greatly assisted by an experimental setting where this transition occurs under defined conditions, in a reliable manner, and synchronous in a sufficiently large population. The unique asymmetric cell cycle of *C. crescentus* with its obligate transition from motile swarmer cell to sessile stalked cell makes it a particularly convenient experimental organism for the examination of both cell cycle and cellular differentiation events. *C. crescentus* is a gram negative bacterium belonging to the α-proteobacteria and can be isolated from freshwater environments, including oceans, streams and lakes [99]. The cells are hetero-oligotrophic aerobe, have vibrioid morphology and contain a single, polar cytoplasmic protuberance surrounded by cell wall material; the stalk [100]. In their natural habitat, they can be found attached to submerged biotic and abiotic surfaces including other micro organisms like bacteria and algae [100].

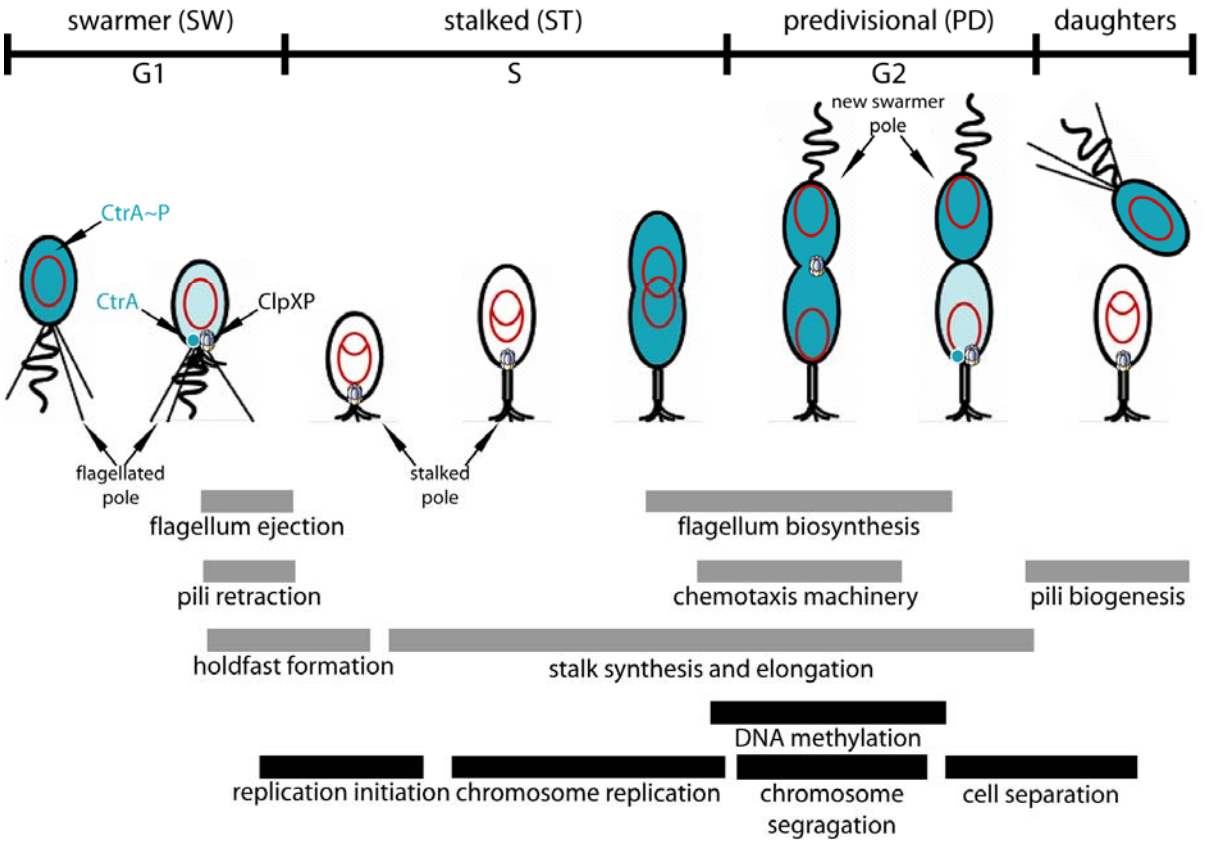

Figure 6: The *Caulobacter crescentus* lifecycle.

The developmental stages of the *C. crescentus* division cycle are shown schematically. Additionally, the spatial distribution of the cell cycle regulator CtrA, as well as its degradation by the protease ClpXP are depicted. CtrA is shown in blue, quiescent chromosomes are represented by circles and replicating chromosomes are indicated by "θ" structures. Morphogenetic events are indicated by grey bars, cell cycle events by black bars. The length and positioning of the bars indicate the initiation and period of events. This figure was adapted from [101].

During its life cycle, *C. crescentus* undergoes an asymmetric cell division (Fig. 6). Each division gives rise to two genetically identical, but morphologically and physiologically distinct daughter cells with different developmental programs. These two cell types comprise a motile swarmer cell and a non-motile stalk bearing cell. The stalked cell progeny can reinitiate chromosome replication almost immediately following cell division [102, 103] and therefore functions as a stem cell, continuously generating new swarmer cells. The planktonic swarmer cells are equipped with a single polar flagellum, polar adhesive pili, are able to perform chemotaxis and their replicative program is blocked [100, 102-105]. This block is mediated by the master cell cycle regulator CtrA [106]. In addition to the direct positive and negative regulation of 96 genes, which are organized in 55 operons (e.g. flagellar class II genes) [107], activated CtrA binds directly to the origin of replication and thereby inhibits replication initiation [106]. To be able to reinitiate chromosome replication and cell division, the swarmer cell has to undergo an obligate differentiation into a stalked cell. During this

transition, CtrA is desphosphorylated and simultaneously located to the incipient stalked pole of the cell, where it is degraded by the ATP dependent protease ClpXP [108-111]. The loss of active CtrA derepresses the origin of replication and DNA replication is initiated. At the same time the flagellum is shed, the pili retract, and the chemosensory apparatus is lost [112]. These organelles are replaced by the stalk, with an adhesive material, the holdfast, located at its tip [113]. The holdfast contains adhesive polysaccharides, whose exact composition is unknown, and mediates strong irreversible attachment of *C. crescentus* cells to solid substrates [57]. The optimal attachment of cells is enabled only during a short window of development, when the flagellum, pili, and the adhesive holdfast are all present at the same pole. Therefore, it has been suggested that the precise timing of the retraction of pili, loss of flagellar activity and assembly of the holdfast is critical for surface colonization (Fig. 7) [47]. During the stalked phase of the cell cycle, the chromosome is completely replicated and both the cell and the stalk continually grow. In the predivisional cell the two chromosomes segregate, a constriction forms and a new flagellum, chemotaxis apparatus, and pilus secretion apparatus are assembled at the pole opposite the stalk (Fig. 6) [101]. Cell division completes the cycle, again resulting in a new motile swarmer cell scavenging for new nutrient resources, and a surface adherent stalked cell.

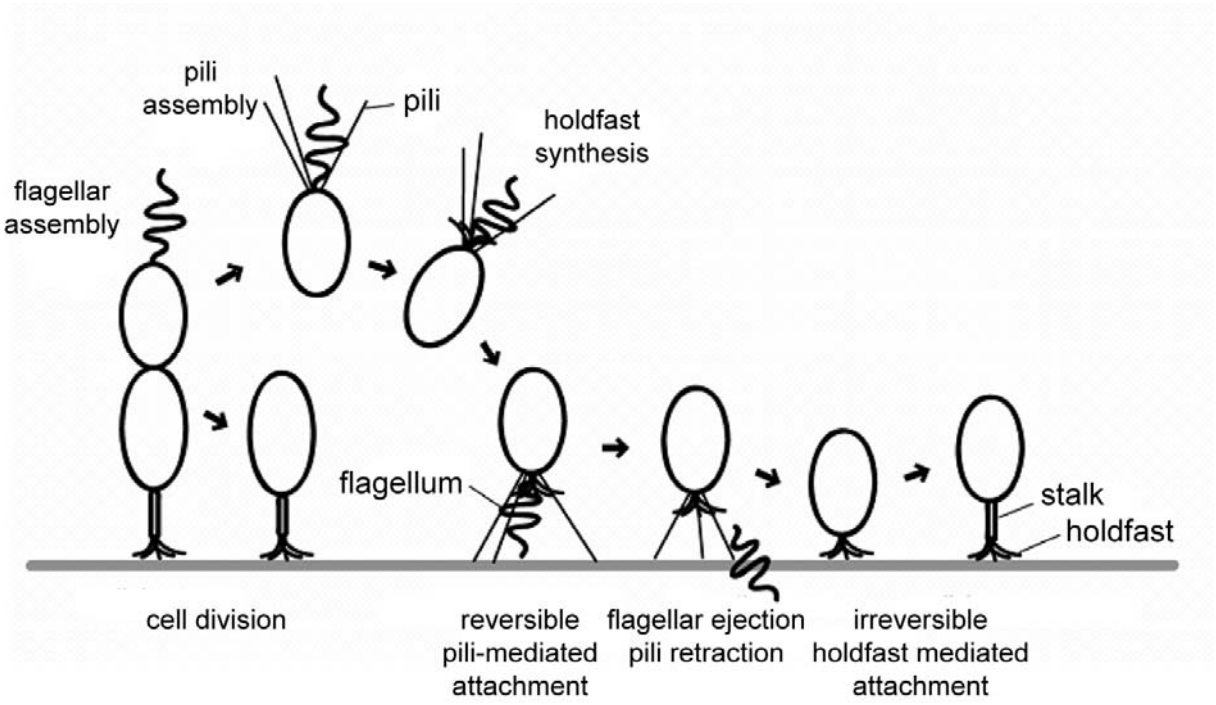

Figure 7: The order of developmental events is important for optimal surface attachment in *Caulobacter crescentus*.

Schematic representation of the development of polar appendices in *C. crescentus*, their timing during the cell cycle and their role in surface attachment.

The morphological and physiological changes that take place during the cell cycle make it easy to visualise the current status of individual cells. This, together with the ability to isolate a pure population of swarmer cells by density gradient centrifugation and to follow their synchronised development facilitates the analysis of the *C. crescentus* cell cycle [114]. The couplings of developmental processes, especially the transition from a motile, planktonic into a non-motile, sessile state, with the cell cycle, as well as its asymmetric division are special features of *C. crescentus*. Together, these unique features made *C. crescentus* one of the preferred bacterial model systems to analyse cell cycle progression, generation of asymmetry and development.

The structure of the *Caulobacter crescentus* flagellum

One possibility of responding to changes in the environment is to move away from adverse, or towards promising conditions. A wide spread way of facilitating locomotion in bacteria is the synthesis of a rotating propeller at the cell surface; the flagellum. During its swarmer and late predivisional phase, *C. crescentus* possesses a single, polar flagellum. Electron microscopy revealed that its structure is similar to the well studied flagella of enteric bacteria [115-117]. The flagellar rotor can be divided into three major components; basal body, hook, and filament (Fig. 8) (reviewed in [118]). The basal body is located in the cytoplasmic membrane and consists of a series of rings attached to each other by a rod. This structure spans both membranes and the peptidoglycan layer and acts as flagellar rotor. The rings are named according to their position in the cell envelope. The C ring is formed by the cytoplasmic part of the basal body, the MS ring lies within the inner membrane and sticks in the periplasm, whereas the P ring is located in the peptidoglycan layer. A *C. crescentus* specific E ring is located between MS and P rings [115]. Finally, the L ring is located in the outer membrane. The rod is attached to the hook, a flexible joint that connects the rod to the filament with the help of adaptor proteins, the hook associated proteins (HAP) (review in [118]). In *C. crescentus* the filament is composed of three different flagellins and converts rotary motion into thrust [119]. The filament is a semi-rigid, hollow tube that comprises most of the flagellar mass and can be up to 10 μM long. It was shown that at least 20 individual proteins are integrated into the complex flagellar structure and another 30 are used for its assembly and function [120].

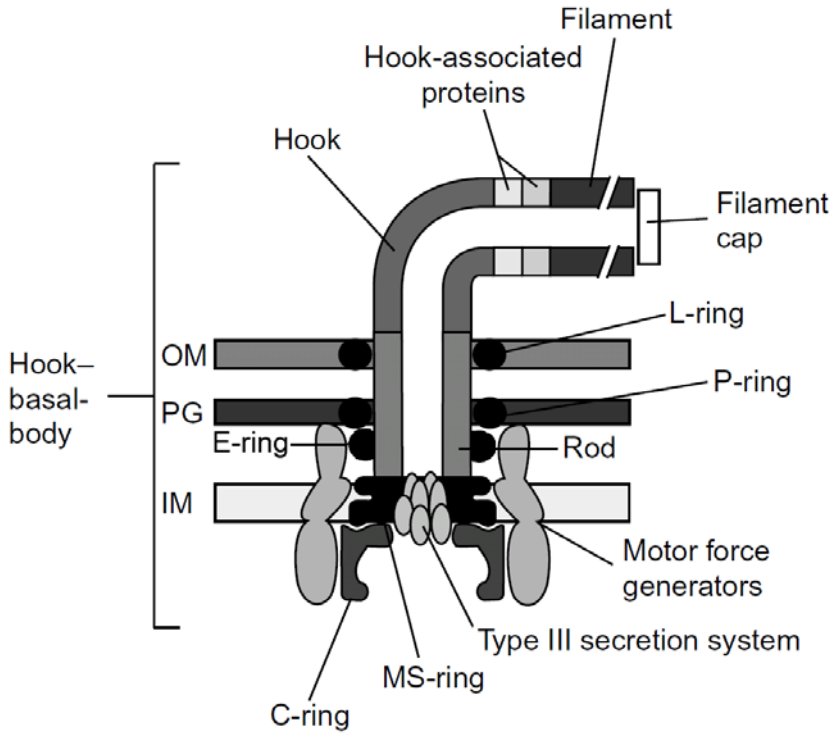

Figure 8: Schematic representation of the flagellar structure.

The flagellum can be subdivided into three substructures: a basal body complex that spans the bacterial membranes, the hook and an external filament. The rotor part of the basal body is associated with the motor force generating proteins MotA and MotB that form the stator. Rotation of the flagellum is achieved via interaction of the motor force generators, which function as proton pumps, with the C-ring. Inner membrane (IM); outer membrane (OM); peptidoglycan layer (PG). This figure was adapted from [121].

The regulation of flagellar gene expression

The regulation of flagellar gene expression is subject to a complex regulatory hierarchy, in which the expression of genes encoding early structures and the functional assembly of their gene products is required for the expression of late gene products [122-127]. In *C. crescentus*, four distinct hierarchical classes can be distinguished (Fig. 9) [128]. The first level of control is mediated by CtrA, which promotes the transcription of the class II genes and links this process to the cell cycle [106, 109, 128, 129]. Class II genes encode the structures of the basal body that are assembled earliest, as well as components of the flagellum-specific type III secretory system and transcription factors (reviewed in [118, 130]). The alternative sigma factor σ^{54} and the transcription activator FlbD, a class II gene product, are essential for the expression of class III genes encoding both the outer basal body and hook structure [131-134]. FlbD and σ^{54} are also a prerequisite for the transcription of the class IV genes encoding the three flagellin subunits of the flagellar filament [131-134]. In contrast to class III genes, the translation of class IV genes requires the completion of the basal body-hook assembly

[135, 136]. At least one flagellin transcript was shown to be destabilized by the negative regulator FlbT prior to the functional assembly of class II and III gene products, suggesting a general role of posttranscriptional control [137, 138].

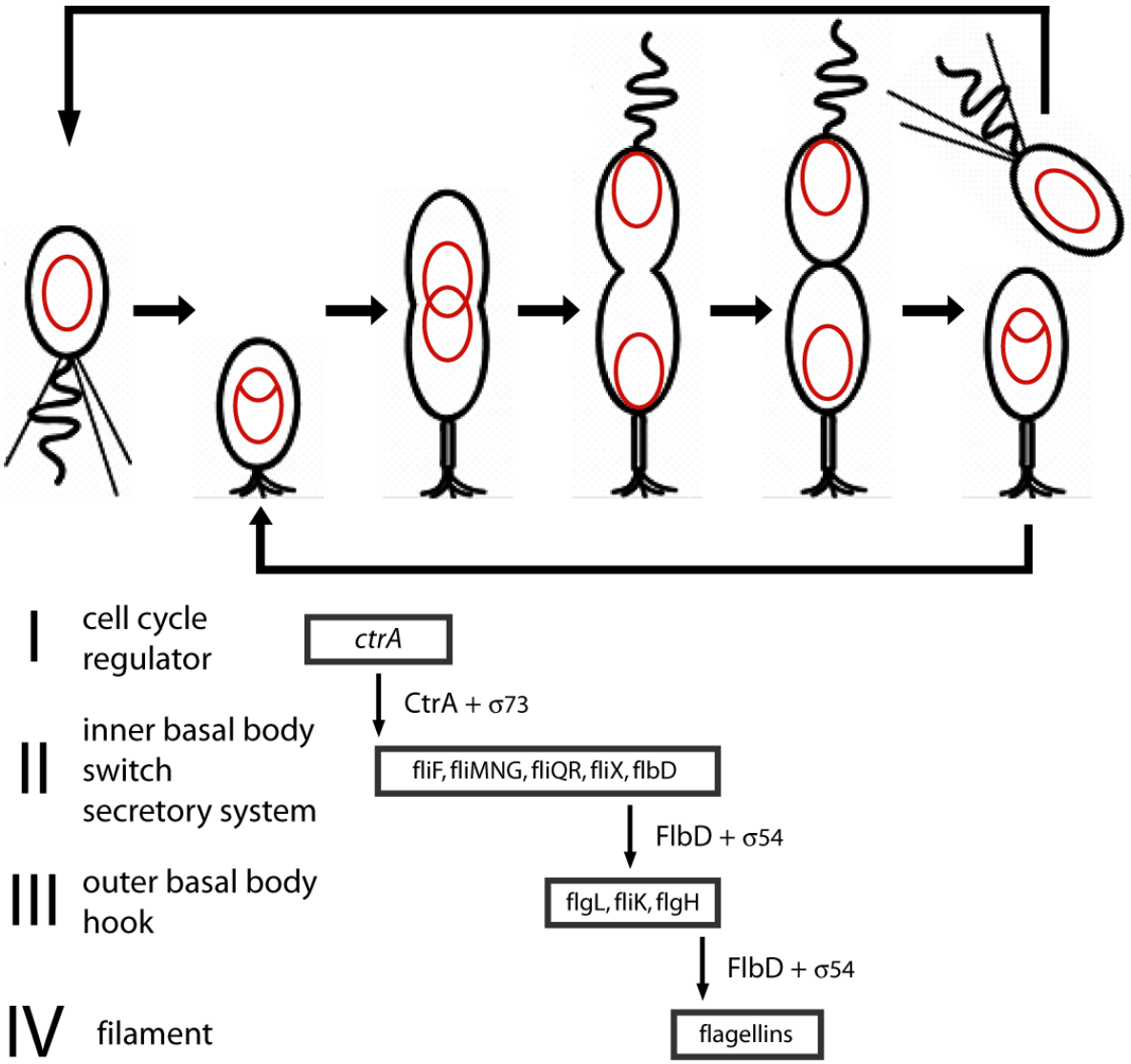

Figure 9: A schematic diagram of the *Caulobacter crescentus* flagellar regulatory hierarchy.

The hierarchical order of flagellar gene expression is depicted with respect to the cell cycle and DNA replication. Example genes for each class are given within blocks that represent the period during the cell cycle in which they are expressed. CtrA coordinates cell cycle events like DNA replication to the synthesis of the flagellum, as it controls the transcription of early, class II flagellar genes. Among others, the transcriptional activator FlbD is a class II gene and after functional assembly of the inner basal body it drives the expression of class III and class IV genes. The class IV genes are further regulated by a posttranscriptional mechanism, which acts on the functional assembly of class III gene products (see text for details). Alternative sigma factors required for gene expression of the respective class are depicted next to the transcription factors. The chromosome is indicated as red circle, as in Fig. 6. This figure was adapted from [139].

The expression of flagellar genes is interconnected twice with the cell cycle. First, CtrA expression, stabilisation and activation by phosphorylation are cell cycle dependent [108, 109, 140, 141]. Second, in addition to its regulated expression, FlbD is also activated by phosphorylation in a cell cycle specific manner [132]. Furthermore, the differential activation of FlbD restricts the expression of class III/IV genes to the incipient swarmer cell compartment in late predivisional cells [132, 142-145].

The assembly of the flagellum

The order of flagellar assembly proceeds, generally speaking, from inner to outer structures (Fig. 10) (reviewed in [118, 130]).

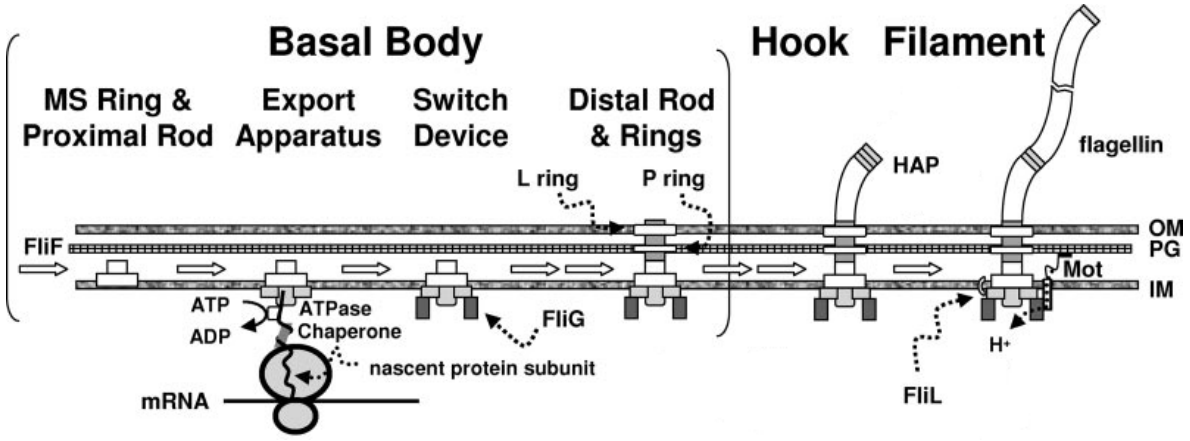

Figure 10: Schematic drawing of the order of flagellar assembly.

The scheme describes the flagellar assembly as it is investigated in the enterics *E. coli* and *S. enterica* serovar Typhimurium. Three major substructures are distinguished, the basal body, the hook, and the filament. The assembly of the basal body is subdivided into four steps, the integration of FliF, the assembly of flagellar specific type three secretion system (TTSS), the C-ring forming switch device and the rod and L/P ring assembly. The order of events is shown as progression from left to right. Inner membrane (IM); peptidoglycan (PG); outer membrane (OM); hook associated proteins (HAP). This figure was adapted from [94].

The first step in assembly is believed to be the insertion of the class II gene product FliF in the inner membrane, where it forms the MS ring [146]. The MS ring is the central structure that houses the flagellar specific type III secretion (TTSS) apparatus, which is assembled next. The C ring is probably assembled on the MS ring by the proteins FliM, FliN, and FliG that together form the switch complex [118], which is required to change the direction of flagellar rotation. The TTSS apparatus is highly selective in transporting its substrates. As soon as the export apparatus is functionally assembled in the MS ring, the rod forming proteins are exported and assembled in the periplasm. Onto the rod, the P ring and the L ring, which are either located in the peptidoglycan layer (P) or in the outer membrane (L),

assemble. These depend on the presence of both the assembled export apparatus and the switch, although the P and L ring proteins are exported by the secretory pathway and not like the other components by the TTSS system. After the whole rod has formed, the completed basal body can now serve as a channel through which subsequent proteins travel across the inner and outer membrane and through the peptidoglycan layer to their assembly site. The first molecules to be secreted through this envelope-spanning channel are the hook subunits, which are polymerized at the distal end of the basal body outside of the cell. After export and assembly of hook associated proteins (HAP), the flagellins are secreted and assembled between the HAPs to produce the filament. The stator complex consisting of MotA and MotB proteins that form the proton channel energising the flagellum is assembled at some point during the flagellar synthesis. Flagellar associated stator complexes are in equilibrium with non-associated complexes diffusing in the inner membrane (reviewed in [118]).

The physiology of the flagellar rotation

In some species the flagellum can rotate with a frequency of up to 100,000 rpm [147]. To be able to rotate, the proton (or sodium) gradient that energises the process has to be converted into torque. The protons flow through an ion channel formed by the stators [148-153] which are composed of MotA and MotB proteins with the stochiometry $MotA_4MotB_2$ [118, 154, 155]. Rotation is probably driven by conformational changes in these membrane protein complexes. It is thought that changes occur as protons move on and off a critical aspartate residue in the stator protein MotB [156] and the resulting forces are applied to the rotor protein FliG, which was shown to interact with the stator protein MotA [157]. While the stator protein MotB can interact with the peptidoglycan and is therefore anchored in a fixed position, the rotor part of the flagellum is free to rotate [149, 158-162]. Each stator complex assembles and works independently, so each complex can generate torque on its own [163-166]. In the absence of either MotA or MotB, the flagellum is completely assembled, but paralysed [148, 150, 167-169].

This paralysis of the flagellum resembles a situation with artificially high cellular c-di-GMP levels in *C. crescentus* [14, 33, 61]. Although the exact mechanism leading to the inhibition of flagellar rotation is not clear, the c-di-GMP binding proteins DgrA and DgrB have been implicated in this process [33]. In addition, c-di-GMP interacts with flagellar function on a second level in *C. crescentus*. At the swarmer-to-stalked cell transition, the flagellum is shed off and released from the cell to turn off motility in the stalked cell. This process is dependent on the DGC activity of the GGDEF domain protein PleD [170].

The activation of PleD, a response regulator with a di-guanylate cyclase output domain provides a link between cell cycle cues and polar development

PleD is an unconventional member of the response regulator family of two component signal transduction systems. It contains two N-terminal receiver domains (D1 and D2) arranged in tandem, and a C-terminal GGDEF output domain [14, 16, 17]. Several genetic experiments have indicated that the two sensor histidine kinases PleC and DivJ, and the single domain response regulator DivK act as upstream components required for the activation of the PleD di-guanylate cyclase activity [61, 171, 172]. In agreement with this, direct biochemical experiments have shown phosphotransfer from both DivJ and PleC to PleD, leading to its activation [14, 61, 173]. The essential cell fate determinator protein DivK is transcriptionally coupled to PleD [174]. Although a direct connection to PleD has not yet been established, it has been shown that DivK is regulated by the same sensor histidine kinases as PleD [172, 174, 175]. As in the case of PleD, DivJ transfers phosphate to DivK [174, 175]. In contrast, PleC has the function of a phosphatase [175, 176]. Due to the presence of all three components, DivJ, PleC, and DivK, at the same time in the dividing cell, DivJ and PleC compete for the phosphorylation status of DivK. Because DivJ activity is restricted to the stalked cell, while PleC activity is restricted to the newborn swarmer cell upon cell division (see below), phosphorylated and unphosphorylated DivK are asymmetrically separated [176]. As DivK influences the phosphorylation as well as degradation of the cell cycle regulator CtrA, the asymmetric DivK phosphorylation status directly influences the cell cycle [140].

Dynamical localisation of PleD and its upstream components during the cell cycle

PleD, like its upstream components PleC, DivJ, and DivK, is dynamically localised during the cell cycle. Whereas DivJ is located at the stalked pole of the stalked and predivisional cell, PleC is located at the swarmer pole of swarmer and predivisional cells (Fig. 12) [175]. DivK is recruited to the swarmer pole in newborn swarmer cells and to the stalked pole of stalked cells, whereas in predivisional cells it is located to both poles (Fig. 12) [177]. PleD is delocalised in swarmer cells, but as soon as the cells differentiate into stalked cells it is sequestered to the incipient stalked pole (Fig. 12) [14]. To enable this localisation, wild-type PleD has to be phosphorylated, as mutations of the phosphoryl acceptor ($PleD_{D53N}$), as well as deletions of the sensor histidine kinases DivJ and PleC abolish polar sequestration [14]. Although critical, phosphorylation is not sufficient for localisation, as shown by the

hyperlocalised PleD mutant PleD$^{*}_{D53N}$ that misses the phosphorylation site but mimics the conformation of an activated PleD [14]. Beyond this insight, the mechanism of subcellular sequestration is unknown. Whereas the differential localisation of PleC and DivJ results in a uneven distribution of phosphorylated DivK upon cell division, which then leads to asymmetry and is believed to orchestrate the different cell fates of the *C. crescentus* progenies [176], the role of PleD localisation is currently unclear. It has been speculated that localised PleD could restrict c-di-GMP production to one locus, thereby enabling the specificity of its signalling pathway [7, 8, 14]. PleD localisation could also ensure that upon division, active PleD stays in the stalked progeny to keep the swarmer cell free of active PleD.

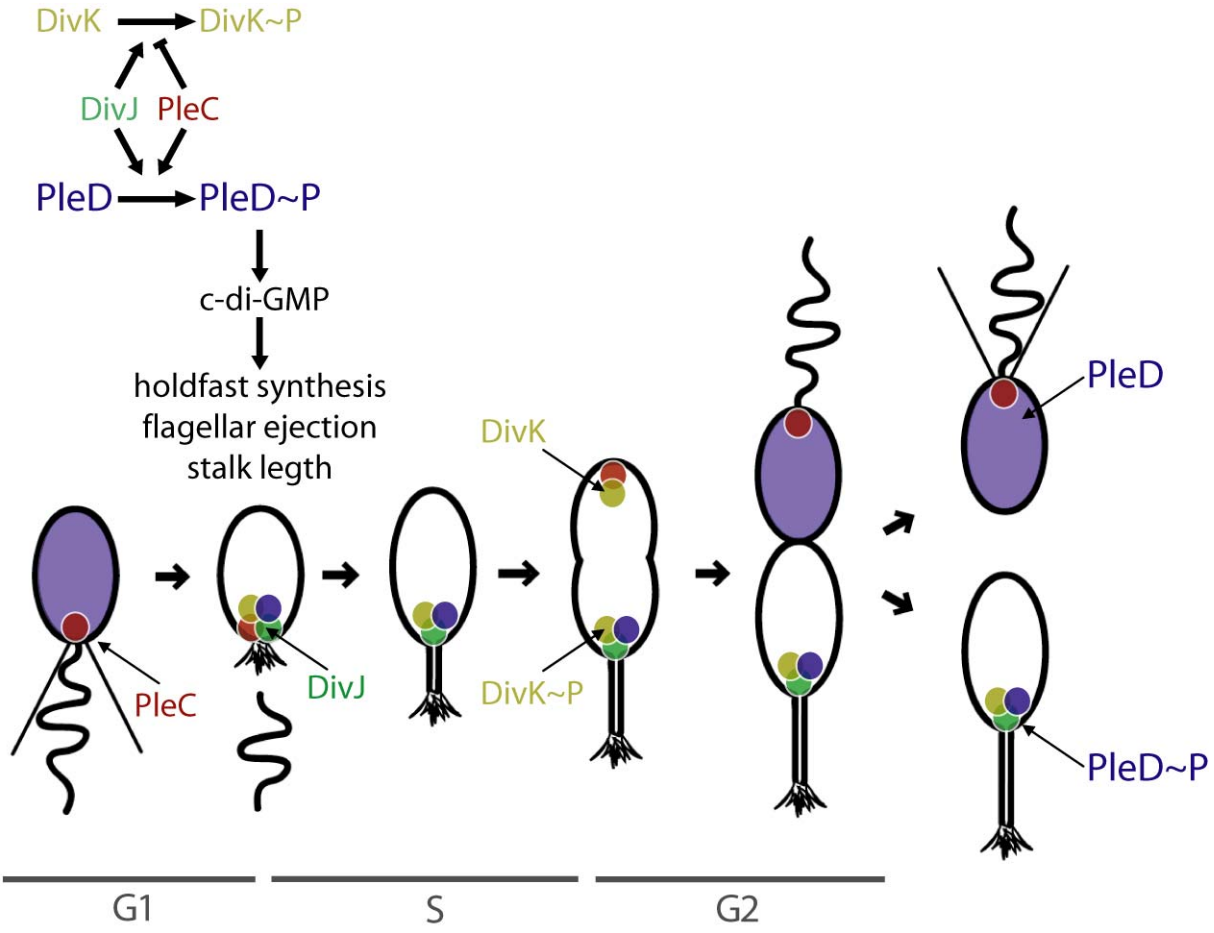

Figure 11: Schematic drawing of the subcellular localisation of PleD and its upstream components during the *Caulobacter crescentus* cell cycle.

PleC is depicted in red, DivJ in green, DivK in yellow, and PleD in blue. Delocalised (and unphosphorylated) PleD is shown in light blue. The enzymatic activities of DivJ and PleC towards DivK and PleD, the cell cycle and key developmental events are schematically represented. While PleD is not phosphorylated and therefore not localised in the swarmer cell, it is activated by PleC and DivJ during the swarmer-to-stalked cell transition. Upon activation PleD is sequestered to the incipient stalked pole of the cell, where it stays for the rest of the cell cycle. Delocalised PleC, DivJ and DivK are not shown for clarity.

Structural insights in the function of PleD

The crystal structures of unphosphorylated as well as activated PleD have been solved and give important insights into a possible activation mechanism (Fig. 11) [16, 17]. Only the first of the two receiver domains resembles the consensus sequence of response regulator input domains. The second receiver domain lacks the aspartate phosphorylation site and a functionally important lysine residue [174]. Upon phosphorylation of Asp53 in the first receiver domain, it is believed that the two receiver domains of PleD change their domain arrangement and allow dimerisation of two PleD molecules with isologous interchain contacts between D1 and D2. In particular, Tyr26 and its surrounding are suggested to play an important role in the potential dimerisation process, as this residue sticks out of the D1 domain and connects it with the D2 domain of the second PleD molecule in both crystal structures. Being in close contact, the GGDEF domains of PleD, both having bound the substrate GTP, are believed to be able to line up in an antiparallel orientation. In this way, the 3`-hydroxyl groups of the bound substrates are brought in close proximity to the α-phosphate of the other GTP molecule and can simultaneously perform a nucleophilic attack onto Pα from the side opposing the susceptible Pα-Pβ diester bond and thereby from the product c-di-GMP [17].

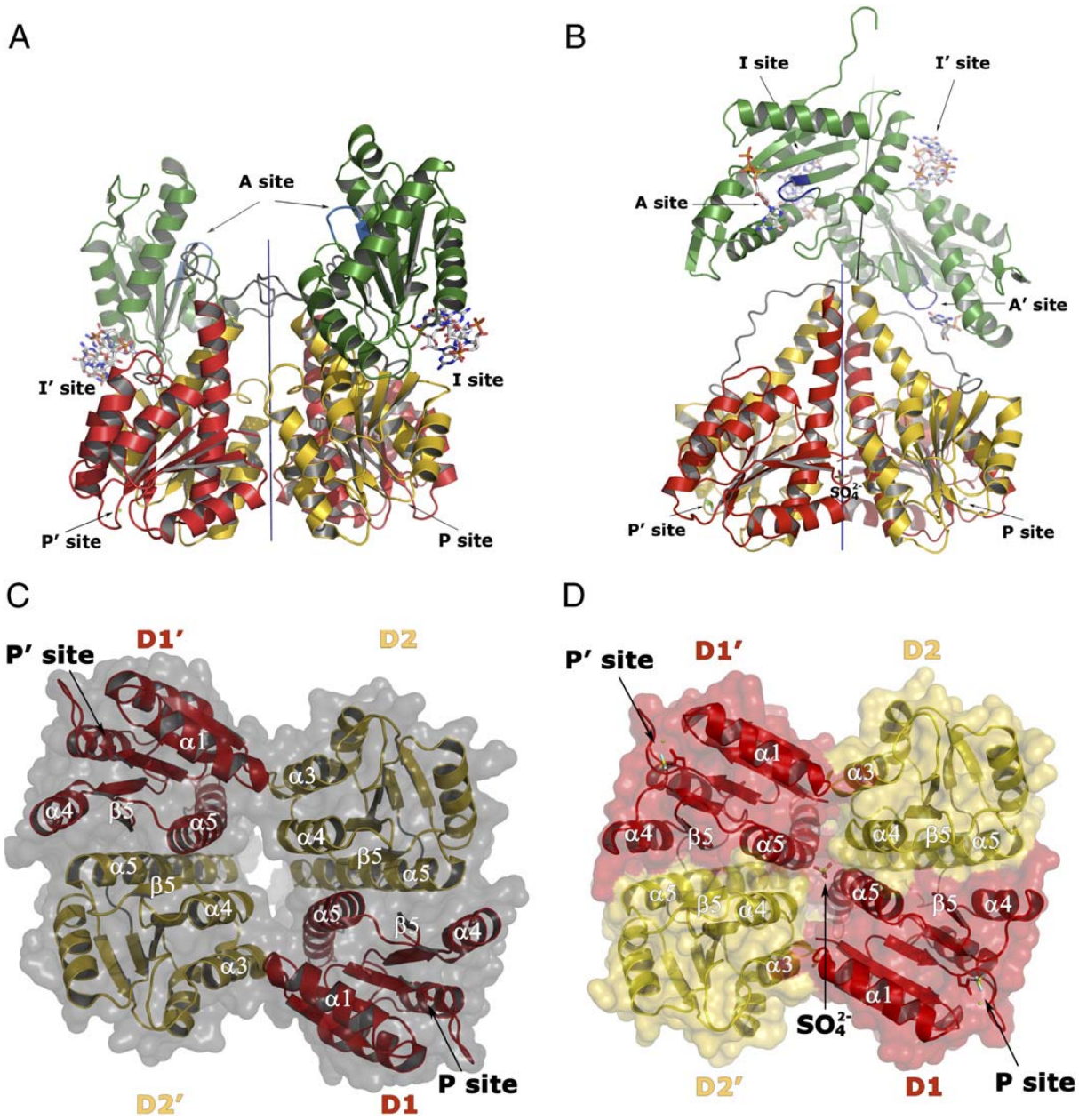

Figure 12: Ribbon diagrams of the crystal structures of non-activated PleD and activated PleD.

The first receiver domain (D1) is coloured in red, the second receiver domain (D2) in yellow and the GGDEF domain in green. The GG(D/E)F motif in the GGDEF domain is highlighted in blue. Disordered parts are depicted in grey, two-fold symmetry axes are indicated by a grey line. The active site (A-site), allosteric inhibition site (I-site) and phosphorylation site (P-site) are indicated; symmetry-related elements are specified by a prime. (A) and (B) present perpendicular views to the two-fold axis of the stem, whereas in (C) and (D) the view is rotated by 90° around a horizontal axis with respect to the top panels, showing the bottom view of the $(D1/D2)_2$ stem with the DGC domains in the rear clipped off for clarity. (A and C) Non-activated PleD [16]. Intercalated $(c\text{-}di\text{-}GMP)_2$ dimers are bound to allosteric inhibition sites I and I`, which are formed by the primary inhibition site in the GGDEF domain (I_p: Arg359, Asp362, Arg390) and a secondary site on the adaptor domain ($I_{S,D2}$: R148, R178). (B and D) In the activated structure [17], the phosphorylation site (P site) is modified by BeF_3^- and Mg_2^+. The active site (A site) harbours GTPαS/Mg_2^+. Intercalated $(c\text{-}di\text{-}GMP)_2$ dimers are bound to the I and I` sites. In this structure, the site are comprised of the primary I_P site, as in the non-activated structure, and a secondary I site of the symmetry-related DGC ($I_{S,DGC}$: R313). In both structures, the crosslinking of two half I-sites by c-di-GMP results in the immobilisation of the GGDEF domains in a way that the A-sites are not productively arranged, rendering the enzyme catalytically incompetent. This figure was adopted from [17].

PleD not only possesses an enzymatic active site (A-site), which binds GTP and catalyses its condensation to c-di-GMP, but also an inhibitory site (I-site) that mediates feedback inhibition upon binding to c-di-GMP [16, 17, 19]. In PleD the I-site is split into three different motifs. Firstly, c-di-GMP is bound by the residues Arg359 and Asp362 of the RXXD motif together with Arg392, all located in the GGDEF domain. These form the so called primary I-site (I_P) [16, 17] Secondly, two alternative secondary binding sites, one formed by residues Arg148 and Arg178 of the D2 domain ($I_{S, D2}$) [16] and one formed by Arg313 of the adjacent GGDEF domain ($I_{S, DGC}$) [17], can bind to c-di-GMP. This binding of c-di-GMP between two sites crosslinks two domains, either the GGDEF with the D2 or alternatively the two GGDEFs of a presumed PleD dimer. This crosslinking reduces the mobility of the GGDEF domain and prevents productive arrangements of the GGDEF active sites. This mechanism was therefore called "inhibition by domain immobilisation" [16, 17]. In addition, the comparison of atomic simulations of PleD having bound c-di-GMP to the I-site with PleD having an unoccupied I-site indicated reduced flexibility of PleD domains upon c-di-GMP binding. This led to the conclusion that c-di-GMP binding to the I-site may influence the dimerisation rate of the molecule and therefore also activity [177]. The finding that mutations in the $I_{S, D2}$ site displayed a 20-fold higher DGC activity compared to wild-type PleD is consistent with that interpretation [19]. Thus, it is possible that c-di-GMP binding to the I-site affects PleD activity in several ways.

Cellular functions of PleD

PleD influences several aspects of polar development in *C. crescentus*. As described above, in the absence of PleD, the flagellum is not released during the swarmer-to-stalked cell transition. In the wild-type situation, this process coincides with degradation of FliF by the ClpAP protease, which is also inhibited in the absence of PleD [170, 178, 179]. Thus, deletion of PleD leads to ectopic flagella at the tip of the stalk during the stalked and predivisional phase of the cell cycle [61]. These flagella are functional, resulting in a "hypermotile" phenotype, characterised by swimming of all cell types in liquid culture [61, 170]. In contrast, on semi-solid agar plates Δ*pleD* cells form smaller colonies compared to the wild type, which was explained by a chemotaxis defect of the mutant strain [14, 61, 180]. When a constantly activated mutant of PleD ($PleD^*$) is expressed in *C. crescentus*, this leads to normally flagellated but non-motile cells, as the rotation of the flagellum is inhibited [61]. Whereas a Δ*pleD* mutant possesses short stalks, the $PleD^*$ expressing cells have increased stalks, indicating a function for *pleD* in stalk growth or length determination [61, 170]. It was further

shown that the production of the holdfast is not properly timed in a Δ*pleD* strain. Instead of holdfast synthesis during the swarmer-to-stalked cell transition, the onset of synthesis is delayed, which leads to suboptimal attachment to surfaces [47]. Taken together, these findings illustrate that the DGC PleD is involved in the inverse regulation of motility and surface attachment. Its activity is controlled on multiple levels to ensure correct timing at the swarmer-to-stalked cell transition. Furthermore, PleD activation is linked to a system controlling asymmetry in *C. crescentus* and itself is involved in polar development.

2. Aim of the thesis

The second messenger c-di-GMP is a key signalling molecule that has a major influence on the lifestyle of bacteria as it antagonistically regulates motility and non-motility, as well as single cell dispersal and biofilm formation. In this work, the model organism for bacterial development, *Caulobacter crescentus*, and its cell cycle embedded transition between motile swarmer cell and sessile stalked cell will be employed to gain a deeper insight into the enzymatic regulation and biological role of c-di-GMP in the control of lifestyle change. One approach used will be the systematic functional analysis of all 14 GGDEF and/or EAL domain proteins from *C. crescentus* with a focus on phenotypes relevant for the swarmer-to-stalked cell transition. The key regulators identified herein will be more closely analysed to understand their role and interconnection in this developmental process. In another approach, the di-guanylate cyclase PleD, that is already known to be involved in the regulation of the swarmer-to-stalked cell transition of *C. crescentus*, will be characterized in more detail. Here, especially the mechanisms and environmental influences underlying its activation and localisation will be investigated, to understand more details of its regulation and the function of polar localisation.

3. Results

3.1 A Phosphodiesterase and its Cognate Di-guanylate Cyclases Antagonistically Control Polar Development in *Caulobacter crescentus*

Sören Abel, Marc Folcher, Urs Jenal

Statement of my work

All plasmids and strains used in this study have been generated by me, unless otherwise stated in table S1. I also performed all motility (Fig. 1, 2A, 3A, 5), attachment (Fig. 1, 5), holdfast stain (Fig. 6A, 6B), Western blot (Fig. 2B, 7A, 7B, 7C, 9B), synchronisation (including dominant negative ClpX expression) (Fig. 6B, 7A, 7C, 8A, 8B, 9B), and light-/fluorescence microscopy (Fig. 8A, 8B, 9A) experiments of this study. Furthermore, I generated and analysed the motile suppressors of the Δ*pdeA* mutant (Fig. 3B, 3C), performed the computational analysis of EAL/GGDEF domains (Fig. S2), and determined the strain growth rates (Fig. S3) given in this manuscript. Finally, I analysed the enzymatic assays of DgcB and the electron micrographs (Fig. 2C).

Abstract

The second messenger c-di-GMP positively regulates surface attachment and negatively regulates single cell based motility. In *Caulobacter crescentus* c-di-GMP plays a key role in the developmental transition from the planktonic swarmer cell to the sessile stalked cell, which involves remodelling of the cell poles. As this irreversible process determines the fate of the bacterium, the decision when to undergo this obligate transition is of critical importance and has to be carefully regulated. To gain further insight into the regulation of pole morphogenesis in this organism, a systematic functional analysis of all GGDEF, EAL and GGDEF/EAL composite proteins from *C. crescentus* was conducted. This identified the phosphodiesterase PdeA as a novel component involved in the regulation of the motile-to-sessile transition. Mutants lacking PdeA are non-motile, fail to restrict holdfast synthesis to the stalked cell type and, as a result, show an increased propensity for surface attachment. PdeA is only present in the late predivisional and swarmer phase of the cell cycle. During transition into stalked cells, it is recruited to the incipient stalked cell pole, where it is degraded by the ATP dependent protease ClpXP. Furthermore, we identify the novel di-guanylate cyclase DgcB that acts as a specific antagonist of PdeA. Evidence is provided that this pair exerts its function in flagellar control via a pathway that does not converge with an already known pathway comprising the di-guanylate cyclase DgcA and the c-di-GMP effector proteins DgrA and DgrB. DgcB controls holdfast biogenesis and surface attachment together with the well-characterised di-guanylate cyclase PleD. Genetic data suggest that both di-guanylate cyclases feed into a c-di-GMP pool that is degraded by PdeA. Cumulatively, these findings result in a model in which PdeA acts as a gatekeeper that prevents the premature surface attachment and loss of motility of the swarmer cell by reducing the concentration of c-di-GMP produced by DgcB. The specific degradation of PdeA together with the activation of PleD trigger the developmental processes towards a non-motile, surface attached stalked cell.

Introduction

C-di-GMP is a ubiquitous second messenger in eubacteria. Several studies have proposed this molecule as key regulator controlling the switch between a planktonic, free living lifestyle and sessile community behaviour of bacterial cells. In particular, an increasing number of reports have linked high levels of c-di-GMP to sessility and biofilm production via synthesis of a number of different adhesion factors, including exopolysaccharides, pili, curli fimbriae, or surface exposed proteinaceous adhesins [23, 30, 46, 49, 72, 81, 86, 181, 182]. In contrast, low levels of c-di-GMP were shown to promote cell motility and a unicellular lifestyle (reviewed in [7-10]).

Synthesis of c-di-GMP is catalyzed by proteins containing a GGDEF domain, whereas the degradation of c-di-GMP is mediated by EAL or HD-GYP domain proteins [13, 14, 20-22, 25, 62]. These domains are highly conserved and widespread in the bacterial kingdom [12]. Most bacteria possess an intermediate number (5-20) of GGDEF or EAL domain proteins (e.g. *Caulobacter crescentus*), a few contain none (e.g. *Haemophilus influenzae*), and others contain up to 100 (e.g. *Shewanella oneidensis, Vibrio vulnificus*) of these proteins. The GGDEF, EAL and HD-GYP domains are often found fused to each other in various combinations, as well as associated in a modular fashion with a wide range of regulatory, sensory input and structural domains. It is therefore believed that the production of c-di-GMP is directly controlled by environmental or internal stimuli [7, 8, 12].

C-di-GMP controls cellular functions via an interaction with downstream receptors. Despite an allosteric c-di-GMP binding site (I-site) in the GGDEF domain itself [16, 17, 19], the PilZ domain has been shown to effect cellular functions upon c-di-GMP binding [27, 28, 33, 34, 36]. This small effector domain can be found alone or associated with regulatory proteins and enzymes and may function as switch protein or as an allosteric regulator [27]. The PilZ domain was found to be involved in regulation of exopolysaccharide (EPS) production [31, 33, 34, 36, 90] as well as flagellar rotation [33]. The latter was found to be regulated by the only *C. crescentus* PilZ domain proteins DgrA and DgrB [33].

The motile-to-sessile switch of *C. crescentus* that is integrated in its division cycle make this organism a suitable model system to investigate c-di-GMP signalling. Upon division the bacterium produces two distinct daughter cells with different morphologies and developmental programs: a sessile stalked cell and a motile swarmer cells [100]. While the newborn stalked cell immediately initiates a new round of chromosome replication and cell

division, the swarmer cell is not able to replicate its chromosome, as the origin of replication is blocked by the cell cycle regulator CtrA [102, 103, 106]. The swarmer cell is propelled by its polar flagellum, performs chemotaxis, and is piliated. Before the cell starts to initiate a new round of cell division, it undergoes a differentiation step from motile to sessile cell. During this transition pili retract, the flagellum is shed, and a stalk with an adhesive holdfast at its tip is produced [101]. The holdfast contains exopolysaccharides of unknown composition through which the cells irreversibly attach to surfaces. Surface attachment peaks during a short window of development, when the flagellum, pili, and the adhesive holdfast are all present at the same pole. It was proposed that the precise timing of assembly and loss of polar organelles is critical for optimal *C. crescentus* surface colonization [47]. At the same time CtrA is inactivated and localised to the developing stalked pole that is occupied by its cognate protease ClpXP, where it is proteolytically degraded. This deblocks the origin of replication and allows the duplication of the chromosome. As the stalked cell elongates and initiates cell division, a new flagellum is synthesised. Flagellar biogenesis in *C. crescentus* is a hierarchically ordered process, which requires the functional assembly of one regulation class, before the genes of the following class are expressed (reviewed in [118, 126, 130]). Prior to cell division, the new flagellum is completed and together with the chemotaxis apparatus and pilus secretion apparatus assembled at the pole opposite the stalk. A constriction is formed and cells divide, again resulting in a swarmer and a stalked cell.

The genome of *C. crescentus* contains 14 genes encoding GGDEF, EAL, or GGDEF/EAL composite proteins (Fig. S1). Three of these proteins and their function in the regulation of motility and attachment have already been characterised in more detail. The EAL domain protein TipF was shown to be a prerequisite of flagellar assembly and positioning and is also required for proper pili expression. Therefore, a Δ*tipF* strain is non-motile and can be assumed to have an attachment defect [183]. Although TipF was predicted to contain an EAL domain, important residues for enzymatic activity are not conserved, making it unlikely that TipF has PDE activity (Fig. S2). In agreement with that, *in vitro* studies failed to show any enzymatic activity involved in c-di-GMP metabolism (M. Folcher unpublished).

PopA is predicted to contain a GGDEF domain. However, like in TipF, widely conserved residues that have been shown to be critical for enzymatic activity are missing (Fig. S2) [14, 18, 19]. Indeed, *in vitro* experiments failed to demonstrate DGC activity [26]. In contrast, residues of the I-site implicated in allosteric binding of c-di-GMP that normally lead to feedback inhibition of the enzymatic activity, are present and still function as c-di-GMP

binding site in PopA [19, 26]. Regulated by c-di-GMP and together with the adaptor protein RcdA [26, 184], PopA was shown to recruit CtrA and perhaps other proteins during the swarmer-to-stalked cell transition and to localise them to the stalked pole, where they are degraded by the protease ClpXP [26]. Furthermore, the deletion of *popA* leads to reduced motility on semi-solid agar plates [185]. The reason for this is unclear, although the presence of a degenerate A-site makes it likely that the observed phenotype of the Δ*popA* strain is rather caused by the disrupted degradation of ClpXP substrates than by direct variations of the c-di-GMP level.

One GGDEF domain protein was recently implicated in the periodic remodelling of the cell pole. The di-guanylate cyclase PleD promotes the transition from swarmer-to-stalked cell by directing flagellar ejection as well as stalk formation and timing of holdfast biogenesis [14, 47, 61, 186]. Like many enzymes involved in c-di-GMP metabolism, PleD has a modular structure with a catalytic GGDEF domain and two regulatory N-terminal CheY-like receiver domains [16, 17]. PleD is activated during the swarmer-to-stalked cell transition through phosphorylation-mediated dimerisation by two sensor histidine kinases, DivJ and PleC [61, 171, 172, 174, 186, 187]. Dimerisation of PleD is necessary for its ability to produce c-di-GMP and leads to its localisation to the incipient stalked pole of the cell [14, 186]. Differential phosphorylation coupled to polar sequestration ensures that PleD activity is restricted to the correct time and place during the *C. crescentus* cell cycle and development. Consistent with its role in timing of holdfast biogenesis, a deletion in *pleD* reduced surface attachment to about 40 % compared to wild type. Furthermore, it leads to a significant reduction of the colony size on motility plates. This unexpected negative effect on motility was suggested to be the result of a chemotaxis defect [61, 180].

The finding that three of the 14 GGDEF/EAL domain proteins are engaged in different aspects of the motile-to-sessile transition and cell cycle control, raised the question if and how the remaining proteins of this family take part in these processes. In particular, the role of phosphodiesterases that counteract the activity of di-guanylate cyclases is still poorly defined. Here, we present a systematic functional analysis of all *C. crescentus* genes predicted to code for GGDEF/EAL domain protein with a focus on the regulation of motility and attachment. This led to the identification of a new pair of enzymes, a di-guanylate cyclase and a phosphodiesterase, which antagonistically control pole morphogenesis during the swarmer-to-stalked cell transition. First insights are gained on how the phosphodiesterase activity is limited to the motile cell cycle phases, where it acts as a gatekeeper, preventing the cells from

premature development into the sessile form. Furthermore, we present evidence for a spatial or temporal separation of enzyme activities towards c-di-GMP within the cell. Together, these findings add an additional layer of complexity to the regulation of pole morphogenesis in *C. crescentus* and the role of the second messenger c-di-GMP therein.

Results

A systematic mutational analysis of genes coding for GGDEF and/or EAL domain proteins reveals proteins that inversely regulate motility and attachment

According to the paradigm of c-di-GMP signalling, the deletion of a di-guanylate cyclase should result in decreased surface attachment and increased motility. In contrast, elevated c-di-GMP levels in the absence of a phosphodiesterase should have the opposite phenotype. To systematically investigate the role of GGDEF and EAL domain proteins in *Caulobacter crescentus*, single in frame deletions of the 14 genes predicted to code for proteins containing GGDEF and/or EAL domains were generated by allelic exchange. Systematic assays for motility and attachment phenotypes were established. To control for a possible influence on growth, which would confound the attachment and motility assays, the growth rate was determined for all mutant strains (Fig. S3). Importantly, none of the deletions affected growth.

Mutations in *tipF*, *pleD*, and *popA* had been described before and served as a controls for the experiments. For motility, all three deletion strains behaved as described in the literature. The absence of PleD reduced colony size to about 60 % of the wild type due to its chemotaxis effect and a Δ*popA* strain showed a about 50 % reduction (Fig. 1) [185]. The *tipF* deletion is non-motile as it can not assemble a flagellum and the observed colony size of about 5 % of the wild type reflects this (Fig. 1) [183]. The attachment of a Δ*pleD* strain (about 40 % of the wild type) is in good agreement with the published data (Fig. 1) [47]. Interestingly, while it was described that the Δ*popA* strain has no attachment phenotype [185], we found that this mutant showed a decrease of attached biomass to about 50 % compared to wild type (Fig. 1). Similarly, a Δ*tipF* mutant showed a severely decreased attachment to about 20 % of the wild type (Fig. 1).

The other 11 deletion strains can be grouped into three classes according to their phenotypes: a) decreased attachment and increased motility, b) increased attachment and reduced motility, and c) no obvious phenotype. The first class includes deletions in *cc0740*, *cc0857*, *dgcA*, and *dgcB*, which all reduced attachment to about 70 % and increased motility to about 150 % of the wild type (Fig. 1). The second class of mutants contains deletions in the *pdeA* and *cc0091* genes. While the Δ*pdeA* strain severely reduced motility to about 20 % of the wild type, the motility phenotype of the Δ*cc0091* mutant is very mild (about 90 % of the wild type) (Fig. 1). The other five deletion strains, Δ*cc0655*, Δ*cc0896*, Δ*cc1086*, Δ*cc3094*, and

Δ*cc3148*, showed no apparent phenotype in surface attachment or cell motility under the conditions tested. The reason why deletions of these genes did not show a phenotype remains unclear. They might not be expressed under the assay conditions, there might be redundancy so a phenotype is only detectable upon deletion of more than one gene or they simply do not influence the measured phenotypes.

Strains lacking *pdeA* show reduced motility although the flagellum is completely assembled

As the Δ*pdeA* strain showed an attachment and motility phenotype expected for a phosphodiesterase mutant it was decided to further investigate this gene. It was shown earlier that increased cellular levels of c-di-GMP result in a paralysed flagellum [33, 61]. Therefore, it was reasoned that the motility defect of the *pdeA* mutant would have a similar effect, since a reduction of the overall PDE activity is likely to increase the cellular c-di-GMP concentration. To make sure that the observed phenotype was indeed caused by a mutation in *pdeA*, a plasmid harbouring the *pdeA* gene was constructed and this construct was introduced both into wild type and into the mutant strain. In a wild type background, plasmid-driven expression of *pdeA in trans* slightly increased the swarm size on semi-solid agar plates, arguing that PdeA has indeed a direct role in motility control (Fig. 2A). In support of this, motility of the Δ*pdeA* mutant strain was completely restored to wild-type levels (Fig. 2A). Next, the abundance of several proteins involved in building the flagellum or in the regulation of motility was analysed. Because flagellar biogenesis is organized in a hierarchical manner (reviewed in [126, 130]), the levels of members of all four regulation classes of the flagellar hierarchy were compared in the wild type and the Δ*pdeA* mutant. As shown in Fig. 2B, no difference was observed for CtrA (class I), FliF, FliM, and FlbD (class II), FlgH (class III), or the flagellins (class IV). This indicates that the structural and regulatory flagellar components are normally expressed and that the first two checkpoint substructures of the flagellum are assembled properly. The level of FliL, a protein required for motor function but not assembly, whose gene is not part of the flagellar hierarchy [188] was also analysed. Like for the other flagellar proteins tested, FliL levels showed no differences in the Δ*pdeA* strain as compared to the wild type (Fig. 2B).

As the Δ*pdeA* strain has no apparent defect in expressing flagellar proteins, the motility defect of the mutant could either be caused by inhibiting flagellar function or by an impaired assembly of class IV filament proteins. To investigate the latter, electron microscopy was used to analyse flagellar filament structures of mutant and wild type. As indicated in Fig. 2C,

the *pdeA* mutant strain had visible flagella that were morphologically indistinguishable from wild type. Taken together, these experiments indicate that in the Δ*pdeA* mutant strain the flagellum is assembled properly. Thus, the motility defect of this strain is likely caused by an impaired motor function.

Mutations in *dgcB* but not in *dgrA* and *dgrB* suppress the motility defect of Δ*pdeA*

It was shown recently that ectopic expression of the di-guanylate cyclase *dgcA* leads to a non-motile phenotype and a paralysed flagellum [33]. The motility block in this strain was partially suppressed when either *dgrA* or *dgrB*, both coding for small c-di-GMP effector proteins, were deleted [33]. To be able to test whether these small effector proteins are also involved in motility control in the Δ*pdeA* mutant, strains were constructed that in addition to the absence of PdeA contained deletions in *dgrA* and/or *dgrB*. The deletion of *dgrA*, *dgrB*, or both failed to restore motility in the Δ*pdeA* mutant, arguing that the inhibition of flagellar rotation in the absence of PdeA is not mediated via the DgrA or DgrB effector proteins (Fig. 3A). Consistent with this, a point mutation in *rpsA*, coding for the ribosomal protein S1, was able to restore motility in cell overexpressing *dgrA* [33], but failed to restore motility in the Δ*pdeA* mutant (data not shown). These results imply that an increased cellular concentration of c-di-GMP can inhibit motility via different non-converging pathways and, more specifically, argue that the di-guanylate cyclase DgcA and the phosphodiesterase PdeA do not interfere with the same pool of c-di-GMP to control motility.

To unravel components of the signal transduction pathway that together with PdeA control *C. crescentus* cell motility, we used the paralyzed Δ*pdeA* strain to screen for motile suppressors. In a first approach, a transposon mutagenesis was conducted by randomly integrating *tn*Mariner into the genome of the Δ*pdeA* strain and isolating mutants that regained motility. In a second approach, spontaneous suppressors were generated by selecting for motile colonies on semi-solid agar plates. The following classes of suppressors were expected: a) upregulation of phosphodiesterases that decrease the cellular c-di-GMP concentration; b) downregulation or elimination of di-guanylate cyclases that contribute to the c-di-GMP pool normally degraded by PdeA; and c) mutation of effector proteins that transduce the c-di-GMP signal to the flagellum. While the transposon mutagenesis most likely only generates loss-of-function mutations, the spontaneous mutations allow also the identification of gain-of-function mutations. In the transposon screen about 50,000 mutants were tested, resulting in 286 motile suppressor strains. Due to an intermediate selection

procedure (see materials and methods) it is not clear if these are independent events. So far, only two targets could be identified (Fig. 3B). One transposon insertion was mapped to the intergenic region between open reading frame *cc2147* (annotated as a D-isomer specific 2-hydroxyacid dehydrogenase family protein) and *cc2148* (predicted to code for the ATP-binding protein of an ABC transporter) (Fig. 3B). The insertion led to wild-type-like colonies on motility agar plates (data not shown). Marker linkage experiments by transduction confirmed that suppression was due to this transposon insertion. The second target isolated in the screen was *dgcB*. Four independent transposon insertions were mapped in the open reading frame coding for this presumable di-guanylate cyclase (Fig. 3B). Two of them mapped to the 3` end of the gene, which codes for the GGDEF domain, implying that disruption of DgcB mediated c-di-GMP synthesis is the cause for the suppression of the paralyzed flagellum. All four insertions increased motility to about 80 % of the wild-type strain (data not shown).

In addition to the transposon-derived suppressors, eight spontaneous motile suppressor mutants of the Δ*pdeA* strain were isolated. Interestingly, individual mutants showed different levels of suppression and were grouped into three classes according to their performance on motility agar plates. Whereas two of the strains formed colonies on semi-solid agar plates of similar size to wild type, three exhibited intermediate motility of about 80 %, while three others showed increased motility of up to about 150 % of the wild type level (Fig. 3C). Based on the results of the transposon screen, it was first tested if any of the spontaneous suppressor mutations mapped to *dgcB*. A resistance marker in a neutral locus next to *dgcB* (~100 % linkage) was transferred to the suppressor by means of general transduction, replacing the *dgcB* region of the suppressor strain with wild-type *dgcB*. Two of the three suppressors with an intermediate motility could be reverted to the reduced motility phenotype of Δ*pdeA* (Fig. 3C), arguing that the original suppressor mutations mapped to the *dgcB* gene. Western blot analysis failed to show a crossreacting band for DgcB in these two mutants, whereas the protein was detectable in the other six isolated strains (data not shown). This result was further confirmed by sequence analysis, demonstrating that one strain contained a nonsense mutation in *dgcB* and the other contained a deletion of the *dgcB* region (Fig. 3B). The same test was performed with a marker ~100 % linked to *cc2147*, but none of the eight suppressor strains could be reverted to the original paralyzed phenotype of the Δ*pdeA* mutant (data not shown). The heterogeneity of the suppressor phenotypes together with the transduction data indicated that different (possibly downstream) targets are involved. Future work will have to concentrate on mapping the chromosomal loci altered in these additional suppressors.

Because both suppressor screens identified DgcB as a candidate di-guanylate cyclase interacting with PdeA, our studies concentrated on the role of these two proteins in pole morphogenesis.

DgcB is a di-guanylate cyclase

Based on the motility and surface attachment phenotype of a *dgcB* mutant and based on its domain organisation, the DgcB protein was postulated to be a di-guanylate cyclase. To test this, a hexa-histidine-tagged version of DgcB was expressed in *Escherichia coli* and purified to homogeneity on a nickel affinity column. The protein was then used in a standard DGC assay [14, 19]. In the presence of purified DgcB protein, GTP was converted to c-di-GMP (Fig. 4). As control reactions the already characterized DGCs PleD* and DgcA from *C. crescentus* were tested (Fig. 4). Under the assay conditions (~5 μM GTP) both showed a higher specific activity as DgcB. The K_M for GTP conversion was determined to be in the range of about 35 μM. While the active site (GGEEF) is conserved, the RXXD motif of the I-site is not conserved in DgcB (Fig. S2). In agreement with this, DgcB was not subject to non-competitive feedback inhibition by c-di-GMP (data not shown). These results together with the genetic data presented above indicate that DgcB is a di-guanylate cyclase that specifically controls pole morphogenesis in *C. crescentus*.

PdeA and DgcB antagonistically control *Caulobacter crescentus* surface attachment and motility

Because mutations in the di-guanylate cyclase *dgcB* can suppress the phenotype of a mutant strain lacking the phosphodiesterase PdeA, we reasoned that these two opposing enzymes act in the same regulatory pathway by controlling the cellular levels of c-di-GMP. To confirm the suppression data and to rule out polar effects of the transposon insertions, attachment and motility were scored in double mutants with markerless, in frame deletions of both *pdeA* and *dgcB*. As shown in Fig. 5, the Δ*pdeA* mutant showed an increased relative attachment and decreased motility, whereas the opposite phenotype was observed for the Δ*dgcB* mutant. The double deletion strain showed an intermediate phenotype for both readouts and was similar to wild type. This indicated that the two opposing enzyme activities antagonistically control motility and surface attachment. This finding also suggests that DgcB and PdeA activities are not required for motility and surface attachment per se, but rather to regulate these cellular functions during the *C. crescentus* life cycle.

To test if PdeA exclusively interacts with DgcB or if other DGCs also contribute to this pathway, additional mutations were analysed in the Δ*pdeA* mutant background. DgcA is also known to be a DGC *in vitro* [19] and a strain with a single deletion in *dgcA* behaves like a Δ*dgcB* mutant in terms of attachment and motility (Fig. 1, 5). Therefore, a double deletion of *pdeA* and *dgcA* was created and tested. However, as shown in Fig. 5, a deletion in *dgcA* had no effect on attachment or on motility in the Δ*pdeA* mutant background. This result indicates that DgcB and PdeA form a specific pair of antagonists that control motility and attachment through the same molecular pathway. Apparently, DgcA, although influencing motility and attachment, does not interfere with the PdeA pathway. In contrast, a mutation in the DGC *pleD* decreased attachment in the Δ*pdeA* background almost to levels of the Δ*pleD* strain and a *dgcB pleD* double mutant showed only background levels of attachment independent of the presence or absence of PdeA (Fig.5). This suggests that that the di-guanylate cyclases DgcB and PleD collectively induce attachment in *C. crescentus* and that the phosphodiesterase PdeA counteracts the action of these two enzymes. In contrast, the motility on semi-solid agar plates of the Δ*pleD* Δ*pdeA* strain was on the level of a Δ*pdeA* mutant. This phenotype is comparable to the Δ*dgcA* Δ*pdeA* strain, indicating that PleD and PdeA influence motility on two non-converging pathways. The colony size formed by the *dgcB pleD* deletion strains shows intermediate motility behaviour between Δ*dgcB* and Δ*pleD*. This is likely because a *pleD* mutant, although being hypermotile in liquid culture, does not perform accordingly on semisolid agar plates [180]. Therefore the deletion of *pleD* reduces the increased motility of the Δ*dgcB* strain. According to the motility behaviour of the Δ*pleD* Δ*pdeA* strain, the additional deletion of *pdeA* should have no influence on motility in the *dgcB pleD* mutant. Indeed, the colony size on semi-solid agar plates of the Δ*dgcB* Δ*pleD* Δ*pdeA* mutant did not differ from the Δ*dgcB* Δ*pleD* strain.

PdeA, DgcB, and PleD control the timing of holdfast biosynthesis during the *Caulobacter crescentus* cell cycle

As the holdfast is the primary adhesin of *C. crescentus* we wondered if PdeA, DgcB and PleD might influence surface attachment via controlling its synthesis. For this, all possible single, double, and triple mutant strains were analysed by staining with a fluorophore coupled to the lectin wheat germ agglutinin, which specifically binds holdfast polysaccharides [47]. The fraction of cells with a strong fluorescence signal was compared in all strains and related to their attachment behaviour. In all cases, attachment directly correlated with the fraction of

cells displaying a stainable holdfast structure (Fig. 6A). Whereas the *pleD* and *dgcB* single mutants both showed reduced holdfast formation, the *dgcB pleD* double mutant showed an almost complete loss of holdfast synthesis (Fig. 6A). Like the attachment defect of the *dgcB pleD* double mutant holdfast formation could not be rescued by an additional deletion of *pdeA* (Fig. 6A). Interestingly, the *dgcB pleD* double and *dgcB pleD pdeA* triple mutant also showed a significant proportion of the cells with filamentous morphology and alterations in the position and number of cell division constriction sites, suggesting a defect in the coordination of cell division events (Fig. 6A).

It has been shown recently that the onset of holdfast production during the swarmer-to-stalked cell transition is delayed in mutants lacking PleD [47], which in turn leads to a reduced number of cells with detectable holdfast in a growing culture. To investigate if DgcB and PdeA are also involved in the timing of holdfast production, the respective mutant strains were analysed. Swarmer cells from wild type, Δ*dgcB*, Δ*pleD* and Δ*pdeA* mutant strains were isolated and the appearance of holdfast was analysed in synchronised populations through one cell cycle. As reported before [47] wild-type swarmer cells have no detectable holdfast adhesin. However, after 20 minutes a large proportion of differentiating cells already had produced a holdfast and after 40 minutes, when no motile cells could be detected anymore, the majority of cells showed strong staining at the cell pole. This behaviour corresponds well with the observed peak of attachment during the swarmer-to-stalked cell transition [47]. A deletion of *pleD* was shown to result in a delay in holdfast synthesis [47]. Consistent with this, the first holdfasts of a Δ*pleD* mutant in this analysis were detectable only after one third of the cell cycle (Fig. 6B). Similarly, a *dgcB* mutant also caused a delayed holdfast synthesis with holdfasts being detectable at the same time when it appeared in a Δ*pleD* strain, although the staining is weak and only very few cells with a holdfast could be detected (Fig.6B). A strong holdfast signal, which is comparable to the wild type, can only be found in early predivisional cells after almost two thirds of the cell cycle. While *dgcB pleD* double mutants failed to develop a holdfast during the cell cycle, holdfast structures appeared prematurely in the Δ*pdeA* mutant strain, with the majority of freshly isolated swarmer cells showing a fluorescence signal (Fig.6B). Together, these experiments indicate that all three enzymes influence the same cellular pathway that triggers holdfast formation and irreversible attachment to surfaces. The di-guanylate cyclases DgcB and PleD positively regulate holdfast synthesis, whereas the phosphodiesterase PdeA negatively regulates the holdfast production. Together, these enzymes are important for the correct timing of holdfast production during the *C. crescentus* cell cycle.

PdeA is subjected to cell cycle dependent proteolysis

To mediate the timing of pole morphogenesis, the activity of regulators involved in this process requires proper temporal control. It has recently been shown that PleD plays an important role in polar morphogenesis and underlies a complex regulatory mechanism that restricts the DGC activity of PleD to the stalked and predivisional cells [14, 186, 187]. However, PleD activity alone is apparently not sufficient to explain the timing of the holdfast production. This raised questions about DgcB and PdeA regulation and their coordination with PleD. Interestingly, transcription of *dgcB* appears to be controlled by the master cell cycle regulator CtrA leading to a sharp burst of *dgcB* transcription in the swarmer cell [141]. To substantiate this apparent temporal control of *dgcB* expression, polyclonal antibodies were raised against the DgcB protein and the distribution of the protein was determined during the cell cycle (Fig. 7A). Despite the transcriptional regulation of *dgcB*, the DgcB protein levels remained constant over the cell cycle. In contrast, PdeA levels fluctuated during the cell cycle. PdeA was present in swarmer cells but then rapidly disappeared until it reappeared in late predivisional cells (Fig. 7A). The cell cycle pattern of the protein level was similar to CtrA and FilF. Like for CtrA and FliF [108, 178], the sharp drop of PdeA levels during the swarmer-to-stalked cell transition suggests that this protein is subject to cell cycle specific proteolytic degradation. Interestingly, a PdeA-YFP fusion did not to fluctuate during the cell cycle (Fig. 7A), arguing that the C-terminal YFP stabilizes the protein. It is well known that certain ATP dependant proteases recognize their substrates via “floppy tails” at either N- or C-termini [109]. The bulky C-terminal YFP could thus inhibit the recognition of PdeA by its protease by masking a C-terminal signal sequence. Such an effect was already described for the ClpXP substrate CtrA [109] and for the ClpAP substrate FliF [178]. To test which of the known ATP-dependent proteases from *C. crescentus* is responsible for PdeA turnover, several mutant strains were analysed, including *ftsH*, *lon*, *hslU*, *clpA,* and *clpX*. PdeA levels were determined by immunoblot in strains with a disruption in one of the genes coding for a protease or chaperone. As a control for stabilized PdeA, the chromosomal copy of *pdeA* was replaced with a *pdeA-gfp* fusion. As shown in Fig. 7B, stabilization of PdeA by GFP tagging led to increased protein levels in a mixed population of cells. In contrast, the PdeA levels were unaltered in *ftsH*, *lon*, *hslU*, and *clpA* mutants (Fig. 7B).

The chaperon ClpX, like its cognate protease ClpP [189], is essential for *C. crescentus* growth and survival [108]. Therefore, its potential involvement in PdeA degradation was investigated using an inducible mutant allele coding for a dominant negative ClpX variant [190]. Upon induction, this ClpX mutant forms non-functional hetero-oligomers with wild-

type ClpX [190, 191]. As shown in Fig. 7C, this lead to a rapid reduction of PdeA degradation. Swarmer cells that expressed the toxic *clpX* mutant allele were not able to efficiently degrade PdeA as they developed into stalked cells. In contrast, FliF, which is degraded by ClpAP showed a normal turnover, indicating that the block in PdeA degradation did not stem from an unspecific cell cycle block, but rather was the direct result of depletion of ClpX activity. In contrast, swarmer cells that did not express the mutant allele of *clpX* showed normal degradation of PdeA during the transition (Fig. 7C). Similar to PdeA, degradation of CtrA, a known ClpXP substrate [108], was severely hampered when ClpX activity is reduced and both substrate proteins follow the same degradation kinetics (Fig. 7C). Taken together, these experiments indicate that PdeA is specifically degraded by the ClpXP protease during swarmer-to-stalked cell transition.

Dynamic localization of PdeA and DgcB during the cell cycle

It has been reported recently that ClpXP and one of its substrates, CtrA, transiently sequester to the stalked pole as *C. crescentus* cells enter S-phase [111, 184]. Because PdeA appears to be a ClpXP substrate we thought to analyse its distribution throughout the cell cycle. A low copy number plasmid harbouring *pdeA-yfp* was introduced in the Δ*pdeA* strain. The resulting cells were synchronised and the distribution of the PdeA-YFP fusion was determined by fluorescence microscopy throughout the cell cycle (Fig. 8A). Whereas swarmer cells showed a delocalised signal, PdeA was localised to the ClpXP occupied incipient stalked pole during cell differentiation. Interestingly, PdeA-YFP remained at this subcellular site for the rest of the cell cycle, likely because this fusion protein cannot be removed by the ClpXP protease (Fig. 8A). It will be interesting to analyse the degradation and subcellular distribution of an YFP-PdeA fusion that has an accessible C-terminus.

To examine the subcellular localisation of DgcB, a strain was constructed in which the chromosomal copy of *dgcB* was replaced by a *dgcB-cfp* fusion. DgcB-CFP was delocalised in swarmer and stalked cells, but sequestered to the stalked pole in late stalked cells. As cells elongate and divide, a second focus of DgcB-CFP appeared at the opposite pole of the cell (Fig. 8B). In newly divided cells, DgcB apparently remained at the old poles for a very short period of time, before being delocalised again. Although it is unclear at this point if the distribution of the DgcB-CFP resembles the pattern of DgcB wild type and what the molecular basis and significance of DgcB localization is, the observed localization might reflect different activity states of the protein as was shown for PleD [186].

CtrA localisation factors are not required for the polar sequestration of PdeA

CtrA, the master regulator of the *C. crescentus* cell cycle, requires the two recruitment factors RcdA and PopA to be delivered to the ClpXP occupied stalked pole during swarmer-to-stalked cell transition [26, 184]. Because of the similar localisation pattern of CtrA and PdeA and because both proteins are degraded by ClpXP, it was tested if PdeA localisation and degradation is also dependent on any of these recruitment factors. As indicated in Fig. 9A localisation of the PdeA-YFP fusion was independent of RcdA and PopA. Furthermore, degradation of PdeA during the cell cycle did not require PopA (Fig. 9B). This suggests that degradation of PdeA, although being dependent on the ClpXP protease, is mediated by a different mechanism than CtrA.

Discussion

Surface attachment peaks during cell differentiation when flagella, adhesive pili, and holdfast are concomitantly present at one cell pole [47]. The correct timing of exposure and removal of polar organelles is thus of critical importance for the motile-sessile transition and subject to careful control in response to internal and external cues. It becomes increasingly clear that c-di-GMP is an important component of the regulatory mechanism controlling pole morphogenesis in *Caulobacter crescentus* (reviewed in [7, 8, 94]). One member of the c-di-GMP signalling pathway is the di-guanylate cycle PleD, which is subject to complex regulation restricting its activity to the differentiating cell pole [14, 186, 187]. Here, we examined the role of two additional c-di-GMP signalling proteins, DgcB and PdeA, in pole morphogenesis. We present evidence that the phosphodiesterase PdeA acts as gatekeeper in the swarmer cell to prevent premature loss of motility and holdfast formation. PdeA activity is restricted to the motile cell type through specific proteolysis by the protease ClpXP. The di-guanylate cyclase DgcB, together with PleD, acts as an antagonist of PdeA, initiating pole morphogenesis during the swarmer-to-stalked cell transition upon removal of PdeA.

A systematic functional screen revealed potential di-guanylate cyclases and phosphodiesterases that contribute to cell differentiation

A systematic functional analysis of mutations in genes encoding GGDEF, EAL, or GGDEF/EAL composite proteins revealed several candidates involved in motility and attachment control (Fig. 1). The motility phenotypes of Δ*tipF*, Δ*pleD*, and Δ*popA* mutants have been described before [61, 183, 185] and showed the expected behaviour in this analysis. Similarly, the attachment phenotype of the Δ*pleD* mutant was also as described earlier [47]. In contrast to previous reports [185], surface attachment of the Δ*popA* mutant was reduced to about 50 % compared to wild-type cells (Fig. 1). This discrepancy might be explained by different wild type strain background used in the two studies. While in the former study the CB15 wild type strain LS1250 was used, a strain that might have experienced some laboratory adaptations, this study used a CB15 strain directly derived from the American type tissue collection (ATTC19089). Interestingly, although the *popA* gene is present and unaltered in the genome of strain LS1250 the PopA protein was not detectable by Western blot analysis (A. Dürig unpublished). It is possible that *popA* expression was lost by repeated culturing in the lab and it is therefore not surprising that a *popA* deletion has no phenotype in this strain background. The role of PopA in motility control and surface

attachment is unclear. Since PopA does not appear to be an active di-guanylate cyclase [26], these effects are unlikely to be the result of a direct variation of c-di-GMP levels. The finding that PopA regulates protein degradation upon binding to c-di-GMP [26] suggests that the observed effect may be a cause of disrupted protein hydrolysis of yet uncharacterised proteins by the protease ClpXP. Beside its described loss of motility [183], a deletion in *tipF* also showed a severe reduction of surface attachment (Fig. 1), although the holdfast biosynthesis appeared normal (data not shown). An active flagellum as well as the presence of adhesive pili is required for optimal surface adhesion [47, 192]. Because both flagellar assembly and pili biogenesis are disturbed in a Δ*tipF* mutant [183], this could explain the observed reduction in attachment.

Several mutants including Δ*dgcA*, Δ*dgcB*, Δ*cc0740*, and Δ*cc0857* showed an increase in motility and a reduced surface attachment propensity (Fig. 1). According to the c-di-GMP signalling paradigm, these genes were anticipated to encode for di-guanylate cyclases. Consistent with this, all four genes code for proteins containing a GGDEF domain (Fig. S1). Furthermore, DgcA has recently been shown to possess DGC activity *in vitro* [19]. These findings were complemented in this study by demonstrating that also DgcB is a DGC *in vitro*. The remaining two members of this group, CC0740 and CC0857, show conservation of the residues in their GGDEF domains known to be involved in catalysis (Fig. S2). It is thus anticipated that the two proteins are also active DGCs that contribute the *C. crescentus* cell differentiation.

Two mutants that harbour deletions in *pdeA* and *cc0091*, respectively, showed reduced motility and increased attachment and therefore were predicted to contain a defective PDE (Fig. 1). Both open reading frames code for GGDEF/EAL composite proteins (Fig. S1). Despite the presence of both domains, PdeA is a phosphodiesterase and lacks DGC activity *in vitro* [20]. Similarly, CC0091 has PDE but no DGC activity (A. Levi unpublished). Thus, there is indeed a correlation of the motility/attachment mutant phenotype and the enzymatic activities of the respective gene products. Importantly, because of its pronounced mutant phenotype, the PdeA phosphodiesterase appears to have a key role in controlling attachment and motility.

The loss of PdeA paralyses the flagellum via increased c-di-GMP levels in a distinct pool

As described above, a deletion in PdeA resulted in a severe reduction of motility on semi-solid agar plates (Fig. 1), yet selected flagellar proteins of different classes of the flagellar

regulation hierarchy showed wild-type levels (Fig. 2B) and transmission electron microscopy revealed a morphologically normal flagellum (Fig. 2C). These findings argue that the assembly of the flagellar rotor is not altered in the Δ*pdeA* strain, but rather the rotation of the flagellum is inhibited. The expression of a constitutively active PleD mutant or the overexpression of the di-guanylate cyclase DgcA were shown to paralyse the flagellum via increased c-di-GMP levels [19, 61]. In analogy, the observed reduction in motility of a Δ*pdeA* strain is maybe due to an increased cellular c-di-GMP concentration as it would be expected for the deletion of a PDE. This interpretation is further strengthened by the finding, that the motility defect of the Δ*pdeA* mutant can be partially overcome by the deletion of a DGC (Fig. 5).

For the overexpression of DgcA, it was shown that the paralysis of the flagellum is mediated by the small c-di-GMP effector proteins DgrA and DgrB, probably via the regulation of FliL levels [33]. The deletion of DgrA and/or DgrB did not suppress the motility phenotype of a Δ*pdeA* strain (Fig. 3A). Neither was the FliL level altered (Fig. 2B), nor had a motile suppressor mutant in *rpsA*, which was isolated by Christen et al., any influence on motility in a Δ*pdeA* strain (data not shown). These results match the finding that, in contrast to the solitary deletion of DgcA, its deletion in the Δ*pdeA* background had no effect (Fig. 5). These results indicate that the DgcA-DgrA/B pathway and the PdeA pathway are separated. To be able to act on different non-converging pathways the c-di-GMP pools affected by DgcA and PdeA, respectively, have to be separated. Therefore, these findings present initial evidence on a spatial or temporal segregation of c-di-GMP mediated signalling pathways in the same cell.

Which receptor then transmits the elevated c-di-GMP levels in the Δ*pdeA* strain? So far, two types of c-di-GMP sensors are known (reviewed in [8]), PilZ domain proteins [19, 27, 28, 33, 34] and GGDEF domain proteins with an I-site [19, 26]. Despite DgrA and DgrB, current *in silico* analysis does not predict any more PilZ domain proteins in *C. crescentus*. Candidate receptor proteins possessing an I-site would be PopA, PleD, DgcA, CC0655, and CC3094 (Fig. S2), though DgcA and PleD can be excluded as a double deletion of PdeA and either of these DGCs did not re-establish motility (Fig. 5).

PdeA prevents premature holdfast synthesis in the swarmer cell

The surface attachment of a Δ*pdeA* strain was increased compared to the wild type (Fig. 1), which would be consistent with a high cellular c-di-GMP level. Since the holdfast is a critical component for surface attachment and c-di-GMP is a known allosteric activator of several

EPS producing enzymes [31, 33, 34, 36, 47, 90], the analysis of the holdfast structure was apparent. Indeed, the amount of cells with a stainable holdfast in a mixed population was increased and could be correlated to the attachment level of a Δ*pdeA* strain (Fig. 6A). It was also observed that the holdfast structure appeared earlier in the cell cycle in the absence of PdeA (Fig. 6B). This explains the increased amount of cells with detectable strong holdfast in a mixed population. Together with the premature holdfast synthesis, the fact that in the wild-type situation the drop of PdeA levels (Fig. 7A) and the synthesis of the holdfast (Fig. 6B) concurred, suggests that PdeA activity prevents holdfast synthesis. A candidate protein that regulates holdfast production in response to c-di-GMP is CC0095. This protein was shown to bind to c-di-GMP, is predicted to be a glycosyl transferase and is essential for attachment and holdfast synthesis (A. Levi unpublished). Furthermore, the artificial increase of c-di-GMP results in increased holdfast production in dependence on CC0095 (A. Levi unpublished). It remains to be elucidated whether this protein is also involved in holdfast production in response to a *pdeA* deletion.

The localisation of PdeA to the ClpXP occupied stalked pole concurs with its degradation

Western blot analysis showed that PdeA is only present during the late predivisional and swarmer phase of the cell cycle (Fig. 7A). Furthermore, the expression of a dominant negative ClpX mutant lead to a stabilisation of PdeA (Fig. C), suggesting that its rapid decrease during the swarmer-to-stalked cell transition is mediated by the protease ClpXP. A well characterised example for the cell cycle dependent degradation by ClpXP is the response regulator CtrA [108]. The localisation pattern of the stabilized PdeA-YFP investigated here resembled the localisation pattern of a non-degradable CtrA-YFP fusion [111]. Like CtrA [110, 111, 184], PdeA localisation to the ClpXP occupied stalked pole at the swarmer-to-stalked cell transition concurred with its degradation (Fig. 8A). Due to the stabilization of the PdeA-YFP fusion (Fig. 7A), the YFP focus stayed at the stalked pole (Fig. 8A). Nevertheless, due to the finding that an YFP fusion to PdeA was able to partially complement the Δ*pdeA* phenotype for attachment and motility (data not shown), the localisation pattern during swarmer and late predivisional phase may reflect the wild type situation.

Deletions in the CtrA recruiting factors RcdA and PopA [26, 184] did not abolish localisation of PdeA (Fig. 9A). Furthermore unlike CtrA [26], PdeA was normally degraded in a Δ*popA* strain (Fig. 9B). These results indicate that there are different ways of targeting ClpXP substrates to the protease. One could speculate that other yet uncharacterised

recruitment factors might be existent or that the localisation of PdeA is an intrinsic feature of PdeA itself.

Disruption of DgcB can suppress the Δ*pdeA* phenotype

The so far characterised Δ*pdeA* phenotypes are likely caused by increased c-di-GMP levels during the swarmer phase of the cell cycle. By down-regulating c-di-GMP production of corresponding DGCs these phenotypes should be suppressed. In the screen for motile suppressor mutants of the Δ*pdeA* phenotype, either spontaneously arisen or generated by transposon mutagenesis, DgcB was revealed as a counterpart for PdeA. In addition to DgcB, only one more insertion locus was mapped in the transposon screen, which resides in the intergenic region between *cc2147* and *cc2148*. Although no open reading frame and no overt upstream regulatory element were directly disrupted by the transposon insertion, the possibility remains that the result of this insertion could be due to polar effects on the neighbouring genes. However, for both an effect in motility upon increased c-di-GMP concentration is not overt. Alternatively, the size of the intergenic region between the two genes (141 bp) would be sufficient to harbour a regulatory RNA. As it was suggested that c-di-GMP might bind to RNAs due to its chemical similarity [8], this option has to be further investigated. In this context, it is interesting to note that only one transposon insertion was found in the *cc2147/cc2148* region, while four independent hits were found in *dgcB*. Furthermore, none of the eight isolated spontaneous suppressors harboured a mutation linked to the *cc2147/cc2148* region, yet two strains were found to have a mutation in *dgcB*. Although the number of isolated suppressors is relatively low, one would expect that a target of similar size as *dgcB*, like it is the case for *cc2147* and cc*2148* respectively, should also appear in the screen. This can be taken as a further hint that the transposon integration in the *cc2147/cc2148* intergenic region altered a small target like e.g. a small sized regulatory RNA or caused a specific alteration rather than a disruption.

The finding that despite DgcB and the transposon insertion between *cc2147* and *cc2148* at least three more suppressors, as judged by their performance on semi-solid agar plates, could be isolated in the selection for spontaneous motile suppressors (Fig. 3C) indicates that more components are involved in motility regulation in response to c-di-GMP. As the design of the screen should allow identification of downstream targets of PdeA, the characterisation of these suppressors is of high interest. Especially the class of suppressor that elevate motility levels to 150 % could lead to the identification of such c-di-GMP effector

proteins, as the motility behaviour resembles a single DGC knock out (Fig. 1), without the additional deletion of *pdeA* and could therefore indicate a c-di-GMP "blind" phenotype.

Is DgcB a constitutive active di-guanylate cyclase or is its activity regulated?

The direct comparison of DGC activities between purified, recombinant DgcB, PleD*, and DgcA, showed a relative low specific activity for DgcB under the conditions of this *in vitro* assay (~5 μM GTP) (Fig. 4). This is likely, at least partially, due to the relatively high K_M for GTP. While the K_M for GTP is 8.3 μM in the case of PleD* [193], DgcB, with a K_M for GTP of ~35 μM, requires more than four times more GTP to be half maximal active. This could be relevant for the regulation of its activity in the cell cycle, as GTP concentration in *C. crescentus* was estimated to be in the range of 50 μM in the swarmer cells and drops to about 10 μM for the rest of the cell cycle at the swarmer-to-stalked cell transition [194].

As predicted by the absence of an intact I-site (Fig. S3), addition of c-di-GMP did not decrease enzymatic activity in a non-competitive way. Is DgcB a constantly active DGC with a low K_M for GTP and therefore low turnover, which is why no feedback inhibition is required [8], or is its DGC activity further regulated? Initial evidence indicates that the addition of c-di-GMP may induce the DGC activity, perhaps by changing the oligomerisation state of the protein (M. Folcher unpublished). A coiled-coil region, which are often involved in protein-protein interactions [195], can be found in the N-terminus of DgcB and it remains to be tested if this region plays a role in the regulation of DgcB activity. Furthermore, in the suppressor screens non-functional DgcB resulted in a partial suppression of the motility phenotype of Δ*pdeA*, resulting in 80 % motility compared to the wild type (Fig. 3C). Another group of spontaneous mutants also showed 80 % motility in the Δ*pdeA* background (Fig. 3C), although their mutations were not linked to *dgcB* (Fig. 3C) and DgcB was expressed to wild type levels (data not shown). This raises the possibility, that the mutation altered an activator or repressor of DgcB in a way that DgcB is not active anymore and therefore behaves like a functional knock out.

PdeA and DgcB form a cognate pair of antagonistic enzymes involved in c-di-GMP metabolism

The finding that the deletion of dgcB can partially suppress the Δ*pdeA* phenotype argues that these two proteins are active in the same pathway. As DgcB was shown to be a DGC and PdeA a PDE, it is likely that both enzymes influence the cell by inversely regulating the

cellular c-di-GMP concentration. This is further strengthened by the finding that two transposon insertions in the 5`-end of *dgcB* could suppress the Δ*pdeA* phenotype (Fig. 3B). These insertions are expected to alter only the GGDEF domain and leave the N-terminal part of the protein intact, which was confirmed by Western blot analysis showing a DgcB specific band at slightly lowered molecular weight indicating a truncated DgcB in these mutants (data not shown).

What do we know about the molecular targets of c-di-GMP regulated by DgcB and PdeA? In the absence of PdeA, cells showed a decreased motility due to inhibition of flagellar rotation. In contrast, the deletion of *dgcB* increased motility on semi-solid agar plates (Fig. 1). The direct measurement of swimming speed in liquid culture showed that Δ*dgcB* cells swim faster (111 ±2 % of the wild type swimming speed), which would be consistent with a flagellum that turns faster [185]. Therefore, these results argue that PdeA and DgcB inversely regulate motility by influencing the rotation speed of the flagellum.

A single deletion in *dgcB* decreased attachment and as for Δ*pdeA*, this attachment effect was correlated with the proportion of cells with a stainable holdfast (Fig. 6A). Furthermore, the combined deletion of *pdeA* and *dgcB* showed intermediate attachment levels between the single deletions, close to the wild-type attachment (Fig. 5). Again, this was reflected on the level of holdfast production (Fig. 6A). While in Δ*pdeA* cells the holdfast was already detectable in swarmer cells, the synthesis of the holdfast was delayed in Δ*dgcB* (Fig. 6B), indicating that a certain threshold concentration of c-di-GMP has to be reached to start holdfast production. In the absence of PdeA, this concentration is reached earlier in the cell cycle, whereas in the absence of DgcB this concentration is reached after a longer time. Taken together, these data support a model in which the opposing activities of DgcB and PdeA inversely influence the production and timing of the holdfast.

DgcB is not the only di-guanylate cyclase in the PdeA pathway

If DgcB was the only DGC delivering c-di-GMP to the cellular pool that is accessible to PdeA, then it would be expected that a deletion of *pdeA* has no effect in the Δ*dgcB* background. This is because in the absence of any c-di-GMP influx in the corresponding pool, it would not matter if degrading activity is present or not. The data presented here show that a *pdeA* deletion has a partial influence on motility and attachment in the absence of DgcB (Fig. 5). This finding argues that an additional c-di-GMP source feeds in the cellular pool that is accessible to PdeAs degrading activity. Furthermore, the finding that holdfast production was not completely abolished in Δ*dgcB* mutant, but only delayed also indicates that at least

one other DGC is required for holdfast synthesis (Fig. 6B). The DGC PleD was already shown to affect holdfast synthesis in a way that resembles DgcB (Fig. 6B) [47] and indeed, the double deletion of DgcB and PleD showed a nearly complete abolishment of holdfast production (Fig. 6A). This cumulative phenotype of the two DGCs indicates that they feed into the same c-di-GMP pool which affects attachment and are strictly required for this process. Furthermore, the additional elongated morphology of a *dgcB* and *pleD* double deletion strain indicates a role for c-di-GMP produced by these two enzymes in the regulation of cell division (Fig. 6A). The finding that the additional deletion of *pdeA* in a Δ*dgcB* Δ*pleD* background did not increase attachment or the number of holdfast bearing cells argues that DgcB and PleD are the major, perhaps the only DGCs feeding into the c-di-GMP pool that regulates attachment and is normally degraded by PdeA (Fig. 6A). The situation differs for the regulation of motility. Here, PleD and PdeA are not in the same pathway, as a deletion of *pleD* in the Δ*pdeA* background did not affect the Δ*pdeA* phenotype (Fig. 5). Still, Δ*dgcB* only partially suppressed the motility phenotype of Δ*pdeA* (Fig. 5), arguing hat a third, yet uncharacterised DGC must be involved in this process

What is the implication of cell cycle specific regulation of PleD, DgcB and PdeA?

PdeA could only be detected in the late predivisional and swarmer cell (Fig. 7A), whereas PleD is inactive in the swarmer cell and activated at the swarmer-to-stalked cell transition [14, 186]. Therefore activities of the PDE and DGC overlap only during a short window at the swarmer-to-stalked cell transition. While this timepoint is critical for surface attachment of the cell [47], the regulation of flagellar rotation takes place in the swarmer cell. This can explain why PdeA and PleD act in the same pathway that regulates surface attachment, but in separated pathways that regulate motility.

Can we deduce from the current data when DgcB is active? The finding that a strain with a deletion of *dgcB* produced a holdfast later in the cell cycle (Fig. 6B) together with the results that a Δ*pleD* strain also had a similar phenotype (Fig. 6B) [47] and DgcB and PleD are the major DGC required for holdfast synthesis (Fig. 5) indicates that DgcB is active during the swarmer-to-stalked cell transition and in the stalked cell. It must also be active in the predivisional cell and/or the swarmer cell, as its deletion accelerates swimming speed (Fig. 1) [185]. Furthermore, the finding that the holdfast in Δ*pdeA* cells could be prematurely detected in the swarmer cells but not at the swarmer pole of the late predivisional cell (Fig. 6B) could indicate the DGC activity that is normally counteracted by PdeA is only present in the

swarmer cell. Alternatively, the machinery for holdfast production could be dysfunctional in predivisional cells. Although the assembly of this machinery is not investigated, it has been reported that at least all proteins required for holdfast synthesis are already present in the predivisional cell [47]. The last indication that DgcB might be regulated in a cell cycle specific manner is its dynamic localisation pattern (Fig. 8B). In analogy to PleD, which is only active when localised [186], one could speculate that this localisation pattern might also reflect the activity status of DgcB, but in contrast to PleD the current data would argue that DgcB is inactive while localised to the poles in the predivisional cell.

Taken together, the data discussed so far can be integrated into the following model (Fig. 10). In the swarmer cell DgcB and (an) unknown DGC(s) are active, but they fail to increase the cellular c-di-GMP pool, because PdeA is distributed all over the cell and acts as a gatekeeper that degrades the synthesised second messenger. Therefore the flagellum rotates in the swarmer cell and no holdfast is synthesised. Upon transition of the swarmer cell into a stalked cell, PdeA localises to the ClpXP occupied, incipient stalked pole, where it is degraded. Degradation of PdeA decreases PDE activity in the cell, which allows the increase of the cellular c-di-GMP concentration. At the same time the DGC PleD is activated. Together with DgcB, these enzymes synthesise c-di-GMP, which finally results in activation of holdfast production and leads to non-motility, as the flagellum stops rotation and is shed. As soon as a constriction is formed and the cell starts to divide, DgcB is localised to both cell poles and may loose activity, while active PleD is localised to the stalked pole and therefore restricted to the stalked compartment of the predivisional cell. At the same time, PdeA protein levels increase, the flagellum is assembled and starts to rotate shortly prior to cell division.

Materials and methods

Growth conditions

E. coli strains were grown in Luria-Bertani (LB) broth at 37 °C. *Caulobacter crescentus* strains were routinely grown in peptone yeast extract (PYE) or minimal medium (M2) [196]. All media were supplemented with antibiotics for selection when required. For synchronisation experiments, newborn swarmer cells were isolated by Ludox gradient centrifugation according to Jenal et al. [179], and released into fresh minimal medium either supplemented with 0.2 % glucose (M2G) or 0.3 % D-xylose (M2X). All *C. crescentus* incubation steps were performed at 30 °C. To determine the optical density of *C. crescentus* cultures the optical density was measured at 660 nm using a photo spectrometer (Genesys6, Thermo Spectronic, WI, USA)

Strain generation

The bacterial strains and plasmids used in this study are shown in Table S1. Molecular biology techniques were used as described elsewhere [197]. Plasmids were propagated in *E. coli* strain DH5a or DH10B. For conjugational transfer into *C. crescentus*, plasmids were mobilised from *E. coli* strain S17-1 [196]. For protein purification, recombinant proteins were expressed in BL21(DE3) (pLysS). Markerless in frame deletion was generated by integration of the respective pNPTS128 based deletion constructs followed by double recombination upon *sacB* counter selection. The presence of the deletion was confirmed by PCR. The exact procedure of strain and plasmid construction is available on request.

Phenotypic assays

Motility was scored by stabbing *C. crescentus* strains into PYE semi-solid agar plates (0.3 % agar). After three days, the colony size was quantified by scanning the plates on an Epson Perfection 4870 Photo (Epson, Japan) and using Photoshop CS v8.0 (Adobe, CA, USA) and ImageJ 1.34 (NIH, USA [198]) software package. For all motility experiments the mean of at least five independent colony sizes is shown. Error bars represent the standard deviation.

Attachment was quantified according to the method of O'Toole and Kolter [47, 199]. In brief, cells were grown in PYE filled 96well microtiterplates (Falcon, NJ, USA) for 24 h at 30 °C under shaking (200 rpm). Attached biomass to the polystyrene surface was staining by crystal violet. The staining was quantified using an Elisa plate reader (Molecular Devices) at

600 nm after dissolving the dye with 20 % acetic acid. For each strain the mean of at least six independent experiments is shown. Error bars represent the standard deviation.

The holdfast was stained by fixing cells with 1.5 % formaldehyde and stained with Oregon Green-conjugated wheat germ agglutinin (0.2 mg/ml) (Molecular Probes) for 20 minutes. After washing with water, an appropriate volume of resuspended bacteria were placed on a microscope slide for fluorescence microscopy.

Protein purification and DGC activity assays

E. coli BL21 pLysS cells carrying the expression plasmid pET21c::dgcB were grown in LB medium with ampicillin (100 µg/ml), and expression was induced by adding isopropyl 1-thio-β-D-galactopyranoside at OD_{600} 0.4 to a final concentration of 0.1 mM. After harvesting by centrifugation, cells were resuspended in buffer containing 50 mM Tris-HCl, pH 8.0, 250 mM NaCl, 5 mM Di-thiothreitol, lysed by sonication, and the suspension was clarified by centrifugation for 10 min at 5000 g. Soluble and insoluble protein fractions were separated by a high-spin centrifugation step (100,000 g, 1 h). The supernatant was loaded onto nickel-nitrilotriacetic acid affinity resin (Qiagen, Germany), washed with buffer, and eluted with an imidazol gradient. Protein preparations were examined for purity by SDS-PAGE, and fractions containing pure protein were pooled and dialyzed for 12 h at 4 °C. To determine di-guanylate cyclase activity, the reaction mixtures with 2.5 µg purified hexa-histidine-tagged DgcB contained 25 mM Tris-HCl, pH 8.0, 250 mM NaCl, 10 mM $MgCl_2$ and were started by the addition of 100 µM [^{33}P]GTP (Amersham Biosciences, UK; 3000 Camel). At indicated time intervals the reaction was stopped with an equal volume of 0.5 M EDTA, pH 8.0 and reaction products were analysed on polyethyleneimine-cellulose chromatography plates.
Samples were dissolved in 5 µl of running buffer containing 1:1.5 (v/v) saturated NH_4SO_4 and 1.5 M KH_2PO_4, pH 3.6, and blotted on Polygram® CEL 300 polyethyleneimine-cellulose thin-layer chromatography plates (Macherey-Nagel, Germany). Plates were developed in 1:1.5 (v/v) saturated NH_4SO_4 and 1.5 M KH_2PO_4, pH 3.6, dried, and exposed on a Storage PhosphorScreen (Amersham Biosciences, UK). The intensity of the various radioactive species was calculated by quantifying the intensities of the relevant spots using ImageJ software, version 1.34.

The K_M for GTP was determined by adding increasing amounts of cold GTP (5 µM, 10 µM, 20 µM, 50 mM, 100 µM, and 500 µM). The time dependent production of c-di-GMP was quantified and the initial reaction velocity (V_0) was determined. The initial reaction velocities were potted as a function of the total GTP concentration and the resulting curve was

fitted according to a Michaelis-Menten kinetics using GraphPad Prism 5.01 software (GraphPad Software, CA, USA). For the determination of allosteric inhibition of c-di-GMP, increasing amounts of cold c-di-GMP (1 μM, 5 μM, 10 μM, 25 μM, 50 μM) were added to the reaction mixture. The initial reaction velocities were determined and compared considering the time dependent production of c-di-GMP from radioactive labelled GTP.

Motile suppressor analysis

For the generation of motile suppressors by transposon mutagenesis, a *tn*Marinerd*cat* was randomly introduced into the genome of CB15N Δ*pdeA* (UJ4454) delivered by the suicide plasmid pALMAR2. Resulting chloramphenicol resistant *C. crescentus* were pooled and motile strains were isolated on semi-solid agar plates after incubation for three days. The integration site of the transposon was determined by arbitrary PCR followed by sequencing.
For the generation of spontaneous suppressors, CB15N Δ*pdeA* (UJ4454) was stabbed into semi-solid agar PYE plates and incubated for four days. Motile mutants appeared as flares and were isolated.

For the identification of mutations in *dgcB* or *cc2147/cc2148*, ΦCR30 lysates grown on CB15N::CMS21 (UJ1682) and CB15N::CMS24 (UJ1685), respectively, were used according to the method described by West et *al*. [200]. Both strains (CB15N::CMS21 and CB15N::CMS24) contained a Kan^r marker that is about 100 % linked to *cc1850* or *cc2147/cc2148*. The presence of mutations was confirmed by sequencing relevant strains.

Antibody Production and Immunoblots

PdeA or DgcB fused to a C-terminal hexa-histidine-tag was purified as described above and each injected into rabbits for polyclonal antibody production (Laboratoire d'Hormonologie, Marloie, Belgium). For immunoblots anti-PdeA serum was diluted 1:1000 and anti-DgcB serum was diluted 1:10000.

Western Blot analysis of whole cell lysates was performed as described elsewhere [33]. Primary antibodies were detected by HRP-conjugated swine anti-rabbit secondary antibodies (Dako Cytomation, Denmark). Western blots were developed with ECL detection reagents (Western Lightning, Perkin Elmer, MA, USA).

Light-, fluorescence- and electron microscopy

For the visualisation of the flagellar morphology, *C. crescentus* strains were grown in PYE till exponential phase, harvested by centrifugation and washed with water. Samples were applied

for 1 min to glow-discharged, carbon-coated grids and negatively stained with 2 % (w/v) uranylacetate. The samples were viewed in a Philips Morgagni 268D electron microscope at a nominal magnification of 20,000× and an acceleration voltage of 80 kV.

For fluorescence imaging bacterial culture was placed on a microscope slide layered with a pad of 2 % agarose dissolved in water. An Olympus IX71 microscope equipped with an UPlanSApo 100x/1.40 Oil objective (Olympus, Japan) and a coolSNAP HQ (Photometrics, AZ, USA) CCD camera was used to take differential interference contrast (DIC) (exposure time 0.15 sec) and fluorescence photomicrographs. For Oregon-Green fluorescence FITC filter sets (Ex 490/20 nm, Em 528/38 nm), for YFP fluorescence YFP filter sets (Ex 500/20 nm, Em 535/30 nm), and for CFP fluorescence CFP filter sets (Ex 436/10 nm, Em 470/30 nm) with an exposure time of 1.0 sec were used. The signal to noise ratio for weak fluorescence signals (e.g. PdeA-YFP) was improved by averaging five serial exposures. Images were processed with softWoRx v3.3.6 (Applied Precision, WA, USA) and Photoshop CS v8.0 softwares.

Figure legends

Figure 1: Systematic assays reveal novel candidate di-guanylate cyclases and phosphodiesterases.

Clean in frame deletions of genes predicted to code for GGDEF and/or EAL domain proteins were generated in the *C. crescentus* wild type background CB15. Their attachment behaviour to polystyrene surfaces and motility on semi-solid agar plates was quantified and plotted relative to the wild type. Error bars represent the standard deviation.

Figure 2: The motility defect of Δ*pdeA* is caused by a paralysed flagellum.

(A) The motility phenotype of a Δ*pdeA* strain can be complemented by expressing a plasmid borne copy of *pdeA*. The motility of CB15 Δ*pdeA* harbouring the plasmid ppdeA was compared to wild type cells with an empty control plasmid and CB15 Δ*pdeA* with the same plasmid on semis solid agar plates. As control the wild type harbouring ppdeA was used. Area of the colony size is given as relative value compared to the wild type. Error bars represent the standard deviation.

(B) The levels of flagellar proteins in Δ*pdeA* are like in the wild type.

Western blot analysis of whole cell lysates of mid exponential phase cultures from wild type (CB15N) and Δ*pdeA* were probed with different antibodies raised against the indicated proteins of different flagellar regulation classes. The proteins belong to the following classes: CtrA (class I), FliF, FliM, and FlbD (class II), FlgH (class III), and the flagellins (class IV).

(C) The *pdeA* mutant strain comprises a morphologically normal flagellum.

Representative transmission electron micrographs of negatively stained wild type (CB15N) and Δ*pdeA* cells grown under the same conditions are shown.

Figure 3: Mutations in *dgcB*, but not in *dgrA/B* can suppress the motility phenotype of a *pdeA* deletion.

(A) Deletions in genes coding for the c-di-GMP effector proteins DgrA, DgrB or both do not rescue the Δ*pdeA* motility defect. Clean deletions of *dgrA*, *dgrB* and both genes in the wild type background (CB15N) were compared on semi-solid agar plates to the same deletion in the Δ*pdeA* background. Values are normalized to the wild type. Error bars represent the standard deviation.

(B) Transposon insertions, making the Δ*pdeA* strain motile were isolated in *dgcB* and in the intergenic region between *cc2147* and *cc2148*.

Schematic representation of the genomic locus of *cc2147/cc2148* and *dgcB* retrieved from the KEGG database (http://www.genome.jp/kegg/). The domain structure of DgcB drawn to scale is schematically represented below the gene. Transposon insertion sites are indicated by arrows. Stop codons identified in the screen for spontaneous suppressors (see Fig. 3C) are indicated by a *. The genes are annotated as: *cc2144-2146* = hypothetical proteins, *cc2147* = D-isomer specific 2-hydroxyacid dehydrogenase family protein, *cc2148* = putative ABC transporter ATP-binding protein, *cc2149* = TonB-dependent receptor, *cc1849* = probable coniferyl aldehyde dehydrogenase, *cc1850* = DgcB, *cc1851* enoyl-CoA hydratase/isomerase family protein.

(C) Spontaneous suppressor of the motility defect of Δ*pdeA* show different levels of suppression and only one class maps to *dgcB*.

Suppressor mutants of Δ*pdeA* were isolated by selection on semi-solid agar plates and tested for their motility (black bars). They were grouped into three classes according to their performance on semi-solid agar plates. A representative of each class is shown (class I = UJ4711, class II = UJ4712, class IIIa = UJ4713, and class IIIb = UJ4714). The *dgcB* region of the suppressors was replaced by a wild-type copy of *dgcB* by means of general transduction and the motility of the resulting strain was quantified (grey bars). Only a subpopulation of class IIII reverts to Δ*pdeA* level motility and was indicated as subclass IIIb. Values are normalized to the wild type. Error bars represent the standard deviation.

Figure 4: Purified recombinant DgcB converts GTP into c-di-GMP.

DgcB-His (2.5 μg) was tested for di-guanylate cyclase activity, and the products of the enzymatic reactions were analysed for 0, 5, 15, 30, 60, 90, and 120 min incubation time as indicated. As control reactions purified DgcA (2.5 μg) and PleD* (2.5 μg) were used and the same time points are shown. Radioactive products and educts were identified and labelled according to their RF values.

Figure 5: DgcB and PdeA from a cognate pair of antagonistic enzymes.

The epistasis of DgcA, DgcB, PleD and PdeA was tested. Clean deletions of the different *dgcs* were combined with a deletion in *pdeA* and a double deletion of *dgcB* and *pleD* was investigated. The attachment behaviour on polystyrene plates, as well as the motility on semi-

solid agar plates of the resulting strains was assayed. The quantified data of the indicated strains are presented relative to the wild type. Error bars represent the standard deviation.

Figure 6: DgcB and PdeA inversely regulate the onset of holdfast formation during the cell cycle together with PleD.

(A) The amount of cells with a detectable holdfast reflects the attachment behaviour of the cells. Batch cultures of cells in logarithmic growth phase were stained with an Oregon green coupled lection binding to holdfast exopolysaccharides. The relative number of cells with a stainable holdfast was determined and compared with the attachment data from Fig. 5. For each strain, at least 370 cells were counted. The error bars represent the standard deviation. Representative images of the holdfast stained cells are shown below the graph. Red colour represents the DIC channel, green colour the Oregon green channel.

(B) In contrast to a Δ*dgcB* and Δ*pleD* strain, a Δ*pdeA* mutant shows premature holdfast synthesis. Swarmer cells of wild type (CB15), Δ*dgcB*, Δ*pleD*, and Δ*pdeA* were isolated and resuspended in M2G. The synchronised population was followed through a cell cycle. At indicated phases of the cell cycle, aliquots of cells were probed for the presence of holdfast exopolysaccharides. White arrows highlight the first appearance of detectable holdfast.

Figure 7: PdeA is degraded by the ClpXP protease upon swarmer-to-stalked cell transition and resynthesised in predivisional cells.

(A) In contrast to DgcB, the protein level of PdeA shows cell cycle specific variations. Wild type cells (CB15N) were synchronised and aliquots were taken at the indicated phases of the cell cycle. These were probed in a Western blot analysis with polyclonal antiserum raised against DgcB or PdeA, respectively.

A strain expressing PdeA-YFP from a plasmid in the presence of a chromosomal copy of PdeA was synchronised under the same conditions and cell lysates were tested in a Western blot analysis for PdeA levels.

(B) The *C. crescentus* proteases Lon, FtsH and the chaperons HslU and ClpA are not involved in the degradation of PdeA. Strains with disrupted genes coding for Lon, FtsH, HslU, and ClpA were grown to the same optical density, probed for the PdeA content in a Western blot analysis and compared to the wild type (CB15N). As control for undegradable PdeA, a strain with a *pdeA-yfp* fusion replacing the wild-type chromosomal *pdeA* copy was assayed.

(C) Decreased ClpX activity stabilizes PdeA during the cell cycle. A dominant negative mutant of ClpX on a low copy number plasmid under the control of the xylose promotor was

introduced in wild-type *C. crescentus* (CB15N). The resulting cells were or were not induced with xylose 2 h prior to isolating swarmer cells as indicted. These were followed through a cell cycle and aliquots were taken at indicated phases of the cell cycle. Whole cell lysates were tested with antisera against PdeA, CtrA or FliF in a Western blot analysis.

Figure 8: PdeA and DgcB are dynamically localised during the cell cycle.
(A) PdeA localisation to the incipient stalked pole of the cell coincides with ClpXP localisation during the swarmer-to-stalked cell transition. A C-terminal YFP fusion expressed from a low copy number plasmid under the control of its own promotor was introduced into a *pdeA* deletion strain. These cells were synchronised and the distribution of the fluorescent signal was recorded at indicated phases of the cell cycle using a fluorescence microscope. Differential interference contrast images and fluorescent images were shown as well as a schematic representation.
(B) DgcB is homogenously distributed in swarmer and stalked cell, but localises to both cell poles as soon as cell form a constriction. A suicide plasmid containing the 3`-part of *dgcB* fused to *cfp* was integrated into the chromosomal *dgcB*. The cell cycle dependent localisation of DgcB-CFP was investigated in synchronised cells under the same conditions as described for Fig. 8A.

Figure 9: The mechanism localising and degrading PdeA differs from the CtrA degradation and localisation pathway.
(A) The PdeA localisation is independent of the CtrA localisation factors PopA and RcdA. PdeA-YFP is expressed from a low copy number plasmid in the wild type (CB15N) or in strains with deleted *popA* and disrupted *rcdA*, respectively. The PdeA-YFP distribution is investigated during exponential growth phase and fluorescence as well as differential interference contrast pictures are shown. Fluorescent foci at the stalked pole of the cell are indicated by arrows.
(B) PopA is not required to allow cell cycle specific regulation of PdeA. The PdeA levels were analysed during the cell cycle progression of synchronised Δ*popA* cells at indicated timepoints using Western blot analysis with a PdeA specific antiserum.

Figure 10: Model for the role of PdeA, DgcB, and PleD in the regulation of polar development in *C. crescentus*.

The enzymatic activities of PdeA, DgcB and PleD towards c-di-GMP, together with the effect on the cell are indicated in the box. Furthermore, the cell cycle resolved localisation and regulation of the three enzymes are depicted. The model proposes that PdeA is regulated by the protease ClpXP. Upon degradation of PdeA, the DGC activity of PleD and DgcB can initiate paralysis and shedding of the flagellum and holdfast synthesis. Hatched areas indicate the delocalisation of two proteins. Inactive, delocalised PleD is not depicted in this scheme for clarity.

Figure S1: Schematic representation of the *in silico* predicted domain architecture of *C. crescentus* GGDEF and/or EAL domain proteins.

The prediction of the domain architecture was retrieved from the SMART database [37]. The annotation for CC1842-PopA was manually adjusted. *In vitro* characterised DGCs are highlighted in red, PDEs in blue.

Figure S2: Multiple alignment of either all *in silico* predicted GGDEF or all EAL domains from *C. crescentus*.

The protein sequences were retrieved from the KEGG database (http://www.genome.jp/kegg/). Domain barriers were determined by including all highly conserved residues as determined by Galperin et al. [12] and amino acid positions were indicated behind the protein name. Multiple alignments of all GGDEF or all EAL domains were performed using ClustalW [201]. Black boxes highlight the GG(D/E)F, RXXD and EAL motifs, respectively.

Figure S3: The individual deletion of genes coding for predicted GGDEF and/or EAL domain proteins does not alter the growth rate of cells.

Deletion strains were grown in complex medium (PYE) at 30 °C, the optical density at 660 nm was recorded every 60 min for 12 h and the doubling time was calculated from these data. The mean of three independent experiments is shown. Error bars represent the standard deviation.

Figure 1

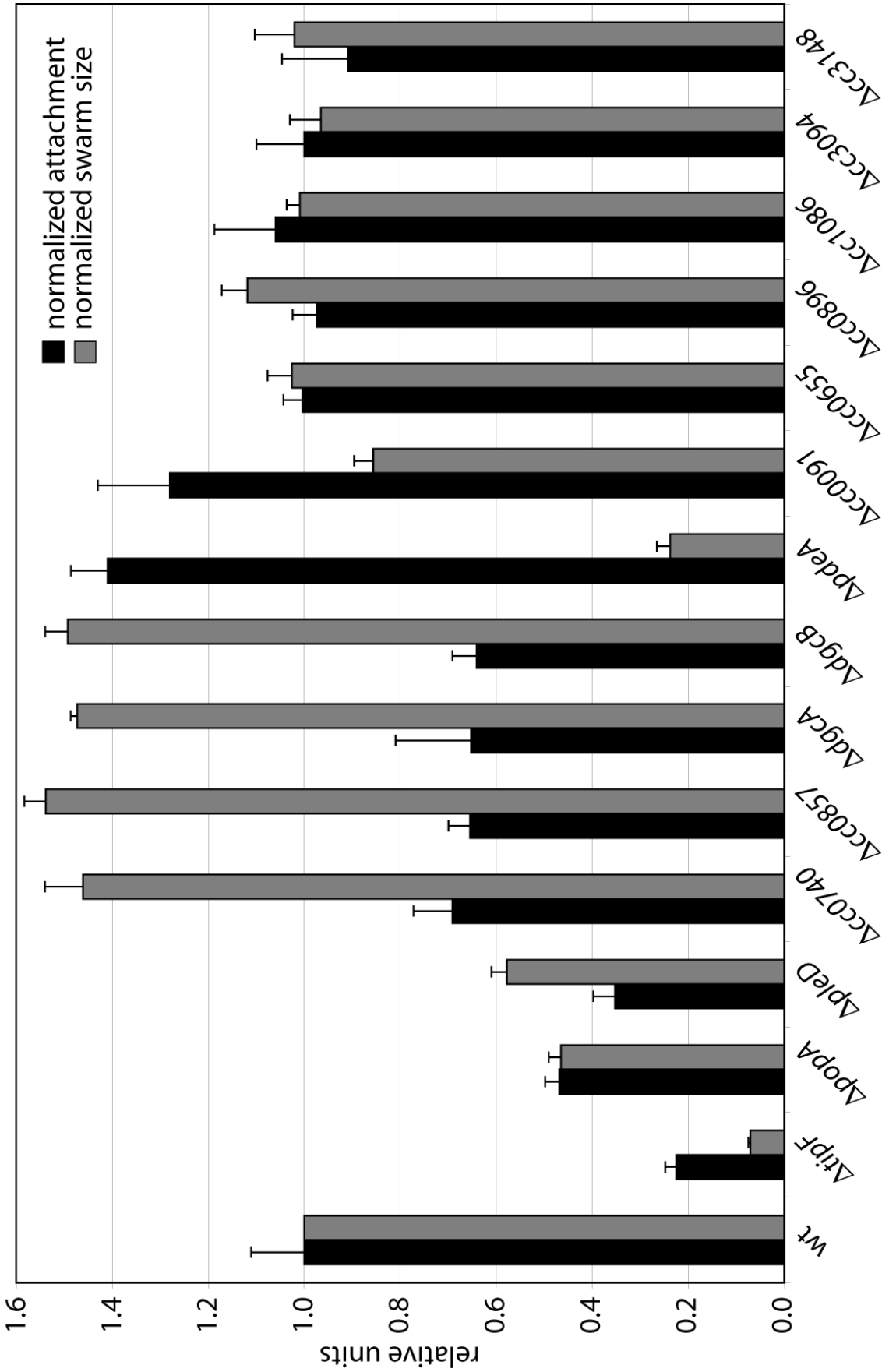
normalized attachment
normalized swarm size
relative units
0.0
0.2
0.4
0.6
0.8
1.0
1.2
1.4
1.6
wt
ΔtipF
ΔpopA
ΔpleD
ΔCC0740
ΔCC0857
ΔdgcA
ΔdgcB
ΔpdeA
ΔCC0091
ΔCC0655
ΔCC0896
ΔCC1086
ΔCC3094
ΔCC3148

Figure 2

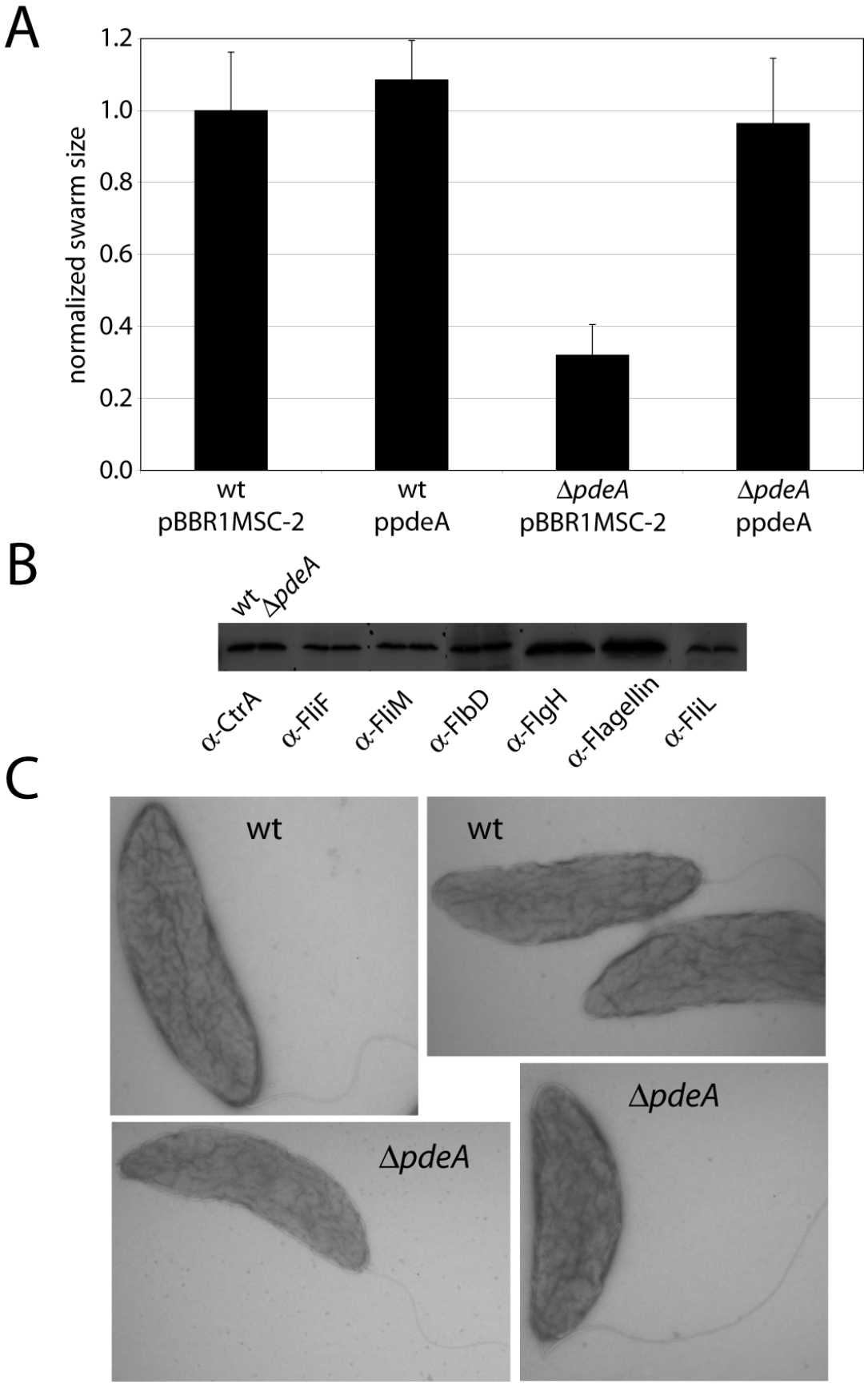
A
normalized swarm size
1.2
1.0
0.8
0.6
0.4
0.2
0.0
wt pBBR1MSC-2
wt ppdeA
ΔpdeA pBBR1MSC-2
ΔpdeA ppdeA
B
wt
ΔpdeA
α-CtrA
α-FliF
α-FliM
α-FlbD
α-FlgH
α-Flagellin
α-FliL
C
wt
wt
ΔpdeA
ΔpdeA

Figure 3

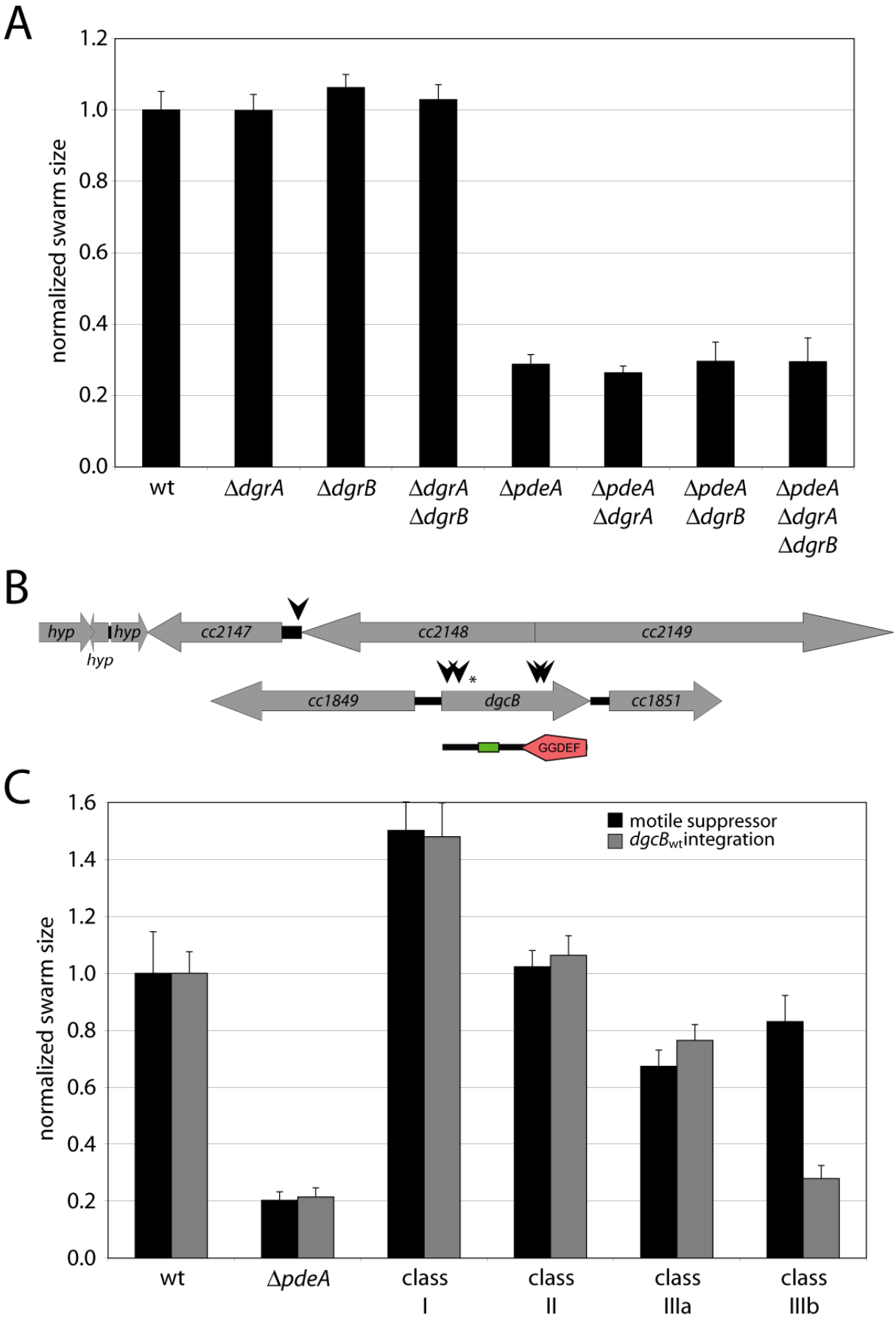
A
normalized swarm size
1.2
1.0
0.8
0.6
0.4
0.2
0.0
wt
ΔdgrA
ΔdgrB
ΔdgrA ΔdgrB
ΔpdeA
ΔpdeA ΔdgrA
ΔpdeA ΔdgrB
ΔpdeA ΔdgrA ΔdgrB
B
hyp
hyp
hyp
cc2147
cc2148
cc2149
cc1849
dgcB
cc1851
*
GGDEF
C
normalized swarm size
1.6
1.4
1.2
1.0
0.8
0.6
0.4
0.2
0.0
motile suppressor
dgcBwt integration
wt
ΔpdeA
class I
class II
class IIIa
class IIIb

Figure 4

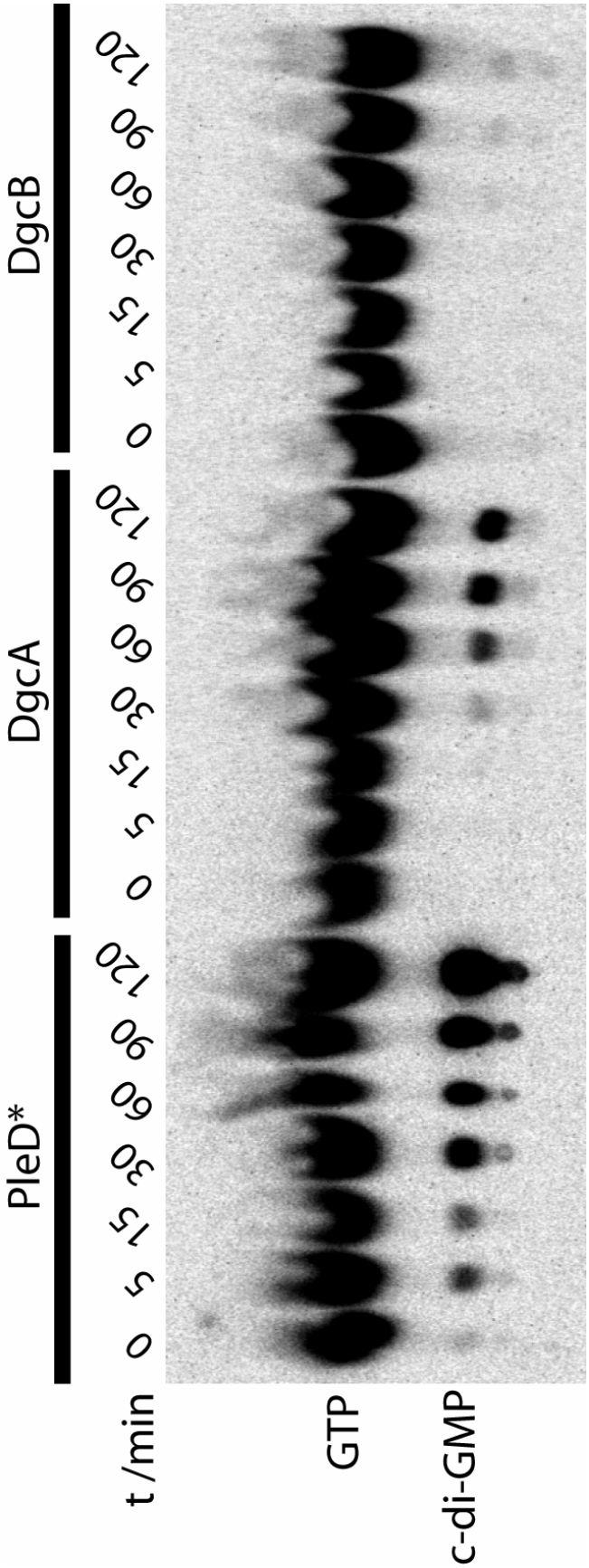

Figure 5

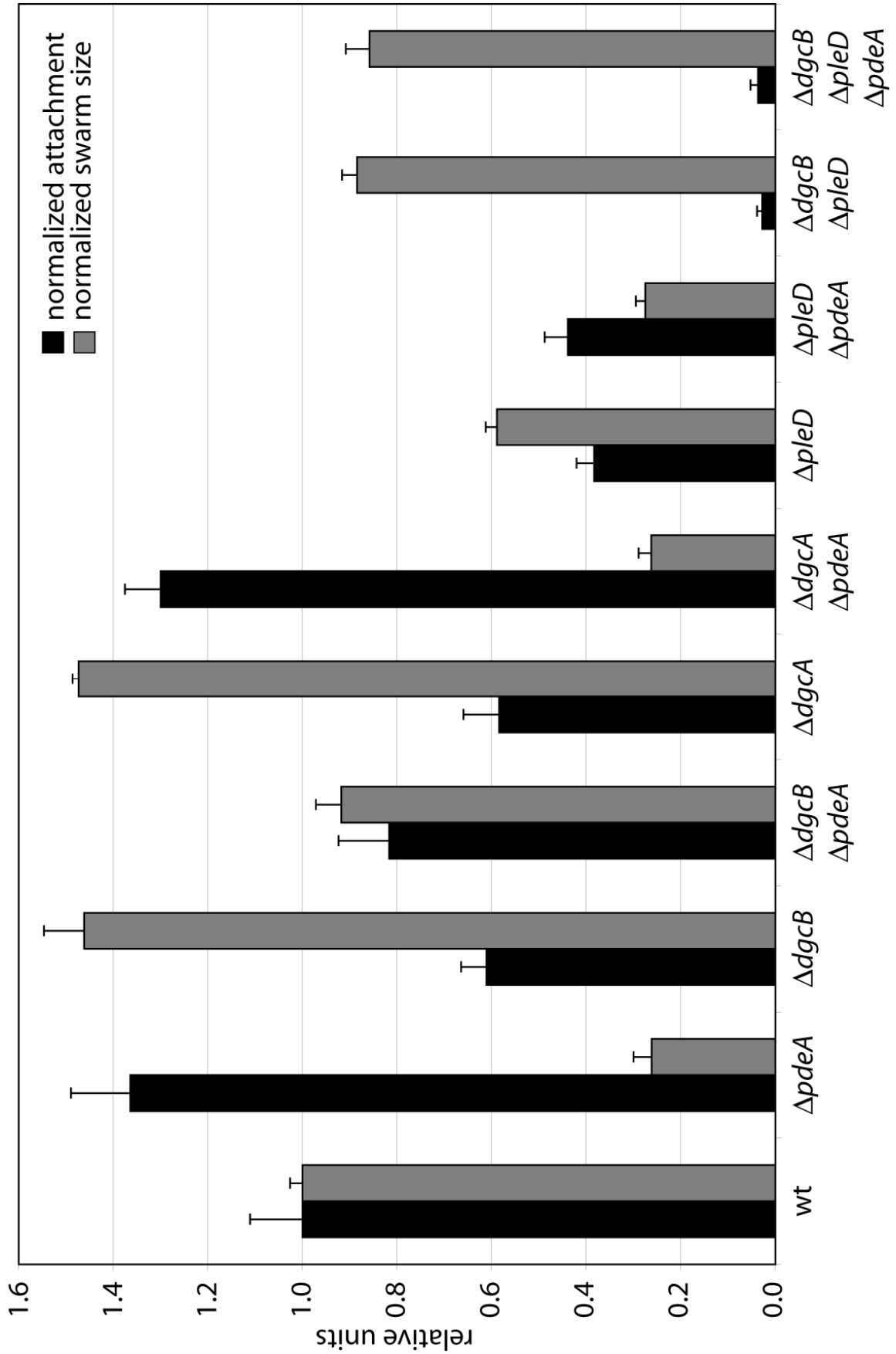
normalized attachment
normalized swarm size
relative units
0.0
0.2
0.4
0.6
0.8
1.0
1.2
1.4
1.6
wt
ΔpdeA
ΔdgcB
ΔdgcB ΔpdeA
ΔdgcA
ΔdgcA ΔpdeA
ΔpleD
ΔpleD ΔpdeA
ΔdgcB ΔpleD
ΔdgcB ΔpleD ΔpdeA

Figure 6

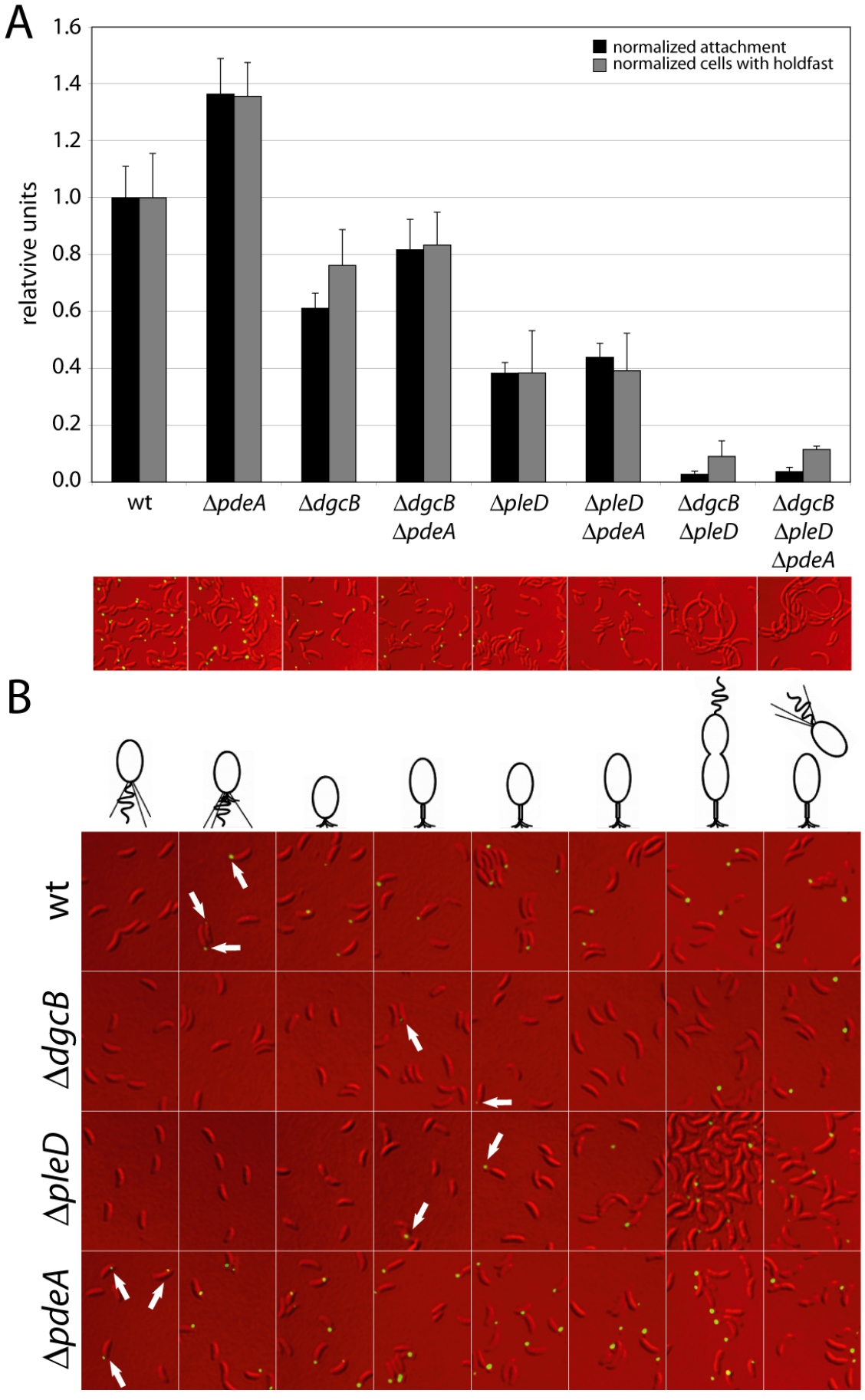
A
1.6
1.4
1.2
1.0
0.8
0.6
0.4
0.2
0.0
relatvive units
normalized attachment
normalized cells with holdfast
wt
ΔpdeA
ΔdgcB
ΔdgcB ΔpdeA
ΔpleD
ΔpleD ΔpdeA
ΔdgcB ΔpleD
ΔdgcB ΔpleD ΔpdeA
B
wt
ΔdgcB
ΔpleD
ΔpdeA

Figure 7

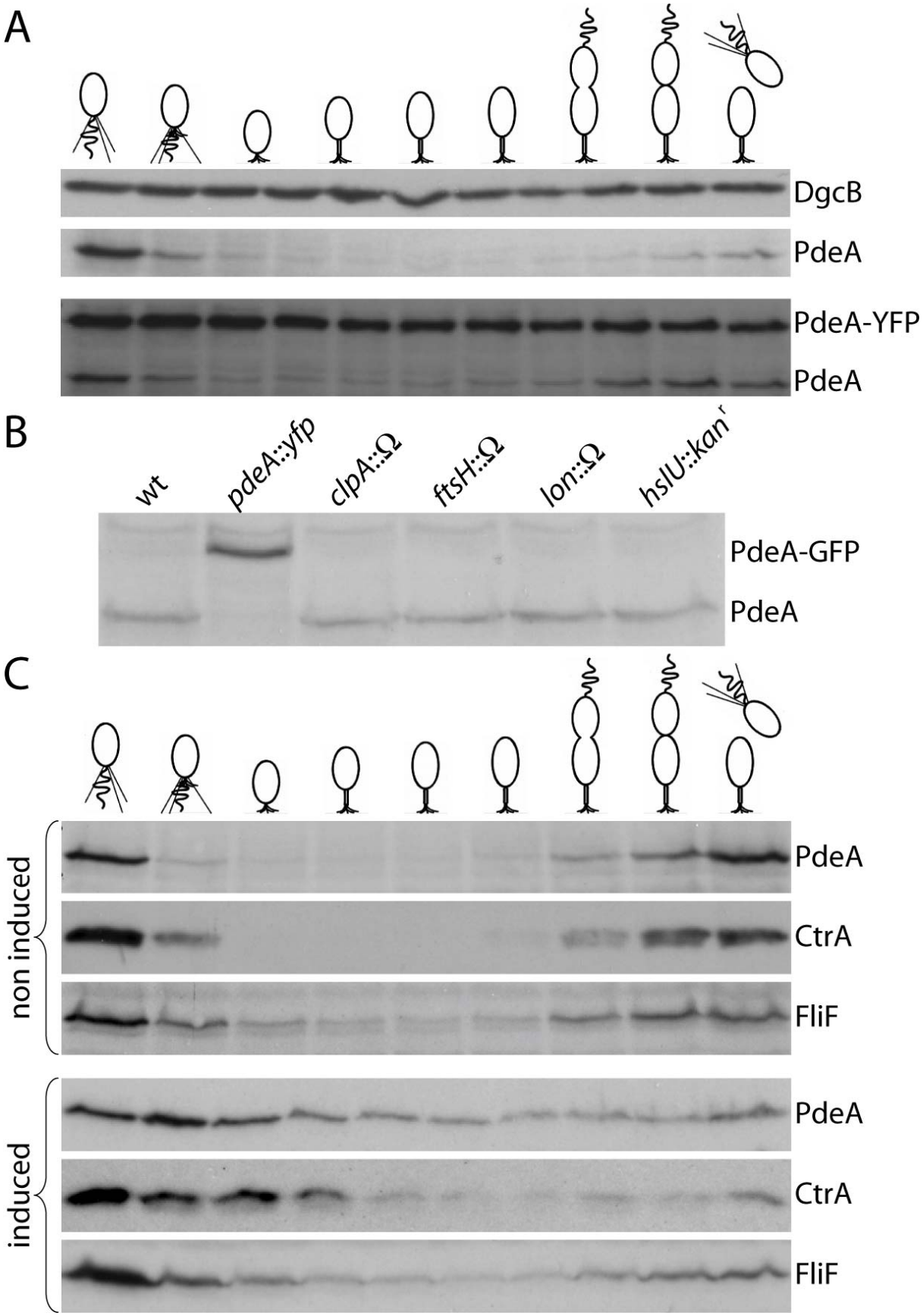
A
DgcB
PdeA
PdeA-YFP
PdeA
B
wt
pdeA::yfp
clpA::Ω
ftsH::Ω
lon::Ω
hslU::kan^r
PdeA-GFP
PdeA
C
non induced
PdeA
CtrA
FliF
induced
PdeA
CtrA
FliF

Figure 8

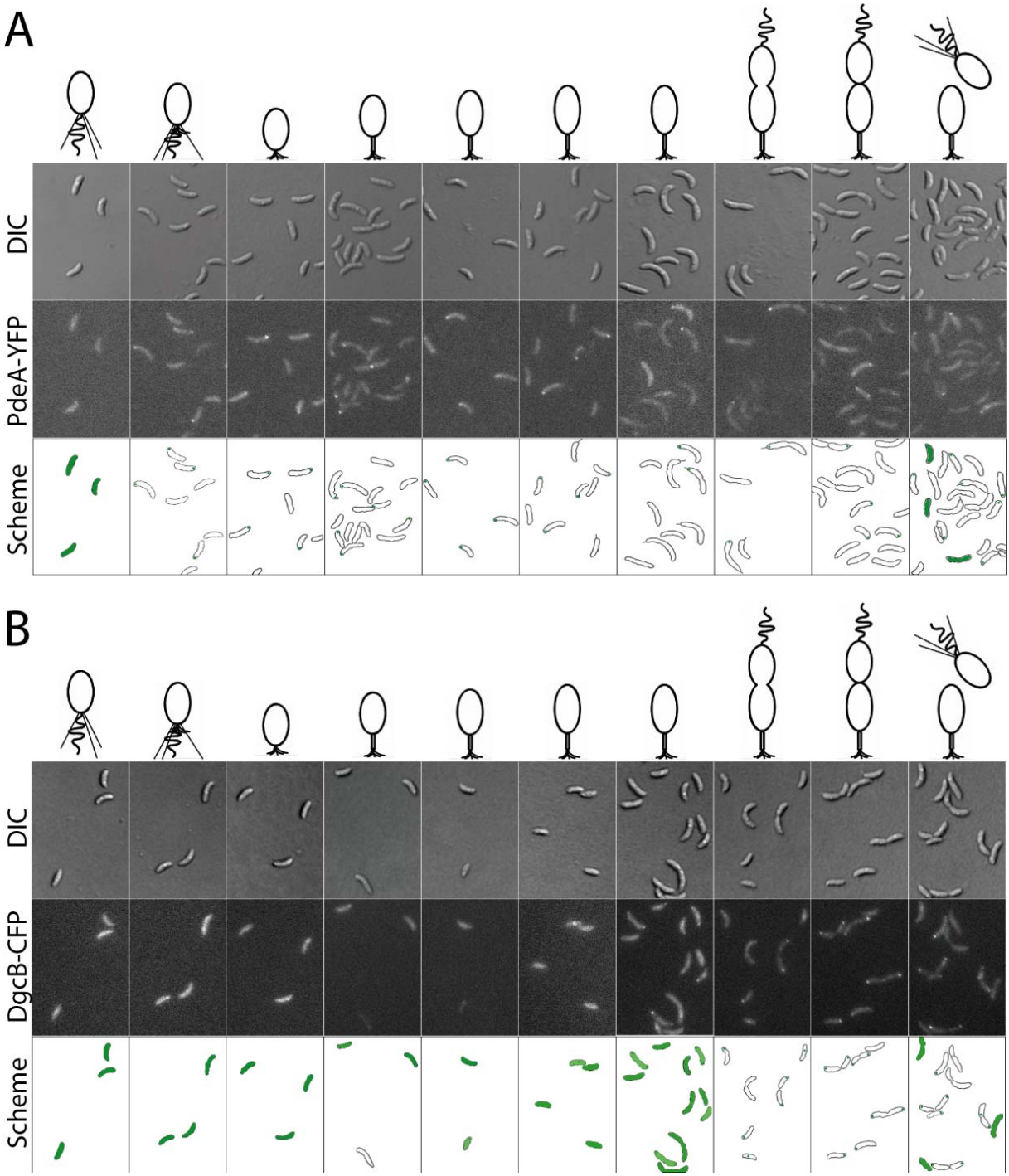

Figure 9

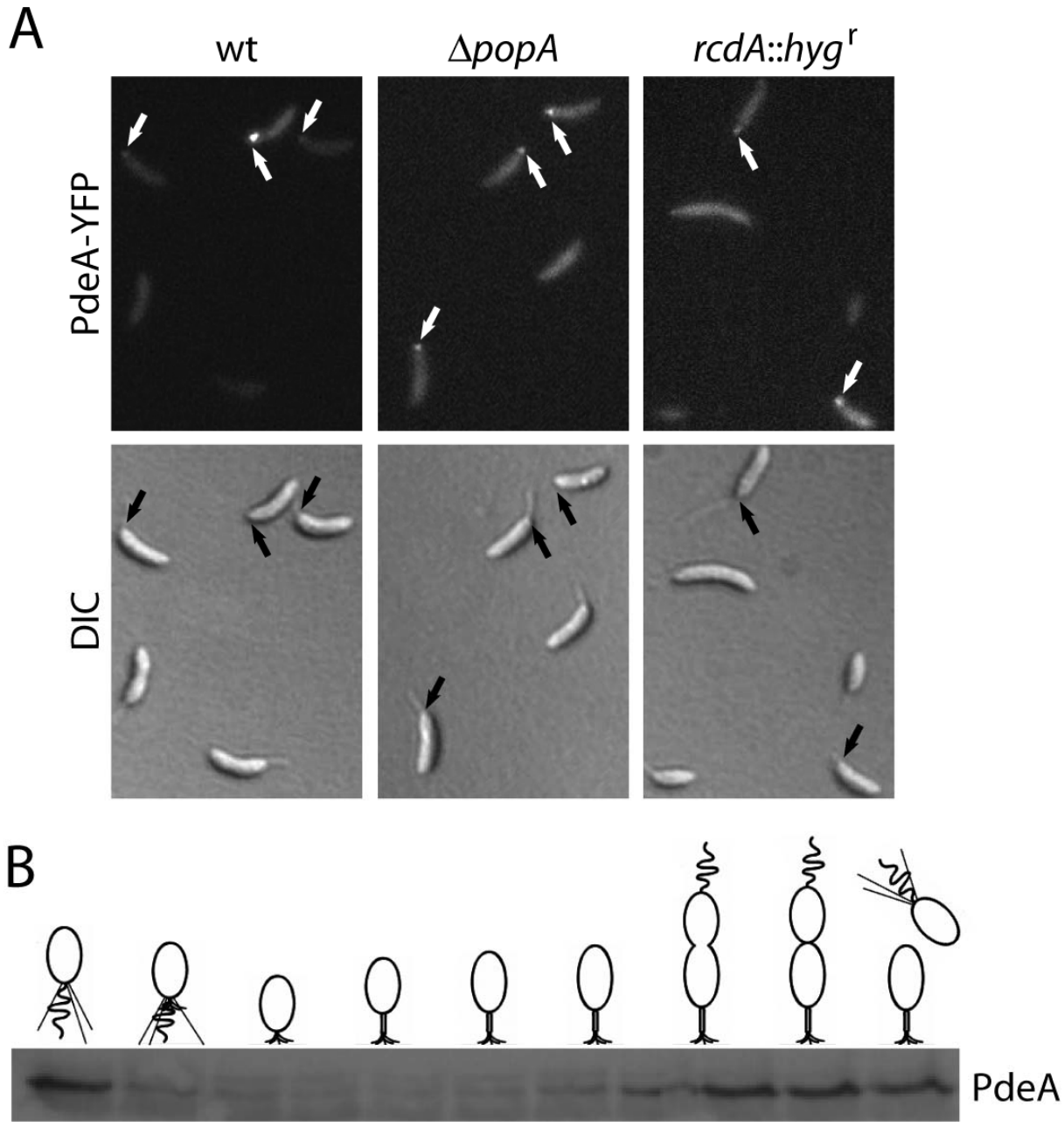

Figure 10

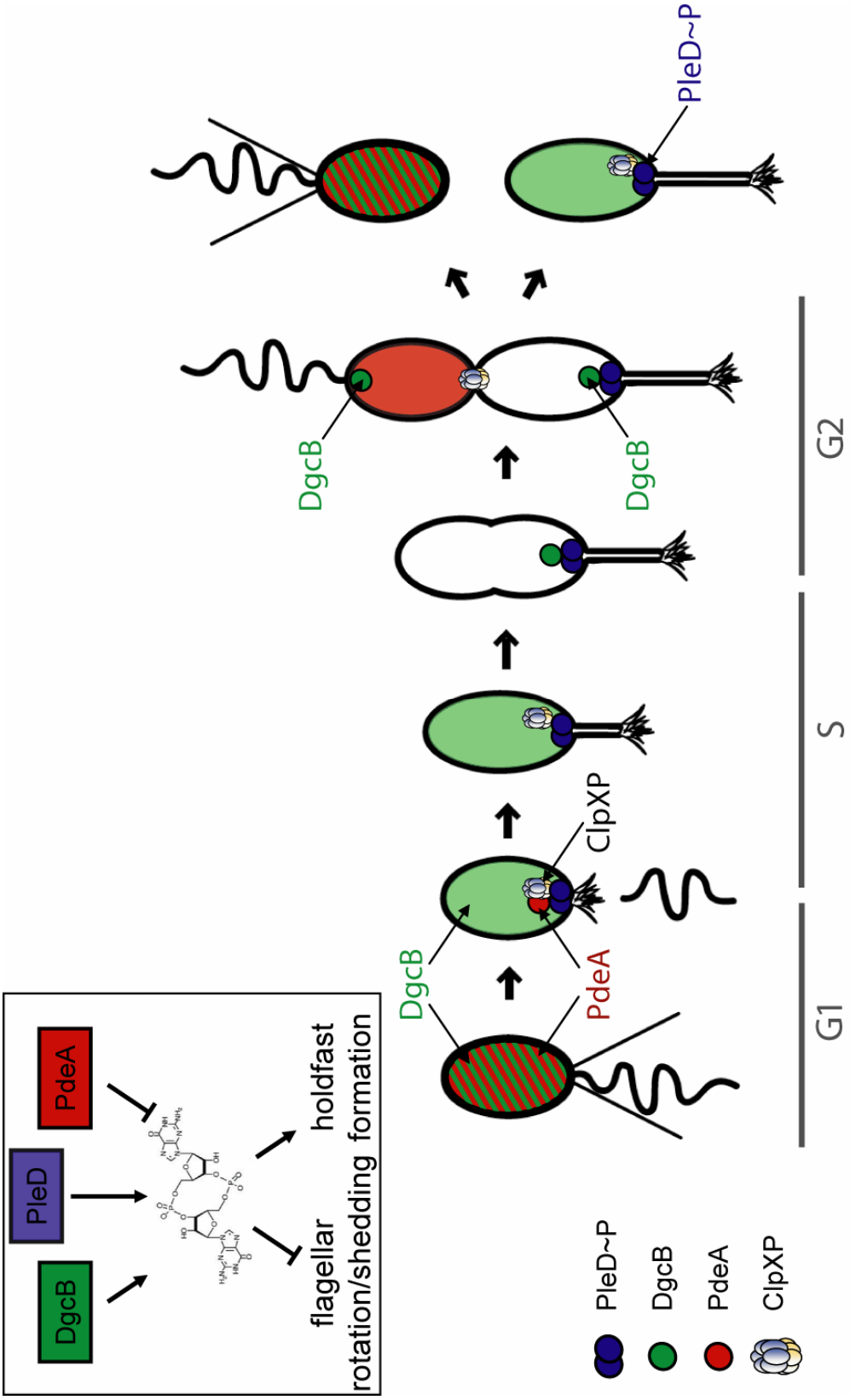
PleD~P
DgcB
DgcB
G2
S
ClpXP
DgcB
PdeA
G1
PleD~P
DgcB
PdeA
ClpXP
PdeA
PleD
DgcB
holdfast formation
flagellar rotation/shedding

Figure S1

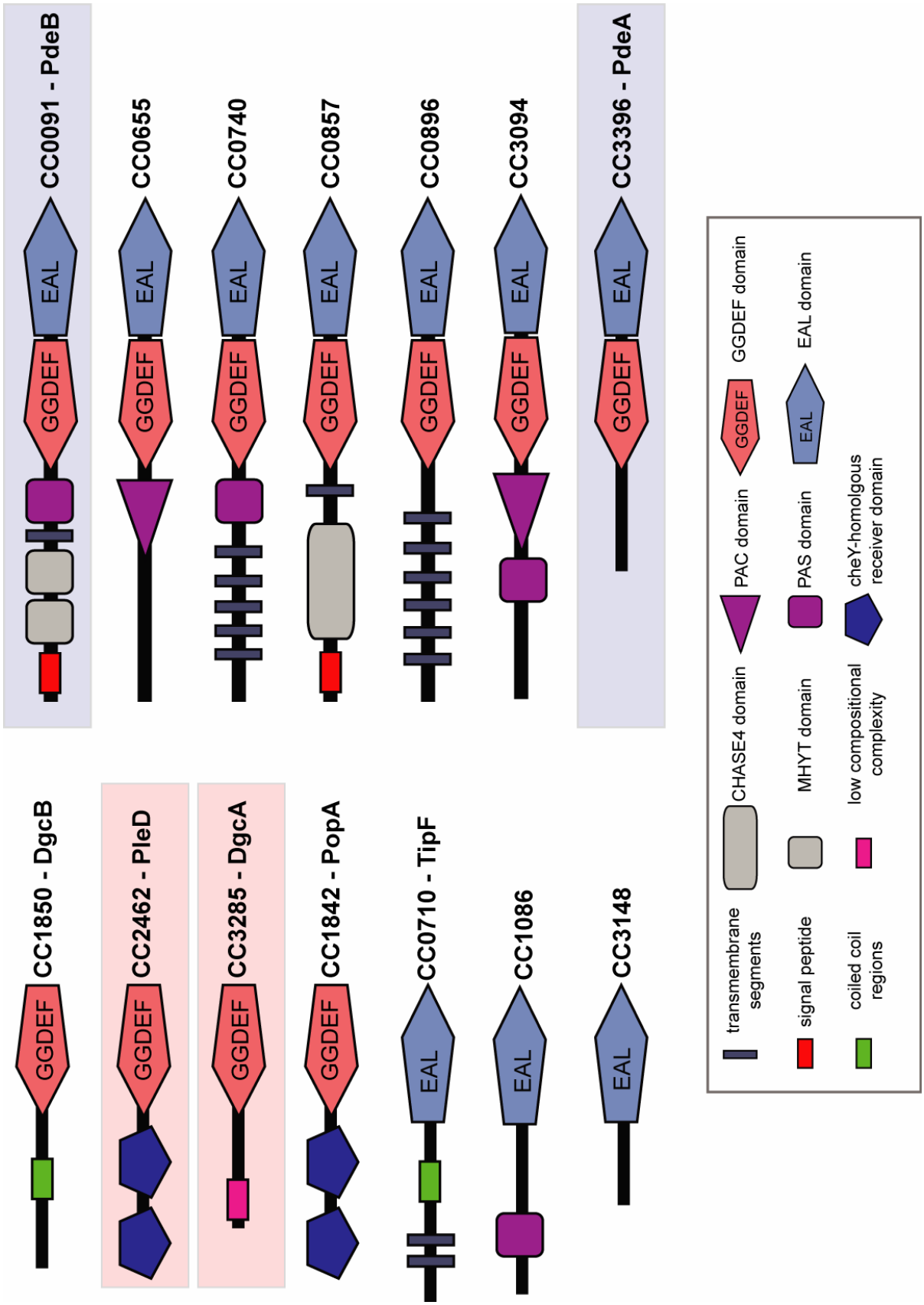
CC0091 - PdeB
EAL
GGDEF
CC0655
CC0740
CC0857
CC0896
CC3094
CC3396 - PdeA
CC1850 - DgcB
CC2462 - PleD
CC3285 - DgcA
CC1842 - PopA
CC0710 - TipF
CC1086
CC3148
transmembrane segments
signal peptide
coiled coil regions
CHASE4 domain
PAC domain
MHYT domain
PAS domain
low compositional complexity
cheY-homolgous receiver domain
GGDEF domain
EAL domain

Figure S2

Figure S3

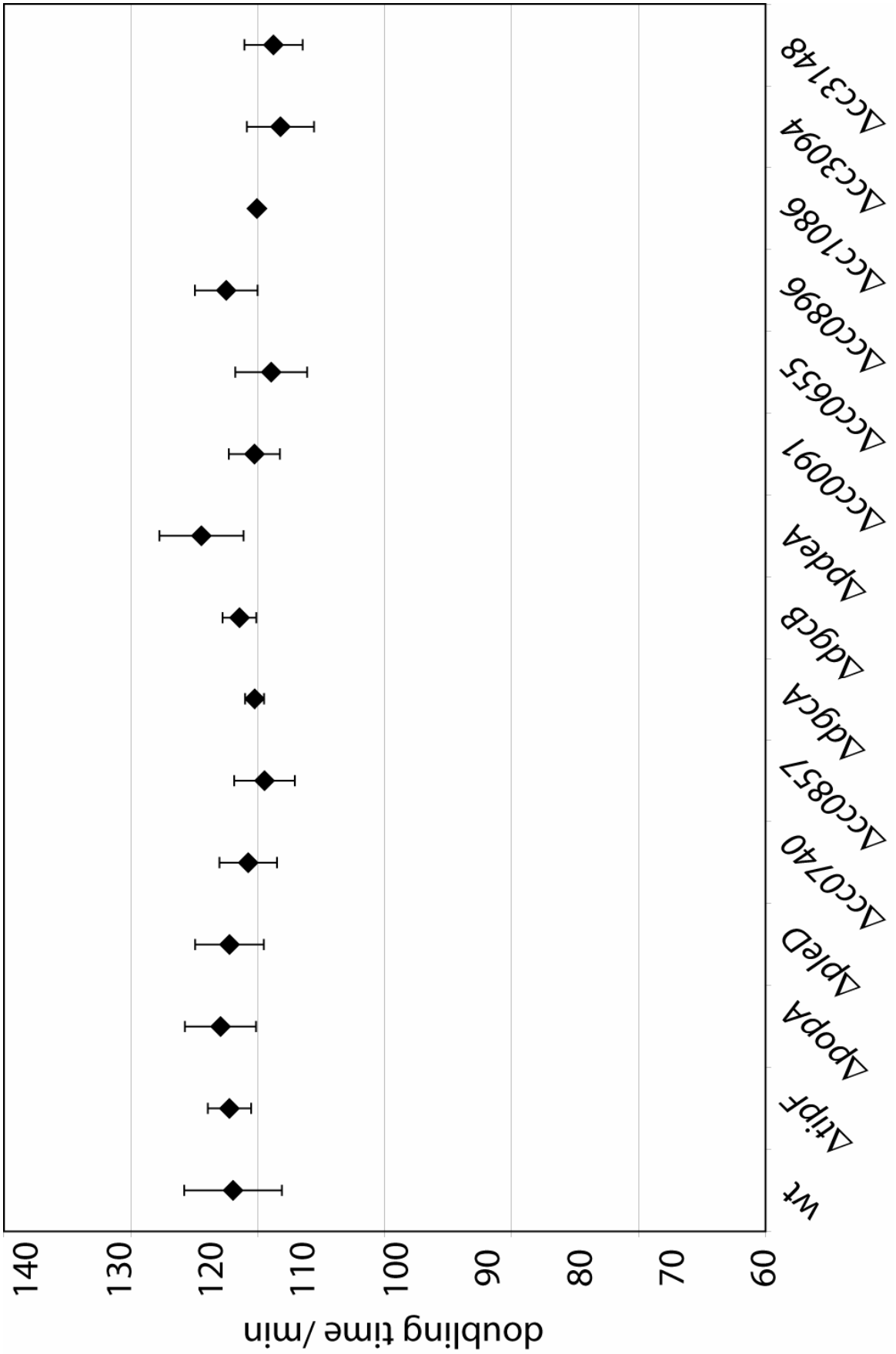
doubling time /min
60
70
80
90
100
110
120
130
140
wt
ΔtipF
ΔpopA
ΔpleD
Δcc0740
Δcc0857
ΔdgcA
ΔdgcB
ΔpdeA
Δcc0091
Δcc0655
Δcc0896
Δcc1086
Δcc3094
Δcc3148

Table S1

Strain or plasmid	Relevant genotype and description	Reference or source
***C. crescentus* strains**		
UJ134	CB15N *hslU*::kan^r	A. Stotz
UJ838	CB15N *clpA*::Ω	M. Osteras
UJ945	CB15N *ftsH*::Ω	[202]
UJ1249	CB15N *xylX*::pMO88	M. Osteras
UJ1267	CB15N - synchronizable variant strain of CB15	[114]
UJ1682	CB15N::CMS21	[200]
UJ1685	CB15N::CMS24	[200]
UJ1855	CB15N *lon*::Ω	[203]
UJ3056	CB15 Δ*cc0091*	A. Levi
UJ3241	CB15 - *C. crescentus* wild type	ATCC19089
UJ4182	BL21(DE3) + pET21c::*dgcB*	M. Christen
UJ4448	CB15N Δ*popA*	this study
UJ4454	CB15N Δ*pdeA*	this study
UJ4455	CB15 Δ*cc0655*	this study
UJ4456	CB15 Δ*tipF*	this study
UJ4457	CB15 Δ*cc0740*	this study
UJ4458	CB15 Δ*cc0857*	this study
UJ4459	CB15 Δ*cc0896*	this study
UJ4460	CB15 Δ*cc1086*	this study
UJ4461	CB15 Δ*popA*	this study
UJ4462	CB15 Δ*dgcB*	this study
UJ4463	CB15 Δ*pleD*	this study
UJ4464	CB15 Δ*cc3094*	this study
UJ4465	CB15 Δ*cc3148*	this study
UJ4466	CB15 Δ*dgcA*	this study
UJ4467	CB15 Δ*pdeA*	this study
UJ4709	CB15 + pBBR1MCS-2	this study
UJ4710	CB15 Δ*pdeA* + pBBR1MCS-2	this study
UJ4711	CB15N Δ*pdeA* motile suppressor class I	this study
UJ4712	CB15N Δ*pdeA* motile suppressor class II	this study
UJ4713	CB15N Δ*pdeA* motile suppressor class IIIa	this study
UJ4714	CB15N Δ*pdeA* motile suppressor class IIIb	this study
UJ4715	CB15 Δ*dgcB* Δ*pdeA*	this study
UJ4716	CB15 ΔdgcA Δ*pdeA*	this study
UJ4717	CB15 + pAL53	A. Levi
UJ4718	CB15 Δ*pdeA* + pAL53	this study
UJ4719	CB15N Δ*dgrA*	this study
UJ4720	CB15N Δ*dgrA* Δ*pdeA*	this study
UJ4721	CB15N Δ*dgrB*	this study
UJ4722	CB15N Δ*dgrB* Δ*pdeA*	this study
UJ4723	CB15 Δ*dgcB* Δ*pleD*	this study
UJ4724	CB15 Δ*dgcB* Δ*pleD* Δ*pdeA*	this study
UJ4725	CB15N Δ*dgrA* Δ*dgrB*	this study
UJ4726	CB15N Δ*dgrA* Δ*dgrB* Δ*pdeA*	this study
UJ4727	CB15N *pdeA*::pSA116	this study
UJ4728	CB15N Δ*pdeA dgcB*::*tn*MarinerdCat integrated at position +2048028 bp	this study
UJ4729	CB15N Δ*pdeA cc2147*::*tn*MarinerdCat integrated at position +2351967 bp	this study

UJ4730	CB15N Δ*pdeA dgcB*::*tn*Marinerd*Cat* integrated at position +2047422 bp	this study
UJ4731	CB15N + pSA120	this study
UJ4732	CB15N Δ*pdeA* + pSA120	this study
UJ4733	CB15N *dgcB*::pSA117	this study
UJ4734	CB15N Δ*pdeA dgcB*::*tn*Marinerd*Cat* integrated at position +2047990 bp	this study
UJ4735	CB15N Δ*pdeA dgcB*::*tn*Marinerd*Cat* integrated at position +2047337 bp	this study
UJ4736	CB15N Δ*popA* + pSA120	this study
UJ4737	CB15N *rcdA*::*hyg*^{r} + pSA120	this study

E. coli strains

BL21(DE3) (pLysS)	F$^-$ *dcm ompT hsdS*(rB$^-$mB$^-$) *gal* l (DE3) [pLysS CAM^r]	Stratagene
DH10B	F- *mcr*A Δ(*mrr*- hsd RMS- *mcr*BC) Φ80d*lacZ*ΔM15 Δ*lac*X74 endA1 recA1 deoR Δ (*ara, leu*)7697 *araD139 galU galK nupG rpsL thi pro hsdR- hsd+ recA RP4-2-Tc*::*Mu-Tn7 supE44* Δ*lac*U169(Φ80 *lacZ*ΔM15) *hsdR17 recA1 endA1gyrA96 thi-1 relA1*	Stratagene
DH5α		[204]
S17-1	RP4-2, Tc::Mu, KM-Tn7	[205]

Plasmids

pALMAR2	pLRS60 carrying a *Tn*Mariner delivering a *Cat* cassette	A. Levi
pBBR1MCS-2	Kan^r broad range medium copy cloning vector	[206]
pET21c::dgcB	pET21c carrying *dgcB* with a C-terminal 6xHis tag	M. Christen
pMO88	pMR20 carrying *clpX* with mutation in ATP binding site under the control of the xylose promotor	M. Osteras and U. Jenal
pNPTS::KO1599	pNPTS138 based deletion construct for *cc1599 - DgrA*	B. Christen
pNPTS::KO3165	pNPTS138 based deletion construct for *cc3165 - DgrB*	B. Christen
ppdeA	pBBR1MCS-2 carrying *pdeA*	A. Levi
pSA116	pNPTS138 carrying 323 bp of the 3`end of *pdeA* fused to *gfp*	this study
pSA117	pPHU281 carrying 620 bp of the 3`end of *dgcB* fused to *cfp*	this study
pSA120	pMR10 carrying *pdeA* under the control of its own promotor fused to *yfp*	this study
pDM1	pNPTS138 based deletion construct for *cc0091*	D. Meyer
pSA93	pNPTS138 based deletion construct for *cc0655*	this study
pSA94	pNPTS138 based deletion construct for *cc0710 - tipF*	this study
pAD2	pNPTS138 based deletion construct for *cc0740*	A. Dürig
pSA91	pNPTS138 based deletion construct for *cc0857*	this study
pSA102	pNPTS138 based deletion construct for *cc0896*	this study
pSA79	pNPTS138 based deletion construct for *cc1086*	this study
pAD8	pNPTS138 based deletion construct for *cc1842 - popA*	A. Dürig
pAD7	pNPTS138 based deletion construct for *cc1850 - dgcB*	A. Dürig
pSA95	pNPTS138 based deletion construct for *cc2462 - pleD*	this study
pSA96	pNPTS138 based deletion construct for *cc3094*	this study
pSA90	pNPTS138 based deletion construct for *cc3148*	this study
pSA80	pNPTS138 based deletion construct for *cc3285 - DgcA*	this study
pSA81	pNPTS138 based deletion construct for *cc3396 - PdeA*	this study

3.2 CC1064, a Transmembrane Protein Required for Flagellar Rotation and Subcellular Protein Localisation Under Environmental Stress Conditions in *Caulobacter crescentus*

Sören Abel, Alexander Böhm, Thomas Egli, Urs Jenal

Statement of my work

The majority of plasmids and strains used in this study have been generated by me. I also performed motility (Fig. 1A, 1B, 1C, 4C, 5, Tab. 2), swimming speed determination (Fig. 3C), attachment (Fig. 1B, 2C, 2D), chemostat (Fig. 2A, 2B), β-galacdosidase activity (Fig. 3A), light-/fluorescence microscopy (Fig. 6, 7, 8, 11), synchronies (Fig. 9C), holdfast stain (Fig. 9C), stalk length determination (Fig. 9A), and growth experiments (S2, S3) of this study. Furthermore, I analysed the electron micrographs (Fig. 3B, 9B), the fatty acid analysis results (Tab. 1) and determined several suppressor mutations in *motA* and *motB* (Fig. 4A).

Abstract

Adaptation to changing environmental conditions requires, among other things, constant remodelling of the bacterial membrane. However, these changes consecutively affect the solvent properties of the lipid bilayer and thus function of membrane embedded and associated proteins. Here, we describe the transmembrane protein CC1064 from *Caulobacter crescentus* that is required for optimal motility, surface attachment and correct subcellular localisation of the di-guanylate cyclase PleD. It is shown that the paralysis the flagellum, as well as the failure to recruit PleD to the developing stalked pole of the cell in the absence of CC1064 is conditional for oxygen and temperature stress conditions. Spontaneous motile suppressors that can compensate for the lack of CC1064 were found to harbour amino acid exchanges in the flagellar motor proteins MotA or MotB. Furthermore, genetic tests suggest that the functional assembly of MotA and MotB is disrupted in the Δ*cc1046* mutant grown under stress conditions and model is discussed that links changes of the cellular fatty acids composition of the membrane to this assembly defect. We demonstrate that mislocalisation of PleD is independent of flagellar paralysis and vice versa. Taken together, we provide evidence for pleiotropic effects of the transmembrane protein CC1064 that influences motor protein assembly, surface attachment and PleD localisation via diverging pathways.

Introduction

Caulobacter crescentus is an obligate aerobe fresh water bacterium with a characteristic asymmetric cell cycle. Upon division, *C. crescentus* cells give rise to two morphologically distinct progenitor cells, a motile swarmer cell and a sessile stalked cell. The latter can act similarly to a stem cell and continuously sprout off motile swarmer cells. These cannot divide and are able to swim with the help of a polar flagellum [99, 100]. In response to external and internal signals the swarmer cells initiates a developmental program and differentiates into a stalked cell. Upon differentiation, the stalked cell gains the ability to undergo DNA replication and initiates a new round of cell division. During this swarmer-to-stalked cell transition, several polar rearrangements take place. The pili retract, the flagellum is released, the stalk starts to develop, and the adhesive holdfast is synthesized. Optimal surface attachment requires the presence and correctly timed development of all these polar organelles [47, 192].

The atypical response regulator PleD, which is localised to the stalked pole, is one factor that was described to control this polar development and therefore influences motility and attachment in *C. crescentus* [14, 47, 61, 170, 174]. PleD is a modular protein with two N-terminal receiver domains arranged in tandem (Rec1 and Rec2) and a C-terminal di-guanylate cyclase output domain (GGDEF domain) [14, 16, 17]. It was shown that in the absence of PleD, the flagellar ejection, the stalk length control and timing of holdfast synthesis during swarmer-to-stalked cell transition are disturbed [47, 61]. The failure of flagellar ejection leads to the occurrence of ectopic flagella at the tip of the stalk and thus hypermotility, while the delayed holdfast synthesis leads to reduced attachment of Δ*pleD* mutants. In contrast, the presence of the constitutively active mutant PleD* results in increased holdfast production, increased stalk length and flagellar paralysis [61].

Activation of c-di-GMP synthesis occurs via phosphorylation of Asp53 in the first receiver domain of PleD. Multiple lines of evidence demonstrate that the sensor histidine kinases DivJ and PleC, as well as the single domain response regulator DivK control the timed activation of PleD [61, 171, 172, 187]. Like PleD, all these signalling proteins change their subcellular localisation in a cell cycle specific manner [175, 177]. Whereas both PleC and DivJ directly phosphorylate PleD [14, 61, 173], DivK was shown to enhance the kinase activity of PleC and DivJ [187]. Phosphorylation leads to dimerisation, bringing two educt charged GGDEF domains into close proximity to allow c-di-GMP synthesis [14, 16, 17].

Dimerisation of PleD was also shown to be a prerequisite for the sequestration of activated PleD to the differentiating *C. crescentus* cell pole [186]. In agreement to this, the hyperactive PleD* was shown have a higher propensity to dimerize *in vitro* and displays hyperlocalisation *in vivo* [14]. However, although the regulators of PleD activity and localisation are defined, the nature of the factor(s) that sequesters active PleD to the cell pole remains unclear.

Another factor that influences motility, but also attachment behaviour of *C. crescentus* is the flagellum itself. The flagellum is a complex structure in the bacterial cell. It spans both the inner and the outer membrane of gram negative bacteria and converts a proton gradient across the inner membrane into mechanical work [207, 208]. Assembly of the flagellum is a highly regulated process involving coordinated expression of over 50 genes in a hierarchical manner [118, 126, 127, 130]. *C. crescentus* flagellar genes can be divided into four regulation classes [128]. By various mechanisms it is ensured, that the gene products of each class are only present in the cell, if the gene products of the preceding regulation class have been functionally assembled [209].

The flagellum can be divided into two substructures; the rotor and the stator. The rotor consists of the C ring, the MS ring, the rod, and the filament [118]. The stator is composed of two integral inner membrane proteins, MotA and MotB [158, 210, 211]. MotA was shown to contain four transmembrane helices [167, 212]. The second and third transmembrane helices are connected by one long cytoplasmic sequence [150], where conserved charged residues are believed to make direct electrostatic contact to FliG, a protein of the cytoplasmatic C-ring of the rotor [157, 213]. MotB has one transmembrane domain with a large C-terminal part in the periplasm [158], where it is believed to anchor the motor proteins to the peptidoglycan cell wall [150, 158, 159, 161, 162, 214]. MotA and MotB form a multimer [160, 214, 215] with the composition $MotA_4MotB_2$ [118, 154, 155] and it has been shown that their transmembrane domains are in close proximity [216, 217]. Individual $MotA_4MotB_2$ complexes form proton channels across the inner membrane that couple proton influx to rotation of the flagellum [148-153]. Therefore, strains lacking MotA or MotB posses paralyzed flagella [148, 150, 167-169].

It is believed that a single flagellar motor is energized by 8-12 $MotA_4MotB_2$ stator complexes [164, 165, 211, 218] and that each complex can act independently from the other stator complexes to generate torque [163-166]. MotA and MotB can pre-assemble in the membrane [219] where about 200 MotB proteins build a pool, that can laterally diffuse in the membrane and rapidly exchange with motor assembled MotB [218]. It was demonstrated that

the pre-assembled $MotA_4MotB_2$ complexes can as a whole be incorporated into pre-assembled flagella [163-165]. The proton channels of pre-formed stator complexes which are not docked to the rotor yet are blocked by an amphipathic helix in MotB, named “the plug”, to prevent premature proton influx [220].

Little is known about specific interactions between the lipid bilayer and the flagellar basal body. Nevertheless, mutations in genes involved in lipid metabolism have been found to cause motility phenotypes in *E. coli* [221] and it is known from a number of integral membrane proteins that they have a preferred lipid composition of the bilayer for optimal functioning [222-226]. Environmental factors such as temperature, oxygen partial pressure, pH, water activity, nutrient availability, pressure and the presence of certain chemicals demand adaptation of the lipid bilayer to ensure both integrity and fluidity of the membrane. Membrane adaptations in response to environmental perturbations are known to involve the alteration of the fatty acid composition (reviewed in [227, 228]). Thus, the question remains if and how the functioning of the highly sophisticated flagellum and other membrane factors is affected by adaptive alterations of the lipid bilayer.

Results

CC1064 affects surface attachment and motility of *Caulobacter crescentus*

To identify genes that are involved in *C. crescentus* surface attachment and motility, a transposon insertion mutagenesis and subsequent screen for attachment mutants was conducted. One mutant harbouring a *Tn*5 insertion in the open reading frame *cc1064* displayed an attachment reduced to 40 % of the wild type. The *cc1064* gene encodes a predicted 297 aa protein with a transmembrane helix at the N-terminus and a large periplasmic domain. We became interested in this gene because it is located next to *divJ* (*cc1063*), a gene encoding a sensor histidine kinase involved in cell division, asymmetry generation and also motility and attachment (Fig. S1). In addition to its attachment phenotype, the *cc1064* mutant also displayed severely impaired motility, leading to a colony size on semi-solid agar plates of only about 20 % compared to the wild type on semi-solid agar plates (Fig 1A/B).

To confirm that the described phenotypes are actually caused by loss of *cc1064* function rather than by a polar effect on a nearby gene, a markerless, in frame deletion of the *cc1064* gene was constructed and the resulting strain was tested for its attachment and motility behaviour. Both effects could be reproduced with this non-polar deletion mutant. In addition, the motility and attachment phenotypes could be restored to wild type by providing a copy of *cc1064* from a low-copy number plasmid (Fig. 1A/B). These complementation experiments demonstrate that CC1064 is required for full motility and attachment in *C. crescentus*.

To examine if the reduced motility on semi-solid agar plates was caused by a defect in motility or a chemotaxis defect, the swimming behaviour of the cells in liquid medium was analysed with the help of light microscopy. Only a very small subpopulation (about 3 %) of *cc1064* mutant cells was found to be motile (Fig. 1C). This was despite the fact that the distribution of swarmer, stalked and pre-divisional cells was not distinguishable from wild type (data not shown) and there were no differences in the growth rate of Δ*cc1064* cells compared to the wild type (Fig. S2). Thus, the CC1064 protein is required for proper motility.

The Δ*cc1064* phenotype is conditional

Surprisingly, it was discovered that the motility phenotype and the attachment phenotype of the *cc1064* mutant is dependent on the culture conditions. When cultures were incubated with vigorous shaking, the fraction of motile mutant cells was indistinguishable from the wild type (Fig. 1C). This suggested that the oxygen concentration in the medium might influence the motility of the mutant cells. Alternatively, an increase in growth rate in response to higher oxygen concentrations might render a larger fraction of the mutant cells motile.

To distinguish between these two possibilities, continuous culture experiments in a chemostat under carbon-limited growth conditions were performed. During the experiment, growth rate and temperature were kept constant and small aliquots of cells were regularly removed and analysed microscopically to determine their motility. When the oxygen supply was reduced without changing the growth rate, mutant cells stopped swimming after about 75 min. This phenomenon was fully reversible, since replenishment of the oxygen supply restored motility, again within about 75 min minutes (Fig. 2A). A control culture of wild-type cells did not show any change in motility upon alterations of the oxygen feed (Fig. 2B). This indicates that the oxygen concentration, but not growth rate is influencing the Δ*cc1064* phenotype and that CC1064 is required for *C. crescentus* motility under conditions of low oxygen concentration.

Since motility was found to be oxygen dependent, it was tested if the attachment defect of the Δ*cc1064* mutant was also oxygen dependent. Cells were grown under high and low oxygen conditions to the same OD_{660} and then tested for attachment to polystyrene surfaces (Fig 2C). While the attachment of cells grown under low oxygen conditions was reduced to 40 % of the wild type, as observed before, the growth with high oxygen supply led to an increase of attachment to about 75 % compared to wild type cells grown under the same conditions. Thus, the attachment phenotype can only be partially restored by increasing the oxygen supply during cell culturing.

It appeared possible that the observed motility defect was caused by alterations of the cell membrane, as environmental parameters are known to influence membrane composition. Apart from oxygen, another factor involved in the regulation of the membrane composition is ambient temperature (reviewed in [227, 229, 230]. Consequently, the motility and attachment behaviour of the Δ*cc1064* strain grown under high oxygen conditions, but at reduced temperatures (16 °C) was tested. Despite the high oxygen concentrations under these conditions, *cc1064* mutant cells showed very few motile cells (data not shown). Similarly, *cc1064* mutant cells grown under high oxygen but low temperature conditions, displayed reduced attachment to the same levels like at optimal growth temperature but low oxygen

(Fig. 2D). This is despite the fact that the oxygen solubility in aqueous solutions is higher at low temperatures [231]. Taken together, both oxygen supply and growth temperature influence motility and surface attachment of the Δ*cc1064* mutant. Whereas the motility defect could be completely restored to wild-type levels, the attachment deficit could only be partially restored upon growth under optimal conditions.

The composition of the lipid bilayer changes upon manipulating the oxygen level of the culture

As pointed out before, it has been shown for several species that changes in the growth temperature or changes of the oxygen supply lead to alterations the composition of the lipid bilayer (reviewed in [227, 229, 230]). The findings described above are consistent with either of two models. CC1064 could play a role for the adjustment of the proper membrane lipid composition under low oxygen and/or low temperature conditions, which in turn might be a necessity for optimal flagellar functioning or assembly. Alternatively CC1064 might by a factor necessary for optimal flagellar functioning or assembly in an altered membrane lipid environment at low oxygen and/or low temperature conditions. To investigate which of these possibilities is correct, an analysis of the total cellular fatty acid content was performed. Samples of wild-type and Δ*cc1064* mutant bacteria were either taken under high or low oxygen growth conditions, the fatty acids were extracted, methylated, and subjected to gas chromatography. It was found that the fatty acid composition differed between the different growth conditions, but no difference between the *cc1064* mutant and the wild type was detected in these experiments (Tab. 1). Low and high oxygen samples mainly differed in the content of unsaturated fatty acids, which was higher under low oxygen conditions. Furthermore, hydroxylated and branched species increased and uneven chain-length fatty acids decreased. This indicates that CC1064 has no influence on the composition of the fatty acids, but may rather be an important factor for flagellar functioning in an altered lipid environment in response to low oxygen and/or low temperature.

The flagellum of a Δ*cc1064* mutant is paralyzed

The expression of bacterial flagellar genes is organised in a highly regulated cascade with different checkpoints. To investigate if the lack of *cc1064* affects one of these flagellar gene expression checkpoints and therefore flagellar function, the activity of representative class II, III and IV promotors and class IV mRNA stability was analysed under conditions where the *cc1064* mutants are non-motile (Fig. 3A). No differences for promotor activities between the

wild type and the Δ*cc1064* mutant could be observed. This indicates full assembly of the flagellar basal body and hook complex. To corroborate this finding and to further examine flagellum morphology, *cc1064* mutant cells were examined with the help of transmission electron microscopy. Flagella of mutant cells grown under conditions where they are non-motile showed no obvious morphological difference compared to the wild type (Fig. 3B). Taken together, the results indicate that *cc1064* is not important for assembly of the basal body, hook or filament, but rather for flagellar functioning, hence flagellar rotation.

An analysis of the swimming speed of the rare motile cells that can be found in a low oxygen culture of a Δ*cc1064* strain showed no difference compared to wild type (Fig 3C). This indicates that the lack of CC1064 leads to either complete loss of flagellar rotation or, in rare cases has no influence at all. Thus, the reason for small swarms on motility agar plates is the strongly reduced proportion of motile cells rather than an overall reduction of the swimming speed.

Suppressor mutations rendering the Δ*cc1064* mutant motile are in *motA* and *motB*

To define the flagellar structures that are altered in the Δ*cc1064* background and lead to non-motility, a screen for spontaneous motile suppressor mutants was performed. Motile suppressors were isolated from motility agar plates after incubation for three days. Genetic mapping experiments and subsequent sequencing identified all suppressor mutants to harbour a single amino acid substitution in MotA or MotB (Fig 4A). All mutants displayed swarming behaviour in semi-solid agar plates that was indistinguishable from wild type (Fig. 4B). Interestingly, all amino acid exchanges in the suppressor mutants are located in or very close (maximal distance 13 aa) to the transmembrane regions of MotA and MotB. It is worth pointing out that several suppressor mutants harboured substitutions of the same amino acid to chemically unrelated amino acids (e.g. Ser52 to Cys, Gly or Arg).

Next, the attachment phenotypes of the motile suppressor mutants were assayed. Attachment for all tested motile suppressor mutants was found to be only partially restored with relative attachment levels of about 70 % compared to the wild type (Fig. 2C/D). These attachment values correspond to levels observed for the parental Δ*cc1064* strain grown under high oxygen conditions, where motility is not affected. Also, the attachment levels of the motile suppressor mutant were found to be insensitive to oxygen as well as temperature (Fig. 2C/D). Together these findings argue for a model where in addition to its motility dependent

attachment phenotype, CC1064 also plays a role for attachment that is independent of its function in motility.

As MotA and MotB form a proton channel across the membrane it appeared possible that the suppressor mutations lead to an increased proton influx, which then might compensate the Δ*cc1064* motility defect. It was shown that elevated ion leakage can lead to growth impairment and is therefore costly [220]. To test if the motile suppressors might exhibit increased influx and therefore might show impaired growth, growth rates of several isolated suppressor mutants were determined. All tested mutants showed the same growth rate as the wild type. To rule out that the suppressor mutations might have a deteriorating effect on growth in the presence of *cc1064* one particular suppressor mutant with a G58D substitution in MotB was chosen and it was tested if the suppressor mutation causes a growth defect in the *cc1064*$^{+}$ background (Fig. S3). In parallel the motility of the generated strain on semi-solid agar plates was investigated (Fig. 4C). Neither growth rate nor swarm size of the *motB* point mutant in the *cc1064*$^{+}$ background was altered compared to the wild type. Together these results indicate that the mutations that render the Δ*cc1064* strain motile have no measurable costs under the conditions of the assay. Furthermore, it can be concluded from these data that the point mutations are no bypass suppressors that would generally increase motility in any strain background. Instead it is likely that the suppressor mutations have a specific influence in the Δ*cc1064* background.

motA or *motB* suppressor alleles are dominant over the respective wild-type alleles

It was shown that the number of functional stator complexes in the flagellum influences the colony size on semi-solid agar plates [160, 164, 165]. This feature of the flagellar motor was employed to find out if wild-type MotB can assemble in a Δ*cc1064* background. Therefore, $motB_{wt}$ and $motB_{sup}$ alleles were co-expressed. It was reasoned that if in the absence of *cc1064* non-functional wild-type MotB can still assemble and form homo-multimers or hetero-multimers with co-expressed mutant MotB proteins this would result in reduced swimming speed due to reduced number of functional stator complexes per motor [164].

Different *motB* suppressor alleles were expressed from a plasmid in the presence of a chromosomal wild-type allele or vice versa and the motility of the respective strains was tested (Fig 5). Overexpression of *motB*, either the wild-type or a mutant, had no effect on motility in the *cc1064*$^{+}$ background. Also in a Δ*cc1064* background the overexpression of wild-type *motB* did not increase the swarm size compared to a control plasmid. Hence,

increased amounts of *motB* do not change swimming behaviour in the wild type or *cc1064* mutant background. However, expression of any $motB_{sup}$ allele in the Δ*cc1064* background led to full restoration of motility, irrespective of the presence or absence of the wild-type *motB* allele on the chromosome or a plasmid. Thus, under all tested conditions the suppressor alleles are fully dominant over wild-type *motB*.

Combinations of *motA* and *motB* suppressor alleles show allele specific motility phenotypes

A possible explanation for the molecular mechanism by which the amino acid exchanges in MotA and MotB lead to suppression of the Δ*cc1064* motility phenotype is that the affected amino acids interfere with the correct functional assembly in the absence of CC1064. To allow function in the Δ*cc1064* background the amino acid substitutions must alter the protein is some way. To investigate the nature of these changes, it was tested if all mutations in *motA* and *motB* are compatible with each other. 45 combinations of point mutations in *motA* and *motB* were created in the in the Δ*cc1064* background and their motility was tested. The individual *motA motB* double mutants showed motility phenotypes ranging from less motile than the Δ*cc1064* $motA^+$ $motB^+$ strain over intermediate to fully motile (Tab. 2). Interestingly, the motility phenotypes were highly allele specific. For example $motA_{A42T}$ combined with $motB_{V29L}$, $motB_{V29M}$ or $motB_{A40V}$ led to fully motile cells, while the combination of $motA_{A42T}$ with $motB_{A40T}$ or $motB_{G58D}$ led to intermediate motility behaviour and all other combinations with $motA_{A42T}$ led to a severely reduced motility (Tab. 2). Likewise $motB_{L44S}$, which shows severely reduced motility in combination with $motA_{A42T}$, showed the whole range of motility phenotypes when combined with the other available *motA* alleles (Tab. 2). Surprisingly, the pattern of allele specificity does not seem to be dependent on the position of the amino acid exchange nor on structural or chemical properties of the side chains of the amino acids. Even mutations that are predicted to locate on different sites of the inner membrane (e.g. $motA_{I28F}$ and $motB_{V29M}$) showed reduced motility. These findings indicate a complex interconnection between the different motor protein variants.

Under low oxygen conditions CC1064 is required for correct subcellular distribution of the response regulator PleD

Because *cc1064* is located next to the *divJ* gene on the *C. crescentus* genome and because DivJ is known to influence PleD phosphorylation and thereby localisation to the incipient stalked pole during swarmer-to-stalked cell transition, the subcellular localization of PleD was

tested. A C-terminal GFP fusion of the response regulator PleD was introduced into wild-type and Δ*cc1064* cells, respectively. PleD localisation of the resulting strains grown under high oxygen conditions was compared to low oxygen conditions. As cultures reached mid exponential phase, the subcellular localisation of PleD was analysed using fluorescence microscopy (Fig. 6). In stalked and predivisional cells grown under high oxygen conditions, PleD was sequestered to the stalked pole in both wild-type and Δ*cc1064* background. About 55 % of the cells showed a localised polar fluorescent focus. In contrast, under low oxygen conditions PleD was found to be uniformly distributed in the majority (91 %) of *cc1064* mutant cell, while the number of cells showing a PleD focus at the stalked pole was only mildly reduced in the wild type under these conditions (37 %). Together, these data suggest that CC1064 either directly or indirectly functions as a localisation factor for PleD under certain environmental conditions, such as low oxygen.

The localisation of the proteins responsible for PleD activation is not affected by the *cc1064* deletion

Polar sequestration of proteins in general may be abolished in a *cc1064* mutant under low oxygen conditions. To test this hypothesis, different GFP fusion proteins, that are known to localise to different addresses in the cell (DivJ, PleC, and DivK), were tested for their subcellular localization under low oxygen conditions. Neither of these proteins showed an altered localisation pattern in the Δ*cc1064* mutant compared to the wild type (Fig. 7). From this it is concluded that the *cc1064* mutant exhibits no general localisation defect.

A phosphorylation independent, hyperlocalised PleD mutant is localised in the Δ*cc1064* background under all conditions

As the *cc1064* deletion mutant seems to have a PleD specific localisation defect, the next question was if CC1064 affects a feature of PleD that is a prerequisite for localisation, for example the phosphorylation or the dimerisation status, or might alternatively affect or constitute itself a PleD receptor at the stalked cell pole. To distinguish between these two possibilities the localisation of the constitutively active, super localised PleD mutant, $PleD^{*}_{D53N}$, was investigated. $PleD^{*}_{D53N}$-GFP clearly displayed polar localisation when cultures were grown under low oxygen conditions, even in the absence of *cc1064* (Fig. 8). Thus it is unlikely that CC1064 affects a receptor or itself functions as a receptor for PleD. Instead, these results support the idea that either phosphorylation or dimer formation of PleD is impaired in the Δ*cc1064* background.

Cells with a deletion in *cc1064* do not show the developmental phenotypes of a Δ*pleD* mutant

Δ*pleD* mutant strains are known to display several developmental phenotypes, including reduced stalk length, failure of efficient flagellar ejection during swarmer-to-stalked cell transition, which results in hypermotility in liquid culture, and finally delayed holdfast synthesis [47, 170, 174]. The latter phenotype has been described as the reason for the observed attachment phenotype of *pleD* mutants [47]. Therefore, it was tested if the Δ*cc1064* mutant displays any features of *pleD* mutants. First, the stalk length of cells grown under oxygen limitation was quantified using light microscopy. In contrast to the Δ*pleD* mutant, which showed a reduced stalk length of 0.6 µm in average, the Δ*cc1064* had a mean stalk length identical to the wild type (1.0 µm) (Fig. 9A).

Cells grown under the same conditions were also investigated under the electron microscope to visualise the position of the flagellum. As described, the Δ*pleD* mutants showed aberrant flagellar positioning at the tip of the stalk. This morphological distinctive feature was not detectable in the *cc1064* deletion strain (Fig. 9B).

Also, newborn swarmer cells were isolated and initiation timepoint of holdfast synthesis of the synchronised population was examined. Again, the Δ*cc1064* strain behaved like the wild type, producing a detectable holdfast as cells differentiated into a stalked cell, whereas the holdfast synthesis in a *pleD* deletion strain was clearly delayed (Fig. 9C). Thus, all organelles known to be controlled by PleD are unimpaired in the *cc1064* mutant. As a consequence, one must conclude that the activity of PleD is not strongly reduced in the *cc1064* mutant background.

Double deletions of *cc1064* and *pleD* lead to an additive motility phenotype

As shown above, the deletion of *cc1064* leads to a paralysed flagellum. The same phenotype is known for the constitutively active PleD* mutant [61]. This is thought to be caused by the ectopic DGC activity of PleD* in the swarmer cell [14, 61, 186]. Following this idea the aberrant PleD localisation pattern of the *cc1064* mutant might lead to PleD activity in the flagellated swarmer cell, which in turn would lead to premature flagellar arrest. If this hypothesis is correct, a *pleD* mutant should be epistatic over Δ*cc1064*. To test this, a *cc1064*, *pleD* double mutant was constructed and its motility behaviour was assayed. It is important to note that, despite the hypermotility phenotype in liquid culture, the Δ*pleD* mutant displays

smaller colonies on semisolid agar plates compared to the wild type size [61]. It was found that the *cc1064 pleD* double mutant displayed an even smaller swarm size compared to the single Δ*cc1064* and single Δ*pleD* mutant, indicating that both deletions lead to a cumulative phenotype (Fig. 10). From this, it is concluded that CC1064 and PleD influence motility via different pathways and that mislocalisation of PleD is not the molecular base for the motility phenotype of the Δ*cc1064* strain

Mutations in *motA* or *motB* cause suppression of the motility phenotype, but do not restore PleD localisation

Little is known about the environmental or internal cues that control PleD activation via DivJ/PleC. Since it has been shown that the flagellum can – in addition to its role for cell locomotion – act as a sensor, that provides the cell with information about for example the viscosity or the wetness of the medium [232, 233] and since *cc1064* was shown here to affect motility and PleD localisation, it appeared possible that the aberrant PleD localisation pattern might be caused by flagellar malfunction. To test this idea PleD localisation was analysed in motile suppressor mutants of a Δ*cc1064* strain. One mutant harbouring a mutation in *motA* and one harbouring a mutation in *motB* were chosen and PleD localisation was tested (Fig. 11). As for the non-motile Δ*cc1064* parental strain, no localised PleD could be observed in the motile suppressors. Thus, it appears unlikely that paralysis of the flagellum is the cause for the PleD localisation defect.

Discussion

CC1064 plays a pleitropic role for motility, PleD localisation and surface attachment

Among many genes that were discovered in a screen for loss of attachment mutants [35] the open reading frame *cc1064* caught our attention because it is located next to *divJ* (Fig. S1) and affected, in addition to attachment, also motility (Fig. 1A, B). Furthermore, both phenotypes were found to be temperature and oxygen dependent (Fig. 1 C, 2A-D). The genetic proximity of *cc1064* and the gene encoding the PleD activator DivJ, together with the involvement of PleD in both motility and attachment control [47, 61] suggested that PleD and CC1064 might act in the same pathway. However, several lines of evidence indicate that CC1064 rather plays a pleitropic role which affects several systems independently.

Firstly, Δ*pleD* Δ*cc1064* double mutants showed an even smaller swarm size than the *pleD* or *cc1064* single mutants (Fig. 10). Hence, the combination of both mutations causes a cumulative motility phenotype which argues against a role for both gene products in the same linear pathway. It rather indicates that the few cells that are motile despite the lack of *cc1064* (Fig. 1C) and therefore are likely responsible for the residual swarming behaviour of the Δ*cc1064* mutants are now experiencing an additional chemotaxis defect caused by the lack of PleD [180].

Secondly, whereas motility and PleD localisation was completely restored under high oxygen conditions at 30 °C (Fig. 1C, 2A, and 6), the attachment behaviour of the Δ*cc1064* mutant could only be partially recovered under these optimal conditions (Fig. 2C, D). It is worth noting in this context that reduced surface attachment has been described as results of loss of motility [47, 192]. The finding that optimal growth conditions could restore surface attachment to ~75 % in a Δ*cc1064* mutant (Fig. 2C, D), together with the finding that fully motile suppressor mutants showed the same relative level of surface attachment independent on the growth conditions (Fig. 2C, D) makes it likely that the conditional part of the Δ*cc1064* attachment defect is caused by the reduced motility. Nevertheless, neither optimal growth conditions nor the motile suppressor mutations could completely restore attachment behaviour to wild-type levels. Thus it is concluded that *cc1064* is required for optimal attachment under any tested condition in addition to its conditional effect on motility.

Thirdly, it appeared possible that malfunction of the flagellar motor might lead to the PleD described mislocalisation. This idea was based on several reports that describe an

additional role of the flagellum as a sensor. One study reports that a decrease in the flagellar rotation rate of the sodium-driven motor of *Vibrio parahaemolyticus* results in a changed flux of sodium ions. The decrease in the rotation rate is explained by sterical inhibition of flagellar turning due to a surface in vicinity. The sodium flux difference was shown to be coupled to the induction of lateral flagellum transcription [232]. Another report suggests that the block of flagellar rotation in *Vibrio cholerae* is a signal for exopolysaccharide synthesis, presumably by influencing the phosphorylation of the regulatory response regulator VpsR [234]. Due to these findings it was considered before that the flagellum of *C. crescentus* could also act as a mechanosensor for surfaces and be part of a signalling cascade required for optimal expression of adhesive properties upon surface contact [47]. PleD is a key mediator for the timing of the transition from swarmer-to-stalked cell [47]. Although delocalisation of PleD is not the reason for the motility defect of the Δ*cc1064* mutant (see above), it appeared possible that the paralysis of the flagellum might cause the localisation defect of PleD. The isolation of motile suppressors of the Δ*cc1064* mutant enabled a test of this idea. However, the finding that PleD is still delocalised in these suppressor mutants (Fig. 11) indicates that it is not motor malfunction which is causing the PleD localisation defect. Localisation experiments in *motA* deletion strains further support this finding and excludes the motor protein itself from being a PleD localisation factor (data not shown). These data indicate that CC1064 influences the spatial distribution of PleD and motor functioning via divergent mechanisms. In summary, the motility phenotype, the delocalisation of PleD and the attachment phenotype are not linked to each other.

Are changes of the lipid bilayer composition responsible for the conditional nature of the Δ*cc1064* phenotype?

The Δ*cc1064* mutant showed similar phenotypes at low ambient temperature and at low oxygen supply (Fig. 2 C, D). Therefore, it was reasoned that the molecular cause for the pleitropic effects must be influenced by both growth conditions. As low oxygen supply (Fig. S2) and low temperature both lead to a decrease of the growth rate it was considered that both external parameters might cause the pleitropic phenotypes by slowing down *C. crescentus* growth. However, in a carbon limited Δ*cc1064* chemostat cultures at a constant, slow growth rate the motility of the cells could be modulated by regulating the oxygen supply (Fig. 2A). This finding indicates a specific function for oxygen in the regulation of motility, despite its influence on growth rate. Therefore, it is concluded that low oxygen supply and likely also

low growth temperature are causing the motility defect independently of their effect on growth rate.

What else could be the reason for the pleitropic phenotype of a *cc1064* mutant and why can the motility and PleD localisation phenotypes only be observed under certain environmental conditions? Several findings point at an involvement of the lipid bilayer. Firstly, temperature and oxygen supply are known to alter the fatty acid composition of the bacterial membrane (reviewed in [227, 229, 230]). Generally speaking, the reduction of growth temperature requires the increase of membrane fluidity. A common response to preserve membrane fluidity is an increase of the proportion of short chain fatty acids and to increase the degree of non-saturated and branched fatty acids [235-239]. Furthermore, the ratio of even and odd chain-length fatty acids has also been demonstrated to increase in response to decreased growth temperature [240]. For the effect of an alteration of the oxygen supply during growth, the fatty acid analysis performed here showed that *C. crescentus* increased the proportion of hydroxylated and branched fatty acids upon decreased oxygen levels (Tab. 1). Although the relative abundance of different unsaturated fatty acid species showed a heterogeneous picture, the overall level of unsaturated fatty acids evidently increased under low oxygen conditions while the number of uneven chain length species droped (Tab. 1). Thus, the changes in the fatty acid composition are qualitatively comparable for both, growth at low temperature and growth at low oxygen.

The second hint towards an involvement of the membrane comes from the time scale on which the bacterial swimming behaviour responds to changes of the oxygen supply. After changing the oxygen input in chemostat experiments, Δ*cc1064* cells responded in approximately 75 min with altered swimming behaviour, which corresponds to 0.25 generation times under these conditions (Fig. 2A). Thus, the changes in swimming behaviour do not reflect a division cycle, as it would be expected for e.g. the *de novo* synthesis of a flagellum. The time scale is rather consistent with the remodelling of a complex system, for example the rearrangement of the lipid bilayer composition.

The last and strongest indication that CC1064 is needed for adaptation of membrane proteins to changing lipid environments comes from the characterisation of motile suppressors mutants. All mutations were found to change residues in or very close to transmembrane regions of the motor proteins MotA and MotB. This close proximity of the position of amino acid exchanges to the membrane suggests a functional relationship. Based on these data, it was reasoned that *cc1064* might have an influence on the membrane composition or alternatively might be required to react adequately to changes in the lipid bilayer. The former

was tested by the analysis of the fatty acid composition in a Δ*cc1064* strain grown under low and high oxygen conditions. Because no severe difference was found when compared to the wild type under the respective conditions (Tab. 1), it was concluded that CC1064 has no influence on the overall fatty acid composition, unless CC1064 does affect the headgroups of the lipids, which have not been examined in the fatty acid analysis, rather than the fatty acid tails. However, one argument speaks against this possibility. A decrease in temperature triggers the Δ*cc1064* phenotype. Therefore, CC1064 must be required under these conditions. However, changes of the lipid headgroup composition are rarely documented under the influence of low temperature [241]. CC1064 may also affect a low abundance fatty acid, which might be below the detection limit in the global fatty acid analysis. Such a fatty acid may be distributed unevenly in the cell in a way that a small global change may lead to a strong local concentration change. Localised lipid species have been reported recently in *Bacillus subtilis* and *Escherichia coli*, where different lipid species specific fluorescent dyes revealed the heterogeneity of the bacterial membrane [242-244]. The same dyes (FM4-64 and NAO) have been tested in *C. crescentus*, but no irregular staining was observed (data not shown). Although this does not rule out the possibility that such lipid domains exist in *C. crescentus*, so far no experimental evidence could be found.

Flagellar paralysis is caused by a stator assembly defect

The transcription of selected flagellar genes in a Δ*cc1064* strain was comparable to the wild type (Fig. 3A) and also examination of the flagellum of *cc0164* mutant cells by electron microscopy showed a morphologically normal filament structure (Fig. 3B). Since flagellar assembly proceeds in a hierarchical manner and because the filament is only assembled after the entire basal body and hook structures are functionally assembled [122-126] this indicates that the cause for the motility defect of the Δ*cc1064* strain is on a functional level or due to the misassembly of proteins that are not part of the flagellar regulation hierarchy. This notion is further corroborated by the finding that all motile suppressors of the Δ*cc1064* strain harbour changes in MotA and MotB (Fig. 4A) and non-functional *motA* or *motB* alleles cause a paralysis of the flagellum [148, 150, 167-169].

It is interesting to note in this context that even under low oxygen conditions and under low temperature conditions, a small subpopulation of cells was found able to swim and that these cells showed a fully functional flagellum as judged by their wild-type swimming speed (Fig. 3C). This digital phenotype, completely non-motile or fully functional, indicates that CC1064 itself is not required for motility. It rather facilitates some molecular event, like e.g. motor

assembly, that is required for motility. By chance, few cells may be able to carry out this function even in the absence of CC1064 and these cells then display wild-type swimming behaviour.

A total of 18 amino acid exchanges in either MotA or MotB were found to suppress the motility defect of Δ*cc1064* cells. Interestingly, all of these mutations were equally effective in overcoming the flagellar blockage and no intermediate phenotypes could be observed. It is also worth noting here that the suppressor mutations are specific for the *cc1064* background, as they do not increase swimming performance in general e.g. in the wild type (*cc1064*$^{+}$) background (Fig. 4C) and are thus unlikely to be bypass suppressors. Together, the finding that the flagellum is paralysed in a Δ*cc1064* strain grown under certain conditions together with the finding that MotA and MotB can specifically suppress this defect indicates that wild-type MotA and MotB are not functional under these conditions.

But what is the nature of the defect of the motor proteins and how can we link this defect to the finding that CC1064 is required for adaptation to changes of the membrane composition? All suppressor mutations in *motA* and *motB* lead to amino acid exchanges that are in or very close to the membrane and it is known that changes in the lipid composition, for example in response to low temperature or oxygen, change the solvent properties of the lipid bilayer for many membrane-embedded or -associated proteins [245]. Furthermore, the conformational state of membrane proteins is dependent on these solvent features [246] and molecular assembly in the membrane milieu depends on specific characteristics of the molecules in the lipid fraction [245]. Thus it was considered that the MotA/B complex might either not function correctly or might not be assembled correctly in the absence of CC1064 in an altered lipid environment.

To test if motor unit assembly is affected, wild-type *motB* and suppressor alleles of *motB* were coexpressed. If one assumes that complex formation occurs with comparable probability for both MotB species, one would expect different stator complex species. These would consist of $MotB_{wt}$ homodimers, $MotB_{wt}MotB_{sup}$ heterodimers and MotBsup homodimers. Block et al. [165] showed that the successive incorporation of functional $MotA_4MotB_2$ complexes in a paralyzed motor is able to restore rotation in a stepwise manner. This experiment is known as motility resurrection. Importantly, it was shown that the rotation speed of the flagellum increases stepwise and linearly with the number of assembled stator complexes. Reid et al. [164] found that swimming speed changes were consistent with the incorporation of stators and Garza et al. [160] showed that the colony size on a semi-solid agar plate is correlated with the rotational velocities of tethered cells. Thus one can infer the

number of functional MotA/B complexes per flagellar motor from the swarm size on semi-solid agar plates. In the experiment performed here, overexpression of a mutant *motB* in the *motB*$^+$ Δ*cc1064* background and vice versa the wild-type *motB* overexpression in a *motB*$_{sup}$ Δ*cc1064* background showed wild-type motility behaviour (Fig. 5). This finding indicates that all assembled stator complexes in the flagellar structure are functional and thus argues for a model where only MotB$_{sup}$ molecules and no wild-type MotB can be assembled into the flagellum in the Δ*cc1064* background under low oxygen or low temperature conditions.

Interestingly, one suppressor mutation characterised here lead to an amino acid substitutions in MotB that has been characterised before in a different context in *E. coli*. It was reported that *E. coli* MotB$_{Tyr61}$ is essential for the plug function that prevents proton flux in unassembled stator complexes [220]. When this residue was exchanged for cysteine and overexpressed together with wild type MotA, the cells stopped growing, probably due to a massive influx of protons that acidified the cytoplasm. *E. coli* MotB$_{Tyr61}$ corresponds to MotB$_{Tyr62}$ in *C. crescentus*, which was also found to be exchanged against cysteine in one of the suppressors isolated in this work (Fig. 4A). Although no connection between the plug-function as described by Hosking et al. and the suppression of the Δ*cc1064* motility phenotype could be found here, it was reported that this residue in addition to other residues between Pro52 and Pro65 form an amphipathic helix that is crucial for protein-membrane lipid interaction. This helix and its amphipathic character appear to be conserved in *C. crescentus*. In addition to the Tyr62Cys mutation, two more exchanges have been found in this region, Gly58D and Asp60Thr (Fig. 4A). Both mutations lead to a substitution of uncharged amino acids for charged and polar residues, respectively. Thus, it is concluded that this region of MotB is not only preventing premature proton flux, but is also important for assembly.

Which feature of motor assembly is defective?

Interestingly, a mutation in either MotA or MotB can overcome the stator assembly defect of the *cc1064* mutant. This argues for a model in which not MotA or MotB alone are dysfunctional, but the internal or external interactions of the MotA/B complex are disturbed. To elucidate the nature of this disturbance it was tested whether combinations of the suppressor mutants in *motA* are compatible with those in *motB*. Combinations of different *motA* and *motB* suppressor alleles led to a variety of motility phenotypes ranging from wild-type like colony sizes to less motility than in the Δ*cc1064* strain expressing wild-type *motA* and *motB* (Tab. 2). Furthermore, no obvious pattern was observed when compatible and

incompatible combinations were analysed with respect to the nature and position of the affected amino acid. The most striking example comes from the Ser52 in MotB that could be exchanged for the physico-chemically unrelated amino acids cysteine, glycine, and arginine (Fig. 4A). This led to the conclusion that is not important to gain a specific function, but rather to loose the serine or a small polar amino acid at this particular position. All three Ser52 variants were incompatible with almost all *motA* suppressor mutants (Tab. 2). However, $MotA_{T189A}$ was compatible with the three Ser52 exchanges. This indicates that $MotA_{T189A}$ differs in some respect from all other mutants, though the molecular mechanism is not obvious. In contrast, the exchanges at positions $MotB_{V29L}$ and $MotB_{V29M}$ or $MotB_{A40T}$ and $MotB_{A40V}$ showed completely different compatibility patterns with MotA variants depending on the nature of the amino acid substitution (Tab. 2). Whereas in some cases exchanges with drastically different physico-chemical properties like G58D were widely tolerated, such mild differences like I204L were largely incompatible (Tab. 2). Furthermore, even exchanges that are predicted to be located at different sites of the membrane like for example $MotA_{I28F}$ and $MotB_{V29M}$ were incompatible (Fig. 4A, Tab. 2). It is therefore unlikely that the observed allele specificity reflects direct interaction of the altered amino acids.

Despite the lack of a molecular explanation for these findings, at least two scenarios could explain these results. For example, the different mutations could suppress the Δ*cc1064* phenotype in a number of independent ways of which some are compatible, but some are not. If this explanation were true, one would expect the substitutions to fall into different categories. These categories should result in compatibility patterns that allowed distinguishing between pathways that tolerate and those that exclude each other. The fact that the found suppressor mutations each seem to form a unique category argues against this hypothesis. However, it is conceivable that such a pattern would emerge when extending the suppressor mutant combinations. Alternatively, all the different substitutions may allow motility by targeting one common mechanism. In this case, combination of mutants would likely result in a cumulative effect on this mechanism. As one mutation already renders the motor proteins in a functional state, the combination of two such mutations may lead to a change that exceeds some tolerance threshold over which the stators are not fully functional anymore.

In summary this leads to a model in which CC1064 is required for the correct assembly of motor protein complexes in a lipid environment that is established upon oxygen or temperature stress. The absence of CC1064 results in non- or misassembled stator complexes that can not interact with the rotor of the flagellum. Consequently, the flagellum is paralysed and cells can not swim.

CC1064 is required for PleD localisation under adverse conditions

In addition to the motility and attachment defect, it was realised that the GGDEF domain protein PleD did not localise in the Δ*cc1064* background. Like flagellar paralysis, but unlike the attachment defect, this phenotype is conditional and the localisation of PleD could be re-established under high oxygen conditions. This effect does not appear to be based on a general disturbance of polar identity, as the spatial distribution of polar organelles like the stalk and the flagellum and the subcellular localisation of DivJ, DivK, and PleC was found to be normal. Rather, this defect appears to be specific for PleD. Although the polar identity of *C. crescentus* is not affected by the lack of CC1064, it is striking that all affected processes, like attachment, stator assembly, and PleD localisation are polar processes and employ localised components. What could be the cause for the permanent delocalisation in the Δ*cc1064* background? Either prerequisites for PleD localisation that act on PleD itself, for example phosphorylation [14] or dimerisation [186], are insufficient or a putative factor that recruits PleD to the pole is altered or missing. The finding that $PleD^{*}_{D53N}$ variant which is known to be constitutively active and has a strong propensity to form dimers [14, 61, 186], was localised even under low oxygen conditions in the Δ*cc1064* background (Fig. 8) is an argument that putative recruitment factors are not altered. Therefore it is likely, that the PleD phosphorylation or dimerisation is insufficient in Δ*cc1064* cells.

What is the role of cell cycle dependent PleD localisation?

According to the current knowledge, a defect in phosphorylation or dimerisation is predicted to disrupt PleD activity. Thus, if the absence of polar sequestration of PleD in a *cc1064* mutant at low oxygen conditions is a result of reduced phosphorylation or reduced dimerisation, at least a partial *pleD* phenotype would be expected. However, none of the known *pleD* phenotypes could be detected in a Δ*cc1064* strain (Fig. 4A-C). Especially, the finding that the timing of the holdfast is not delayed, together with the conditional nature of PleD localisation, rule out PleD as the cause for the reduced attachment defect of the Δ*cc1064* mutant under all conditions. Furthermore, the normal localisation pattern of DivK in the Δ*cc1064* cells under low oxygen conditions (Fig. 7) is an indication that the kinase function of the cognate PleD kinase DivJ is not affected, as DivK localisation is dependent on DivJ catalytic activity [177, 247]. Together, these data indicate that the activity of PleD is not altered by the deletion of *cc1064*. These findings raise questions regarding the role of PleD localisation for *C. crescentus* development.

What causes the delocalisation of PleD in the Δ*cc1064* background?

While the localisation experiments with PleD$^{*}_{D53N}$ (Fig. 8) indicate that the PleD localisation defect is caused by an intrinsic feature of PleD, the finding that no Δ*pleD* phenotype could be detected (Fig. 9A-C) argues for the opposite. The molecular reason for the delocalised PleD in a Δ*cc1064* background at low oxygen conditions is therefore unclear. From the finding that PleD can localise at high oxygen growth conditions (Fig. 6), as well as from the PleD$^{*}_{D53N}$ data, one can conclude that CC1064 itself can not be the receptor for PleD. Instead it is possible that CC1064 can influence a polar receptor, perhaps by a similar mechanism as discussed for the motor proteins, without completely abolishing its function. While the hyperlocalised PleD$^{*}_{D53N}$ may still show full polar sequestration, the affinity of wild-type PleD for a polar receptor may be insufficient to be detected. Alternatively, the absence of CC1064 could also reduce the activation of PleD in a way that its activity is still sufficient to maintain PleD function and prevent a Δ*pleD* phenotype. Still, the residual active and therefore localised PleD could be present at too low levels to allow a visualisation in the background noise when expressed as a GFP fusion from a plasmid. Finally, PleD$^{*}_{D53N}$ differs from wild-type PleD not only in its propensity to form dimers, but it also lacks the phosphoryl acceptor site and can therefore not be phosphorylated. This difference may be relevant to establish a localisation phenotype in the Δ*cc1064* background.

Materials and Methods

Growth conditions

E. coli strains were grown at 37 °C in Luria-Bertani (LB) media, *Caulobacter crescentus* strains were grown at 30 °C in peptone-yeast extract (PYE) supplemented with the appropriate antibiotics [196, 197]. For low oxygen conditions 5 ml cell cultures were grown in 14 ml reaction tubes on a rotary wheel at 100 rpm and for high oxygen conditions 5 ml cell cultures were grown 100 ml bevelled Erlenmeyer flasks were used on a gyratory shaker at 200 rpm. Cell density of bacterial cultures were determined by measuring the OD_{660} using a photo spectrometer (Genesys6, Thermo Spectronic, WI, USA).

Continuous culture

To ensure carbon limited growth for chemostat experiments a modified M2 minimal media [196] was used. The basal medium consisted of 12.25 mM Na_2HPO_4, 7.75 mM KH_2PO_4, and 18.70 mM NH_4Cl. The following salts and trace elements were added as a 100-fold concentrated solution after autoclaving the basal medium: 0.50 mM $MgSO_4$, 0.05 mM $FeSO_4$ stabilized with 0.05 mM Na_4EDTA, 0.50 mM $CaCl_2$. Glucose was always autoclaved separately and added after cooling to a final concentration of 1.11 mM. The medium also contained 0.15 ml silicone anti-foam (Fluka) per litre. For continuous culture, computer-controlled glass and stainless steel bioreactors (MBR, Wetzikon, Switzerland) were used and run at a volume of 1 l. pH was kept at 6.5±0.2 by automatic addition of a solution of 0.5 M NaOH and 0.5 M KOH and the temperature was set at 30±0.1 °C. The stirrer speed was set to 25 rpm and the dilution rate was 0.021±0.006 h^{-1}. Oxygen was supplemented at a rate of 50 ml min^{-1} for high oxygen conditions and 15 ml min^{-1} for low oxygen condition. At the indicated time points 1 ml aliquots were taken for further analysis of changes in motility and OD_{660}.

Strain and plasmid generation

The bacterial strains and plasmids used in this study are shown in Table S1. Molecular biology techniques were used as described elsewhere [197]. Plasmids were propagated in *Escherichia coli* strain DH5α or DH10B and introduced into *C. crescentus* via S17-1 by conjugation [196]. The markerless Δ*cc1064* in frame deletion was generated by integration of pNPTS128-deltacc1064 followed by double recombination upon *sacB* counter selection. The presence of the deletion was confirmed by PCR. The different *motA* and *motB* alleles were

transferred between strains by means of general transduction with phage CR30 [196]. As selectable markers, highly cotransducible (~100 % linkage) *tn5*d*cat* transposon insertions in *cc0762* for *motA*, or *tn5*d*kan* insertions in *cc1578* for *motB* were used, respectively. The presence of the mutation was either confirmed with the help of functional assays or sequencing. Exact procedures for strain and plasmid constructions are available upon request.

Phenotypic assays

For attachment assays 200 µl aliquots of logarithmically growing *C. crescentus* cells were transferred to 96 well microtiter plates (Falcon, NJ, USA). Comparable cell density was confirmed (OD_{660} ±0.05) and cells were allowed to bind to the plastic surface for exactly 15 minutes either with (high oxygen conditions) or without (low oxygen conditions) shaking at 200 rpm on a rocking platform for at 30 °C, unless otherwise stated. Attached cells were subsequently quantified by staining with a 0.1 % crystal violet solution (in 5 % 2-propanol and 5 % methanol) and quantification of the retained dye with the help of an Elisa plate reader (Molecular Devices, CA, USA) at 600 nm after dissolving the dye with 20 % acetic acid as described before [47]. For all attachment experiments the mean of at least eight measures is displayed. Error bars represent the standard deviation.

Motility of *C. crescentus* strains was determined using semi-solid agar plates composed of PYE plus 0.3 % agar. Semi-solid agar plates were routinely incubated at 30 °C for 3 days. The colony size was quantified by scanning the plates on an Epson Perfection 4870 Photo scanner (Epson, Japan) and using Photoshop CS v8.0 (Adobe, CA, USA) and ImageJ 1.34 (NIH, USA [198]) software package. For all motility experiments the mean of at least five independent colony sizes is shown. Error bars represent the standard deviation.

Light-, fluorescence- and electron microscopy

An Olympus IX71 microscope equipped with an UPlanSApo 100x/1.40 Oil objective (Olympus, Germany) and a coolSNAP HQ (Photometrics, AZ, USA) CCD camera were used to take fluorescence images. For GFP and Oregon green fluorescence FITC filter sets (Ex 490/20 nm, Em 528/38 nm) were used with an exposure time of 0.5 sec and 1.0 sec respectively. To determine the number of motile cells and the velocity of individual cells, a microchamber using double sided tape (Tesa, USA) was build on a microscope slide. 20 µl of logarithmically growing *C. crescentus* expressing GFP constitutively from plasmid pAD6 were placed in the chamber, which was sealed with a coverslip. Motile cells appeared as bright trail on the photomicrograph. The length of the trail was taken as measure for

swimming velocity. Images were processed with softWoRx v3.3.6 (Applied Precision, WA, USA) and Photoshop CS v8.0 (Adobe, CA, USA) softwares. The same microscopic setup was used to subjectively determine motility of the cells under differential interference contrast (DIC).

To visualise the flagellum of *Caulobacter crescentus* strains, logarithmically growing cultures were washed three times with water, applied for 1 min to glow-discharged, carbon-coated grids and negatively stained with 2 % (w/v) uranylacetate. The samples were viewed in a Philips Morgagni 268D electron microscope at a nominal magnification of 20,000× and an acceleration voltage of 80 kV.

Fatty acid analysis

Cellular fatty acid analysis was performed at the DSMZ (Germany) using a fatty acid methyl-ester analysis (FAME) according to the MIDI microbial identification system (Kim 2001). In brief, exponentially growing bacteria were harvested by centrifugation and lyophilised. The dried bacteria were resuspended in 1 ml 3.8 M NaOH in 50 % methanol and boiled for 35 min. For methylation of fatty acids 2 ml of a 55 % hydrochloric acid solution in methanol was added and heated for 10 ±1 minutes at 80 ± 1 °C. The fatty acid methyl esters were extracted in 1.25 ml 50 % hexane 50 % methyl tert-butyl ether. The organic phase is washed with 3 ml 0.3 M NaOH and subjected to gas chromatography. A 25 m x 0.2 mm phenyl methyl silicone fused silica capillary column was used in combination with a flame ionisation detector and the Sherlock automated pattern recognition software attached to a database (MIDI, DE, USA). The temperature profile for each run was 170 °C to 270 °C at a ramp of 5 °C per minute. Hydrogen is used as carrier gas.

β-Galactosidase activity assays

For β-Galactosidase assays *Caulobacter crescentus* strains were grown in PYE medium, harvested at OD_{660} of 0.4, permeabilized with chloroform, and assayed for β-galactosidase activity according to the method of Miller [248]. The resulting o-nitrophenol product absorption was measured at 420 nm in a photo spectrometer (Genesys6, Thermo Spectronic, WI, USA).

Suppressor generation and mapping

To isolate motile suppressor mutants of Δ*cc1064*, UJ2864 was spotted on a semi-solid agar plate. After 3-4 days of incubation at 30 °C, flares of motile cells became visible and were isolated by restreaking twice on PYE plates.

For determining the locus of suppressor mutations, a Mariner transposon was randomly integrated into the mutant chromosome delivered by pALMAR-1 or pALMAR-3, respectively. A ΦCR30 lysate was prepared on the pooled resulting colonies and transduced in UJ2864 (CB15N Δ*cc1064*). Recombinants were screened for a linked motile phenotype on semi-solid agar plates and the cotransduction frequency of positive hits was determined. The integration site of the transposon was mapped with arbitrary PCR followed by sequencing. The distance between transposon insertion site and mutation was estimated according to West et al. [200]. The resulting area of interest was sequenced.

Synchronization and holdfast staining

Homogenous populations of swarmer cells were isolated as described before [179], resuspended in M2G minimal medium [196] to an optical density of approximately OD_{660} 0.3, and allowed to proceed synchronously throughout the cell cycle. Aliquots of cells were taken every 30 minutes, fixed with 1.5 % formaldehyde and stained with Oregon Green-conjugated wheat germ agglutinin (0.2 mg/ml) for 20 minutes. After washing with water, an appropriate volume of resuspended bacteria was placed on a microscope slide layered with a pad of 2 % agarose dissolved in water and analysed.

Figure legends

Figure 1: CC1064 is required for surface attachment and motility.

(A) An in frame non-polar deletion of *cc1064* can be complemented *in trans*. Wild type (CB15N) and Δ*cc1064* cells with a control vector (pMR10) or a plasmid encoded copy of *cc1064* were spotted in duplicates on a semi-solid agar plate and incubated for 3 days.

(B) Quantification of the motility and attachment phenotypes of Δ*cc1064* with and without trans complementation. Swarm size and relative attachment for the indicated strains are displayed. All parameters are normalized to the wild type (CB15N for motility, CB15 for attachment). Error bars represent the standard deviation.

(C) A Δ*cc1064* culture has a strongly reduced subpopulation of motile cells.

The percentage of motile and non-motile cells for a batch culture of the wild type (CB15N) and Δ*cc1064* were determined as described in material and methods under low oxygen or high oxygen conditions. Note that the high percentage of non-motile cells for the wild type culture is due to the presence of non-motile stalked and predivisional cells.

Figure 2: The Δ*cc1064* phenotypes are oxygen and temperature conditional.

(A/B) Continuous culture experiments. The Δ*cc1064* mutant (A) or the wild type (CB15N) (B) were grown in a chemostat under carbon limitation and constant growth rate as described in material and methods. The oxygen input (air feed given in ml min^{-1}), cell density (OD_{600}) and dilution rate (D given in h^{-1}) are indicated. Motility behaviour of the cells at various time points during continuous culture is indicated by plus (motile) or minus (non-motile) signs below the graph.

(C) The attachment phenotype of Δ*cc1064* cells could only be partially rescued by growth at high oxygen levels. Fast attachment assays with cultures grown at high or low oxygen conditions (see material and methods) with wild type (CB15), *cc1064*::*tn5* and different motile suppressors harbouring *motA* or *motB* suppressor alleles were performed. Values are normalized to the wild type grown under the respective conditions. Error bars represent the standard deviation.

(D) Low growth temperatures lead to an attachment defect of the Δ*cc1064* mutant. Strains and experimental setup are as for Fig. 1C except that incubations were carried out under high oxygen conditions but 16°C (experimental culture) or 30°C (control culture).

Figure 3: The Δ*cc1064* cells harbour a morphologically intact but paralysed flagellum.

(A) Δ*cc1064* mutants do not display defective flagellar gene expression. Specific β-galactosidase activities of Δ*cc1064* cells and wild type control cells (CB15N) carrying plasmids that harbour lacZ reporter fusions to the indicated representative flagellar genes/promotors or a control plasmid (pMR20) are shown. The mean of at least three independent experiments is shown. Error bars represent the standard deviation.
(B) Δ*cc1064* mutants have an apparently intact flagellum. Representative transmission electron micrographs of negatively stained bacteria grown under conditions where the Δ*cc1064* strain is non-motile are shown.
(C) The rare motile cells in Δ*cc1064* cultures under low oxygen conditions display the same swimming speed as wild type cells (CB15N). Swimming speed for individual cells in cultures grown under high or low oxygen conditions was determined as described in material and methods. Average swimming speed of wild type cells and Δ*cc1064* mutant cells are displayed. For wild type and Δ*cc1064* under high oxygen conditions at least 180 cells, for Δ*cc1064* under low oxygen conditions 25 cells were measured. Error bars represent the standard deviation.

Figure 4: Single amino acid exchanges in or close to the transmembrane regions of the flagellar motor proteins suppress the non-motility phenotype of a Δ*cc1064* mutant.
(A) Schematic drawing of the membrane topology of MotA and MotB. Residues predicted to be in the membrane are drawn in light blue; residues altered in the suppressor mutants are shown in red. Transmembrane region were predicted based on the following programs: HMMTOP [249], DAS [250], SOSUI [251-253], TMHMM [254, 255], Mpred [256].
(B) The motility behaviour of *motA* and *motB* suppressor mutants is indistinguishable from wild type. Wild-type *Caulobacter crescentus* (CB15N), the Δ*cc1064* mutant and different motile suppressor mutants were spotted on a semi-solid agar plate and incubated for 3 days. Suppressor mutations in *motA* are indicated in red; those in *motB* are labelled in black.
(C) The suppressor mutations neither cause a growth disadvantage nor increased motility in the *cc1064*$^{+}$ background. The colony areas of wild type (CB15N), Δ*cc1064*, Δ*cc1064* *motB*$_{G58D}$ and *motB*$_{G58D}$ in the *cc1064*$^{+}$ background from a motility-agar plate are displayed. Values are normalized to the wild type. Error bars represent the standard deviation.

Figure 5: *motB* suppressor alleles are fully dominant over the *motB* wild-type allele

The swarm sizes for the indicated mutants or the wild type control (CB15N) harbouring the indicated *motB* alleles on a plasmid or the empty vector (pMR20), respectively, are indicated. Swarm sizes are normalized to the wild type harbouring the control plasmid. Error bars represent the standard deviation.

Figure 6: PleD is delocalised in a Δ*cc1064* background under low oxygen conditions.

The wild type (CB15N) and Δ*cc1064* expressing a plasmid borne copy of *pleD-egfp* were grown under high or low oxygen conditions and analysed for their PleD localisation. Representative images are shown. Arrows indicate PleD-GFP foci.

Figure 7: The *cc1064* mutant has no general localisation defect.

Δ*cc1064* cells expressing either *divJ-gfp*, *pleC-gfp* or *divK-gfp*, respectively, were grown under low oxygen conditions and the subcellular localisation of the various fusion proteins was checked with fluorescence microscopy. Representative pictures are shown. Arrows indicate polar foci of GFP fusion proteins.

Figure 8: A constitutively active PleD mutant is still localised in Δ*cc1064*.

Fluorescence microscopic pictures of wild type (CB15) and Δ*cc1064* cells expressing a plasmid driven copy of $PleD^{*}_{D53N}$-GFP grown under low oxygen conditions. Arrows indicate $PleD^{*}_{D53N}$-GFP foci at the stalked pole of the cells in representative images.

Figure 9: Phenotypes attributed to loss of PleD activity are not altered in Δ*cc1064* mutants.

(A) The stalk length of Δ*cc1064* mutants is not reduced.

The stalk length of the wild type (CB15N), a Δ*cc1064* and a Δ*pleD* mutant grown under low oxygen conditions was measured from differential interference contrast microscopic pictures. Mean stalk length values of at least 50 cells is displayed. Error bars represent the standard deviation.

(B) Δ*cc1064* mutants do not show misplaced flagella.

Cells were grown under low oxygen conditions till mid exponential phase and the morphology of Δ*cc1064* and Δ*pleD* mutants was analysed with the help of transmission electron microscopy. Please note, that due to preparation artefacts flagellar filaments were

frequently sheared, but short fragments attached to the stalk were still detectable in Δ*pleD* mutants as indicated by the arrow.

(C) The onset of holdfast formation is not delayed in the Δ*cc1064* mutant.

Swarmer cells from low oxygen cultures of the wild type (CB15), a Δ*pleD* mutant and a *cc1064*::*tn*5 mutant were isolated and followed through a cell cycle. At indicated phases of the cell cycle, aliquots of cells were probed for the presence of holdfast exopolysaccharides with the help of an Oregon green coupled lection. Red colour represents the DIC channel, green colour the Oregon green channel.

Figure 10: CC1064 does not affect motility via the same pathway as PleD.

The motility behaviour on semi-solid agar plates of the indicated mutant strains was quantified. Values are normalized to the swarm size of the wild type (CB15N) and present means of five independent experiments with the standard deviations indicated as error bars.

Figure 11: Motile suppressor mutants of Δ*cc1064* display dispersed PleD.

PleD localisation was analysed in the indicated motile suppressor mutants of the parental Δ*cc1064* strain expressing a plasmid borne copy of *pleD-gfp*. The strains were grown under low oxygen conditions. Representative pictures are shown.

Figure S1: *cc1064* is located next to *divJ*.

Schematic drawing of the genomic locus of *cc1064*. Structure and annotation were retrieved from the KEGG database (www.genome.jp/kegg).

Figure S2: The Δ*cc1064* mutant has the same growth rate as the wild type.

Wild type (CB15N) and Δ*cc1064* cultures were grown in complex medium at low or high oxygen conditions as described in material and methods and the optical density at 660 nm was determined at indicated time points. The natural logarithm of the cell density is plotted over time.

Figure S3: Growth rates of wild type, Δ*cc1064* mutant or motile suppressor mutants are identical.

Cultures of the indicated strains were grown as described in material and methods. The natural logarithm of the cell density is plotted over time.

Table 1: The oxygen level, but not the absence of *cc1064* has an influence on the fatty acid composition of the *Caulobacter crescentus* membrane.

Wild type (CB15N) and Δ*cc1064* were grown under high and low oxygen conditions to the same OD_{660}, lyophilised and the fatty acid composition was analysed as described in material and methods. Given retention time (RT) values relate to the wild type at high oxygen and fatty acid concentrations are peak areas in arbitrary units.

Table 2: Combinations of $motA_{sup}$ and $motB_{sup}$ alleles show an allele specific motility phenotype in the Δ*cc1064* background.

Mean swarm sizes normalized to the wild type (CB15N) ± standard deviation of Δ*cc1064* strains harbouring the indicated combinations of *motA* and *motB* alleles are shown.

Figure 1

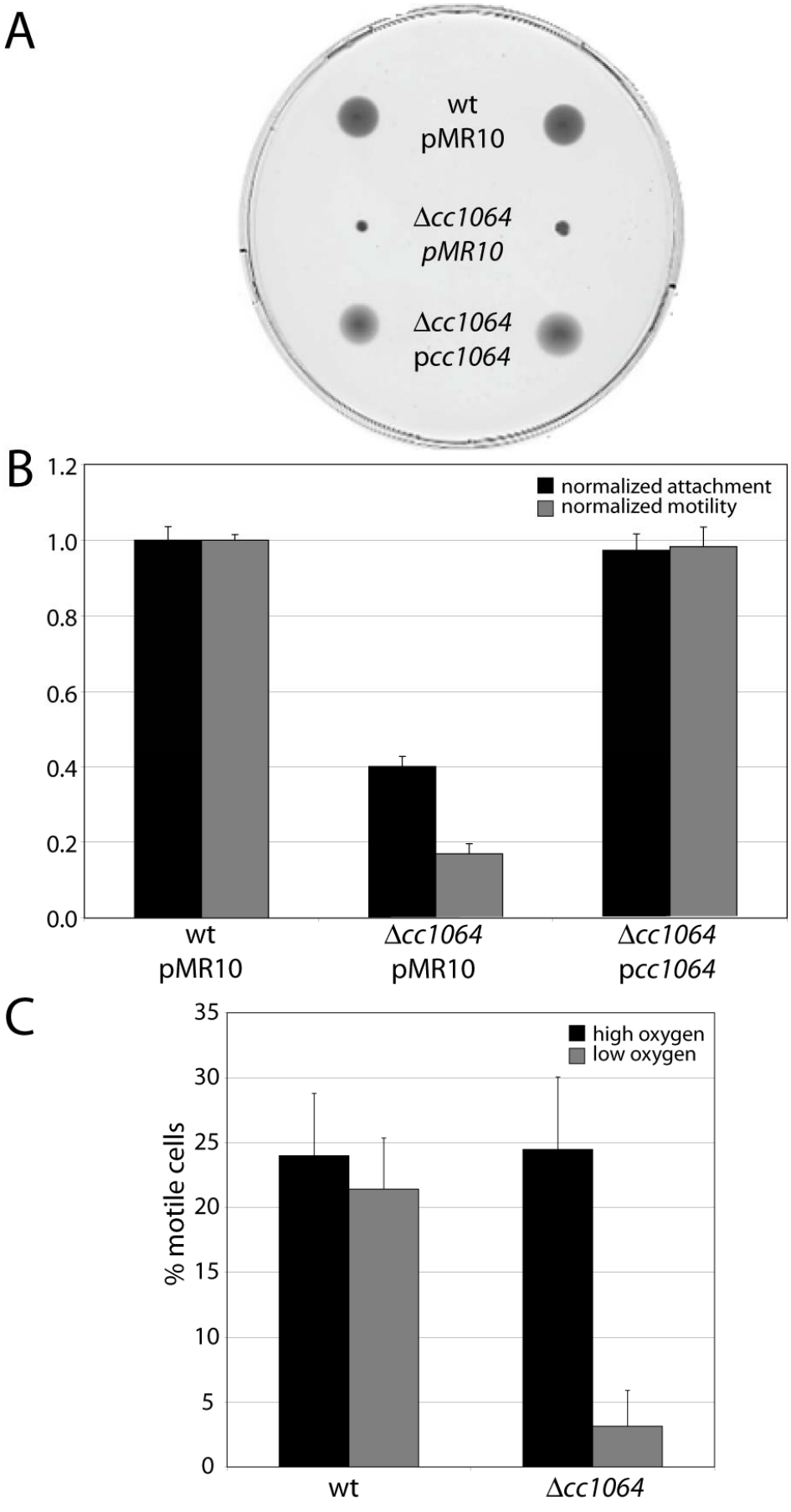
A
wt
pMR10
Δcc1064
pMR10
Δcc1064
pcc1064
B
normalized attachment
normalized motility
1.2
1.0
0.8
0.6
0.4
0.2
0.0
wt
pMR10
Δcc1064
pMR10
Δcc1064
pcc1064
C
high oxygen
low oxygen
% motile cells
35
30
25
20
15
10
5
0
wt
Δcc1064

Figure 2

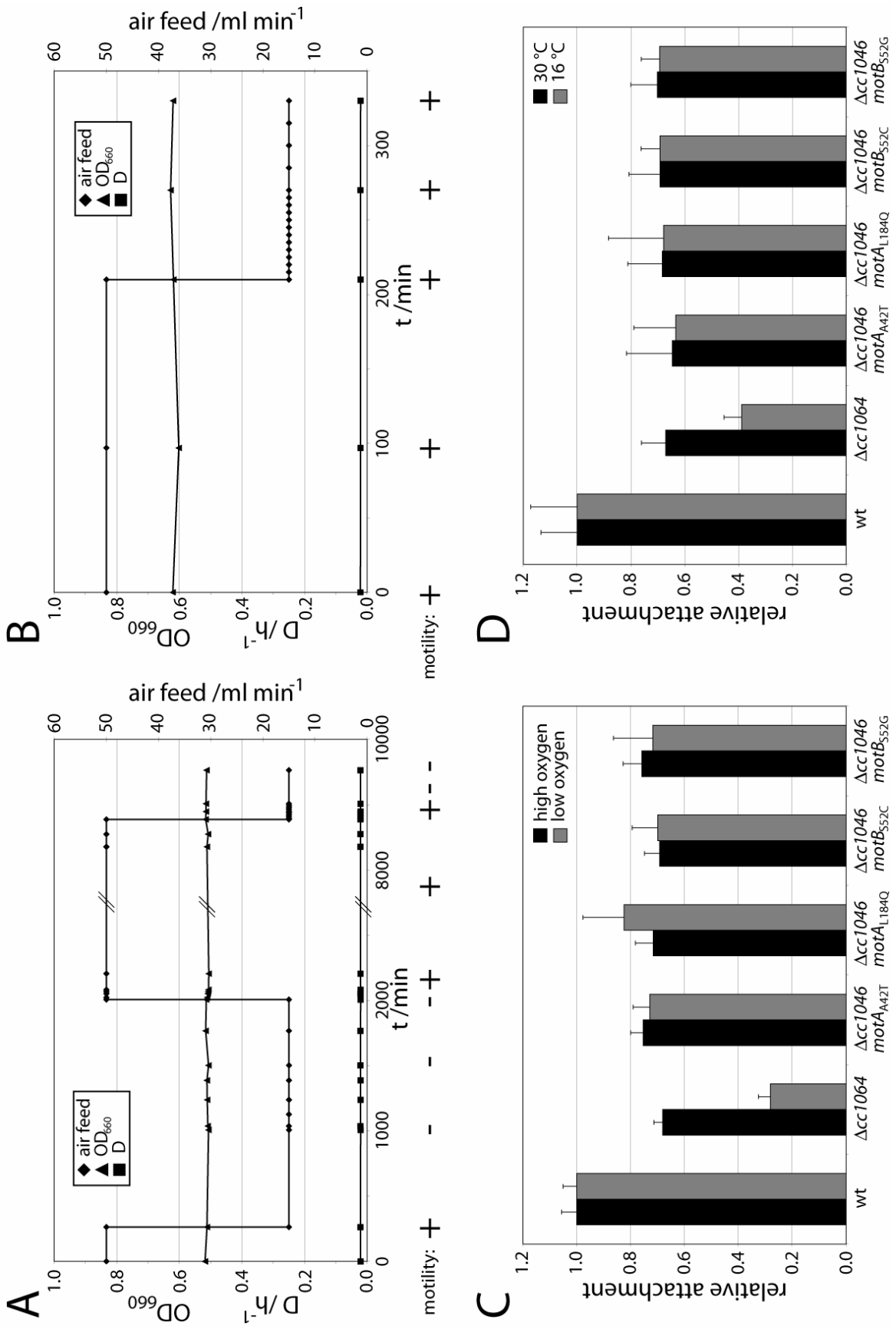
A
B
C
D
air feed /ml min-1
air feed
OD660
D
OD660
D /h-1
t /min
motility:
high oxygen
low oxygen
30 °C
16 °C
relative attachment
wt
Δcc1064
ΔccA42T
ΔccL184Q
Δcc1046 motB552C
Δcc1046 motB552G

Figure 3

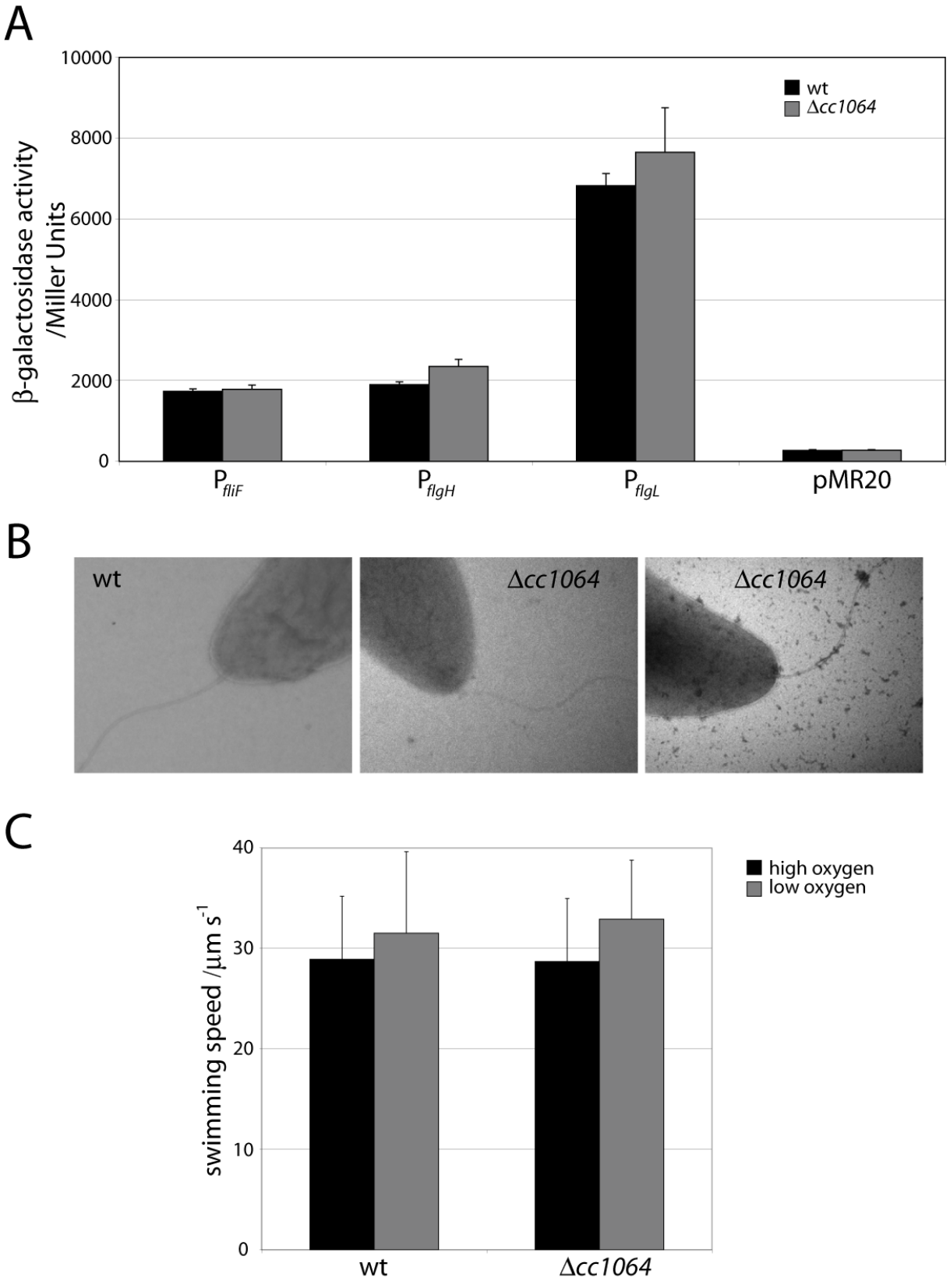
A
10000
8000
6000
4000
2000
0
β-galactosidase activity /Miller Units
wt
Δcc1064
P fliF
P flgH
P flgL
pMR20
B
wt
Δcc1064
Δcc1064
C
40
30
20
10
0
swimming speed /µm s-1
high oxygen
low oxygen
wt
Δcc1064

Figure 4

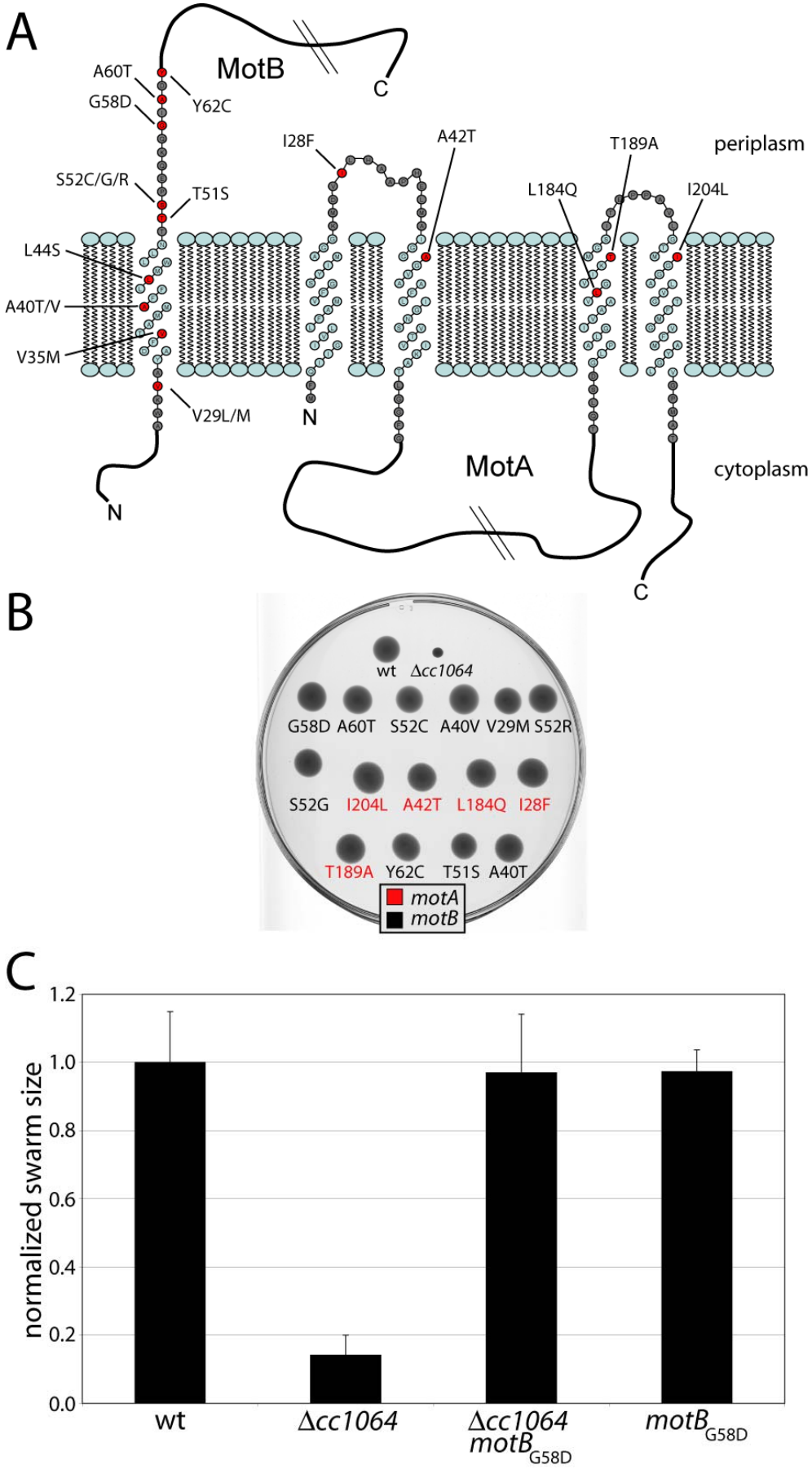
A
MotB
C
A60T
G58D
Y62C
I28F
A42T
T189A
periplasm
S52C/G/R
T51S
L184Q
I204L
L44S
A40T/V
V35M
V29L/M
N
N
MotA
cytoplasm
C
B
wt Δcc1064
G58D A60T S52C A40V V29M S52R
S52G I204L A42T L184Q I28F
T189A Y62C T51S A40T
motA
motB
C
normalized swarm size
1.2
1.0
0.8
0.6
0.4
0.2
0.0
wt
Δcc1064
Δcc1064 motB G58D
motB G58D

Figure 5

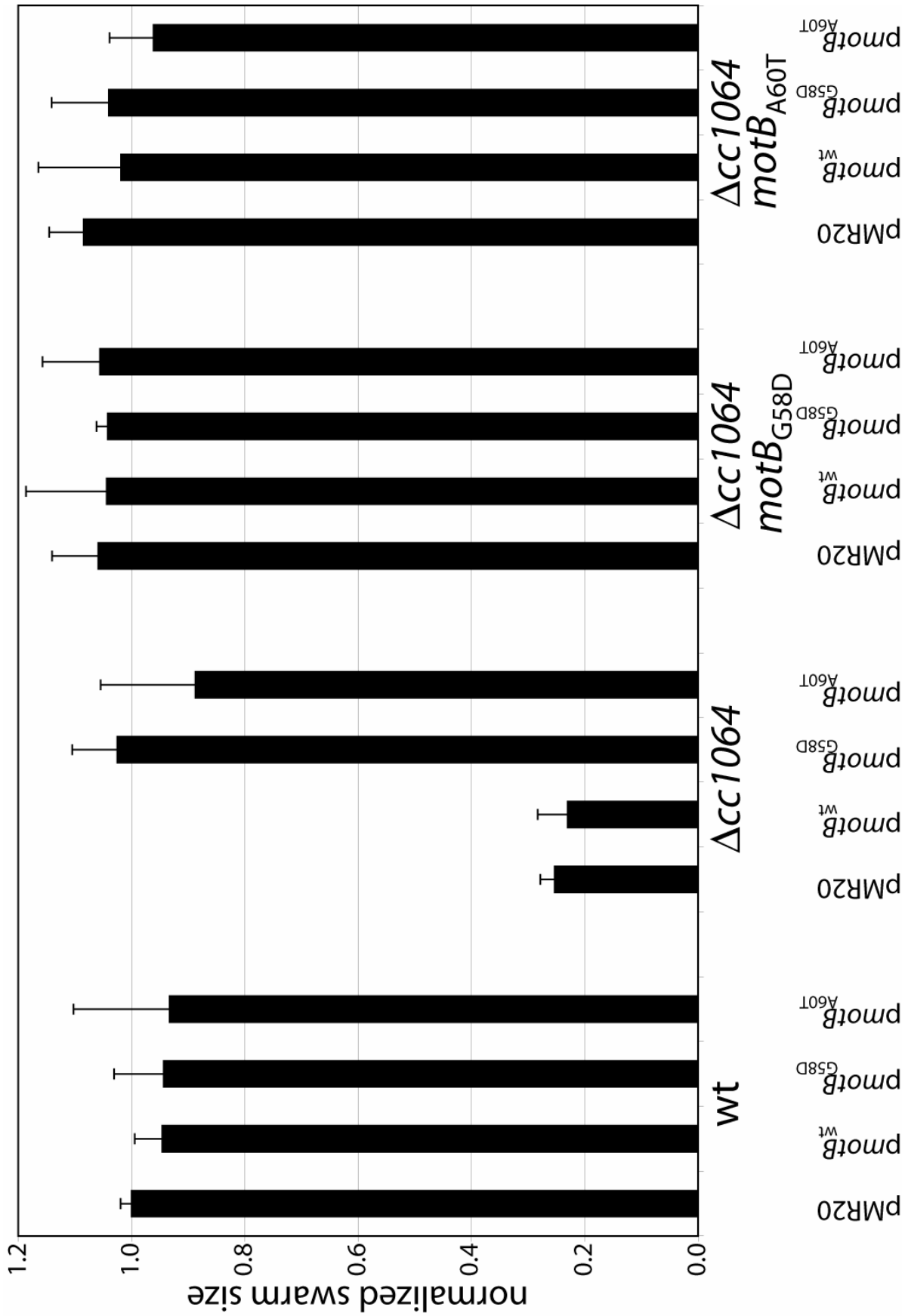
normalized swarm size
0.0
0.2
0.4
0.6
0.8
1.0
1.2
wt
Δcc1064
Δcc1064 motB G58D
Δcc1064 motB A60T
pMR20
pmotB wt
pmotB G58D
pmotB A60T

Figure 6

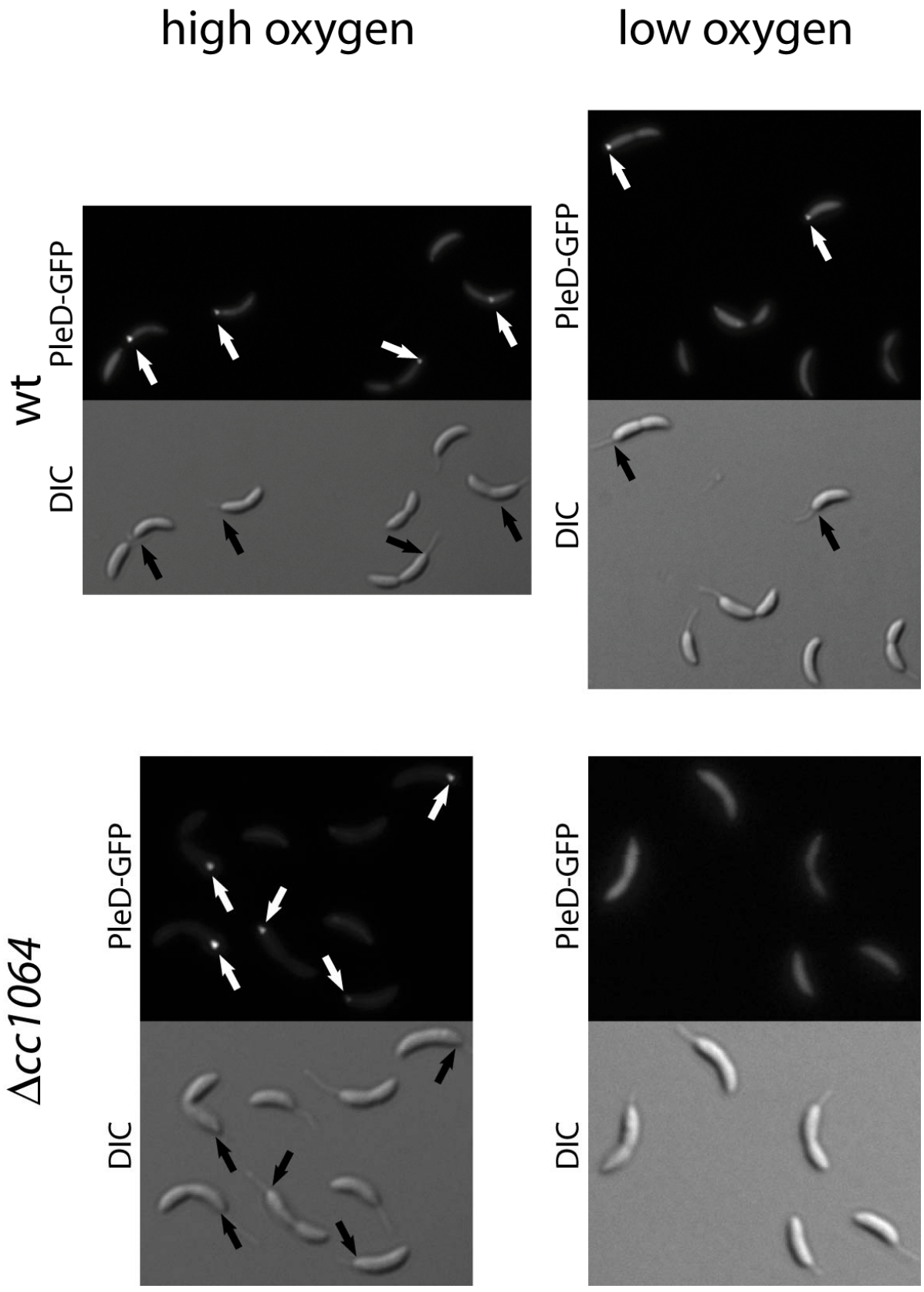
high oxygen
low oxygen
wt
PleD-GFP
DIC
PleD-GFP
DIC
Δcc1064
PleD-GFP
DIC
PleD-GFP
DIC

Figure 7

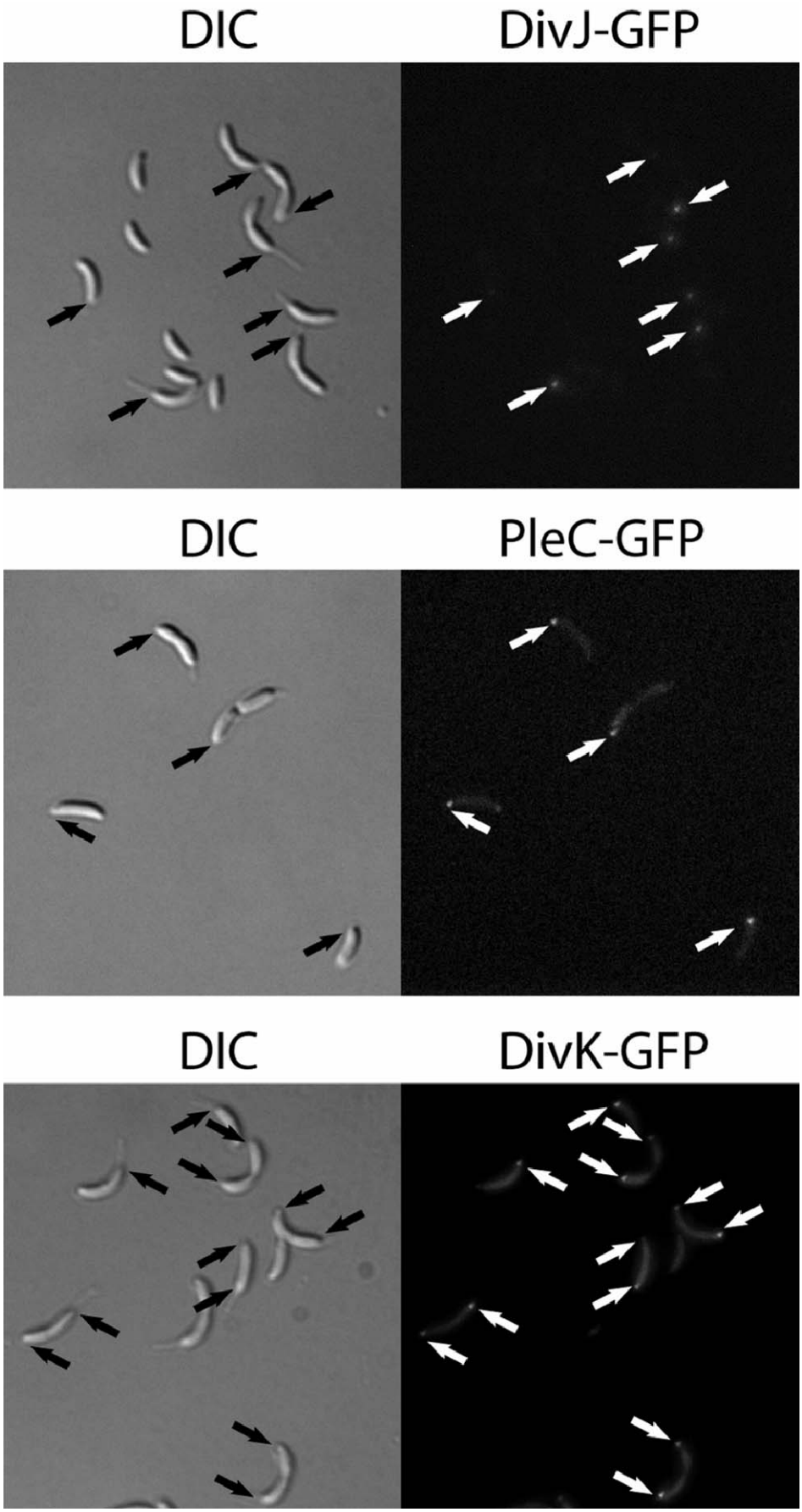

Figure 8

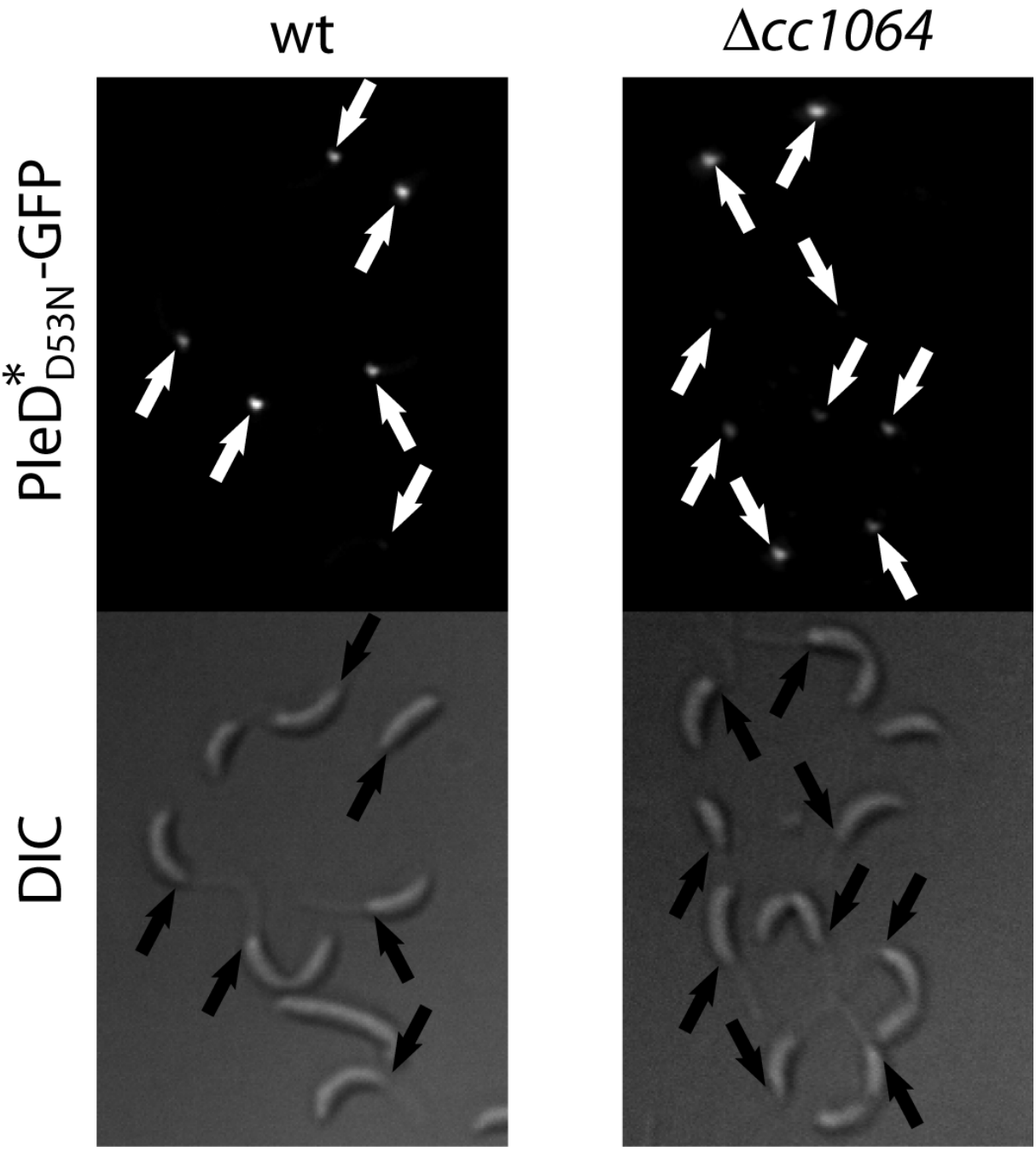

Figure 9

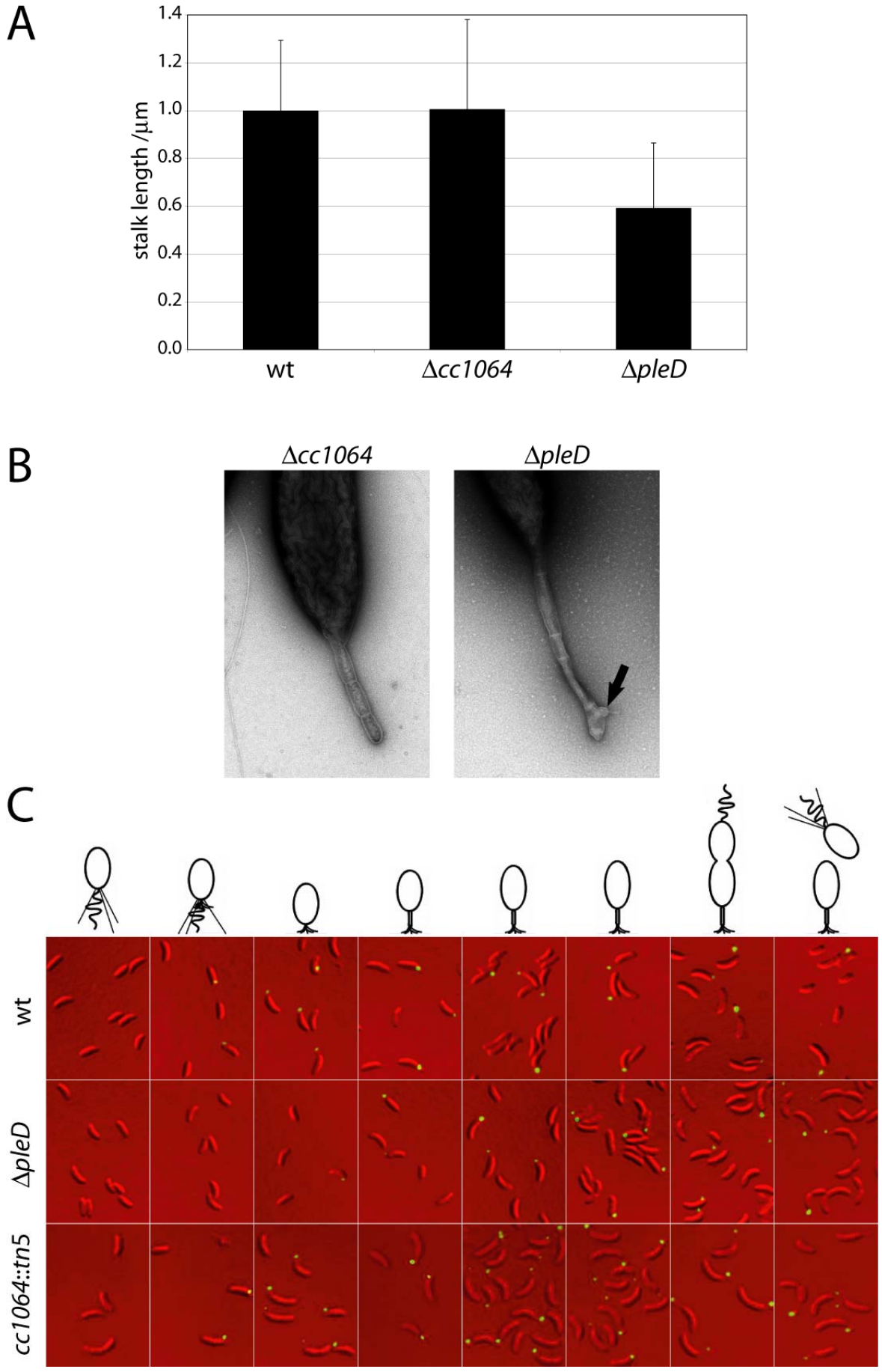
A
stalk length /µm
1.4
1.2
1.0
0.8
0.6
0.4
0.2
0.0
wt
Δcc1064
ΔpleD
B
Δcc1064
ΔpleD
C
wt
ΔpleD
cc1064::tn5

Figure 10

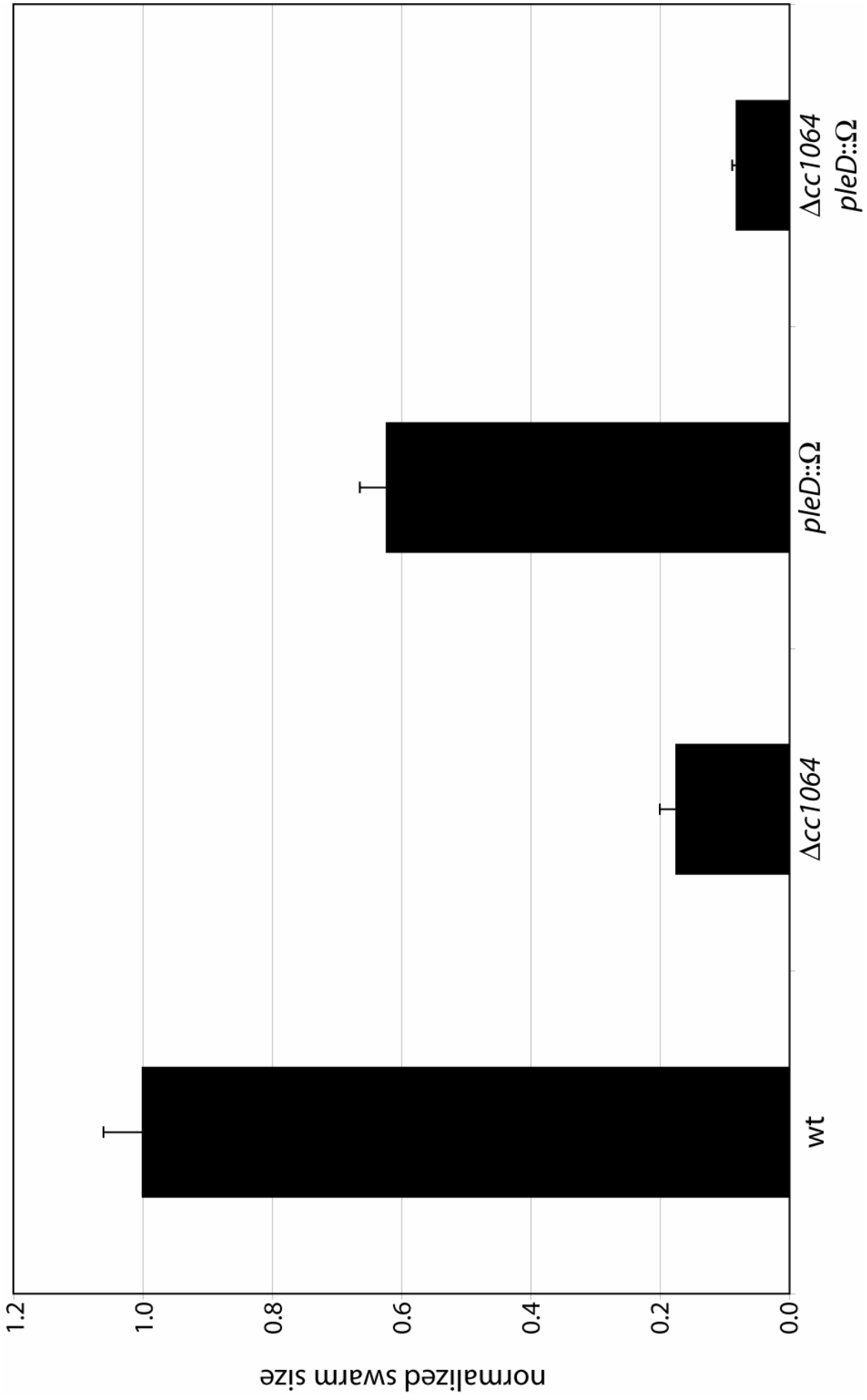
normalized swarm size
0.0
0.2
0.4
0.6
0.8
1.0
1.2
wt
Δcc1064
pleD::Ω
Δcc1064 pleD::Ω

Figure 11

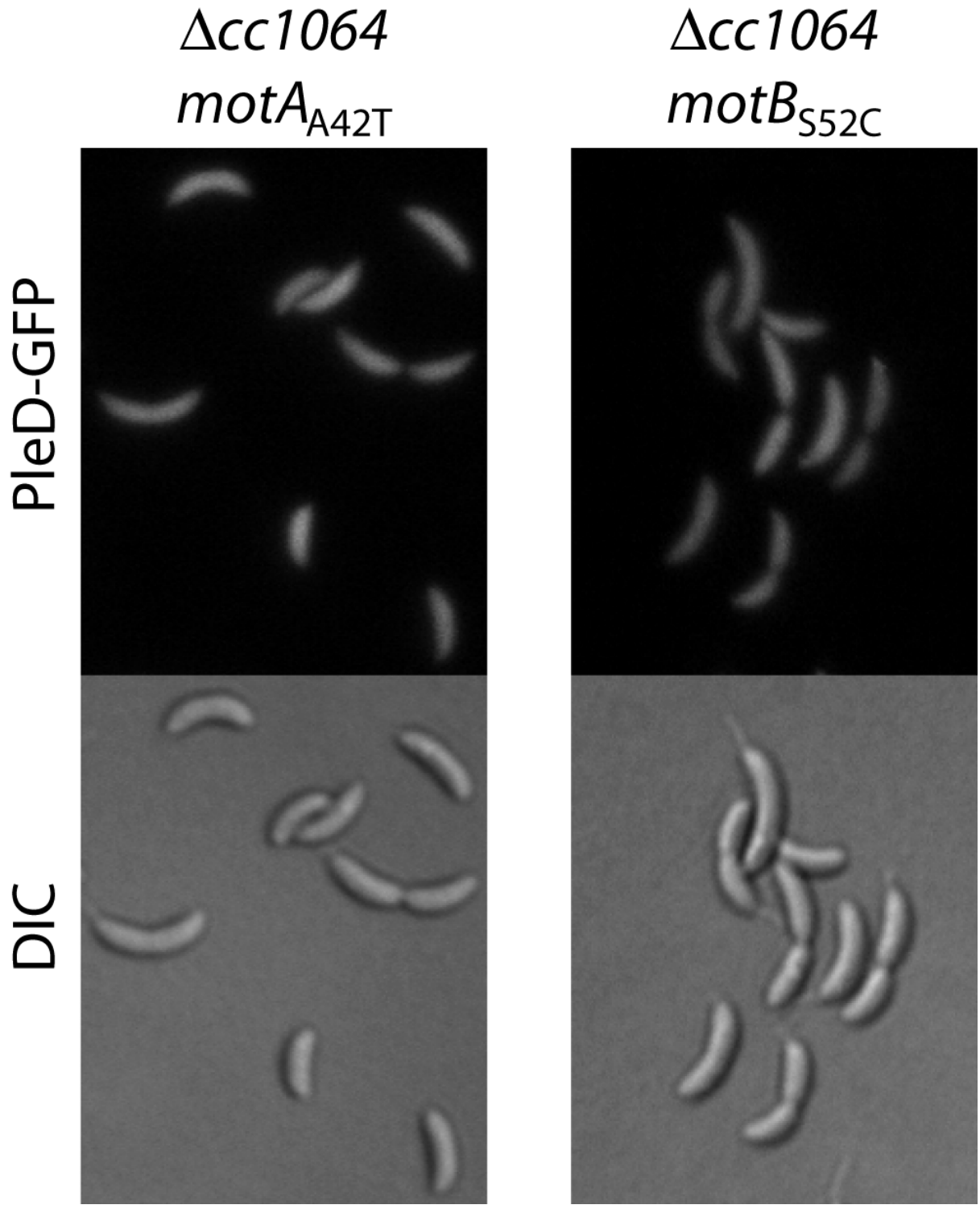

Table 1

RT		6.511	6.742	7.500	8.466	8.722	9.050	9.382	10.411	10.721	12.094	12.215	12.462	12.531	13.915	14.229	14.369	15.624
substance		21:1 3OH	12:0 3OH	14:0	15:0 ISO	15:1 ω8c	15:0	14:0 2OH	16:1 ω7c	16:0	17:1 ω8c	17:1 ω6c	17:0	16:1 2OH	18:1 ω7c	18:0	11 methyl 18:1 ω7c	15:0 ISO 2OH /16:1 ω7c
wt	high oxygen	1.03	0.54	1.67	0.18	0.14	7.03	0.20	10.65	16.68	3.46	2.38	2.42	6.22	43.18	0.43	2.33	10.65
	low oxygen	1.19	0.69	2.59	0.44	n.d.	1.14	0.30	14.18	20.03	0.56	0.34	n.d.	4.15	50.78	0.42	1.57	14.18
Δ*cc1064*	high oxygen	0.98	0.55	1.64	0.21	0.13	6.60	0.22	10.52	16.87	3.23	2.17	2.34	6.19	43.89	0.45	2.70	10.52
	low oxygen	1.24	0.69	2.52	0.45	n.d.	0.92	0.22	13.99	20.35	0.47	0.29	n.d.	3.79	51.70	0.47	1.26	13.99

Table 2

Δ*cc1064*	*motB*$^+$	V29L	V29M	A40T	A40V	L44S	S52C	S52G	S52R	G58D	A60T
motA$^+$	0.289 ±0.029	wt	wt	wt	wt	wt	wt	wt	wt	wt	wt
I28F	wt	wt	0.851 ±0.067	wt	wt	0.262 ±0.019	0.486 ±0.310	0.542 ±0.049	0.624 ±0.044	wt	0.821 ±0.080
A42T	wt	wt	wt	0.480 ±0.020	wt	0.147 ±0.023	0.194 ±0.016	0.206 ±0.018	0.241 ±0.017	0.424 ±0.046	0.227 ±0.013
L184Q	wt	wt	wt	wt	wt	wt	0.583 ±0.073	0.656 ±0.075	0.901 ±0.054	wt	wt
T189A	wt	wt	0.854 ±0.060	wt	0.636 ±0.025	0.891 ±0.062	wt	wt	wt	wt	0.710 ±0.033
I204L	wt	0.400 ±0.032	0.388 ±0.034	wt	0.374 ±0.022	wt	0.724 ±0.038	0.674 ±0.071	0.645 ±0.032	wt	0.556 ±0.043

Figure S1

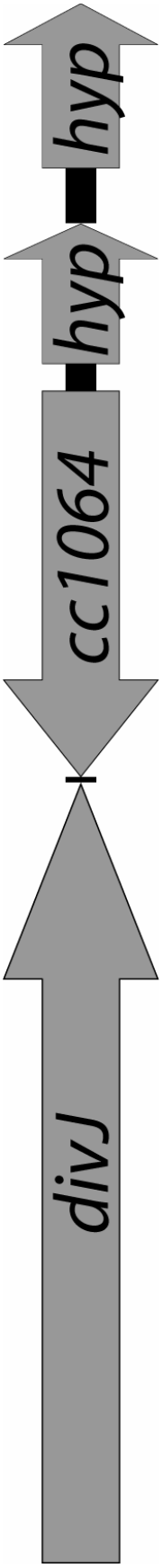

Figure S2

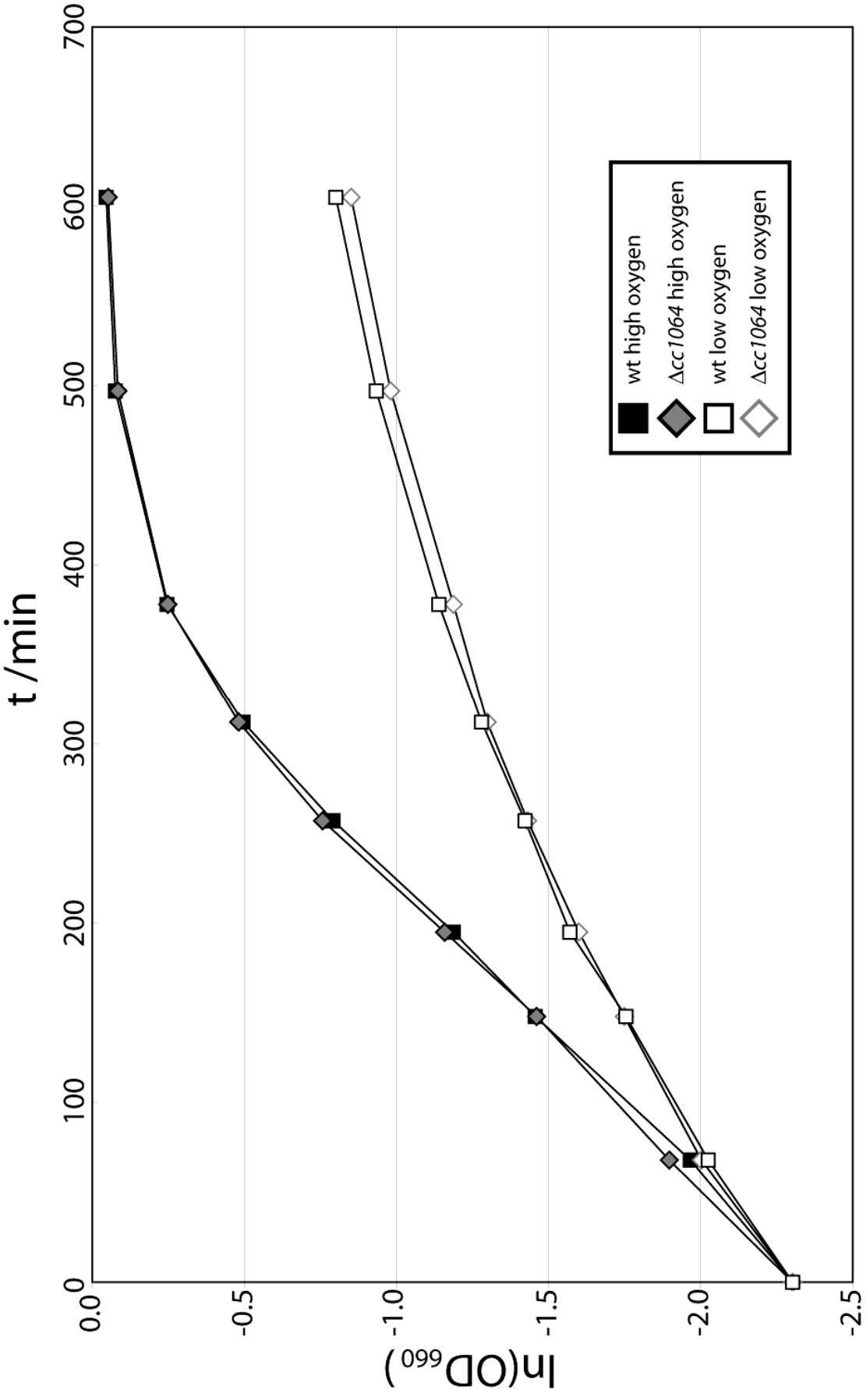
t /min
ln(OD660)
0
100
200
300
400
500
600
700
0.0
-0.5
-1.0
-1.5
-2.0
-2.5
wt high oxygen
Δcc1064 high oxygen
wt low oxygen
Δcc1064 low oxygen

Figure S3

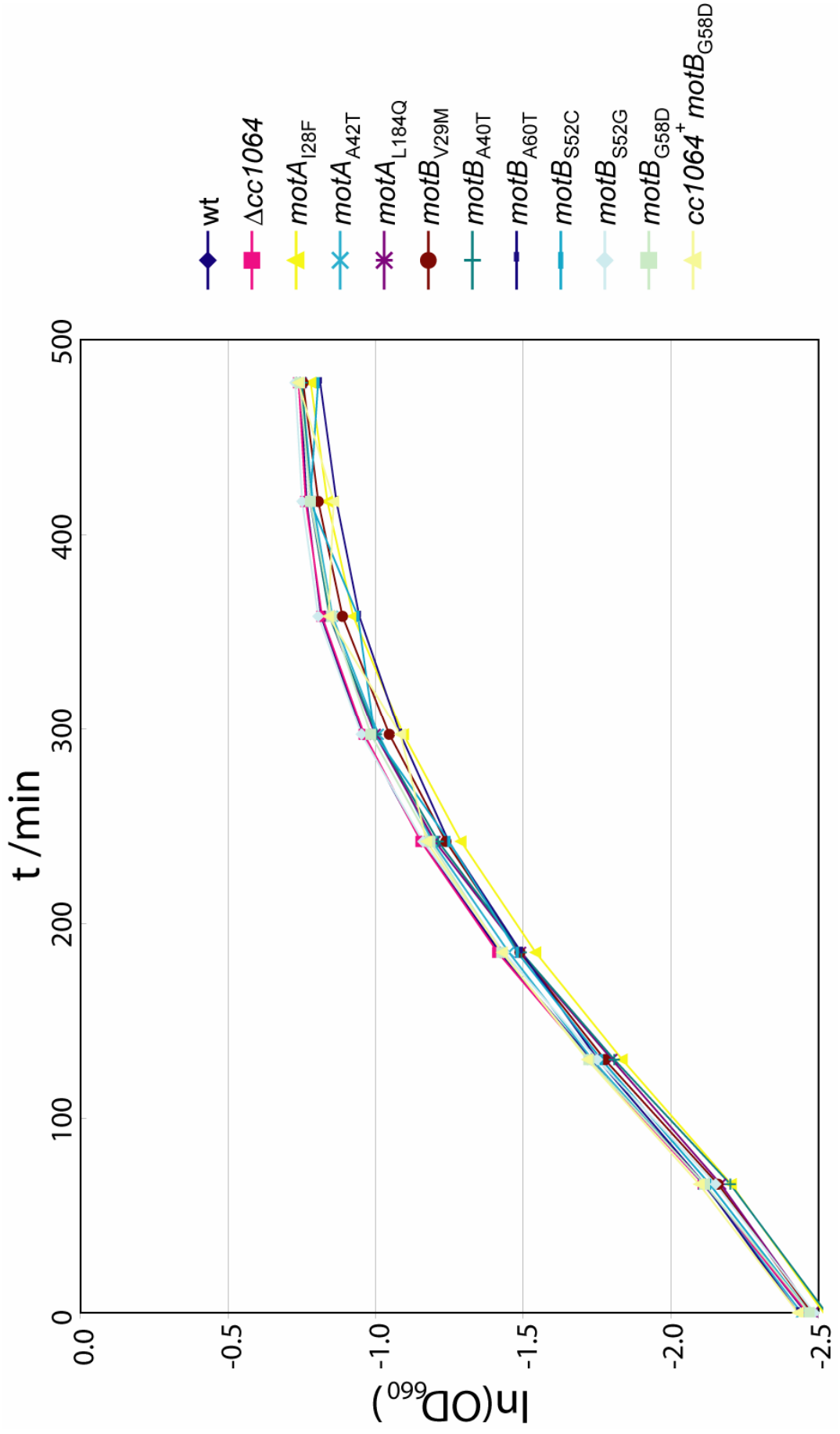
wt
Δcc1064
motA I28F
motA A42T
motA L184Q
motB V29M
motB A40T
motB A60T
motB S52C
motB S52G
motB G58D
cc1064+ motB G58D
t /min
0
100
200
300
400
500
0.0
-0.5
-1.0
-1.5
-2.0
-2.5
ln(OD660)

Table S1

Strain or plasmid	Relevant genotype and description	Reference or source
***C. crescentus* strains**		
UJ195	CB15N *pleD*::Ω	[170]
UJ418	CB15N + pMR20	P. Aldridge
UJ730	CB15 Δ*pleD*	[47]
UJ998	CB15N *divJ*::Ω	[61]
UJ1267	CB15N - synchronizable variant strain of CB15	[114]
UJ2591	CB15 *motA*::*tn*5	A. Levi
UJ2712	CB15N + pOP-290-2	A. Stotz
UJ2713	CB15N + pCM4	[257]
UJ2714	CB15N + pflgL-lacZ	[132]
UJ2715	CB15N Δ*cc1064* + pOP-290-2	this study
UJ2716	CB15N Δ*cc1064* + pCM4	this study
UJ2717	CB15N Δ*cc1064* + pflgL-lacZ	this study
UJ2718	CB15N Δ*cc1064* + pMR20	this study
UJ2719	CB15N Δ*cc1064 divJ*::pdivJgfp	this study
UJ2720	CB15N Δ*cc1064* + pMR10divK-egfp	this study
UJ2724	CB15N + pSA41	this study
UJ2730	CB15N Δ*cc1064* + p*cc1064*	this study
UJ2731	CB15N + pMR10	this study
UJ2742	CB15N Δ*cc1064* + ppleC-egfp	this study
UJ2743	CB15 *cc1064*::*tn*5 $motA_{A42T}$	this study
UJ2747	CB15 *cc1064*::*tn*5 $motA_{L184Q}$	this study
UJ2749	CB15 *cc1064*::*tn*5 $motB_{S52C}$	this study
UJ2750	CB15 *cc1064*::*tn*5 $motB_{S52G}$	this study
UJ2815	CB15N + pAD6	A. Dürig
UJ2864	CB15N Δ*cc1064*	this study
UJ2865	CB15N Δ*cc1064 pleD*::Ω	this study
UJ2912	CB15N Δ*cc1064* + pSA41	this study
UJ2926	CB15N Δ*cc1064 divJ*::Ω	this study
UJ2929	CB15N Δ*cc1064* $motB_{G58D}$	this study
UJ2930	CB15N Δ*cc1064* $motB_{A60T}$	this study
UJ2931	CB15N Δ*cc1064 cc1578*::*tn*Marinerd*NptI* $motB_{G58D}$	this study
UJ2935	CB15N Δ*cc1064* $motB_{S52C}$	this study
UJ2938	CB15N Δ*cc1064* $motB_{A40V}$	this study
UJ2939	CB15N Δ*cc1064* $motB_{V29M}$	this study
UJ2940	CB15N Δ*cc1064* $motB_{S52R}$	this study
UJ2941	CB15N Δ*cc1064* $motB_{S52G}$	this study
UJ2946	CB15N Δ*cc1064 cc1578*::*tn*5	this study
UJ2947	CB15N *cc1578*::*tn*5 $motB_{G58D}$	this study
UJ2997	CB15N Δ*cc1064* + pMR10	this study
UJ3024	CB15N Δ*cc1064* $motA_{A42T}$	this study
UJ3025	CB15N Δ*cc1064* $motA_{L184Q}$	this study
UJ3026	CB15N Δ*cc1064* $motA_{I28F}$	this study
UJ3028	CB15N Δ*cc1064* $motB_{Y62C}$	this study
UJ3029	CB15N Δ*cc1064* $motB_{T51S}$	this study

UJ3030	CB15N Δ*cc1064 motB*$_{A40T}$	this study
UJ3110	CB15N Δ*cc1064* + pAD6	this study
UJ3142	CB15N Δ*cc1064 motB*$_{S52C}$ + pSA41	this study
UJ3143	CB15N Δ*cc1064 motA*$_{A42T}$ + pSA41	this study
UJ3157	CB15N Δ*cc1064 motA*$_{I204L}$ *cc0762*::*tn*Marinerd*Cat*	this study
UJ3158	CB15N Δ*cc1064 motA*$_{T189A}$ *cc0762*::*tn*Marinerd*Cat*	this study
UJ3197	CB15N + pmotB$_{wt}$	this study
UJ3199	CB15N + pmotB$_{G58D}$	this study
UJ3201	CB15N + pmotB$_{A60T}$	this study
UJ3203	CB15N Δ*cc1064* + pmotB$_{wt}$	this study
UJ3205	CB15N Δ*cc1064* + pmotB$_{G58D}$	this study
UJ3207	CB15N Δ*cc1064* + pmotB$_{A60T}$	this study
UJ3208	CB15N Δ*cc1064 motB*$_{G58D}$ + pMR20	this study
UJ3210	CB15N Δ*cc1064 motB*$_{G58D}$ + pmot*B*$_{wt}$	this study
UJ3212	CB15N Δ*cc1064 motB*$_{G58D}$ + pmotB$_{G58D}$	this study
UJ3214	CB15N Δ*cc1064 motB*$_{G58D}$ + pmotB$_{A60T}$	this study
UJ3215	CB15N Δ*cc1064 motB*$_{A60T}$ + pMR20	this study
UJ3217	CB15N Δ*cc1064 motB*$_{A60T}$ + pmotB$_{wt}$	this study
UJ3219	CB15N Δ*cc1064 motB*$_{A60T}$ + pmotB$_{G58D}$	this study
UJ3221	CB15N Δ*cc1064 motB*$_{A60T}$ + pmotB$_{A60T}$	this study
UJ3241	CB15 - *C. crescentus* wild type	ATCC19089
UJ3385	CB15 *cc1064*::*tn*5	this study
UJ3712	CB15N *cc1578*::*tn*5	this study
UJ3748	CB15N *motA*$_{wt}$ *motB*$_{wt}$ *cc0762*::*tn*Marinerd*Cat* *cc1578*::*tn*Marinerd*NptI*	this study
UJ3749	CB15N Δ*cc1064 motA*$_{wt}$ *motB*$_{wt}$ *cc0762*::*tn*Marinerd*Cat* *cc1578*::*tn*Marinerd*NptI*	this study
UJ3750	CB15N Δ*cc1064 motA*$_{wt}$ *motB*$_{G58D}$ *cc0762*::*tn*Marinerd*Cat* *cc1578*::*tn*Marinerd*NptI*	this study
UJ3751	CB15N Δ*cc1064 motA*$_{wt}$ *motB*$_{A60T}$ *cc0762*::*tn*Marinerd*Cat* *cc1578*::*tn*Marinerd*NptI*	this study
UJ3752	CB15N Δ*cc1064 motA*$_{wt}$ *motB*$_{S52C}$ *cc0762*::*tn*Marinerd*Cat* *cc1578*::*tn*Marinerd*NptI*	this study
UJ3753	CB15N Δ*cc1064 motA*$_{wt}$ *motB*$_{A40V}$ *cc0762*::*tn*Marinerd*Cat* *cc1578*::*tn*Marinerd*NptI*	this study
UJ3754	CB15N Δ*cc1064 motA*$_{wt}$ *motB*$_{V29M}$ *cc0762*::*tn*Marinerd*Cat* *cc1578*::*tn*Marinerd*NptI*	this study
UJ3755	CB15N Δ*cc1064 motA*$_{wt}$ *motB*$_{S52R}$ *cc0762*::*tn*Marinerd*Cat* *cc1578*::*tn*Marinerd*NptI*	this study
UJ3756	CB15N Δ*cc1064 motA*$_{A42T}$ *motB*$_{wt}$ *cc0762*::*tn*Marinerd*Cat* *cc1578*::*tn*Marinerd*NptI*	this study
UJ3757	CB15N Δ*cc1064 motA*$_{A42T}$ *motB*$_{G58D}$ *cc0762*::*tn*Marinerd*Cat cc1578*::*tn*Marinerd*NptI*	this study
UJ3758	CB15N Δ*cc1064 motA*$_{A42T}$ *motB*$_{A60T}$ *cc0762*::*tn*Marinerd*Cat cc1578*::*tn*Marinerd*NptI*	this study
UJ3759	CB15N Δ*cc1064 motA*$_{A42T}$ *motB*$_{S52C}$ *cc0762*::*tn*Marinerd*Cat cc1578*::*tn*Marinerd*NptI*	this study

UJ3760	CB15N Δ*cc1064 motA*$_{A42T}$ *motB*$_{S52R}$ *cc0762*::*tn*Marinerd*Cat cc1578*::*tn*Marinerd*NptI*	this study
UJ3761	CB15N Δ*cc1064 motA*$_{L184Q}$ *motB*$_{wt}$ *cc0762*::*tn*Marinerd*Cat cc1578*::*tn*Marinerd*NptI*	this study
UJ3762	CB15N Δ*cc1064 motA*$_{L184Q}$ *motB*$_{S52C}$ *cc0762*::*tn*Marinerd*Cat cc1578*::*tn*Marinerd*NptI*	this study
UJ3763	CB15N Δ*cc1064 motA*$_{L184Q}$ *motB*$_{S52R}$ *cc0762*::*tn*Marinerd*Cat cc1578*::*tn*Marinerd*NptI*	this study
UJ3764	CB15N Δ*cc1064 motA*$_{I28F}$ *motB*$_{wt}$ *cc0762*::*tn*Marinerd*Cat cc1578*::*tn*Marinerd*NptI*	this study
UJ3765	CB15N Δ*cc1064 motA*$_{I28F}$ *motB*$_{A60T}$ *cc0762*::*tn*Marinerd*Cat cc1578*::*tn*Marinerd*NptI*	this study
UJ3766	CB15N Δ*cc1064 motA*$_{I28F}$ *motB*$_{S52C}$ *cc0762*::*tn*Marinerd*Cat cc1578*::*tn*Marinerd*NptI*	this study
UJ3767	CB15N Δ*cc1064 motA*$_{I28F}$ *motB*$_{V29M}$ *cc0762*::*tn*Marinerd*Cat cc1578*::*tn*Marinerd*NptI*	this study
UJ3768	CB15N Δ*cc1064 motA*$_{I28F}$ *motB*$_{S52R}$ *cc0762*::*tn*Marinerd*Cat cc1578*::*tn*Marinerd*NptI*	this study
UJ3769	CB15N Δ*cc1064 motA*$_{I204L}$ *motB*$_{wt}$ *cc0762*::*tn*Marinerd*Cat cc1578*::*tn*Marinerd*NptI*	this study
UJ3770	CB15N Δ*cc1064 motA*$_{I204L}$ *motB*$_{A60T}$ *cc0762*::*tn*Marinerd*Cat cc1578*::*tn*Marinerd*NptI*	this study
UJ3771	CB15N Δ*cc1064 motA*$_{I204L}$ *motB*$_{S52C}$ *cc0762*::*tn*Marinerd*Cat cc1578*::*tn*Marinerd*NptI*	this study
UJ3772	CB15N Δ*cc1064 motA*$_{I204L}$ *motB*$_{A40V}$ *cc0762*::*tn*Marinerd*Cat cc1578*::*tn*Marinerd*NptI*	this study
UJ3773	CB15N Δ*cc1064 motA*$_{I204L}$ *motB*$_{V29M}$ *cc0762*::*tn*Marinerd*Cat cc1578*::*tn*Marinerd*NptI*	this study
UJ3774	CB15N Δ*cc1064 motA*$_{I204L}$ *motB*$_{S52R}$ *cc0762*::*tn*Marinerd*Cat cc1578*::*tn*Marinerd*NptI*	this study
UJ3775	CB15N Δ*cc1064 motA*$_{L189A}$ *motB*$_{wt}$ *cc0762*::*tn*Marinerd*Cat cc1578*::*tn*Marinerd*NptI*	this study
UJ3776	CB15N Δ*cc1064 motA*$_{L189A}$ *motB*$_{A60T}$ *cc0762*::*tn*Marinerd*Cat cc1578*::*tn*Marinerd*NptI*	this study
UJ3777	CB15N Δ*cc1064 motA*$_{L189A}$ *motB*$_{A40V}$ *cc0762*::*tn*Marinerd*Cat cc1578*::*tn*Marinerd*NptI*	this study
UJ3778	CB15N Δ*cc1064 motA*$_{L189A}$ *motB*$_{V29M}$ *cc0762*::*tn*Marinerd*Cat cc1578*::*tn*Marinerd*NptI*	this study
UJ3786	CB15N Δ*cc1064 motA*$_{wt}$ *motB*$_{S52G}$ *cc0762*::*tn*Marinerd*Cat cc1578*::*tn*Marinerd*NptI*	this study
UJ3789	CB15N Δ*cc1064 motA*$_{wt}$ *motB*$_{A40T}$ *cc0762*::*tn*Marinerd*Cat cc1578*::*tn*Marinerd*NptI*	this study
UJ3790	CB15N Δ*cc1064 motA*$_{A42T}$ *motB*$_{S52G}$ *cc0762*::*tn*Marinerd*Cat cc1578*::*tn*Marinerd*NptI*	this study
UJ3791	CB15N Δ*cc1064 motA*$_{A42T}$ *motB*$_{A40T}$ *cc0762*::*tn*Marinerd*Cat cc1578*::*tn*Marinerd*NptI*	this study
UJ3792	CB15N Δ*cc1064 motA*$_{L184Q}$ *motB*$_{S52G}$ *cc0762*::*tn*Marinerd*Cat cc1578*::*tn*Marinerd*NptI*	this study

UJ3793	CB15N Δ*cc1064* $motA_{I28F}$ $motB_{S52G}$ *cc0762*::*tn*Marinerd*Cat* *cc1578*::*tn*Marinerd*NptI*	this study
UJ3794	CB15N Δ*cc1064* $motA_{I204L}$ $motB_{S52G}$ *cc0762*::*tn*Marinerd*Cat cc1578*::*tn*Marinerd*NptI*	this study
UJ3795	CB15N Δ*cc1064* $motA_{A42T}$ $motB_{L44S}$ *cc0762*::*tn*Marinerd*Cat cc1578*::*tn*Marinerd*NptI*	this study
UJ3796	CB15N Δ*cc1064* $motA_{L184Q}$ $motB_{L44S}$ *cc0762*::*tn*Marinerd*Cat cc1578*::*tn*Marinerd*NptI*	this study
UJ3797	CB15N Δ*cc1064* $motA_{I28F}$ $motB_{L44S}$ *cc0762*::*tn*Marinerd*Cat* *cc1578*::*tn*Marinerd*NptI*	this study
UJ3798	CB15N Δ*cc1064* $motA_{L189A}$ $motB_{L44S}$ *cc0762*::*tn*Marinerd*Cat cc1578*::*tn*Marinerd*NptI*	this study
UJ3799	CB15N Δ*cc1064* $motA_{I204L}$ $motB_{V29L}$ *cc0762*::*tn*Marinerd*Cat cc1578*::*tn*Marinerd*NptI*	this study
UJ3802	CB15N Δ*cc1064* Δ$motA_{wt}$ $motB_{L44S}$ *cc0762*::*tn*Marinerd*Cat* *cc1578*::*tn*Marinerd*NptI*	this study
UJ3803	CB15N Δ*cc1064* Δ$motA_{wt}$ $motB_{V29L}$ *cc0762*::*tn*Marinerd*Cat* *cc1578*::*tn*Marinerd*NptI*	this study
UJ4703	CB15 + pMR10	this study
UJ4704	CB15 Δ*cc1064*+ pMR10	this study
UJ4705	CB15 Δ*cc1064*+ pcc1064	this study
UJ4706	CB15 Δ*cc1064*	this study
UJ4707	CB15 Δ*cc1064* + pSW7	this study
UJ4708	CB15 + pSW7	this study

E. coli strains

DH10B	F- *mcr*A Δ(*mrr*- hsd RMS- *mcr*BC) Φ80d*lacZ*ΔM15 Δ*lac*X74 endA1 recA1 deoR Δ (*ara, leu*)7697 *araD139 galU galK nupG rpsL thi pro hsdR- hsd+ recA RP4-2-Tc*::*Mu-Tn7*	Stratagene
DH5α	*supE44* Δ*lac*U169(Φ80 *lacZ*ΔM15) *hsdR17 recA1 endA1gyrA96 thi-1 relA1*	[204]
S17-1	RP4-2, Tc::Mu, KM-Tn7	[205]

Plasmids

pAD6	pMR20 carrying *egfp* under the control of the Lac promotor	A. Dürig
pALMAR-1	*tn*Mariner harbouring a kanamycin resistance cassette	A. Levi
pALMAR-3	*tn*Mariner harbouring a chloramphenicol resistance cassette	A. Levi
pcc1064	pMR10 carrying wild-type *cc1064* under the control of its own promotor	this study
pCM4	*flgH* transcriptional fusion to LacZ on pRKlac290	[257]
pdivJgfp	pEGFP-N2 carrying a C-terminal *egfp* fusion to *divJ*	[175]
pflgL-lacZ	*flgL* translational fusion to LacZ on pRKlac290	[132]
pUT_Km2	Mini-*Tn*5 transposon delivery vector	[258]
pmotBA60T	pMR20 carrying $motB_{A60T}$ under the control of its own promotor	this study
pmotBG58D	pMR20 carrying $motB_{G58D}$ under the control of its own promotor	this study
pmotBwt	pMR20 carrying $motB_{wt}$ under the control of its own promotor	this study

pMR10	Kan^r broad range low copy cloning vector	[259]
pMR10divK-egfp	pMR10 carrying a C-terminal *egfp* fusion to *divK*	[177]
pMR20	Tet^r broad range low copy cloning vector	[259]
pNPTS128-deltacc1064	Kan^r pLitmus38-derived vector with oriT and *sacB* carrying ~830 bp homology region upstream and downstream of *cc1064*, including the first 134 bp and the last 10 bp of the *cc1064* open reading frame	this study
pOP-290-2	*fliF* promotor transcriptional fusion to LacZ on pRKlac290	A. Stotz
ppleC-egfp	pMR20 carrying a C-terminal *egfp* fusion to *pleC*	[175]
pSA41	pBBR1MSC-2nolac carrying a C-terminal egfp fusion to *pleD*	this study
pSW7	pMR20 carrying a C-terminal gfp fusion to pleD$^*_{D53N}$	[61]

3.3 Activation of the Di-guanylate Cyclase PleD by Phosphorylation-mediated Dimerisation

Ralf Paul, Sören Abel, Paul Wassmann, Andreas Beck, Heiko Heerklotz, Urs Jenal

JBC 282:29170-29177 (2007)

Statement of my work

I contributed to this work by generating GFP fusion constructs of diverse PleD mutants. Furthermore, I performed all microscopy experiments required for this work (Fig. 6).

THE JOURNAL OF BIOLOGICAL CHEMISTRY VOL. 282, NO. 40, pp. 29170–29177, October 5, 2007

Activation of the Diguanylate Cyclase PleD by Phosphorylation-mediated Dimerization*[S]

Received for publication, June 7, 2007, and in revised form, July 19, 2007 Published, JBC Papers in Press, July 19, 2007, DOI 10.1074/jbc.M704702200

Ralf Paul, Sören Abel, Paul Wassmann, Andreas Beck, Heiko Heerklotz[1], and Urs Jenal[2]

From Biozentrum, University of Basel, Klingelbergstrasse 70, Basel CH-4056, Switzerland

Diguanylate cyclases (DGCs) are key enzymes of second messenger signaling in bacteria. Their activity is responsible for the condensation of two GTP molecules into the signaling compound cyclic di-GMP. Despite their importance and abundance in bacteria, catalytic and regulatory mechanisms of this class of enzymes are poorly understood. In particular, it is not clear if oligomerization is required for catalysis and if it represents a level for activity control. To address this question we perform *in vitro* and *in vivo* analysis of the *Caulobacter crescentus* diguanylate cyclase PleD. PleD is a member of the response regulator family with two N-terminal receiver domains and a C-terminal diguanylate cyclase output domain. PleD is activated by phosphorylation but the structural changes inflicted upon activation of PleD are unknown. We show that PleD can be specifically activated by beryllium fluoride *in vitro*, resulting in dimerization and c-di-GMP synthesis. Cross-linking and fractionation experiments demonstrated that the DGC activity of PleD is contained entirely within the dimer fraction, confirming that the dimer represents the enzymatically active state of PleD. In contrast to the catalytic activity, allosteric feedback regulation of PleD is not affected by the activation status of the protein, indicating that activation by dimerization and product inhibition represent independent layers of DGC control. Finally, we present evidence that dimerization also serves to sequester activated PleD to the differentiating *Caulobacter* cell pole, implicating protein oligomerization in spatial control and providing a molecular explanation for the coupling of PleD activation and subcellular localization.

Cyclic 3′,5′-guanylyl and adenylyl nucleotides function as second messengers in signal transduction pathways of eukaryotes and prokaryotes. The synthesis of these molecules is catalyzed by a wide variety of nucleotidyl cyclases, which are active as homo- or heterodimers (1). Monocyclic nucleotidyl cyclases that catalyze the formation of cAMP or cGMP are regulated by small molecules, endogenous domains, or exogenous protein partners, many of which alter the interface of the catalytic domains and therefore the integrity of the catalytic site. Much less is known about catalysis and regulation mechanisms of the recently discovered family of diguanylate cyclases (DGCs).[3] DGCs are responsible for the synthesis of cyclic di-GMP, a ubiquitous second messenger involved in bacterial biofilm formation and persistence (2). Cellular levels of c-di-GMP are controlled through the opposing activities of DGCs and phosphodiesterases, which form two large families of output domains found in bacterial one- and two-component systems (3). The DGC activity is contained within the highly conserved GGDEF domain, whose three-dimensional fold is similar to the catalytic core of adenylate cyclase and the "palm" domain of DNA polymerases (4, 5). Because GGDEF domains are often associated with sensory input domains, it was proposed that these regulatory proteins serve to directly couple environmental or internal stimuli to a specific cellular response through the synthesis of the second messenger c-di-GMP. Similar to monocyclic nucleotidyl cyclases, the controlled formation of catalytically competent GGDEF domain dimers may be a key mode of DGC regulation (2, 5, 6). A simple model proposes that dimerization mediates an antiparallel arrangement of two DGC domains, each of which is loaded with one GTP substrate molecule. Such an arrangement would allow deprotonation of the GTP 3′OH groups and subsequent intermolecular nucleophilic attacks onto the α-phosphate to occur (5).

The diguanylate cyclase PleD controls pole morphogenesis during the *Caulobacter crescentus* cell cycle (4, 7–10). PleD is an unorthodox member of the response regulator family of two-component signal transduction systems with two receiver domains arranged in tandem fused to a GGDEF output domain (5). Phosphorylation by two cognate kinases, PleC and DivJ, is required for the activation and dynamic sequestration of PleD to the differentiating pole (4, 9). Although the first receiver domain (Rec1) serves as phosphoryl acceptor (at the conserved Asp-53 residue), the second receiver domain (Rec2) was proposed to function as an adaptor for dimerization of activated PleD (5, 9). A simple mechanistic model for the activation of PleD proposes that phosphorylation at the conserved Asp-53 of Rec1 induces repacking of the Rec1/Rec2 interface. This in turn would mediate dimer formation by isologous Rec1-Rec2 contacts across the interface and thereby facilitate reorientation and assembly of two C-terminal DGC domains (5). Here we demonstrate that PleD activity can be greatly stimulated *in vitro*

* This work was supported by Swiss National Science Foundation Fellowship 3100A0-108186 (to U. J.). The costs of publication of this article were defrayed in part by the payment of page charges. This article must therefore be hereby marked "*advertisement*" in accordance with 18 U.S.C. Section 1734 solely to indicate this fact.

[S] The on-line version of this article (available at http://www.jbc.org) contains supplemental Figs. S1–S3 and Table S1.

[1] Present address: Leslie Dan Faculty of Pharmacy, University of Toronto, Toronto, Ontario M5S 3M2, Canada.

[2] To whom correspondence should be addressed: Tel.: 41-61-267-2135; Fax: 41-61-267-2118; E-mail: urs.jenal@unibas.ch.

[3] The abbreviations used are: DGC, diguanylate cyclase; c-di-GMP, cyclic diguanylic acid; SEC, size-exclusion chromatography; ITC, isothermal titration calorimetry; DSS, disuccinimidyl suberate; PVDF, polyvinylidene difluoride; GFP, green fluorescent protein.

TABLE 1
Activities of PleD wild-type and mutant proteins
5 μM of each protein was incubated in reaction buffer (see "Materials and Methods") with 100 μM ^{33}P-labeled GTP. For BeF_3 activation 1 mM $BeCl_2$ and 10 mM NaF were added to the reactions.

Protein	Without BeF_3	With BeF_3
	nanomoles of c-di-GMP min^{-1} mg^{-1}	
PleD	3.32 (±0.7)[a]	159.97 (±22.6)
$PleD_{D53N}$	2.38 (±0.3)	1.10 (±0.2)
$PleD_{Y26A}$	ND[b]	0.036 (±0.017)

[a] In parentheses: standard deviation.
[b] ND, not detectable.

by the phosphoryl mimic BeF_3 and that activation of PleD results in dimer formation. Cross-linking experiments revealed that the DGC activity resides entirely in the dimer fraction of activated PleD. Furthermore, controlled dimerization not only modulates DGC activity but is also employed to couple PleD activity to its subcellular sequestration. This is the first demonstration that GGDEF protein dimers represent the active conformation of diguanylate cyclases and confirms that oligomerization can be used to regulate the activity of this abundant class of signaling proteins.

MATERIALS AND METHODS

Strains, Plasmids, and Media—Bacterial strains and plasmids used in this study are shown in Table 1. *Escherichia coli* strains were grown in Luria Broth (LB) media supplemented with antibiotics for selection, when necessary. The exact procedure of strain and plasmid construction is available on request.

Expression and Purification of PleD—*E. coli* cells carrying the respective expression plasmid were grown in 200 ml of LB medium with ampicillin (100 μg/ml), and expression was induced by adding isopropyl 1-thio-β-D-galactopyranoside to 0.4 mM final concentration. After harvesting by centrifugation, the cells were resuspended in TN buffer (50 mM Tris-HCl at pH 8.0, 500 mM NaCl, 5 mM β-mercaptoethanol) and lysed by passage through a French press cell. The suspension was clarified by centrifugation, followed by a high spin centrifugation step (100,000 × *g*, 1 h). The supernatant was loaded onto Ni-NTA affinity resin (Qiagen), washed with TN buffer, and eluted with an imidazole gradient. Elution fractions were examined for purity by SDS-PAGE, and fractions containing pure protein were pooled. PleD was extensively dialyzed first against 500 mM NaCl, 50 mM Tris-HCl, pH 8.0, 5 mM EDTA, pH 8.0, 5 mM β-mercaptoethanol, and than against 250 mM NaCl, 25 mM Tris-HCl, pH 7.8, 5 mM β-mercaptoethanol. Prior to cross-linking experiments PleD was dialyzed against a buffer containing 250 mM NaCl, 5 mM PO_4, and 5 mM β-mercaptoethanol. Analytical size exclusion chromatography (SEC) was performed with a Superdex 200 column on a SMART system (Amersham Biosciences) at a flow rate of 50 μl/min. Preparative SEC to quantitatively strip nickel-nitrilotriacetic acid-purified PleD from bound c-di-GMP was performed on a preparative scale Superdex 200 column on an AEKTA system (Amersham Biosciences).

Enzymatic Assays—Diguanylate cyclase assays were adapted from procedures described previously (Paul *et al.* 4). The standard reaction mixtures with purified PleD contained 50 mM Tris-HCl, pH 7.8, 250 mM NaCl, 10 mM $MgCl_2$ in a 50-μl volume and were started by adding 100 μM GTP/[α-^{33}P]GTP (PerkinElmer Life Sciences, 0.01 μCi/μl). To calculate the initial velocity of product formation, aliquots were withdrawn at regular time intervals, and the reaction was stopped with an equal volume of 50 mM EDTA, pH 6.0. Reaction products (2 μl) were separated on polyethyleneimine-cellulose plates (Macherey-Nagel) in 1.5 M KH_2PO_4/5.5 M $(NH_4)_2SO_4$ (pH 3.5), mixed in a 2:1 ratio. Plates were exposed to a phosphorimaging screen, and the intensity of the various radioactive species was calculated by quantifying the intensities of the relevant spots using ImageQuaNT software (Amersham Biosciences). Measurements were always restricted to the linear range of product formation.

Cross-linking Assays—The purified protein (20 or 25 μM in 100 mM NaCl, 5 mM $NaPO_4$, pH 7.8, 10 mM $MgCl_2$, 5 mM β-mercaptoethanol, ± 1 mM $BeCl_2$/10 mM NaF) was incubated with 2 mM disuccinimidyl suberate (DSS, Pierce) for 0, 1, 5, and 10 min. The cross-linker was inactivated by adding Tris-HCl, pH 7.8, to 50 mM final concentration. After separation on 10% SDS-PAGE and transfer to a PVDF membrane, PleD monomeric and dimeric forms were detected by staining with an anti-PleD antibody (8).

Isothermal Titration Calorimetry—The interaction of PleD with cyclic-di-GMP was measured with a VP-ITC isothermal titration calorimeter from MicroCal (Northampton, MA), with 3 μM PleD in the cell and 90 μM c-di-GMP in the syringe (buffer: 100 mM NaCl, 25 mM Tris-HCl, pH 7.8, 5 mM $MgCl_2$, and 1 mM β-mercaptoethanol). All solutions were thoroughly degassed and equilibrated to 25 °C before filling into the calorimeter. The delay between the injections was set to 5–10 min to ensure complete re-equilibration between subsequent injections. The heat capacity of the interaction between the inhibitor and the protein was estimated through measurements between 5 and 25 °C.

Microscopy and Photography—*C. crescentus* strains were grown in 5 ml of peptone-yeast extract media containing 5 μg/ml tetracycline (PYE/tet) for 18 h at 30 °C on a roller incubator. The stationary phase cultures were diluted 1/50 and grown for another 8–10 h in 5 ml of PYE/tet. For fluorescence imaging 1 μl of bacterial culture was placed on a microscope slide layered with a pad of 2% agarose dissolved in water. An Olympus IX71 microscope equipped with an UPlanSApo 100×/1.40 oil objective (Olympus) and a coolSNAP HQ (Photometrics) charge-coupled device camera were used to take differential interference contrast and fluorescence photomicrographs. For GFP fluorescence fluorescein isothiocyanate filter sets (Ex 490/20 nm, Em 528/38 nm) were used with exposure times of 0.15 and 1.0 s, respectively. Images were processed with softWoRx version 3.3.6 and Photoshop CS version 8.0.

RESULTS

Activation of the PleD Diguanylate Cyclase by Beryllium Fluoride—To investigate the specific requirements for PleD DGC activity and activation *in vitro*, we first set out to define the optimal reaction conditions with respect to pH, the concentrations of monovalent and divalent cations, and protein concentration. PleD was enzymatically active between pH 6.5 and 10.0, with maximal activity between pH 7.5 and 8.5 (supple-

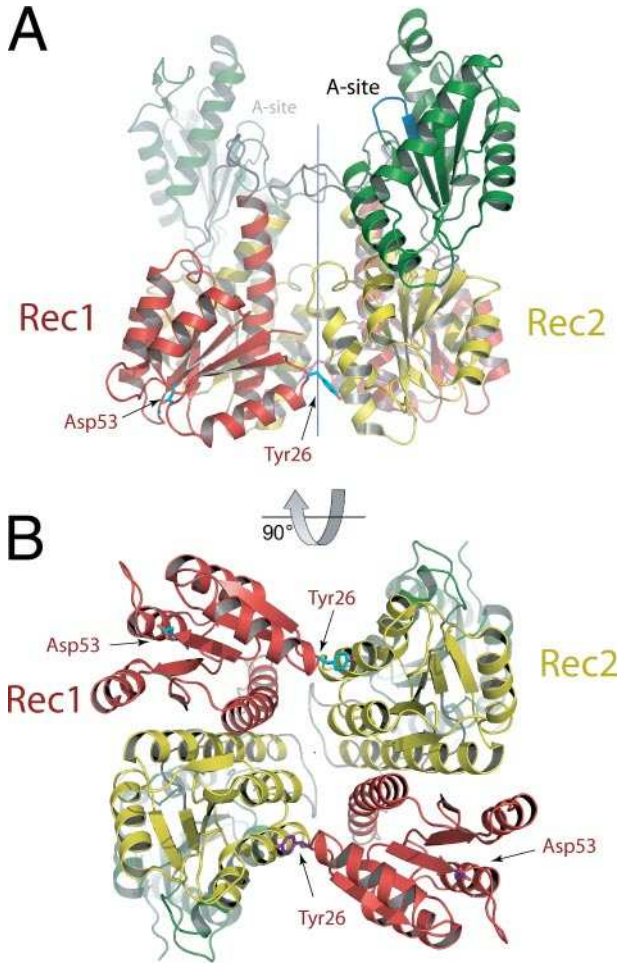

FIGURE 1. **Crystal structure of the non-activated PleD (5).** A front view of a PleD dimer is shown in *A* with the first receiver domain (Rec1) in *red*, the second receiver domain (Rec2) in *yellow*, and the GGDEF domain in *green*. The active site (A-site) loop (*blue*), the phosphoryl acceptor Asp-53, and the position of Tyr-26 are indicated. The 2-fold symmetry axis is drawn in *dark blue*. *B*, *bottom view* along the axis of the Rec1-Rec2 dimerization stem. The domain coloring is equivalent to *A*.

mental Fig. S1). Enzymatic activity was strictly dependent on the presence of either Mg^{2+} (supplemental Fig. S1) or Mn^{2+} (not shown), with Mn^{2+} resulting in a slightly higher activity compared with Mg^{2+}. The strict requirement for bivalent cations is in agreement with the recent finding of coordinating metal ions in the catalytic center of the PleD DGC (11). Activity decreased with increasing NaCl concentration (supplemental Fig. S1). Also, the addition of KCl (25 mM) to reaction assays (4) slightly decreased the enzymatic activity and was omitted in subsequent experiments.

Activation of the PleD DGC *in vitro* and *in vivo* requires the transfer of a phosphoryl group onto the aspartic acid acceptor residue Asp-53 of the first receiver domain (Fig. 1) (4). However, *in vitro* phosphorylation experiments with PleD resulted in an exiguous increase of DGC activity, possibly due to suboptimal assay conditions or to low stability of the phosphorylated form (4). For this reason we tested activation of PleD by beryllium fluoride (BeF_3) a molecular mimic of a phosphoryl group that has been widely used for biochemical and structural studies of bacterial response regulators (12–18). As shown in Fig. 2, BeF_3 significantly stimulated the enzymatic activity of PleD,

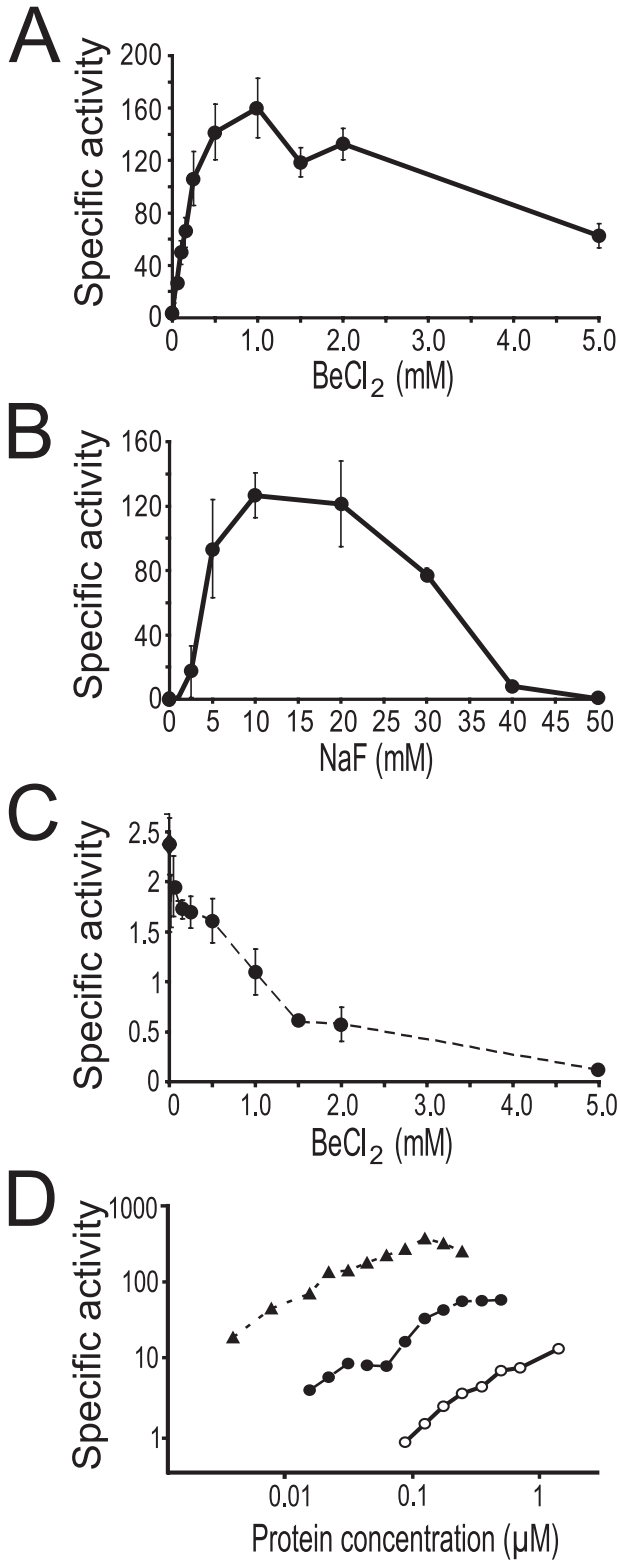

FIGURE 2. **Beryllium fluoride-mediated activation of the PleD diguanylate cyclase.** *A*, PleD (5 μM) activity (nanomoles of c-di-GMP min^{-1} mg^{-1}) as a function of $BeCl_2$ concentration in the presence of 5 mM NaF. *B*, PleD (2.5 μM) activity (nanomoles of c-di-GMP min^{-1} mg^{-1}) as a function of NaF concentration in the presence of 1 mM $BeCl_2$. *C*, $PleD_{D53N}$ (5 μM) activity (nanomoles of c-di-GMP min^{-1} mg^{-1}) as a function of $BeCl_2$ concentration in the presence of 5 mM NaF. *D*, specific activities (nanomoles of c-di-GMP min^{-1} mg^{-1}) for PleD (*open circles*), PleD activated with BeF_3 (*filled circles*), and the constitutively active PleD* mutant protein (*triangles*) as a function of the protein concentration.

with optimal concentrations of 1 mM $BeCl_2$ (Fig. 2*A*) and 10 mM NaF (Fig. 2*B*), respectively. DGC activation was reversible and was immediately abolished upon removal of BeF_3 (data not shown). A PleD mutant protein lacking the phosphoryl acceptor site Asp-53 ($PleD_{D53N}$) could not be activated, suggesting that BeF_3 activates the protein by specifically interacting with this residue in the first receiver domain (Fig. 2*C*). A constitutively active mutant of PleD, PleD* (4) was also stimulated by BeF_3, but only by a factor of 2 (data not shown). This is consistent with the view that PleD* is locked in an active state (see below). Concentrations of $BeCl_2$ or NaF above 1 mM and 10 mM, respectively, had a negative effect on DGC activity (Fig. 2, *A–C*). At these concentrations BeF_3 probably interacts non-specifically with surface residues that are required for diguanylate cyclase activity.

BeF_3 Activation Results in PleD Dimerization—The specific activities of non-activated and BeF_3-activated PleD wild-type protein and of the constitutively active PleD* mutant increased with increasing protein concentration (Fig. 2*D*). This suggested that PleD might be active in a dimeric (or oligomeric) form, with dimer formation being concentration-dependent. The observation that PleD* and BeF_3 activated PleD reach an activity plateau at much lower protein concentrations than non-activated PleD further suggested that the PleD dimerization constant is affected either by genetic changes or by chemical activation of the protein. To test this hypothesis, cross-linking studies were performed with PleD using the chemical cross-linker DSS (see "Materials and Methods"). We reasoned that the amount of covalently cross-linked dimers was proportional to the amount of dimers in solution. When the DSS cross-linker was incubated with non-activated wild-type PleD or $PleD_{D53N}$ at a protein concentration of 20 μM (well below the estimated dissociation constant K_d of dimerization of 104 μM (11)), only a minor fraction of the protein was captured as covalently cross-linked dimers (Fig. 3*A*). This is consistent with the low basal level of enzymatic activity observed for non-activated PleD (Table 1). Activation of PleD by BeF_3 not only increased DGC activity (Table 1) but also the amount of cross-linked dimer species (Fig. 3*A*). In contrast, the non-activable $PleD_{D53N}$ (Fig. 2 and Table 1) showed no increase in cross-linked dimers (Fig. 3*A*).

The crystal structure of non-activated PleD predicted a specific dimerization interface in the Rec1-Rec2 receiver domain stem with a small contact patch around the surface exposed Tyr residue at position 26 of the first receiver domain (Fig. 1). Tyr-26 is strictly conserved in PleD homologs that share a Rec1-Rec2-DGC domain structure, but not in response regulators with a different domain architecture (supplemental Fig. S2). To test if this residue plays a role in PleD dimerization, DGC activity and dimerization behavior of the $PleD_{Y26A}$ mutant protein were analyzed. Indeed, $PleD_{Y26A}$ was completely inactive in the absence and only marginally active in the presence of BeF_3 (Table 1). Consistent with this, only a minor fraction of the protein could be cross-linked in the dimer form, irrespectively of the presence of BeF_3 (Fig. 3*A*). In agreement with these *in vitro* data, the *$pleD_{Y26A}$* allele failed to complement the pleiotropic developmental defects of a *C. crescentus pleD* null mutant. Together these results strongly support the

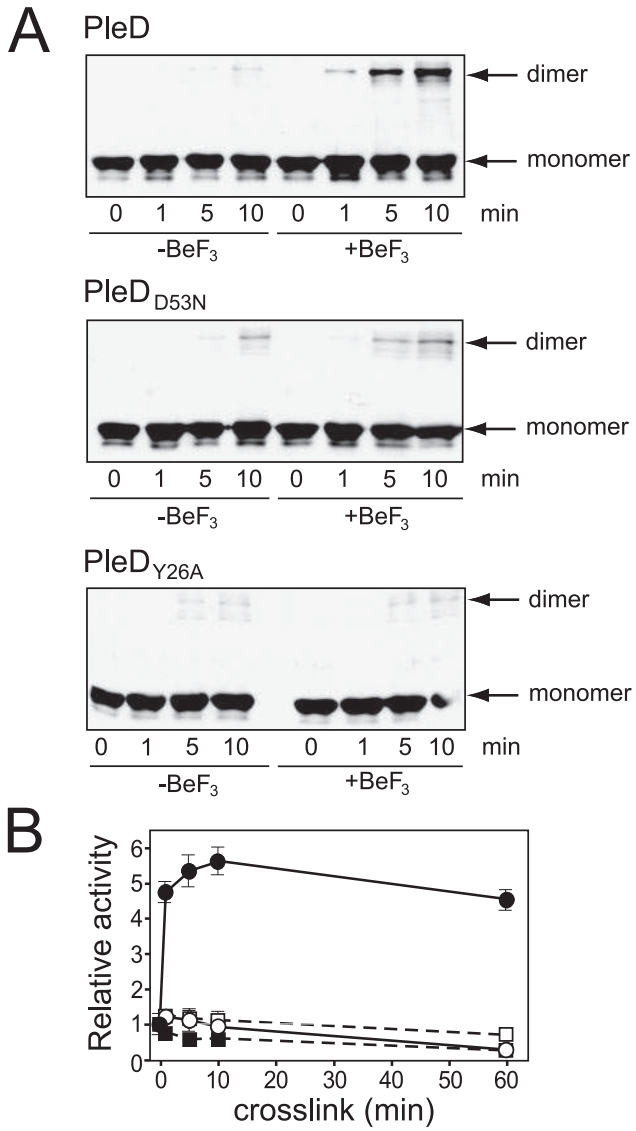

FIGURE 3. **Beryllium fluoride induces PleD dimerization and activation.** *A*, cross-link assays with PleD, $PleD_{D53N}$, and $PleD_{Y26A}$. 20 μM of the purified proteins with or without BeF_3 was incubated with 2 mM DSS (Pierce) for 0, 1, 5, and 10 min. PleD monomers and dimers were separated on SDS-polyacrylamide gels, transferred to PVDF membranes, and detected by immunoblot analysis with an anti-PleD antibody. *Arrows* mark the monomeric and dimeric forms of PleD. *B*, PleD cross-linked in the presence of BeF_3 shows increased DGC activity. 20 μM of PleD (*circles*) or $PleD_{D53N}$ (*squares*) with (*filled symbols*) or without BeF_3 (*open symbols*) were incubated with 2 mM DSS for 0, 1, 5, 10, and 60 min. The reactions were diluted 1:10, and DGC activities were determined as indicated under "Materials and Methods."

view that Tyr-26 residue forms part of the interaction surface of PleD dimers. This is consistent with the finding that, although additional inter-chain contacts are formed in the crystal structure of BeF_3 activated PleD, the specific contact around Tyr-26 is maintained (11).

The Diguanylate Cyclase Activity of PleD Resides in the Dimer Fraction—As indicated by cross-linking, PleD forms dimers in the presence of BeF_3. To investigate if the enzymatic activity coincided with the cross-linked PleD fractions, reactions were diluted 10-fold immediately after DSS treatment and quenching. At this BeF_3 concentration PleD showed only residual DGC activity (Fig. 2). As shown in Fig. 3*B*, cross-linking of BeF_3-activated PleD resulted in a 6-fold increase of DGC activity as

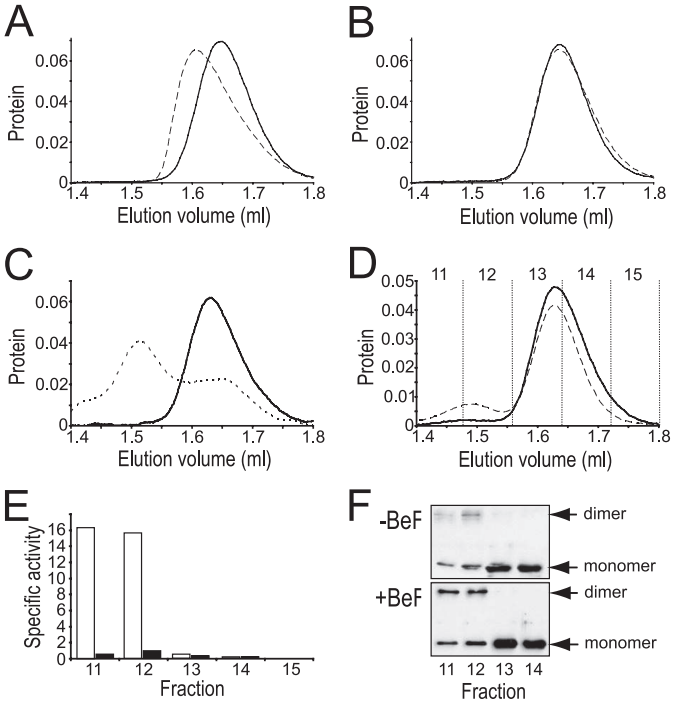

FIGURE 4. **The enzymatic activity of PleD is contained within the dimer fraction.** SEC of PleD (50 μg) in the presence (*stippled line*) or absence (*solid line*) of BeF_3 (*A*); $PleD_{D53N}$ (50 μg) in the presence (*stippled line*) or absence (*solid line*) of BeF_3 (*B*); PleD (*solid line*) and PleD* (*stippled line*) (*C*); and PleD cross-linked with 2 mM DSS in the absence (*solid line*) or presence (*stippled line*) of BeF_3 (*D*). *E*, enzymatic activity (nanomoles of c-di-GMP min^{-1} mg^{-1}) of the PleD SEC fractions 11–15 from *D* with (*open bars*) or without (*black bars*) BeF_3. *F*, immunoblot analysis of PleD SEC fractions 11–15 from *D* with anti-PleD antibody. *Arrows* mark the monomeric and dimeric forms of PleD.

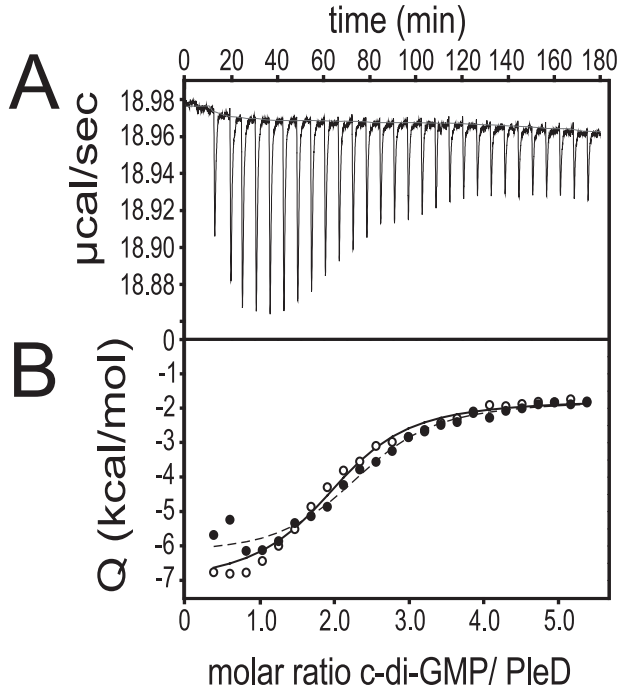

FIGURE 5. **c-di-GMP binding to the allosteric site of PleD is not affected by BeF_3-mediated activation of the protein.** *A*, raw data of ITC with 90 μM c-di-GMP titrated into 3 μM non-activated PleD at 25 °C. *B*, integration of the titration peaks for the binding of c-di-GMP (90 μM) to non-activated (*open symbols*) and BeF_3-activated PleD (*solid symbols*). The fitted binding curves are indicated by the *stippled line* for the non-activated, and by the *solid line* for the BeF-activated protein.

compared with non-cross-linked samples. In contrast, cross-linking of PleD in the absence of BeF_3 and cross-linking of $PleD_{D53N}$ either in the presence or absence of BeF_3 did not result in increased DGC activity. Taken together, these results suggested that, in the presence of BeF_3, a fraction of the PleD protein is trapped by DSS cross-link in a dimerized form and that the dimer represents the active conformation of PleD. To further substantiate this idea we attempted to separate active dimers from inactive monomers by SEC (see "Materials and Methods"). Only PleD, but not $PleD_{D53N}$, changed its apparent molecular size in the presence of BeF_3 (Fig. 4, *A* and *B*). However, in contrast to the constitutive active PleD*, which is present predominantly as a dimer (Fig. 4*C*), BeF_3-activated PleD did not show resolved monomer and dimer peaks. Rather, the broadening of the PleD peak and its shift to a higher apparent molecular mass are consistent with a rapid equilibrium between monomers and dimers for the activated PleD. Only when BeF_3-activated PleD was cross-linked with DSS before SEC, defined monomer and dimer peaks were observed (Fig. 4*D*). The peak corresponding to cross-linked PleD dimers was considerably smaller than the monomer peak indicating that only a minor fraction of PleD was trapped in the dimeric form. This was confirmed by immunoblot experiments with anti-PleD antibodies that also showed an increase of the dimer form (fractions 11 and 12) in BeF_3-treated samples (Fig. 4*F*). Nevertheless, the dimer fractions almost exclusively accounted for the detectable DGC activity (Fig. 4*E*). The observations that BeF_3 treatment increased the proportion of PleD dimers and that isolated dimers exhibited high DGC activity are in support of an "activation by dimerization" mechanism.

DGC Activity Is Not Required for PleD Dimerization—To demonstrate that dimerization is required, but not sufficient for diguanylate cyclase activity, we analyzed if the $PleD_{E370Q}$ mutant formed dimers. The conserved Glu-370 residue is part of the A-site signature sequence GG(E/D)EF of the PleD diguanylate cyclase domain and was proposed to coordinate a Mg^{2+} ion in the active site required for deprotonation of the 3′-OH group of one GTP substrate molecule and its subsequent nucleophilic attack onto the α-phosphate of the other GTP molecule. As predicted, the $PleD_{E370Q}$ mutant lacked detectable enzymatic activity both in the presence and absence of BeF_3 (data not shown). We even failed to detect any enzymatic activity when the protein concentration was increased to >50 μM and with prolonged incubation times. However, in contrast to $PleD_{Y26A}$ the lack of activity was not due to a failure to dimerize. When BeF_3-activated $PleD_{E370Q}$ was used in cross-link experiments, the behavior of the mutant form was indistinguishable from PleD wild type (supplemental Fig. S3). Thus, dimerization is clearly a prerequisite for, rather than a consequence of diguanylate cyclase activity.

Activation of the PleD Diguanylate Cyclase Does Not Interfere with Feedback Inhibition—The diguanylate cyclase activity of PleD is subject to strong product inhibition through binding of c-di-GMP to an allosteric I-site widely conserved among GGDEF domain proteins (5, 19). To test if PleD activation with BeF_3 interferes with allosteric control, binding of c-di-GMP to the I-site was directly measured using ITC (Fig. 5). Integration

of the titration peaks of c-di-GMP injected from the syringe into the cell of the calorimeter containing PleD produced a sigmoidal enthalpy curve for the interaction between PleD and c-di-GMP. The slope of the binding curve implies a dissociation constant of 0.3 μM ($\pm$0.1 μM). This is in good agreement with the K_i of 0.5 μM determined earlier (5, 19). In support of a c-di-GMP dimer bound at each I-site (5) the binding stoichiometry was measured as 2.1:1 ($\pm$0.2) (c-di-GMP:PleD) (Fig. 5).

When binding of c-di-GMP to PleD was compared in the non-activated and BeF_3-activated conformation, both binding affinity (0.4 $\pm$ 0.1 μM) and stoichiometry (2.1:1 $\pm$ 0.2) did not change significantly upon activation. In agreement with this, the IC_{50} values for PleD inhibition measured at a protein concentration of 5 μM were very similar for the non-activated (5.1 $\pm$ 1.4 μM) and the BeF_3-activated (5.9 $\pm$ 1.3 μM) PleD. From these data we conclude that activation of PleD by dimerization does not interfere with allosteric control of the protein. It should be noted that the calorimetric data show a deviation at very low c-di-GMP concentrations that cannot be described in terms of the simple binding model used here. This may be related to the varying degree of dimerization of c-di-GMP in solution (20). Because this effect is limited to the first few injections and does not interfere with the sigmoidal part of the binding curve, we have eliminated the first three data points from the fit (Fig. 5*B*) rather than introducing a more complex model with additional parameters of questionable relevance. A surprising result was obtained when measuring the heat capacity for the interaction between c-di-GMP and PleD by plotting the binding enthalpy *versus* the temperature between 5 °C and 25 °C (dCp = dH/dT). The heat capacity was fitted as −0.43 kJ/(mol K) (data not shown). The negative value suggests a hydrophobic interaction between the inhibitor and the protein. However, in the crystal structure c-di-GMP interacts predominantly in a hydrophilic manner with charged amino acid residues (5). It is conceivable that the binding of c-di-GMP to PleD might cause a conformational change in the protein, with a corresponding change of the protein-solvent interactions.

A PleD Mutant Unable to Dimerize Fails to Sequester to the Cell Pole—During the *C. crescentus* cell cycle PleD dynamically sequesters to the developing pole in response to activation by phosphorylation (4). However, the molecular basis for pole discrimination between active and inactive PleD is unclear. To analyze if phosphorylation itself or rather phosphorylation-induced dimerization is required for polar sequestration, we fused $PleD_{Y26A}$ to GFP and compared its subcellular localization to GFP fused versions of $PleD_{D53N}$ and $PleD^*_{D53N}$. As shown in Fig. 6, $PleD_{D53N}$ fails to localize to the pole, whereas $PleD^*_{D53N}$, the non-phosphorylatable but constitutive active form is found exclusively at the *C. crescentus* stalked cell pole. Similar to $PleD_{D53N}$, $PleD_{Y26A}$ fails to sequester to the cell pole, arguing that the ability to form dimers is critical for polar localization of PleD (Fig. 6). When the Y26A mutation was introduced into the constitutive active form PleD*, the resulting $PleD^*_{Y26A}$-GFP fusion protein also failed to localize to the pole (Fig. 6). Levels of both $PleD_{Y26A}$ and $PleD^*_{Y26A}$ GFP fusion proteins were normal, arguing that the Y26A mutation did not affect the protein stability *in vivo* (data not shown). In summary, these data suggested that the oligomerization state of PleD provides the structural basis for cell cycle dependent dynamic recruitment of the protein to the cell pole.

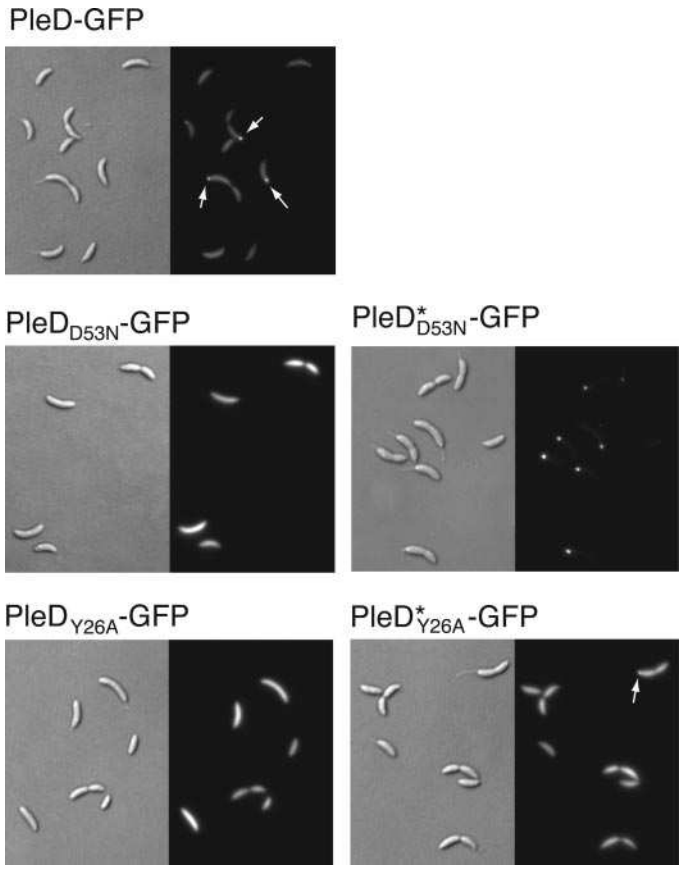

FIGURE 6. **A PleD dimerization mutant fails to dynamically localize to the cell pole.** Differential interference contrast (*left panels*) and fluorescent images (*right panels*) are shown for *C. crescentus* NA1000 wild-type expressing GFP fusion proteins of the indicated PleD variants. Polar fluorescent foci are marked by *arrows*.

DISCUSSION

Dimerization is a common property of proteins utilized to provide stability, transmit signals, or channel reagents across membranes (21). Dimer formation can also be a mechanism to control enzyme activity, as exemplified by the cell death protease caspase 9 (22) or the cytokine antagonist p40 (23). Here we present an example for dimerization-induced activation of an enzyme, diguanylate cyclase, which takes advantage of an associated regulatory domain that couples dimerization to phosphorylation input.

The crystal structure of the non-activated form of the PleD response regulator suggested an "activation by dimerization" mechanism (5). However, because monomeric proteins can form non-physiological dimers or higher order oligomers in crystals, this hypothesis required experimental validation. In the crystal structure PleD forms a dimer with the two receiver domains mediating weak monomer-monomer interactions between a small contact patch around Tyr-26 of Rec1 and α3-α4 of Rec2 (Fig. 1). Thus, the apo structure not only provided the structural basis for activity control of PleD but also proposed the interaction surface for dimerization. Here we tested the hypothesis that, upon activation, PleD engages in

dimer formation, and we analyzed the specific role of Tyr-26 in this process. Because we failed to efficiently activate PleD *in vitro* by phosphorylation through one of its cognate kinases (4) we used the phosphoryl mimic BeF_3 to analyze the effect of activation on PleD oligomerization and activity (12, 15). Our results not only provide biochemical evidence for an "activation by dimerization" mechanism but also confirm an important role for Tyr-26 in dimerization. Both a genetically active form of PleD, PleD* (4), and BeF_3 activated PleD-stimulated DGC activity and oligomerization. Because stimulation of PleD DGC activity by BeF_3 specifically required the phosphoryl acceptor side Asp-53, the changes in structure and activity observed most likely reflect the activation mechanism normally evoked by phosphorylation. Because the constitutive active form PleD* still showed ~10-fold higher DGC activity and formed more stable dimers than BeF_3-modified PleD, it is possible that PleD is only partially activated by BeF_3 in the non-toxic concentration range used (Fig. 2). Alternatively, the PleD* mutant protein, which contains several amino acid changes contributing to the "locked-on" state (4, 9), might form particularly stable dimers. To demonstrate that the DGC activity specifically associates with PleD dimers, we chemically cross-linked BeF_3-activated protein and subsequently separated PleD dimers from non-cross-linked monomers by SEC. The finding that the cross-linked dimer fraction had a greatly increased enzymatic activity as compared with monomers strongly implied that PleD dimers represent the active form of the enzyme and argued that phosphorylation-mediated dimerization represents the main mechanism of PleD diguanylate cyclase activity control. A possible role for dimerization or oligomerization of diguanylate cyclases was suggested previously. Several full-length GGDEF domain proteins, and isolated GGDEF domains, that were expressed as fusions to maltose-binding protein, behaved as dimers or trimers when analyzed by SEC (6). However, although the significance of trimer formation is unclear, no correlation was reported between the oligomeric state and enzymatic activity of these proteins.

In contrast to PleD wild type, the $PleD_{Y26A}$ mutant failed to efficiently form dimers upon activation with BeF_3. This, and the observation that, in the presence of BeF_3, $PleD_{Y26A}$ showed an almost 10,000-fold lower DGC activity as compared with PleD wild type, is consistent with a specific requirement of residue Tyr-26 for PleD oligomerization. The weak monomer interactions observed in the PleD apo structure around Tyr-26 predicted that if this residue is part of the dimerization interface additional contacts would have to be formed upon activation to stabilize the complex. In agreement with the data presented here, the interaction surface around Tyr-26 is maintained in the crystal structure of the activated form of PleD (11) with Tyr-26 making specific contacts to Asp-209 and Arg-212 in the second receiver domain of the other chain. However, a series of additional inter-chain contacts are formed in the activated structure resulting in a tightening of the dimer interface (11). The Tyr residue at position 26 of the first receiver domain is strictly conserved in PleD homologs with an identical Rec1-Rec2-GGDEF domain structure (supplemental Fig. S2). In contrast, this residue is not conserved in response regulators with a different domain structure or composition (supplemental Fig. S2). Similarly, residues Asp-209 and Arg-212, the interaction partners of Tyr-26 in the crystal structure of activated PleD, show strict conservation only in proteins with a PleD-like domain structure (data not shown). Together with the experimental data presented here, this strongly suggested that Tyr-26 forms part of the dimerization surface of this protein family.

Diguanylate cyclases catalyze the formation of a symmetric product by condensing two identical GTP substrate molecules. In contrast to monocyclic nucleotidyl cyclases, which form non-symmetric products, dimerization is an apparent necessity for the catalytic mechanism of DGCs, because it creates a fully symmetrical active site at the interface of two subunits. In the simplest model two substrate-charged GGDEF domains would meet in a symmetric but antiparallel arrangement to properly position the 3′-OH groups for an intermolecular nucleophilic attack onto the α-phosphate of the opposite substrate molecule. Moreover, because it is a prerequisite for catalysis, oligomerization of the DGC domains is obviously exploited to control PleD enzyme activity. Although phosphorylation-mediated dimerization of PleD represents the first example of controlled dimerization of a DGC, it is possible that promoting or inhibiting dimerization is a key mechanism of DGC activity control in general. The preponderance of potential DGCs present in many bacteria predicts complex signaling mechanisms and makes it obligatory for the cell to tightly control these enzymes (2). Although most DGCs have been postulated to be subject to strict product inhibition (19), little is known about how DGCs are activated in response to specific environmental or internal signals. Although it can be assumed that all GGDEF domains that are fused to receiver domains of two-component systems exhibit PleD-like phosphorylation-mediated control, GGDEF domains, which are associated with other signal input domains like GAF (24, 25), PAS (26), BLUF (27), or HAMP (28, 29), might function similarly. It is worth mentioning that most regulatory mechanisms used to control monocyclic nucleotidyl cyclases involve the formation or dissolution of catalytically competent active sites, caused by rearrangement of the two catalytic domains of the dimer relative to each other (reviewed in Ref. 1). Future studies will show if this regulatory principle can be extended to the large family of bacterial DGCs.

Oligomerization of PleD is not only used to temporally control DGC activity but also contributes to its spatial distribution. PleD activity is required for the morphological changes that take place during the *C. crescentus* swarmer-to-stalked cell transition (7–9). During this cell differentiation step, PleD is activated by phosphorylation and as a result sequesters to the differentiating pole (4). The observation that non-phosphorylatable forms of PleD fail to localize to the cell pole, whereas the constitutively activated mutant form PleD* is predominantly found at this subcellular site, suggested that activation of PleD during development is directly coupled to its dynamic subcellular positioning (4). However, the molecular basis for this coupling event and for PleD recognition at the pole remained unclear. In principle, a polar interaction partner could recognize activated PleD by its phosphorylation status, by an altered monomer conformation, or by its oligomerization state. The observation, that PleD molecules lacking Tyr-26 not only fail to dimerize but also fail to sequester to the pole, suggested that the

oligomerization state dictates subcellular distribution of PleD during the *C. crescentus* cell cycle. Enzymatically active dimers of PleD would thus specifically sequester to the differentiating cell pole resulting in the predominant formation of c-di-GMP at this cellular localization. Because *Caulobacter* possesses markers that are laid down during or after cell division to tag the new poles (30–32), it is reasonable to assume that PleD interacts with one or several pre-existing proteins, which are able to discriminate between its monomeric and dimeric forms. Dimerization of PleD might increase the interaction diversity by enabling simultaneous binding of two interacting proteins or by creating new binding sites for additional proteins (21). Both of these possibilities could provide a molecular explanation for the discrimination of PleD oligomers at the differentiating pole. Spatial discrimination based on receiver domain-mediated oligomerization could very well be a general cellular phenomenon in bacteria. Like PleD, the response regulator DivK dynamically localizes to the *C. crescentus* cell poles in a phosphorylation-dependent manner (33). It is not clear how the poles discriminate between activated and non-activated DivK, but it is attractive to speculate that oligomerization might also play a role in this behavior. CikA, a sensor histidine kinase and a key component of the circadian clock input pathway in the cyanobacterium *Synecococcus elongatus*, also localizes to the pole where it is believed to interact with a complex of clock-related proteins (34). Polar sequestration of CikA depends on a C-terminal pseudo-receiver domain that lacks the conserved phosphoryl acceptor side. It has been proposed that, through a docking/activation mechanism, pseudo-receiver domain couples the activity of CikA to its subcellular location (34). Because histidine kinases are active as dimers, the pseudo-receiver domain might serve as an adaptor between the oligomeric state and polar positioning of CikA. Like the pseudo-receiver domain, the Rec2 receiver domain of PleD is not conserved and likely fulfills an adaptor function. It is possible that the Rec1-Rec2-GGDEF domain structure that arose through duplication of the receiver domains in PleD homologs has evolved to provide for additional surface for the interaction with specific polar receptors. In such a scenario, Rec1 would be interacting with the histidine kinase and would provide dimerization surface. Rec2, in turn, would also be engaged in dimerization but in addition would mediate interaction with a polar receptor. If so, a distinct subcellular localization of enzymatically active DGCs might be common to all PleD homologs. Future studies are geared at identifying the polar receptor(s) for PleD, characterizing the molecular mechanisms required for the discrimination between PleD monomers and dimers, and analyzing the biological relevance of sequestering an enzymatically active form of PleD to this particular subcellular site.

Acknowledgments—We thank Jacob Malone and Tilman Schirmer for helpful discussions.

REFERENCES

1. Sinha, S. C., and Sprang, S. R. (2006) *Rev. Physiol. Biochem. Pharmacol.* **157,** 105–140
2. Jenal, U., and Malone, J. (2006) *Annu. Rev. Genet.* **40,** 385–407
3. Ulrich, L. E., Koonin, E. V., and Zhulin, I. B. (2005) *Trends Microbiol.* **13,** 52–56
4. Paul, R., Weiser, S., Amiot, N. C., Chan, C., Schirmer, T., Giese, B., and Jenal, U. (2004) *Genes Dev.* **18,** 715–727
5. Chan, C., Paul, R., Samoray, D., Amiot, N. C., Giese, B., Jenal, U., and Schirmer, T. (2004) *Proc. Natl. Acad. Sci. U. S. A.* **101,** 17084–17089
6. Ryjenkov, D. A., Tarutina, M., Moskvin, O. V., and Gomelsky, M. (2005) *J. Bacteriol.* **187,** 1792–1798
7. Hecht, G. B., and Newton, A. (1995) *J. Bacteriol.* **177,** 6223–6229
8. Aldridge, P., and Jenal, U. (1999) *Mol. Microbiol.* **32,** 379–391
9. Aldridge, P., Paul, R., Goymer, P., Rainey, P., and Jenal, U. (2003) *Mol. Microbiol.* **47,** 1695–1708
10. Levi, A., and Jenal, U. (2006) *J. Bacteriol.* **188,** 5315–5318
11. Wassmann, P., Chan, C., Beck, A., Heerklotz, H., Paul, R., Jenal, U., and Schirmer, T. (2007) *Structure* **15,** 915–927
12. Yan, D., Cho, H. S., Hastings, C. A., Igo, M. M., Lee, S. Y., Pelton, J. G., Stewart, V., Wemmer, D. E., and Kustu, S. (1999) *Proc. Natl. Acad. Sci. U. S. A.* **96,** 14789–14794
13. Cho, H., Wang, W., Kim, R., Yokota, H., Damo, S., Kim, S. H., Wemmer, D., Kustu, S., and Yan, D. (2001) *Proc. Natl. Acad. Sci. U. S. A.* **98,** 8525–8530
14. Hastings, C. A., Lee, S. Y., Cho, H. S., Yan, D., Kustu, S., and Wemmer, D. E. (2003) *Biochemistry* **42,** 9081–9090
15. Wemmer, D. E., and Kern, D. (2005) *J. Bacteriol.* **187,** 8229–8230
16. Toro-Roman, A., Wu, T., and Stock, A. M. (2005) *Protein Sci.* **14,** 3077–3088
17. Toro-Roman, A., Mack, T. R., and Stock, A. M. (2005) *J. Mol. Biol.* **349,** 11–26
18. Bachhawat, P., Swapna, G. V., Montelione, G. T., and Stock, A. M. (2005) *Structure* **13,** 1353–1363
19. Christen, B., Christen, M., Paul, R., Schmid, F., Folcher, M., Jenoe, P., Meuwly, M., and Jenal, U. (2006) *J. Biol. Chem.* **281,** 32015–32024
20. Zhang, Z. Y., Kim, S., Gaffney, B. L., and Jones, R. A. (2006) *J. Am. Chem. Soc.* **128,** 7015–7024
21. Marianayagam, N. J., Sunde, M., and Matthews, J. M. (2004) *Trends Biochem. Sci.* **29,** 618–625
22. Renatus, M., Stennicke, H. R., Scott, F. L., Liddington, R. C., and Salvesen, G. S. (2001) *Proc. Natl. Acad. Sci. U. S. A.* **98,** 14250–14255
23. Heinzel, F. P., Hujer, A. M., Ahmed, F. N., and Rerko, R. M. (1997) *J. Immunol.* **158,** 4381–4388
24. Aravind, L., and Ponting, C. P. (1997) *Trends Biochem. Sci.* **22,** 458–459
25. Hurley, J. H. (2003) *Sci. STKE 2003*, PE1
26. Ponting, C. P., and Aravind, L. (1997) *Curr. Biol.* **7,** R674–R677
27. Gomelsky, M., and Klug, G. (2002) *Trends Biochem. Sci.* **27,** 497–500
28. Aravind, L., and Ponting, C. P. (1999) *FEMS Microbiol. Lett.* **176,** 111–116
29. Galperin, M. Y., Nikolskaya, A. N., and Koonin, E. V. (2001) *FEMS Microbiol. Lett.* **203,** 11–21
30. Viollier, P. H., Sternheim, N., and Shapiro, L. (2002) *Proc. Natl. Acad. Sci. U. S. A.* **99,** 13831–13836
31. Huitema, E., Pritchard, S., Matteson, D., Radhakrishnan, S. K., and Viollier, P. H. (2006) *Cell* **124,** 1025–1037
32. Lam, H., Schofield, W. B., and Jacobs-Wagner, C. (2006) *Cell* **124,** 1011–1023
33. Jacobs, C., Hung, D., and Shapiro, L. (2001) *Proc. Natl. Acad. Sci. U. S. A.* **98,** 4095–4100
34. Zhang, X., Dong, G., and Golden, S. S. (2006) *Mol. Microbiol.* **60,** 658–668

SUPPLEMENTAL MATERIAL:

Figure S1: Characterization of PleD DGC activity as a function of pH **(A)**, $MgCl_2$ concentration **(B)**, and NaCl concentration **(C)**. The specific activity was determined as nmol c-di-GMP min^{-1} mg^{-1}. 10 μM PleD was assayed in 50 μl volume (250 mM NaCl, 50 mM Tris-HCl pH 7.8, 10 mM $MgCl_2$, 5mM β- Mercaptoethanol) and 100 μM ^{33}P-labelled GTP, with varying NaCl or $MgCl_2$ concentrations in the respective assays. The pH-dependence was determined with assays containing 75 mM Tris-Propane (pH 6-7, 9-10.5), or 75 mM Tris-HCl (pH 7-9).

Figure S2: Exclusive conservation of Tyr26 in the phosphoryl-acceptor domain of PleD-like response regulators. Sequence logos representing amino acid conservation of different response regulator families were generated by the WebLogo tool (http://weblogo.berkeley.edu; (35)) from alignments produced by BLAST and edited by Jalview (36). The domain structure of the different families was generated with SMART (37) and is indicated above the WebLogos. **(A)** PleD-like family of response regulators sharing the same Rec1-Rec2-GGDEF (DUF1) domain structure and composition. The numbering of the amino acid residues refers to *C. crescentus* PleD. **(B)** Response regulators with duplicated receiver domains, a PleD-like GGDEF domain (DUF1), and additional signaling domains. The numbering of the amino acid residues refers to the N-terminal receiver domain of protein NSE_0512 from *Neorickettsia sennetsu* **(C)** Response regulators with a single receiver domain and a GGDEF output domain. The numbering of the amino acid residues refers to *Pseudomonas fluorescens* WspR (38). **(D)** Response regulators consisting of a single receiver domain. The numbering of the amino acid residues refers to *C. crescentus* DivK (39).

Figure S3: Beryllium fluoride induces dimerization of a catalytically inactive PleD mutant protein. **(A)** Size exclusion chromatography (SEC) of $PleD_{E370Q}$ crosslinked with 2 mM DSS in the presence (stippled line) or absence (solid line) of BeF_3. **(B)** Immunoblot analysis of PleD SEC fractions 11-15 from (A) with anti-PleD antibody. Arrows mark the monomeric and dimeric forms of PleD.

Table S1: Strains and Plasmids

Strain	**Relevant genotype or description**	**Reference or source**
Escherichia coli		
DH10B	F$^-$ *mcr*A Δ(*mrr*- hsd RMS- *mcr*BC) Δ80d*lacZ* ΔM15 Δ*lac*X74 endA1 recA1 deoR Δ(*ara, leu*)7697 *araD139 galU galK nupG rpsL thi pro hsdR- hsd+ recA RP4-2-Tc* Δ*Mu-Tn7*	(40)
BL21 (DE3)	F$^-$ *dcm ompT hsdS*(rB-mB-) pLysS *gal* Δ(DE3) [pLysS CAMr]	Stratagene
Caulobacter crescentus		
UJ626	CB15N Δ*pleD* pPA53-4	(4)
UJ1909	CB15N Δ*pleD* pSW6	(4)
UJ1910	CB15N Δ*pleD* pSW7	(4)
UJ2722	CB15N Δ*pleD* pSA38	This study
UJ2745	CB15N Δ*pleD* pSA39	This study

Plasmid	**Relevant genotype or description**	**Reference or source**
pCC2	pET11; *pleD*, C-terminal His_6 tag	(4)
pRP87	pET11; $pleD_{D53N}$, C-terminal His_6 tag	(4)
pRP89	pET11; *pleD**, C-terminal His_6 tag	(4)
pRP100	pET11; $pleD_{E370Q}$, C-terminal His_6 tag	This study
pRP106	pET11; $pleD_{Y26A}$, C-terminal His_6 tag	This study
pPA53-4	pMR10; *pleD-gfp*	(4)
pSA38	pMR10; $pleD_{Y26A}$-*gfp*	This study
pSA39	pMR10; $pleD^*_{Y26A}$-*gfp*	This study
pSW6	pMR10; $pleD_{D53N}$-*gfp*	(4)
pSW7	pMR10; $pleD^*_{D53N}$-*gfp*	(4)

Figure S1

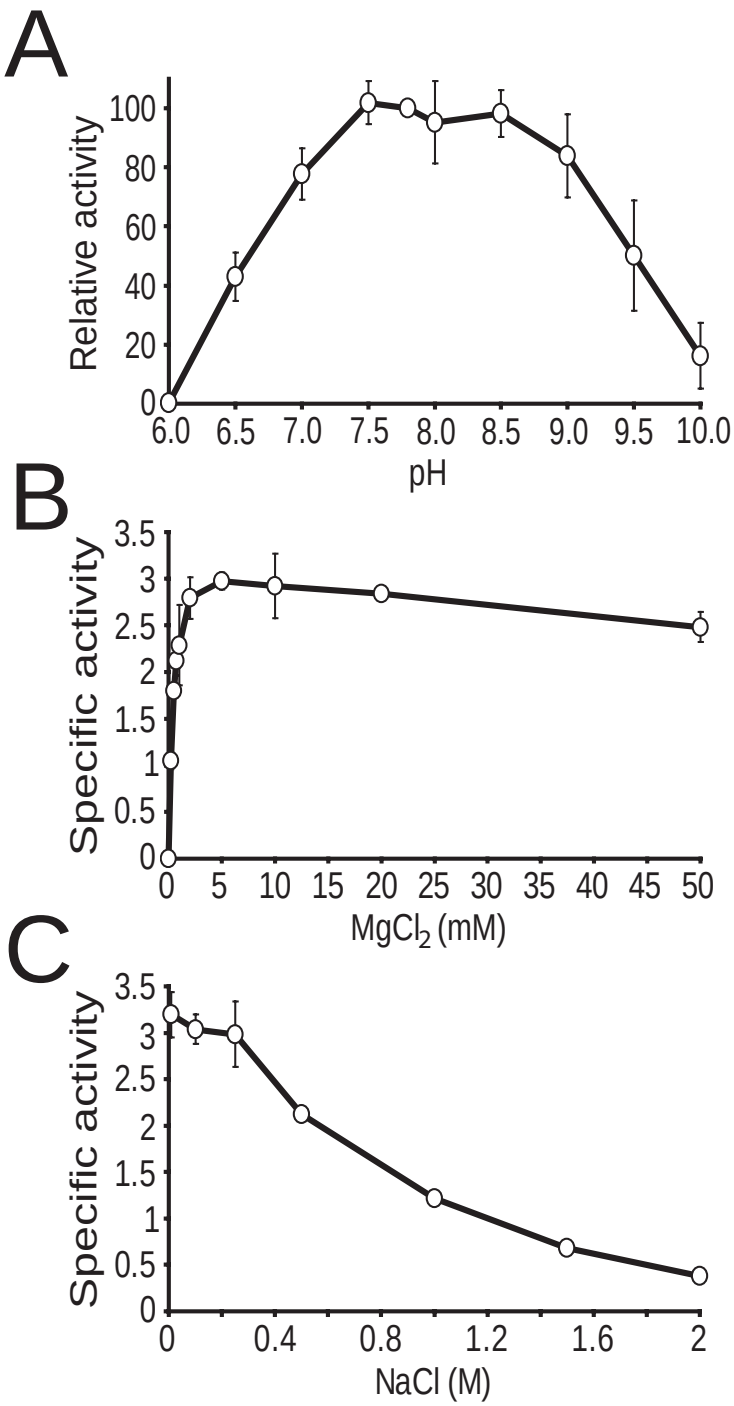
A
Relative activity
100
80
60
40
20
0
6.0
6.5
7.0
7.5
8.0
8.5
9.0
9.5
10.0
pH
B
Specific activity
3.5
3
2.5
2
1.5
1
0.5
0
0
5
10
15
20
25
30
35
40
45
50
MgCl2 (mM)
C
Specific activity
3.5
3
2.5
2
1.5
1
0.5
0
0
0.4
0.8
1.2
1.6
2
NaCl (M)

Figure S2

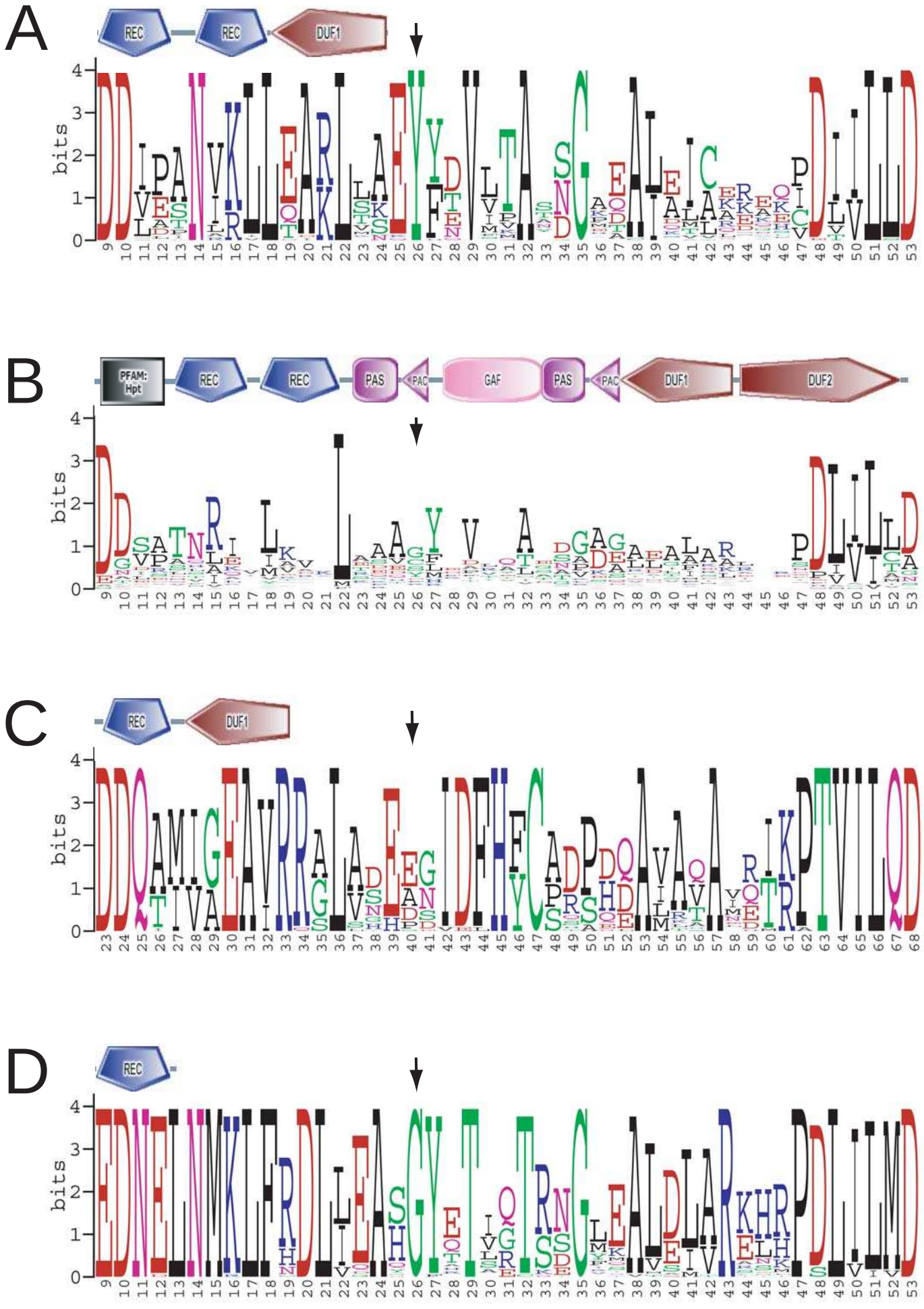
A
REC
REC
DUF1
bits
B
PFAM: Hpt
REC
REC
PAS
PAC
GAF
PAS
PAC
DUF1
DUF2
bits
C
REC
DUF1
bits
D
REC
bits

Figure S3

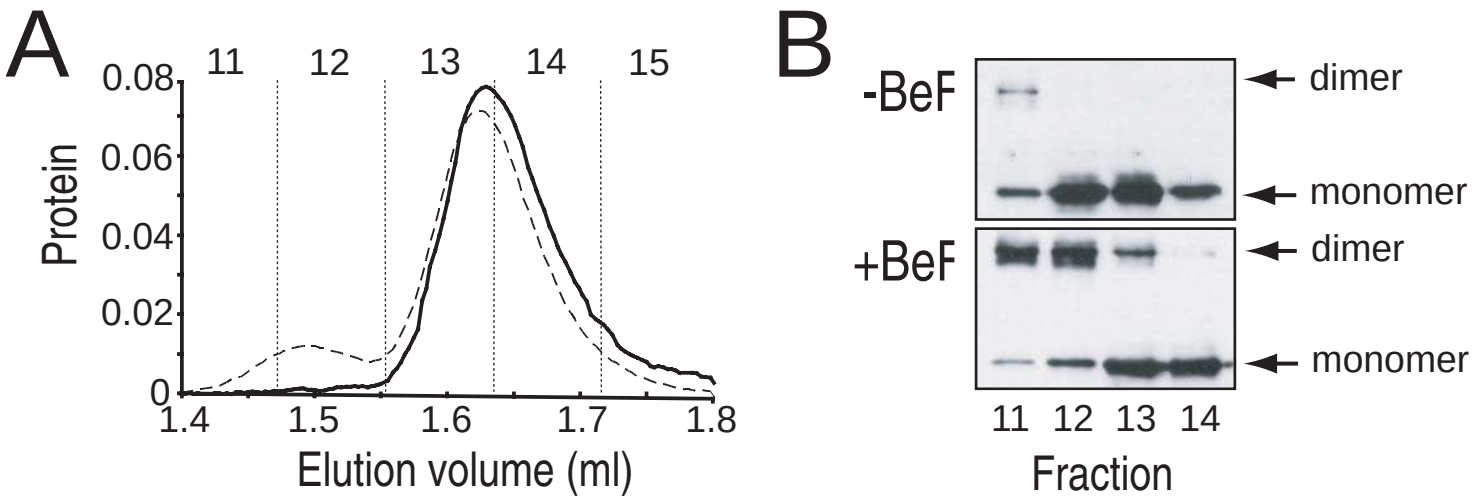
A
11
12
13
14
15
0.08
0.06
0.04
0.02
0
Protein
1.4
1.5
1.6
1.7
1.8
Elution volume (ml)
B
-BeF
+BeF
dimer
monomer
dimer
monomer
11
12
13
14
Fraction

3.4 Allosteric Regulation of Histidine Kinases by their Cognate Response Regulator Determines Cell Fate

Ralf Paul, Tina Jaeger*, Sören Abel*, Irene Wiederkehr, Marc Folcher, Emanuele G. Biondi, Michael T. Laub, Urs Jenal

*Authors contributed equally to the manuscript

Cell, manuscript accepted

Statement of my work

I contributed to this work by generating strains expressing fluorescent protein fusions to DivJ, PleC and DivK. In addition, I performed the cell cycle resolved colocalisation experiments (Fig. 6C) and took part in all further microscopy analysis required for this work (Fig. 6A S9A).

Please cite this article in press as: Paul et al., Allosteric Regulation of Histidine Kinases by Their Cognate Response Regulator Determines Cell Fate, Cell (2008), doi:10.1016/j.cell.2008.02.045

Cell

Allosteric Regulation of Histidine Kinases by Their Cognate Response Regulator Determines Cell Fate

Ralf Paul,[1] Tina Jaeger,[1,3] Sören Abel,[1,3] Irene Wiederkehr,[1] Marc Folcher,[1] Emanuele G. Biondi,[2] Michael T. Laub,[2] and Urs Jenal[1,*]

[1]Biozentrum, University of Basel, Klingelbergstrasse 70, 4056 Basel, Switzerland

[2]Massachusetts Institute of Technology, Department of Biology, 77 Massachusetts Avenue Cambridge, MA 02139, USA

[3]These authors contributed equally to this manuscript.

*Correspondence: urs.jenal@unibas.ch

DOI 10.1016/j.cell.2008.02.045

SUMMARY

The two-component phosphorylation network is of critical importance for bacterial growth and physiology. Here, we address plasticity and interconnection of distinct signal transduction pathways within this network. In *Caulobacter crescentus* antagonistic activities of the PleC phosphatase and DivJ kinase localized at opposite cell poles control the phosphorylation state and subcellular localization of the cell fate determinator protein DivK. We show that DivK functions as an allosteric regulator that switches PleC from a phosphatase into an autokinase state and thereby mediates a cyclic di-GMP-dependent morphogenetic program. Through allosteric activation of the DivJ autokinase, DivK also stimulates its own phosphorylation and polar localization. These data suggest that DivK is the central effector of an integrated circuit that operates via spatially organized feedback loops to control asymmetry and cell fate determination in *C. crescentus*. Thus, single domain response regulators can facilitate crosstalk, feedback control, and long-range communication among members of the two-component network.

INTRODUCTION

Asymmetric cell division underlies the fundamental basis for the developmental evolution of organisms. It refers to the capability of stem cells to simultaneously produce a continuous output of differentiated cells and to maintain their own population of undifferentiated cells. The regulation of asymmetric division is achieved by the controlled segregation of basally localized cell fate determinants, which leads to the polarization of the stem cell along its axis (Betschinger and Knoblich, 2004). In the bacterium *Caulobacter crescentus*, asymmetry is established by members of the two-component signaling systems, which control various aspects of bacterial physiology including cell differentiation and virulence. Two sensor histidine kinases, DivJ and PleC, are positioned to opposing poles of the *Caulobacter* predivisional cell (McAdams and Shapiro, 2003). A cylindrical extension of the cell body, the stalk, and an adhesive holdfast occupy the DivJ-marked pole, while the PleC-occupied pole bears a rotating flagellum and adhesive pili (Figure 7A). Upon division the stalked cell re-enters S-phase immediately, whereas the motile-swarmer cell takes advantage of the replication inert G1 phase to spread out before it undergoes reprogramming into a surface adherent stalked cell.

C. crescentus cell fate is implemented by the essential single domain response regulator DivK (Hecht et al., 1995; Matroule et al., 2004). DivK localizes to both poles of the predivisional cell in a phosphorylation-dependent manner, but is released from the flagellated pole after completion of cytokinesis (Figure 7A) (Jacobs et al., 2001). While the DivJ autokinase is the main phosphodonor for DivK and responsible for its sequestration to the cell poles (Lam et al., 2003), the PleC phosphatase activity displaces DivK from the flagellated pole by maintaining DivK∼P levels low in the swarmer cell (Lam et al., 2003; Matroule et al., 2004). Compartmentalization of the DivJ kinase and the PleC phosphatase during cell division results in the sudden reduction of DivK∼P levels in the swarmer cell and the initiation of the swarmer-specific developmental program (Matroule et al., 2004). Conversely, a rapid DivJ-mediated increase of DivK phosphorylation during the G1-to-S transition is critical for G1-to-S transition and cell differentiation (Hung and Shapiro, 2002; Jacobs et al., 2001; Wu et al., 1998). Activated DivK has recently been proposed to control cell cycle progression and development via the CckA-ChpT pathway, which regulates the activity of the master cell cycle regulator CtrA (Biondi et al., 2006).

Although it is clear that DivK phosphorylation by DivJ and dephosphorylation by PleC are vital for *C. crescentus* cell cycle control and development, the significance of the spatial behavior of DivK and its molecular role remain unclear. Here we propose that DivK together with PleC and DivJ form the core of an integrated regulatory circuitry that operates via spatially organized cellular feedback loops. We show that DivK directly interacts with both polar proteins to strongly boost their kinase activities. By switching PleC from the phosphatase into the autokinase mode and by forming a strong positive feedback loop with the

DivJ autokinase, DivK effectively and robustly mediates G1-to-S transition.

One of the readouts of the DivK-driven network is the synthesis of the second messenger cyclic di-GMP via the activation of the response regulator PleD (Aldridge et al., 2003; Paul et al., 2004). PleD phosphorylation results in dimerization-based activation of the C-terminal diguanylate cyclase domain and sequestration of the regulator to the differentiating pole where it directs flagellar ejection, holdfast biogenesis, and stalk formation (Levi and Jenal, 2006; Paul et al., 2007, 2004). Genetic experiments indicated that DivJ, PleC, and DivK are upstream components required for the activation of the PleD diguanylate cyclase (Aldridge et al., 2003; Sommer and Newton, 1991). Consistent with this, in vivo and in vitro experiments had shown a direct role for PleC and DivJ in modulating phosphorylation, diguanylate cyclase activity, and polar localization of PleD (Aldridge et al., 2003; Paul et al., 2004). This indicated that PleC, in addition to functioning as phosphatase in swarmer cells, also plays a role as autokinase and contributes to the stalked cell-specific program via PleD activation. We present in vitro and in vivo evidence that DivK together with the DivJ and PleC kinases serves to activate and sequester the PleD diguanylate cyclase during the G1-to-S transition. DivK contributes to the specific phosphorylation of PleD by acting as a specific and effective enhancer of the PleC and DivJ autokinases. Our findings propose a regulatory role for single domain response regulators in two component signal transduction pathways as diffusible modulators of their cognate sensor histidine kinases.

RESULTS

DivK Stimulates the PleD Diguanylate Cyclase Activity in a PleC-Dependent Manner

To explore the regulatory link between PleD, PleC, and DivK, activation of PleD diguanylate cyclase activity was assayed in vitro in the presence of PleC and DivK. In line with earlier results (Paul et al., 2004) PleC alone only marginally stimulated PleD activity (Figure 1A). Surprisingly, in the presence of DivK or $DivK_{D53N}$, a mutant that cannot be phosphorylated because it lacks the phosphoryl acceptor site, PleD diguanylate cyclase activity was dramatically stimulated (Figures 1A and 1B). Stimulation by DivK wild-type was less effective, presumably because DivK itself can use PleC∼P as phosphodonor (Hecht et al., 1995) and thus can sequester some of the available phosphoryl groups. DivK-dependent stimulation of PleD activity required ATP, PleC autokinase activity, and the PleD phosphoryl acceptor site Asp53 (Figure 1B). In particular, purified $PleC_{F778L}$, a mutant that lacks autokinase activity but shows normal phosphatase activity (Matroule et al., 2004) failed to support DivK-dependent stimulation of PleD. Because PleD is activated by dimerization (Paul et al., 2007), residual diguanylate cyclase activity can be detected at this protein concentration (5 μM) even in the absence of phosphorylation (the K_d for dimerization of nonactivated PleD is 100 μM [Wassmann et al., 2007]) (Figure 1B). It is interesting to note that when all three proteins were present PleD diguanylate cyclase activity decreased below the basal level of nonactivated PleD under conditions that did not allow phosphorylation (no ATP, no PleC autokinase activity) (Figure 1B). Altogether, these experiments demonstrate that the single domain response regulator DivK is able to efficiently stimulate the in vitro activity of PleD and that this activation requires an active histidine protein kinase PleC.

DivK Stimulates PleC Autokinase but Not Phosphatase Activity

The above experiments suggested that DivK activates PleD by interfering with PleC autokinase activity. To test this, PleC autophosphorylation activity was monitored in the presence and absence of DivK. Because PleC readily phosphorylates DivK in vitro (Hecht et al., 1995; Wu et al., 1998), we used $DivK_{D53N}$ to avoid a reduction of PleC∼P by phosphotransfer to DivK. As shown in Figure 2A and Figure S1A (available online), $DivK_{D53N}$ stimulated levels of PleC∼P in a concentration dependent manner. Because the stability of PleC∼P was not affected by DivK (Figure S1B), $DivK_{D53N}$ seems to specifically stimulate PleC autophosphorylation activity. As a consequence of this stimulation, phosphotransfer from PleC to PleD (Figure 2B) as well as PleD dimerization (Figure S2) was increased when both response regulators were present in the reaction. This is consistent with the observed increase in c-di-GMP synthesis in reactions containing PleD, PleC and DivK (Figure 1). Likewise, phosphotransfer from PleC∼P to DivK was stimulated in the presence of $DivK_{D53N}$ (Figure 3A). Stimulation of PleC autokinase activity did not result from a DivK-mediated in vitro artifact (e.g., through DivK assisted folding of PleC), as solubility, quarternary structure, and activity of PleC preincubated with or without $DivK_{D53N}$ was indistinguishable (Figure 3). Finally, we tested if $DivK_{D53N}$ was able to stimulate PleC phosphatase activity. Purified DivK∼P was mixed with PleC in the presence or absence of $DivK_{D53N}$ to assay dephosphorylation rates. In contrast to PleC mediated phosphorylation of DivK, dephosphorylation of DivK was not increased in the presence of $DivK_{D53N}$ (Figures 3A–3C). Rather, the rate of DivK∼P dephosphorylation was reduced in the presence of $DivK_{D53N}$. In conclusion, these experiments provide strong evidence that the response regulator DivK is able to selectively stimulate the kinase but not the phosphatase activity of its cognate histidine kinase PleC.

DivK and PleD Compete for Phosphorylation by the DivJ Kinase

Because DivK and PleD also interact with DivJ, we tested if the response regulators also showed some synergistic behavior with respect to DivJ or if they would compete for DivJ kinase. As shown in Figure 1C, the PleD diguanylate cyclase was activated by DivJ, but the addition of DivK efficiently blocked PleD activation. PleD activation was restored only when DivK was diluted below a molar ratio of 1:10. $DivK_{D53N}$ also reduced DivJ-mediated PleD activation but was less efficient than DivK wild-type (Figure 1C). These results suggested that PleD and DivK compete for the phosphodonor DivJ∼P. This was confirmed by monitoring phosphotransfer from DivJ∼P to the two response regulators. Although DivJ∼P readily served as phosphodonor for PleD in the absence of DivK, phosphoryl groups were transferred exclusively to DivK when both response regulators were present in the reaction mixture (Figure 2D). Altogether, these experiments show that DivK and PleD compete for phosphorylation by the stalked pole specific kinase DivJ, and that in vitro DivJ∼P prefers to transfers phosphate to DivK.

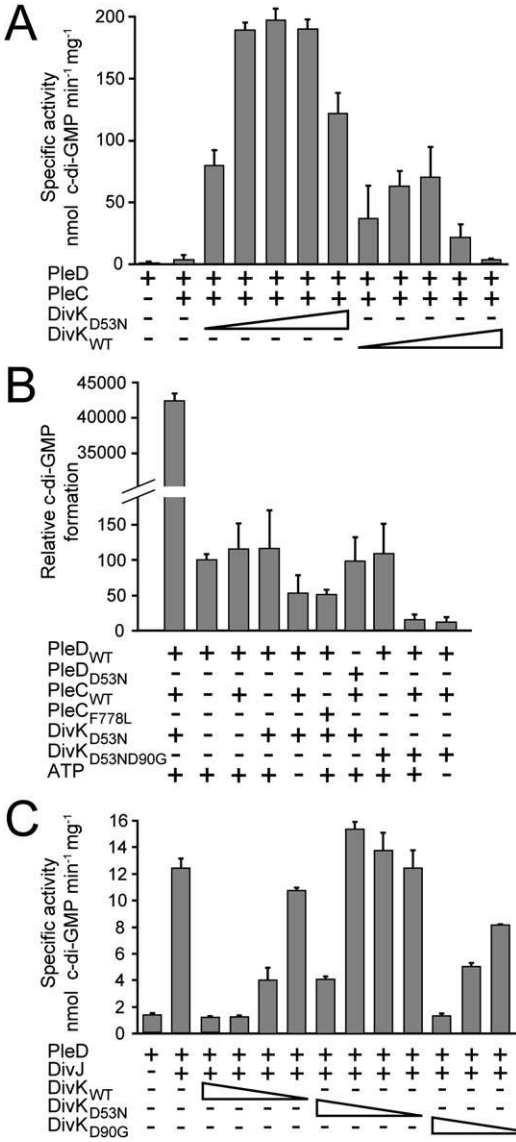

Figure 1. In Vitro Activation of the Diguanylate Cyclase PleD by the Histidine Kinase PleC and the Response Regulator DivK

(A) PleC and PleD were incubated with DivK or $DivK_{D53N}$ in the presence of ATP and [α-^{33}P]GTP. The formation of c-di-GMP was determined as initial velocities of the enzymatic reactions (Paul et al., 2007). Reactions contained 1.25 μM PleD, 10 μM PleC, and increasing amounts of $DivK_{D53N}$ or DivK (0.1 μM, 0.3 μM, 1 μM, 10 μM or 30 μM). Error bars represent the mean ± standard deviation (SD).

(B) Reaction conditions were as indicated in (A). Reactions contained 10 μM PleC wild-type or $PleC_{F778L}$, 5 μM PleD or $PleD_{D53N}$, and 10 μM $DivK_{D53N}$ or $DivK_{D53ND90G}$.

(C) Reaction conditions were as indicated in (A). Reactions contained DivJ (10 μM), PleD (10 μM), and DivK, $DivK_{D53N}$, or $DivK_{D90G}$ (10 μM, 1 μM, 0.3 μM, or 0.1 μM).

DivK Stimulates Autophosphorylation of DivJ

The observation that DivK is able to stimulate PleC autokinase activity in vitro raised the possibility that DivK might also modulate the activity of its other cognate kinase, DivJ. Similar to its observed effect on PleC, $DivK_{D53N}$ efficiently stimulated DivJ autophosphorylation (Figures 4A and S1C), and did not affect the stability of DivJ~P (Figure S1D). As for PleC, pre-incubation of DivJ with $DivK_{D53N}$ did not affect kinase solubility or quarternary structure, and stimulation by DivK was indistinguishable in untreated and DivK pre-treated samples (Figure S4). Activation of DivJ by $DivK_{D53N}$ led to increased phosphotransfer to the response regulators DivK and PleD (Figure 4B). In conclusion, DivK acts both as phosphoryl acceptor and as a potent activator of the stalked pole-specific kinase DivJ. A nonphosphorylatable form of PleD, $PleD_{D53N}$, had no stimulatory effect on DivJ or PleC (Figure S1C), arguing that the activation of the DivJ and PleC autokinase activities by DivK is specific for this response regulator.

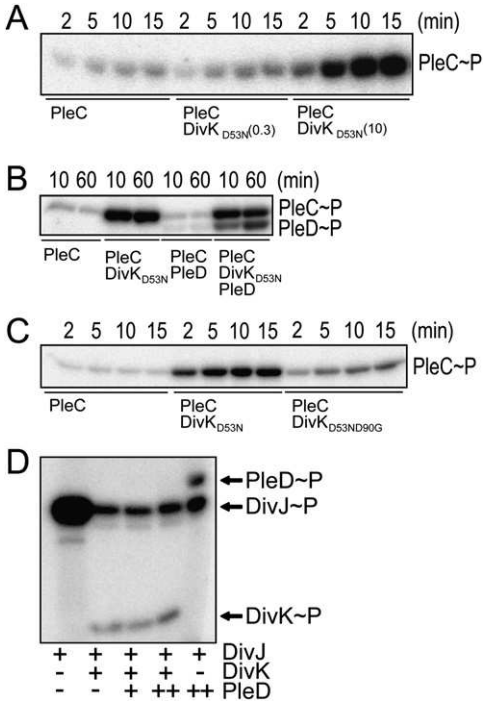

Figure 2. DivK Stimulates Autophosphorylation of the PleC Histidine Kinase

(A) In vitro autophosphorylation with PleC (10 μM) and $DivK_{D53N}$ (0.3, 10 μM).

(B) Phosphotransfer reactions with PleC (10 μM), $DivK_{D53N}$ (10 μM), and PleD (10 μM).

(C) In vitro autophosphorylation of PleC (10 μM) in the presence of $DivK_{D53N}$ (10 μM) or $DivK_{D53ND90G}$ (10 μM).

(D) In vitro phosphotransfer between DivJ (2.5 μM) and the response regulators DivK (2.5 μM) and PleD (2.5 μM or 50 μM). The bands corresponding to the phosphorylated proteins are marked.

The Developmental Mutant $DivK_{D90G}$ Fails to Stimulate PleD Activation by PleC

Consistent with the postulated cell-cycle role of DivK during the G1-to-S transition, the cold-sensitive *$divK_{D90G}$* mutant arrests in G1 at the restrictive temperature (Wu et al., 1998). At the permissive temperature, this strain shows a developmental phenotype strikingly similar to mutants lacking PleD (see below). To test if altered interactions of the mutant protein with DivJ or PleC account for this phenotype we analyzed the ability of $DivK_{D90G}$ to

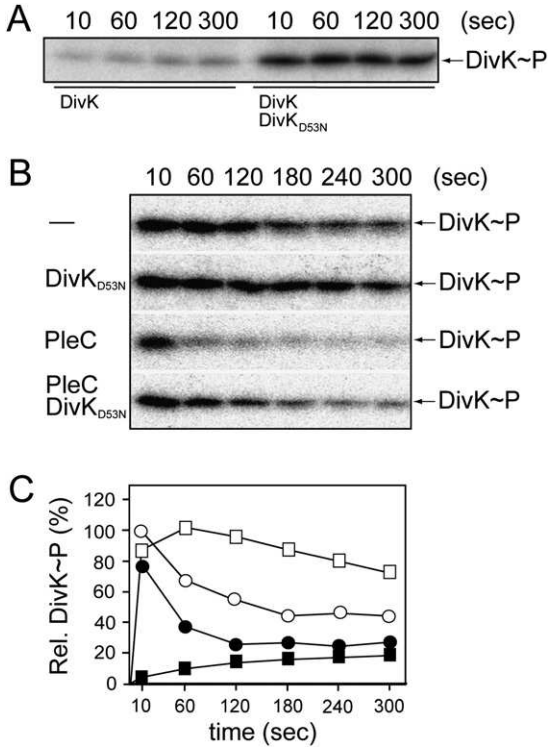

Figure 3. DivK Does not Stimulate PleC Phosphatase Activity

(A) PleC-mediated phosphorylation of DivK. PleC (10 μM) and DivK (10 μM) were incubated with [γ-^{32}P]ATP in the presence or absence of DivK$_{D53N}$ (15 μM) for the times indicated.

(B) PleC-mediated dephosphorylation of DivK. Purified DivK∼P was incubated alone (top row), with DivK$_{D53N}$ (15 μM; second row), with PleC (2.5 μM; third row), or with DivK$_{D53N}$ and PleC (bottom row) for the times indicated.

(C) Quantification of PleC-mediated DivK phosphorylation (squares) and dephosphorylation (circles) in the presence (open symbols) or absence of DivK$_{D53N}$ (closed symbols). The phosphatase assays were normalized for DivK auto-phosphatase activity.

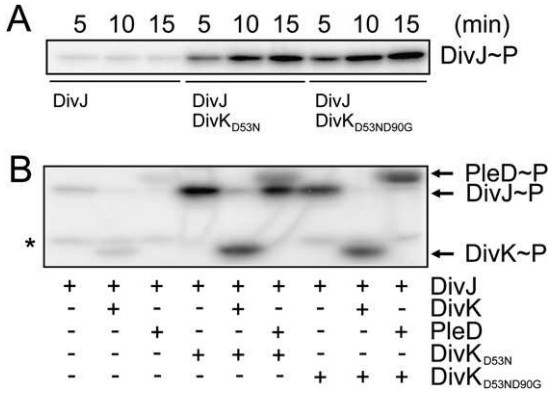

Figure 4. A Positive Feedback Mechanism Stimulates DivK Phosphorylation by DivJ

(A) DivK stimulates DivJ autophosphorylation. DivJ (10 μM) was incubated with [γ-^{32}P]ATP with DivK$_{D53N}$ (30 μM) or DivK$_{D53ND90G}$ (30 μM) for the indicated times.

(B) Phosphotransfer reactions with DivJ (10 μM), DivK (10 μM), PleD (10 μM), DivK$_{D53N}$ (10 μM), and DivK$_{D53ND90G}$ (10 μM). The bands corresponding to the phosphorylated proteins are indicated. The band labeled with an asterisk is not visible on the Coomassie-stained gel and most likely represents a gel artifact.

activate the DivJ and PleC autokinases. DivK$_{D90G}$ was slightly less efficient in competing with PleD for the activation by DivJ (Figure 1C). To analyze the interaction of DivK$_{D90G}$ with the DivJ and PleC kinases, we constructed a double mutant protein that lacked the phosphoryl acceptor Asp53. DivK$_{D53ND90G}$ was still able to stimulate DivJ autophosphorylation and phosphotransfer to DivK or PleD (Figure 4B). In contrast, DivK$_{D53ND90G}$ was unable to stimulate PleD and PleC autophosphorylation (Figures 1B and 2C), and failed to stimulate PleD activation by PleC (Figure 1B). Phosphotransfer from PleC∼P to DivK$_{D90G}$ was similar to DivK wild-type (Figure S5), and DivK$_{D53ND90G}$ did not affect PleC phosphatase activity (Figure S6). Together, these experiments show that the D90G mutation specifically affects the ability of DivK to stimulate PleC autokinase.

PleD-Dependent Pole Morphogenesis Requires the PleC Autokinase

Although the phosphatase activity of PleC is sufficient to initiate pole development and induce motility in the swarmer cell (Matroule et al., 2004), it has not been tested if PleC kinase activity plays a role during the next, PleD-dependent step of pole morphogenesis. Because PleC and DivK are able to efficiently activate PleD in vitro, we analyzed the role of PleC kinase in promoting PleD-dependent developmental processes like motility, stalk formation, holdfast synthesis, and surface attachment (Aldridge and Jenal, 1999; Aldridge et al., 2003). For this purpose, we generated a *ΔpleC* single and a *ΔpleCΔpleD* double mutant in the surface-binding wild-type strain CB15 (ATCC19089) and used these strains for complementation experiments with *pleC* alleles encoding PleC variants with kinase and phosphatase activity (K^+P^+; $pleC_{WT}$), with only phosphatase activity (K^-P^+; $pleC_{F778L}$), or lacking both activities (K^-P^-; $pleC_{T614R}$) (Matroule et al., 2004). To corroborate that the F778L mutation specifically affects PleC autokinase but not phosphatase activity in vivo, we showed that DivK∼P levels were similarly reduced in swarmer cells of strains harboring $pleC_{WT}$ or $pleC_{F778L}$, respectively (Figure S7).

C. crescentus surface binding is developmentally controlled and requires an active flagellum, the formation of polar pili, and synthesis of an adhesive holdfast (Levi and Jenal, 2006). Because of its block in pole development, the *ΔpleC* mutant completely failed to attach to plastic surfaces, whereas a *ΔpleD* mutant inefficiently adhered to surfaces because of a delay in holdfast formation (Levi and Jenal, 2006) (Figure 5A). Complementation with *pleC* wild-type fully restored surface attachment of the *ΔpleC*, but not of the *ΔpleCΔpleD* double mutant. In contrast, the $pleC_{F778L}$ (K^-P^+) allele partially restored surface binding of the *ΔpleC* mutant to the same level observed for a *ΔpleD* mutant (Figure 5A), arguing that in strains lacking PleC kinase activity development is initiated but cannot proceed past the stage of PleD activation. In comparison, expression of PleC$_{T614R}$ (K^-P^-) in the *ΔpleC* strain showed no effect (Figure 5A). Reduced attachment was the result of inefficient formation of the primary cell adhesin, the holdfast, during development. Synchronized cultures of *ΔpleC* mutant cells complemented with *pleC*

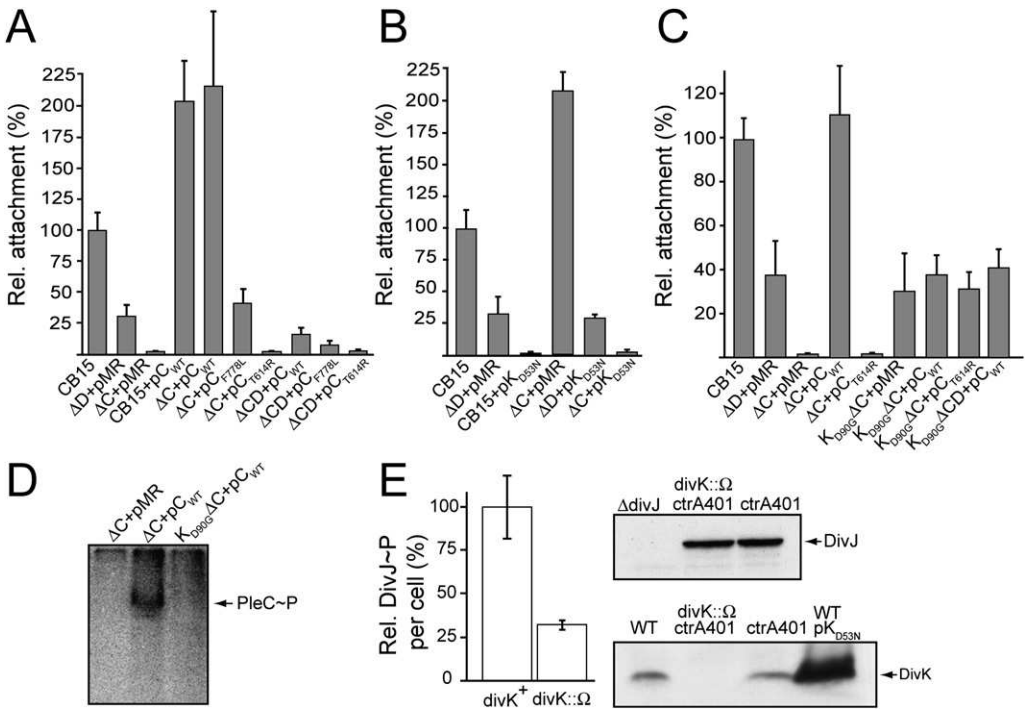

Figure 5. DivK Stimulates PleC and DivJ Autokinase Activities in Vivo

(A) PleC kinase activity is required for PleD-dependent surface attachment. Attachment of cells to polystyrene was measured for the following strains as described in (Levi and Jenal, 2006): CB15 wild-type, *ΔpleC* (ΔC), and *ΔpleC ΔpleD* (ΔCD). As indicated, the strains contained an empty vector (pMR) or a plasmid copy of the following *pleC* alleles: *pleC* wild-type (pC$_{WT}$), *pleC$_{F778L}$* (pC$_{F778L}$), or *pleC$_{T614R}$* (pC$_{T614R}$). Error bars represent the mean ± SD.

(B) and (C) Surface attachment of the following strains was measured: CB15 wild-type, *ΔpleD* (ΔD), *ΔpleC* (ΔC), *divK$_{D90G}$ ΔpleC* (K$_{D90G}$ΔC), and *divK$_{D90G}$ ΔpleC ΔpleD* (K$_{D90G}$ΔCD). The strains contained an empty vector (pMR) or a plasmid copy of the *pleC* wild-type (pC$_{WT}$) or *pleC$_{T614R}$* (pC$_{T614R}$) allele as indicated.

(D) Levels of PleC∼P in the *ΔpleC* deletion strain containing an empty vector (ΔC+pMR), the *ΔpleC* deletion strain containing a plasmid copy of the *pleC* wild-type (ΔC+pC$_{WT}$), and the *divK$_{D90G}$ ΔpleC* double mutant containing a plasmid copy of the *pleC* wild-type (K$_{D90G}$ΔC+pC$_{WT}$). The band corresponding to PleC∼P is marked.

(E) Levels of DivJ∼P per cell in a *C. crescentus divK$^+$* strain and a *divK:Ω* null mutant (left panel). Immunoblots with anti-DivJ and anti-DivK antibodies, respectively, are shown on the right. Error bars represent the mean ± SD.

wild-type developed a visible holdfast 15–30 min after swarmer cells were released into fresh medium (Figure 6A). A similar pattern was observed for *C. crescentus* wild-type cells (Levi and Jenal, 2006). In contrast, cells expressing *pleC$_{F778L}$* (K$^-$P$^+$) showed a severe delay in holdfast synthesis and reduced surface attachment during the swarmer-to-stalked cell differentiation (Figure 6A). Because activation of the PleD response regulator results in the production of c-di-GMP (Paul et al., 2004), we next tested if PleD-dependent pole morphogenesis correlates with the production of the second messenger during development. A pronounced peak of c-di-GMP was observed early in the *C. crescentus* cell cycle coincident with the onset of holdfast biogenesis both in wild-type (data not shown) and in the *ΔpleC* mutant complemented with wild-type *pleC* (Figure 6B). Because c-di-GMP levels failed to increase in *pleD* mutant cells or in cells lacking PleC kinase activity (K$^-$P$^+$), we conclude that both activities are necessary to increase second messenger concentration during *Caulobacter* cell differentiation.

Likewise, motility control and stalk biogenesis during *C. crescentus* cell differentiation required both PleD and an active PleC autokinase (Figure S8). Together these findings suggest that while PleC phosphatase activity is sufficient to activate the motility program in newborn swarmer cells, consecutive steps in pole development during the G1-to-S transition require PleC autokinase activity to activate the PleD diguanylate cyclase.

DivK Stimulates the PleC-PleD Signal Transduction Pathway Involved in Cell Fate Determination

To investigate the in vivo role of DivK in pole development we first tested if increased cellular concentrations of DivK$_{D53N}$ could stimulate PleC- and PleD-dependent surface attachment. Cells containing an additional plasmid-borne copy of *divK$_{D53N}$* showed increased surface attachment as compared to cells harboring a control plasmid (Figures 5B and 5E). Importantly, attachment was not increased in strains lacking PleD or PleC autokinase activity, arguing that higher levels of DivK$_{D53N}$ increased attachment in a PleC- and PleD-dependent manner.

Next, we compared surface attachment of *C. crescentus* wild-type with that of a *divK$_{D90G}$* mutant strain. The observation that DivK$_{D90G}$ failed to stimulate PleD activity through the PleC kinase in vitro suggested that the PleD-dependent pathway controlling pole development might be inactive in the *divK$_{D90G}$* mutant at the permissive temperature. As shown in Figure 5C, the complete deficiency of the *ΔpleC* mutant to attach to surfaces was

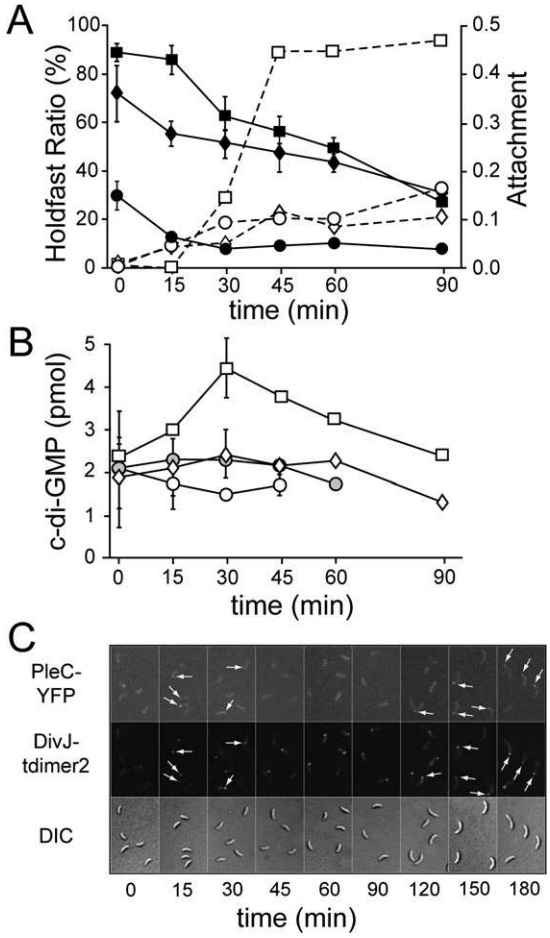

Figure 6. PleD-Dependent c-di-GMP Synthesis and Holdfast Formation during Development Requires DivK and PleC Kinase Activity

(A) Holdfast formation (open symbols) and attachment (closed symbols) during the G1-to-S transition. Swarmer cells of the following strains were isolated and suspended in M2G medium: *ΔpleC* deletion strain containing a plasmid copy of the *pleC* wild-type (squares), *ΔpleC* deletion strain containing a plasmid copy of the $pleC_{F778L}$ allele (diamonds), and a $divK_{D90G}$*ΔpleC* double mutant containing a plasmid copy of the *pleC* wild-type (circles). Error bars represent the mean ± SD.

(B) Measurements of c-di-GMP levels during the G1-to-S transition. The following strains were analyzed: *ΔpleC* deletion strain containing a plasmid copy of the *pleC* wild-type (squares), *ΔpleC* deletion strain containing a plasmid copy of the $pleC_{F778L}$ allele (circles), *ΔpleC ΔpleD* deletion strain containing a plasmid copy of the *pleC* wild-type (diamonds), and a $divK_{D90G}$*ΔpleC* double mutant containing a plasmid copy of the *pleC* wild-type (gray circles).

(C) PleC-mYFP and DivJ-tDimer2 localization was examined by epi-fluorescence microscopy in synchronized cell populations of UJ4507 at the indicated time points. Arrows indicate polar foci.

partially suppressed in the presence of the $divK_{D90G}$ allele. This is consistent with the observation that $divK_{D90G}$ is able to bypass the cell division checkpoint of cells lacking the PleC phosphatase (Matroule et al., 2004; Sommer and Newton, 1991). However, attachment of a *ΔpleC* $divK_{D90G}$ double mutant remained at an intermediary level typically observed for cells lacking PleD, and an extrachromosomal copy of the *pleC* wild-type gene could not restore wild-type levels of attachment in this mutant background (Figure 5C). Finally, a *ΔpleC ΔpleD* $divK_{D90G}$ triple mutant when complemented with *pleC* wild-type showed the same intermediary attachment level, arguing that PleD was not activated in the presence of the $divK_{D90G}$ allele. Like mutants lacking PleD or the PleC autokinase activity, $divK_{D90G}$ mutant cells showed a severe delay in holdfast synthesis during the swarmer-to-stalked cell differentiation (Figure 6A) and were unable to produce the characteristic PleD-dependent peak of c-di-GMP during the G1-S transition (Figure 6B).

Altogether, these experiments corroborate the results obtained in vitro and suggest that DivK is required for the activation of the PleC autokinase in vivo. Based on this we propose that PleC, DivK and PleD define a pathway required for c-di-GMP mediated pole morphogenesis during *C. crescentus* cell differentiation.

DivK Stimulates PleC and DivJ Kinase Activity In Vivo

An attractive model to explain how DivK activates PleC autokinase during the G1-to-S transition combines the in vitro and in vivo data presented above with the spatial dynamics of DivK during the cell cycle (Jacobs et al., 2001; Matroule et al., 2004). In such a model the appearance of DivJ during swarmer cell differentiation activates DivK and mediates its localization to the PleC-occupied pole. An increase of DivK levels at this site would then activate the PleC autokinase and trigger c-di-GMP production through PleD phosphorylation. If so, one would predict that in differentiating cells the autokinase activities of both PleC and DivJ are dependent on DivK. To test this we measured the in vivo levels of PleC∼P and DivJ∼P in dependence of DivK. PleC∼P was readily detectable in wild-type cells but was greatly reduced in $divK_{D90G}$ mutant cells at the permissive conditions (Figure 5D). Because $DivK_{D90G}$ was still able to stimulate DivJ in vitro (Figure 4), we generated a *divK* null mutant strain to test the influence of DivK on DivJ activation in vivo. The *divK* gene was inactivated in the *ctrA401* mutant background, which shows reduced activity of the cell cycle master regulator CtrA (Quon et al., 1998). Consistent with the observation that *ctrA* mutant alleles can restore viability of *divK* null mutants (Wu et al., 1998), a *divK::Ω ctrA401* double mutant was fully viable. As shown in Figure 5E, DivJ∼P levels were significantly reduced in *ΔdivK ctrA401* double mutant as compared to the isogenic *ctrA401* single mutant. These results support the conclusion that DivK is required to stimulate PleC and DivJ autokinase activities in vivo.

The model outlined above predicts that PleC and DivJ colocalize at the differentiating pole at the time when PleD is activated and the holdfast is synthesized. To test this we analyzed the localization patterns of PleC and DivJ in synchronized cells expressing a PleC-YFP and a DivJ-tDimer2 fusion (Matroule et al., 2004; Wheeler and Shapiro, 1999). PleC-YFP is localized in swarmer cells but disperses from the emerging stalked pole between 30 and 45 min after the initiation of development when cellular levels of PleC drop (Figures 6C and S9). At later stages of the cell cycle, PleC-YFP concentrates at the pole opposite the stalk (Figure 6C). In contrast, in newborn swarmer cells DivJ levels are low and DivJ-tDimer2 is absent at the flagellated pole. In parallel with an increase of DivJ, DivJ-tDimer2 concentrates at the emerging stalked pole already after 15 min (Figures 6C and S9). As a result, DivJ-tDimer2 and PleC-YFP coexist at

the differentiating pole during a time window that overlaps with PleD-mediated c-di-GMP production and holdfast synthesis (Figures 6A–6C and S9). Localization studies with PleC-YFP and DivK-CFP as well as with DivJ-YFP and DivK-CFP indicated that DivK-CFP is also present at the differentiating cell pole during the same time window (data not shown).

DISCUSSION

Our data establish posttranslational feedback loops as important elements of the regulatory machinery that determines cell fate in *C. crescentus*. At the heart of this regulatory mechanism is the diffusible single domain response regulator DivK, which is required for cell cycle progression and the establishment of asymmetry (Hecht et al., 1995; Hung and Shapiro, 2002; Jacobs et al., 2001; Lam et al., 2003; Matroule et al., 2004). Two antagonistic players, PleC and DivJ, localized at opposite poles of the predivisional cell, determine the phosphorylation status and polar localization of DivK during the cell cycle (Jacobs et al., 2001; Lam et al., 2003; Matroule et al., 2004; Wheeler and Shapiro, 1999) (Figure 7). DivK implements cell cycle control through CtrA (Biondi et al., 2006; Hung and Shapiro, 2002; Wu et al., 1998), a DNA-binding response regulator that is controlled by phosphorylation (Biondi et al., 2006; Domian et al., 1997; Quon et al., 1996), but the molecular basis for this interaction is unknown. Based on our data we propose that DivK primarily acts by modulating the activities of DivJ and PleC, and possibly other sensor histidine kinases involved in *C. crescentus* polarity and cell cycle control (Ohta and Newton, 2003; Wheeler and Shapiro, 1999). DivK∼P negatively controls the CckA-ChpT pathway that regulates CtrA phosphorylation and stability during the cell cycle (Biondi et al., 2006). However, as there is no evidence that this interaction is direct, important regulatory components of the DivK network might still be missing. A potential candidate for such a component is the unorthodox sensor kinase DivL (Wu et al., 1999). Not only were *divL* alleles isolated in a genetic screen together with *divK, divJ, pleC,* and *pleD* (Ohta et al., 1992; Sommer and Newton, 1991), but the DivL kinase also localizes to the cell poles (Sciochetti et al., 2005). Because in vitro experiments failed to identify additional kinases stimulated by $DivK_{D53N}$ (E.G.B. and M.T.L., unpublished data), we propose that DivK is a specific regulator of DivJ, PleC, and possibly DivL.

In vitro and in vivo studies suggest that DivK is a potent activator of the PleC kinase that changes the cell's developmental program by switching PleC from its default phosphatase into an autokinase mode during the G1-to-S transition. These data are in agreement with the observed synergistic effect between PleC and DivK (Hecht et al., 1995). The only direct targets of bifunctional PleC identified so far are DivK and PleD, with DivK∼P being a substrate of the PleC phosphatase in swarmer cells (Matroule et al., 2004; Wheeler and Shapiro, 1999) and PleC∼P acting as a phosphodonor for PleD in stalked cells. PleC, once activated by DivK, might also contribute to DivK phosphorylation in stalked and predivisional cells. But if DivK∼P is a substrate for the PleC phosphatase in swarmer cells and then switches PleC into the autokinase mode during differentiation, what triggers this transition? DivJ, the main kinase of DivK is present at very low concentrations in swarmer cells (Jacobs et al., 2001; Wheeler and Shapiro, 1999). As DivJ levels rise during G1-to-S, DivJ localizes to the differentiating pole. At this stage DivJ-mediated phosphorylation localizes DivK∼P to the cell pole, where it forces PleC into the autokinase mode (Figure 7). Because DivK also activates DivJ, the two proteins might form a positive feedback loop that leads to a strong stimulation of DivJ in stalked cells. Upregulation of the DivJ autokinase by DivK might be particularly important to quickly and robustly switch PleC from the phosphatase to the kinase mode during the G1-to-S transition and in the predivisional cell (Figure 7). Conversely, the feedback loops can also explain how the system is quickly reset as cells enter G1. The dominant role of DivJ in DivK phosphorylation and polar localization suggests that its loss results in the dissolution of DivK from the poles (Jacobs et al., 2001; Matroule et al., 2004). Therefore, exclusion of DivJ from the swarmer compartment during cytokinesis will reduce DivK∼P levels and decrease DivK concentration at the flagellated pole below a threshold level required for PleC autokinase activation. As a result, PleC switches back into its phosphatase mode, thereby installing the swarmer cell program. Thus, the feedback loops described here might give rise to sharp and robust developmental transitions. The recurring spatial mixing and separation of the default phosphatase PleC and its dominant inhibitor, the DivJ-DivK kinase loop, would contribute to the oscillation of the system between stalked and swarmer programs (Figure 7A). The role of DivK is to facilitate long-range communication between the asymmetric DivJ and PleC antagonists and coordinate their activities.

This model makes the critical assumption that localization of DivK∼P to the cell poles increases DivK concentration at this subcellular site above a threshold level required for the activation of the PleC and DivJ kinases. The model predicts that polar localization of DivJ and PleC is critical for the DivK-mediated feedback loops to operate. Indeed, mutants lacking the SpmX muramidase fail to recruit DivJ to the emerging stalked pole and are unable to activate DivJ kinase and spark DivK phosphorylation in stalked cells (Radhakrishnan et al., 2008). Conversely, mutants lacking PodJ fail to localize PleC to the flagellated cell pole and show distinct pole development defects (Viollier et al., 2002; Wang et al., 1993). Intriguingly, *podJ* and *spmX* expression is controlled reciprocally by activated CtrA∼P (Figure 7B) (Crymes et al., 1999; Radhakrishnan et al., 2008) opening up the possibility that DivJ and PleC, through DivK, control their own spatiotemporal behavior.

What could be the molecular mechanism through which DivK stimulates the autokinase activities of PleC and DivJ? Efficient stimulation of PleC and DivJ autophosphorylation was obtained at a 1:1 ratio of kinase and $DivK_{D53N}$ and a soluble kinase fragment containing only the DHp (dimerization and histidine phosphotransfer) and CA (catalytic and ATP-binding) domains (Parkinson and Kofoid, 1992; Stock et al., 2000). Thus, DivK modulates autokinase activity by binding to the catalytic core fragment. This is in accordance with results from a yeast two-hybrid screen that indicated DivK binding to a shared 66 amino acid sequence forming the core of the DHp domain of several kinases including PleC and DivJ (Ohta and Newton, 2003). Because DivK did not affect the oligomerization state of PleC and DivJ, interference with kinase dimerization seems unlikely. The observed drop of basal level activity of the PleD diguanylate cyclase under

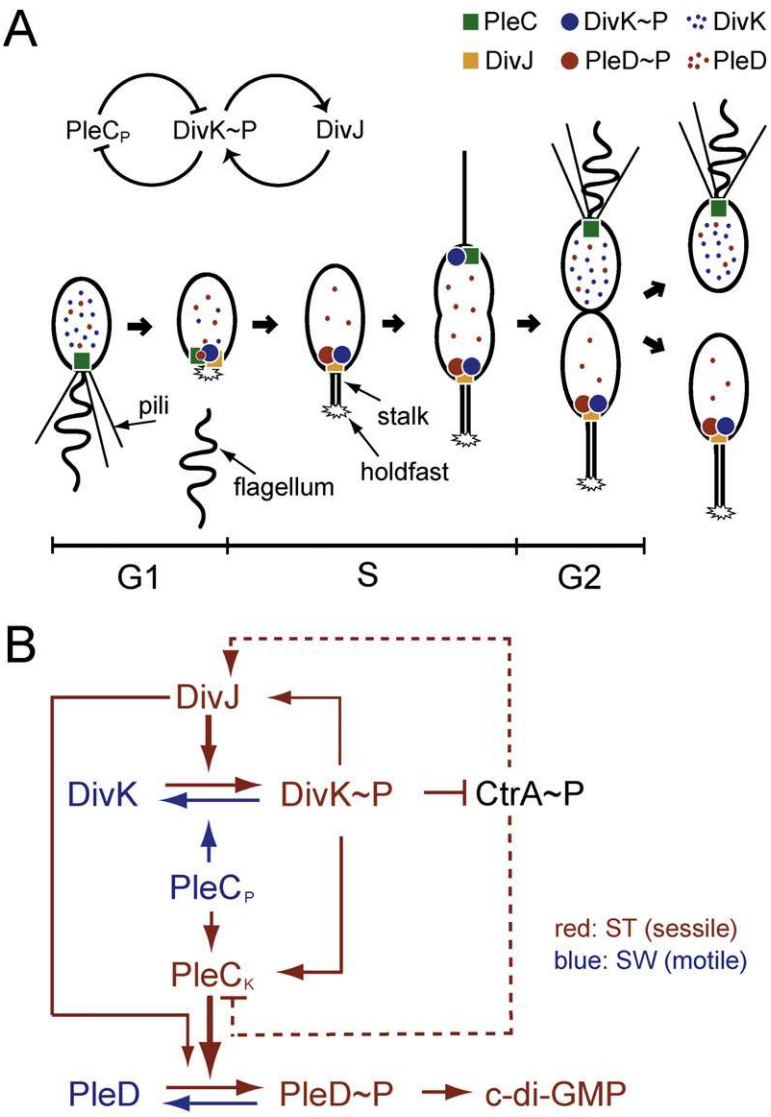

Figure 7. Model for the Regulation of the PleC-DivJ-DivK Cell Fate Control System

(A) Schematic of the *C. crescentus* cell cycle with polar appendices and localization patterns for PleC, DivJ, DivK, DivK∼P, PleD, and PleD∼P. A summary of the posttranslational feedback circuitry with the DivJ kinase, the PleC phosphatase, and the DivK response regulator is indicated.

(B) Diagram of the phosphorylation circuit controlling cell fate and cellular asymmetry in *Caulobacter crescentus*. The model predicts that the sessile-stalked cell program is directed through polar DivK∼P interacting with and activating both PleC and DivJ kinases. Likewise, the motile-swarmer cell program results from the absence of the DivJ kinase, dissolution of DivK from the cell pole, and establishment of the PleC phosphatase activity. The two known molecular targets of the PleC-DivJ-DivK cell fate machinery, PleD and CtrA, are indicated. Stippled lines indicate PleC and DivJ polar localization control through CtrA∼P-regulated expression of *podJ* and *spmX*, respectively (Crymes et al., 1999; Radhakrishnan et al., 2008).

conditions where autophosphorylation is absent or inefficient, indicates the formation of a nonproductive ternary complex that engages PleD in an inactive monomeric form (Paul et al., 2007). Possibly, DivK and PleD monomers interact with the same kinase dimer and DivK bound to one kinase protomer can activate autophosphorylation and phosphotransfer to PleD via the other protomer. The failure of the DivK$_{D90G}$ mutant to stimulate PleC kinase activity in vitro and in vivo could result from an altered interaction with the DHp domain of the kinase. This view is consistent with the position of Asp90 at the N terminus of the DivK receiver domain helix α4. Because this region undergoes structural changes upon phosphorylation (Robinson et al., 2000) and makes specific contacts with the DHp domain (Zapf et al., 2000) it is a good candidate for the interaction surface that mediates the phosphatase-kinase switch of PleC.

In conclusion, our results indicate a role for the abundant class of single domain response regulators in spatially interconnecting different components of the two-component signal transduction circuitry. While recent system level approaches indicated that a one-to-one relationship between histidine kinases and their cognate response regulators prevents unwanted cross-talk (Skerker et al., 2005; Yamamoto et al., 2005) our results add a new level of complexity to this sensory network demonstrating the possibility of widespread inter-connections between apparently insolated signaling systems through retrograde information transfer from response regulators to cognate kinases.

EXPERIMENTAL PROCEDURES

Strains, Plasmids, and Media

The bacterial strains and plasmids used in this study are shown in Table S1. *Caulobacter crescentus* strains were grown in peptone yeast extract (PYE), or in minimal glucose media (M2G, [Ely, 1991]). Newborn SW cells were isolated by Ludox or Percoll gradient centrifugation (Jenal and Shapiro, 1996), and released into fresh M2G medium. For conjugal transfer into *C. crescentus*, *Escherichia coli* strain S17-1 was used as donor. The *divK*$_{D90G}$ mutation (Sommer and Newton, 1991) was introduced into CB15Δ*pleC* (UJ731) by allelic exchange. To generate the *divK* null mutant, the *divK::*Ω allele was transduced from strain CJ403 (Lam et al., 2003) into the *C. crescentus ctrA401* mutant strain (Quon et al., 1996). The exact procedures of strain and plasmid construction are available on request. Unless stated otherwise, pooled data consist of at least three independent experiments and are represented as mean ± standard deviation (SD).

Attachment Assays and Holdfast Staining

For attachment assays, logarithmically growing *C. crescentus* cells were diluted 1:30 in PYE, and cultivated for 24 hr in 96-well microtiter plates at 200 rpm on a rocking platform. Attachment of cells to the polystyrene surface was quantified as described (Levi and Jenal, 2006). For attachment assays of synchronized populations, cell aliquots were transferred to microtiter plates at the time points indicated, and allowed to bind to the plastic surface for 15 min at room temperature before staining. *C. crescentus* holdfast was stained with a mixture of Oregon Green-conjugated wheat-germ agglutinin (0.2 mg/ml) and Calcofluor White (0.1 mg/ml) and was visualized by fluorescence imaging on an Olympus AX70 microscope with a Hamamatsu C4742-95 digital camera (Levi and Jenal, 2006). Images were recorded and processed with Improvision Openlab and the Photoshop CS v8.0 (Adobe, CA) software packages.

Fluorescence Microscopy

For fluorescence imaging bacteria were placed on a microscope slide coated with 2% agarose dissolved in water. An Olympus IX71 microscope equipped with an UPlanSApo 100×/1.40 Oil objective (Olympus, Germany) and a cool-SNAP HQ CCD camera (Photometrics, AZ, United States) were used to take differential interference contrast (DIC) and fluorescence photomicrographs. YFP (Ex 500/20 nm, EM 535/30 nm) Rhodamine filter sets (Ex 555/28 nm, EM 617/73 nm) were used. DIC pictures were taken with 0.15 s and fluorescence pictures with 1.0 s exposure time. Images were processed with softWoRx v3.3.6 (Applied Precision, WA) and Photoshop CS v8.0 softwares.

In Vivo *Phosphorylation*

In vivo phosphorylation experiments were performed as described previously (Domian et al., 1997; Jacobs et al., 2001) with the following modifications. The strains were grown in M5G minimal medium supplemented with 1 mM glutamate until an optical density at 660 nm of 0.15, collected by centrifugation and resuspended in filtered culture medium to an optical density of 0.3. Cells were labeled at 30°C for 5 min with 100 μCi [^{32}P]H_3PO_4 or 30 μCi [^{32}P]ATP, and after lysis immunoprecipitated with 10 μl anti-PleC, anti-DivK, or anti-DivJ serum. Radiolabeled proteins were separated on a 10% polyacryamide gel and visualized with a phosphoimager (Molecular Dynamics, GE Healthcare, NJ).

Nucleotide Analysis

For the analysis of c-di-GMP levels in synchronized *C. crescentus* cultures (OD_{660} 0.4), nucleotides were extracted with 1 M formic acid. Lyophilized samples were analyzed with a 125/4 Nucleosil 4000-1 PEI column (Macherey-Nagel, Germany) on SMART- (GE Healthcare, NJ) or Pro Star HPLC-Systems (Varian, CA). The nucleotides were applied to the column dissolved in buffer A (7 mM KH_2PO_4 [pH 4]), and eluted with a gradient of buffer B (0.5 M KH_2PO_4, 1 M Na_2SO_4 [pH 5.5]) at a flow rate of 50 μl/min. Concentrations were determined by comparison with a standard of chemically synthesized c-di-GMP.

Expression and Purification of Proteins

E. coli cells carrying the respective expression plasmid were grown in LB medium with ampicillin (100 μg/ml), and expression was induced by adding either arabinose (final concentration of 0.2%) or IPTG (final concentration of 0.4 mM). After harvesting by centrifugation, the cells were resuspended in TN-buffer (50 mM Tris-HCl [pH 8.0], 500 mM NaCl, 5 mM β-mercaptoethanol), lysed by passage through a French pressure cell, and clarified by centrifugation. The supernatant was loaded onto Ni-NTA affinity resin (QIAGEN, Germany), washed with TN-buffer, and eluted with an imidazol-gradient. PleD, DivK, a catalytic fragment of DivJ‘ (C-terminal 296 amino acids), and a catalytic PleC‘ fragment containing the complete cytoplasmic domains (540 amino acids) remained soluble and were purified under native conditions. Two additional catalytic PleC‘ fragments (containing the C-terminal 313 or 489 amino acids, respectively) were solubilized from inclusion bodies and renatured after purification (Hecht et al., 1995; Paul et al., 2004). Proteins were examined for purity by SDS-PAGE and fractions containing pure protein were pooled and dialyzed. DivK was concentrated by precipitation with 60% saturated ammonium sulfate (pH 7.0) prior to dialysis; the kinase fragments and PleD were concentrated using Amicon Ultra- or Microcon- Centrifugal Filter Units (Millipore, MA). Analytical size exclusion chromatography was performed with a Superdex 200 column on an ÄKTApurifier (GE Healthcare) system at a flow rate of 0.5 ml/min. Concentrations and molecular weights of proteins were determined by an online refractometer (Optilab rEX, Wyatt Technology) and a miniDAWN light scattering instrumentation (Wyatt Technology, CA). Untagged DivK for in vitro phosphatase assays was obtained by cleaving His-DivK with Thrombin (Novagen, WI, United States) for 1 hr at 25°C, followed by preparative size exclusion chromatography with a Superdex 75 column on an ÄKTApurifier (GE Healthcare, NJ) at a flow rate of 1.5 ml/min.

Enzymatic Assays

Diguanylate cyclase assays were adapted from procedures described previously (Paul et al., 2007, 2004). The standard diguanylate cyclase reaction mixtures contained 50 mM Tris-HCl (pH 7.8), 250 mM NaCl, 10 mM $MgCl_2$ in 50 μl volume and was started by the addition of a mixture of 100 μM GTP/[α-^{33}P]GTP (PerkinElmer; 0.01 μCi/μl). All kinase reactions were supplemented with 25 mM KCl. To calculate the initial velocity of product formation, aliquots were withdrawn at regular time intervals and the reaction was stopped with an equal volume of 50 mM EDTA (pH 6.0). Reaction products (2 μl) were separated on polyethyleneimine-cellulose plates (Macherey-Nagel) in 1.5 M KH_2PO_4/5.5 M $(NH_4)_2SO_4$ (pH 3.5) in a 2:1 ratio. Plates were exposed to a phosphorimager screen, and the intensity of the various radioactive species was calculated by quantifying the intensities of the relevant spots using the ImageQuant software (Molecular Dynamics). Measurements were always restricted to the linear range of product formation. In vitro kinase and phosphatase assays were performed as described earlier (Hecht et al., 1995; Matroule et al., 2004; Paul et al., 2004; Skerker et al., 2005). For kinase assays the proteins were incubated at 25°C for 15 min in phosphorylation buffer (50 mM Tris-HCl at pH 7.8, 25 mM NaCl, 25 mM KCl, 5 mM $MgCl_2$) containing 5 μCi [γ-^{32}P]ATP (Amersham Biosciences, GE Healthcare, NJ), unless stated otherwise. Reactions were stopped with 4× SDS-PAGE sample buffer (250 mM Tris-HCl at pH 6.8, 40% glycerol, 8% SDS, 2.4 M β-mercaptoethanol, 0.06% bromophenol blue, 40 mM EDTA), and ^{32}P-labeled proteins were separated by electrophoresis on 10% SDS-PAGE gels followed by autoradiography on a phosphor-imager screen. DivK-P for phosphatase assays was purified from contaminating His-tagged PleC and $DivK_{D53N}$ by two rounds of batch purification with Ni-NTA resin (QIAGEN, Germany), followed by gel filtration for the removal of ATP.

SUPPLEMENTAL DATA

Supplemental Data include nine figures, one table, and Supplemental References and can be found with this article online at http://www.cell.com/cgi/content/full/133/3/■■■/DC1/.

ACKNOWLEDGMENTS

We thank all members of the Jenal group for valuable discussions and Arnaud Basle, Assaf Levi, Dietrich Samurai, and Paul Wassmann for technical assistance. We are grateful to Y. Brun, T. Costa, C. Jacobs-Wagner, J.-Y. Matroule, A. Newton, N. Ohta, D. Pierce, and P. Viollier for providing mutant strains, plasmids, and antisera. This work was supported by Swiss National Science Foundation Fellowship 3100A0-108186 to U.J.

Received: August 14, 2007
Revised: December 21, 2007
Accepted: February 11, 2008
Published: May 1, 2008

REFERENCES

Aldridge, P., and Jenal, U. (1999). Cell cycle-dependent degradation of a flagellar motor component requires a novel-type response regulator. Mol. Microbiol. *32*, 379–391.

Aldridge, P., Paul, R., Goymer, P., Rainey, P., and Jenal, U. (2003). Role of the GGDEF regulator PleD in polar development of Caulobacter crescentus. Mol. Microbiol. *47*, 1695–1708.

Betschinger, J., and Knoblich, J.A. (2004). Dare to be different: asymmetric cell division in Drosophila, C. elegans and vertebrates. Curr. Biol. *14*, R674–R685.

Biondi, E.G., Reisinger, S.J., Skerker, J.M., Arif, M., Perchuk, B.S., Ryan, K.R., and Laub, M.T. (2006). Regulation of the bacterial cell cycle by an integrated genetic circuit. Nature *444*, 899–904.

Crymes, W.B., Jr., Zhang, D., and Ely, B. (1999). Regulation of podJ expression during the Caulobacter crescentus cell cycle. J. Bacteriol. *181*, 3967–3973.

Domian, I.J., Quon, K.C., and Shapiro, L. (1997). Cell type-specific phosphorylation and proteolysis of a transcriptional regulator controls the G1-to-S transition in a bacterial cell cycle. Cell *90*, 415–424.

Ely, B. (1991). Genetics of *Caulobacter crescentus*. Methods Enzymol. *204*, 372–384.

Hecht, G.B., Lane, T., Ohta, N., Sommer, J.M., and Newton, A. (1995). An essential single domain response regulator required for normal cell division and differentiation in Caulobacter crescentus. EMBO J. *14*, 3915–3924.

Hung, D.Y., and Shapiro, L. (2002). A signal transduction protein cues proteolytic events critical to Caulobacter cell cycle progression. Proc. Natl. Acad. Sci. USA *99*, 13160–13165.

Jacobs, C., Hung, D., and Shapiro, L. (2001). Dynamic localization of a cytoplasmic signal transduction response regulator controls morphogenesis during the Caulobacter cell cycle. Proc. Natl. Acad. Sci. USA *98*, 4095–4100.

Jenal, U., and Shapiro, L. (1996). Cell cycle-controlled proteolysis of a flagellar motor protein that is asymmetrically distributed in the Caulobacter predivisional cell. EMBO J. *15*, 2393–2406.

Lam, H., Matroule, J.Y., and Jacobs-Wagner, C. (2003). The asymmetric spatial distribution of bacterial signal transduction proteins coordinates cell cycle events. Dev. Cell *5*, 149–159.

Levi, A., and Jenal, U. (2006). Holdfast formation in motile Swarmer cells optimizes surface attachment during Caulobacter crescentus development. J. Bacteriol. *188*, 5315–5318.

Matroule, J.Y., Lam, H., Burnette, D.T., and Jacobs-Wagner, C. (2004). Cytokinesis monitoring during development; rapid pole-to-pole shuttling of a signaling protein by localized kinase and phosphatase in Caulobacter. Cell *118*, 579–590.

McAdams, H.H., and Shapiro, L. (2003). A bacterial cell-cycle regulatory network operating in time and space. Science *301*, 1874–1877.

Ohta, N., Lane, T., Ninfa, E.G., Sommer, J.M., and Newton, A. (1992). A histidine protein kinase homologue required for regulation of bacterial cell division and differentiation. Proc. Natl. Acad. Sci. USA *89*, 10297–10301.

Ohta, N., and Newton, A. (2003). The core dimerization domains of histidine kinases contain recognition specificity for the cognate response regulator. J. Bacteriol. *185*, 4424–4431.

Parkinson, J.S., and Kofoid, E.C. (1992). Communication modules in bacterial signaling proteins. Annu. Rev. Genet. *26*, 71–112.

Paul, R., Abel, S., Wassmann, P., Beck, A., Heerklotz, H., and Jenal, U. (2007). Activation of the diguanylate cyclase pleD by phosphorylation-mediated dimerization. J. Biol. Chem. *282*, 29170–29177.

Paul, R., Weiser, S., Amiot, N.C., Chan, C., Schirmer, T., Giese, B., and Jenal, U. (2004). Cell cycle-dependent dynamic localization of a bacterial response regulator with a novel di-guanylate cyclase output domain. Genes Dev. *18*, 715–727.

Quon, K.C., Marczynski, G.T., and Shapiro, L. (1996). Cell cycle control by an essential bacterial two-component signal transduction protein. Cell *84*, 83–93.

Quon, K.C., Yang, B., Domian, I.J., Shapiro, L., and Marczynski, G.T. (1998). Negative control of bacterial DNA replication by a cell cycle regulatory protein that binds at the chromosome origin. Proc. Natl. Acad. Sci. USA *95*, 120–125.

Radhakrishnan, S.K., Thanbichler, M., and Viollier, P.H. (2008). The dynamic interplay between a cell fate determinant and a lysozyme homolog drives the asymmetric division cycle of Caulobacter crescentus. Genes Dev. *22*, 212–225.

Robinson, V.L., Buckler, D.R., and Stock, A.M. (2000). A tale of two components: a novel kinase and a regulatory switch. Nat. Struct. Biol. *7*, 626–633.

Sciochetti, S.A., Ohta, N., and Newton, A. (2005). The role of polar localization in the function of an essential Caulobacter crescentus tyrosine kinase. Mol. Microbiol. *56*, 1467–1480.

Skerker, J.M., Prasol, M.S., Perchuk, B.S., Biondi, E.G., and Laub, M.T. (2005). Two-component signal transduction pathways regulating growth and cell cycle progression in a bacterium: a system-level analysis. PLoS Biol. *3*, e334. 10.1371/journal.pbio.0030334.

Sommer, J.M., and Newton, A. (1991). Pseudoreversion analysis indicates a direct role of cell division genes in polar morphogenesis and differentiation in Caulobacter crescentus. Genetics *129*, 623–630.

Stock, A.M., Robinson, V.L., and Goudreau, P.N. (2000). Two-component signal transduction. Annu. Rev. Biochem. *69*, 183–215.

Viollier, P.H., Sternheim, N., and Shapiro, L. (2002). Identification of a localization factor for the polar positioning of bacterial structural and regulatory proteins. Proc. Natl. Acad. Sci. USA *99*, 13831–13836.

Wang, S.P., Sharma, P.L., Schoenlein, P.V., and Ely, B. (1993). A histidine protein kinase is involved in polar organelle development in *Caulobacter crescentus*. Proc. Natl. Acad. Sci. USA *90*, 630–634.

Wassmann, P., Chan, C., Paul, R., Beck, A., Heerklotz, H., Jenal, U., and Schirmer, T. (2007). Structure of BeF(3)(-)-Modified Response Regulator PleD: Implications for Diguanylate Cyclase Activation, Catalysis, and Feedback Inhibition. Structure *15*, 915–927.

Wheeler, R.T., and Shapiro, L. (1999). Differential localization of two histidine kinases controlling bacterial cell differentiation. Mol. Cell *4*, 683–694.

Wu, J., Ohta, N., and Newton, A. (1998). An essential, multicomponent signal transduction pathway required for cell cycle regulation in Caulobacter. Proc. Natl. Acad. Sci. USA *95*, 1443–1448.

Wu, J., Ohta, N., Zhao, J.L., and Newton, A. (1999). A novel bacterial tyrosine kinase essential for cell division and differentiation. Proc. Natl. Acad. Sci. USA *96*, 13068–13073.

Yamamoto, K., Hirao, K., Oshima, T., Aiba, H., Utsumi, R., and Ishihama, A. (2005). Functional characterization in vitro of all two-component signal transduction systems from Escherichia coli. J. Biol. Chem. *280*, 1448–1456.

Zapf, J., Sen, U., Madhusudan, Hoch, J.A., and Varughese, K.I. (2000). A transient interaction between two phosphorelay proteins trapped in a crystal lattice reveals the mechanism of molecular recognition and phosphotransfer in signal transduction. Structure *8*, 851–862.

Supplementary material

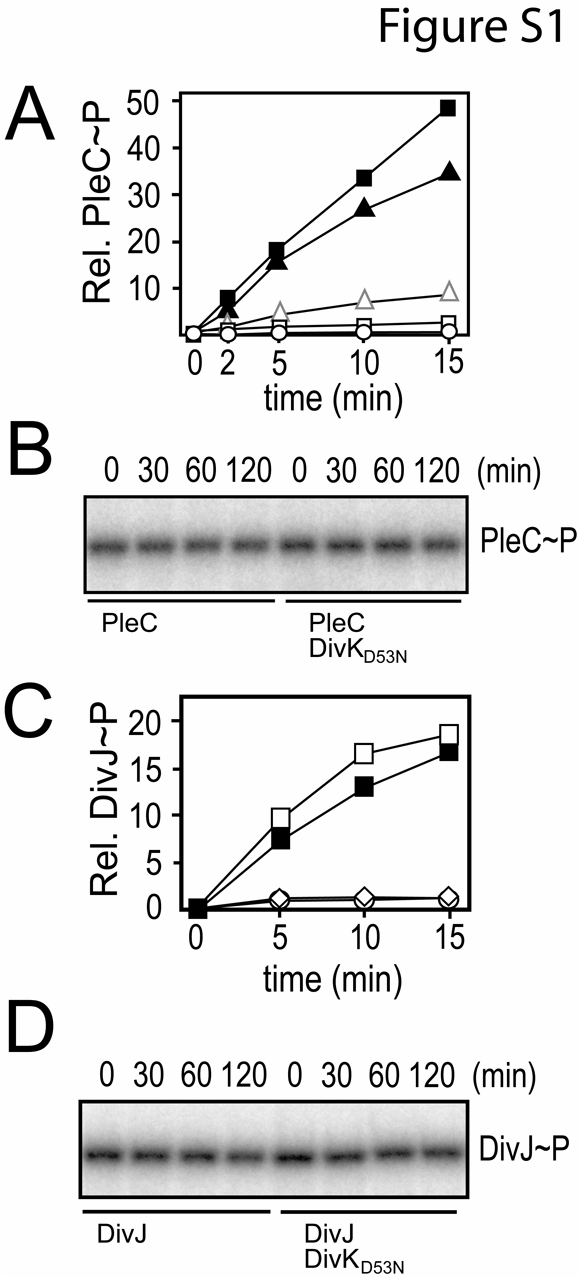

Figure S1: DivK Stimulates Autophosphorylation of the PleC and DivJ Histidine Kinases.

(A) Quantification of PleC autophosphorylation as shown in Fig. 2A with the following concentrations of $DivK_{D53N}$, 0 µM (open circles), 0.3 µM (open squares), 10 µM (filled triangles), 30 µM (filled squares), or 10 µM $DivK_{D53ND90G}$ (open

triangles). Values are averages from three experiments and are normalized to the level of PleC autophosphorylation in the absence of $DivK_{D53N}$ at time point 15 min.

(B) DivK does not affect stability of PleC~P. PleC was phosphorylated in the presence of [γ-^{32}P]ATP, purified, and PleC~P levels were measured after incubation with or without $DivK_{D53N}$.

(C) Quantification of DivJ autophosphorylation as shown in Fig. 4A without additional proteins (open circles), in the presence of $DivK_{D53N}$ (30 µM; closed squares), of $DivK_{D53ND90G}$ (30 µM; open squares), or of $PleD_{D53N}$ (30 µM, diamonds). Values were normalized to the phosphorylation levels at 15 min in the absence of additional protein. The data are averages of two experiments.

(C) DivK does not affect stability of DivJ~P. DivJ was phosphorylated in the presence of [γ-^{32}P]ATP, purified, and DivJ~P levels were measured after incubation with or without $DivK_{D53N}$.

Figure S2

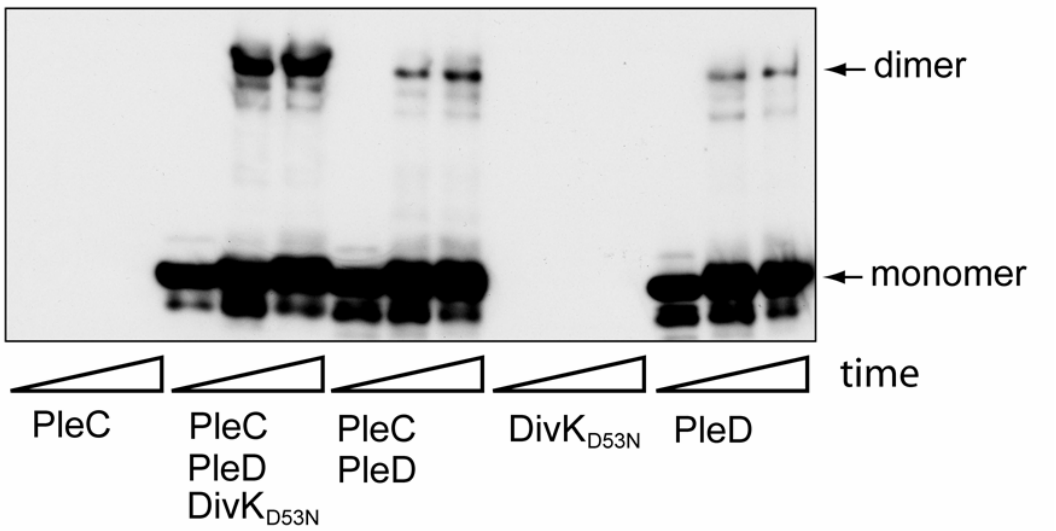

Figure S2: PleC-Mediated Dimerization of PleD Requires DivK.

Crosslink assays with PleD, PleC, and $DivK_{D53N}$ were carried out as described in (Paul et al., 2007). 20 µM of the purified proteins were incubated with ATP and cross-linked for 0, 1, and 5 minutes. PleD monomers and dimers were separated on SDS-polyacrylamide gels, transferred to PVDF-membranes, and detected by immunoblot analysis with an anti-PleD antibody. Arrows mark the monomeric and dimeric forms of PleD.

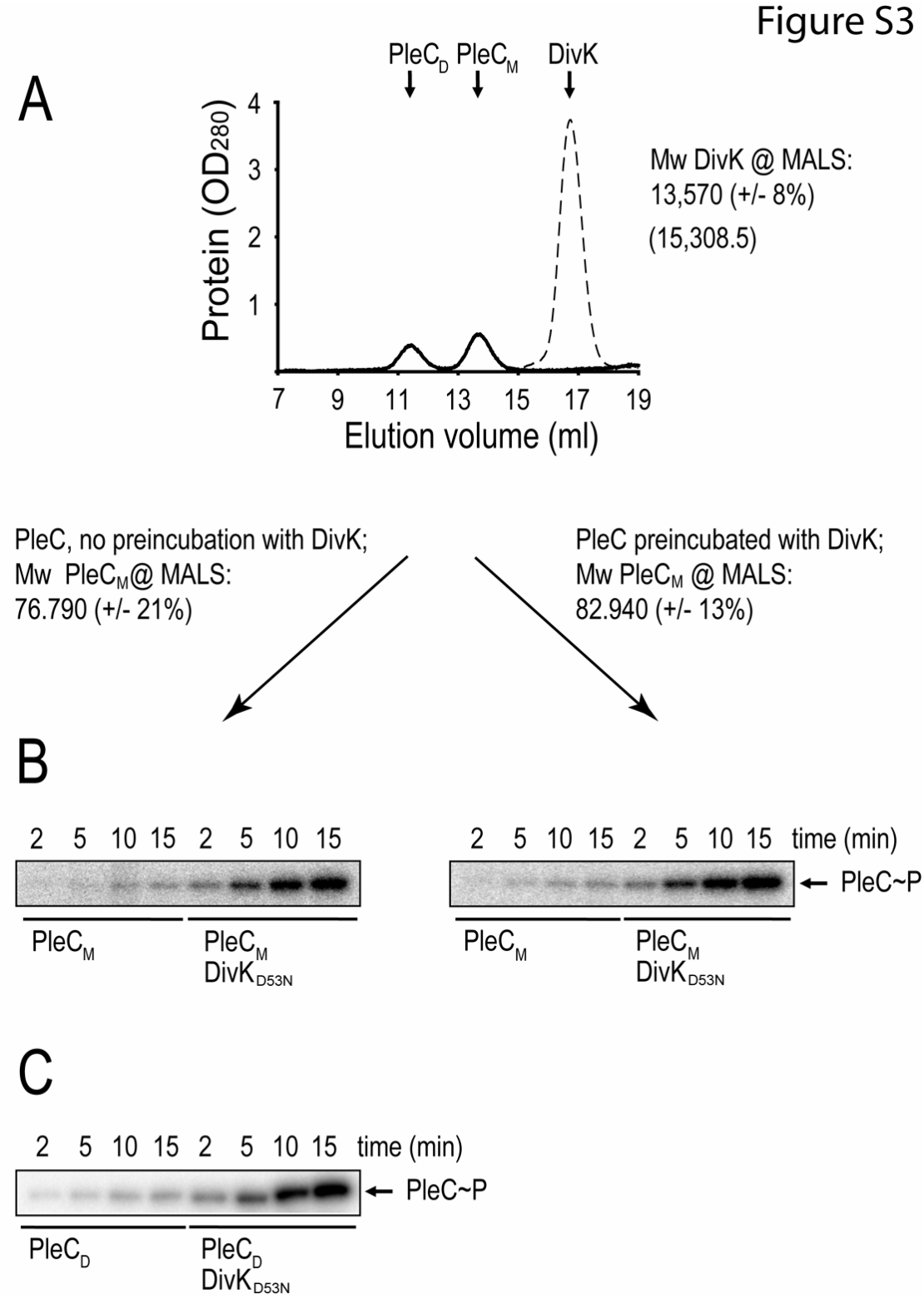

Figure S3: Quarternary Structure and Activity of PleC in the Presence or Absence of DivK.

(A) Size exclusion chromatography of PleC pre-incubated in the presence and absence of DivK. Multi-angle light scattering (MALS) was used to measure the

molecular weight of purified proteins. Measured values are indicated with theoretical values shown in brackets. $PleC_M$ refers to the peak corresponding to monomeric PleC, $PleC_D$ marks the peak corresponding to a PleC dimer. The distribution of PleC monomer and dimer fraction was not affected by preincubation with DivK.

(B) Measurement of kinase activity of purified $PleC_M$ from (A) in the presence or absence of DivK.

(C) Measurement of kinase activity of purified $PleC_D$ from (A) in the presence or absence of DivK.

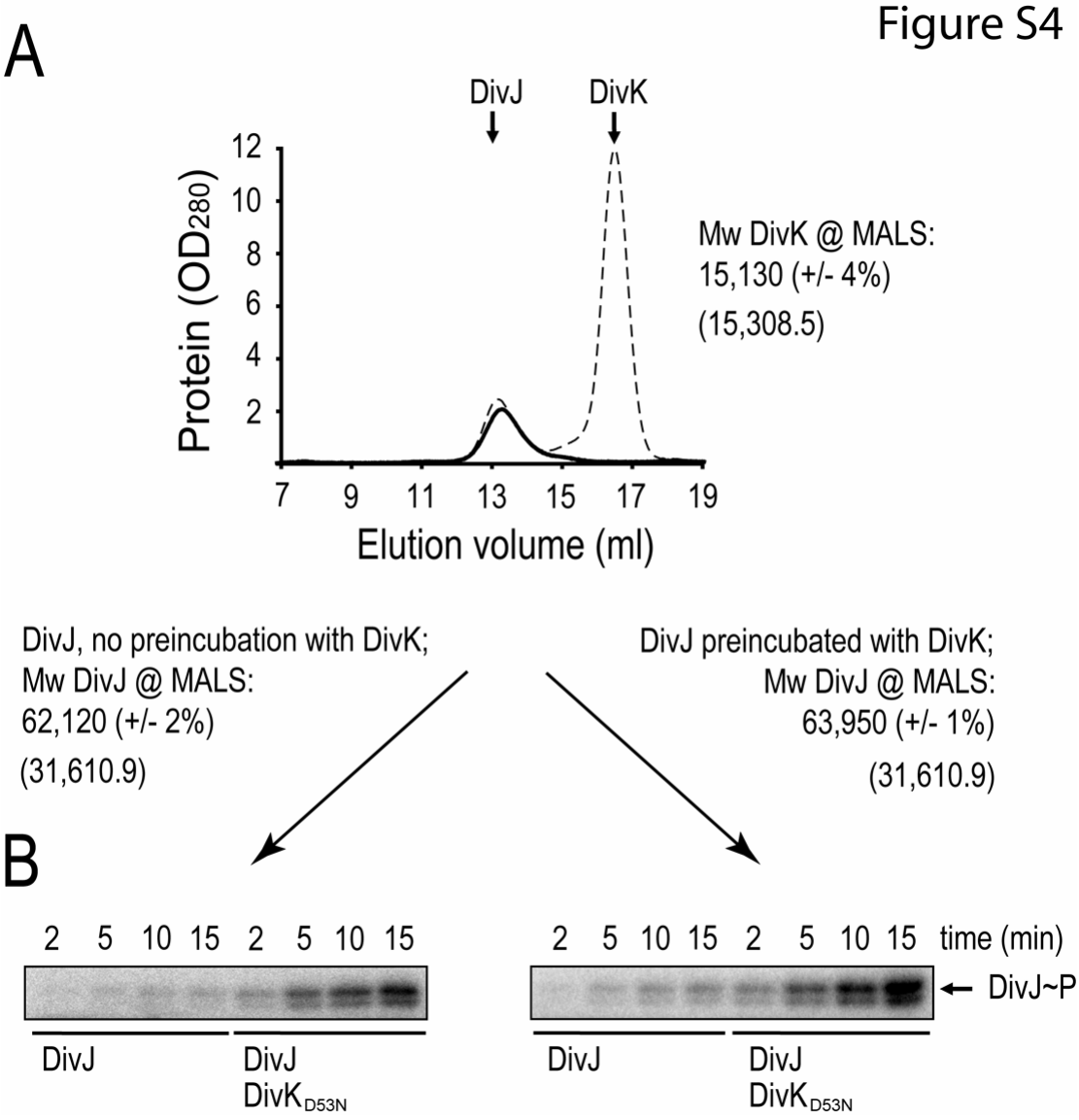

Figure S4: Quarternary Structure and Activity of DivJ in the Presence or Absence of DivK.

(A) Size exclusion chromatography of DivJ pre-incubated in the presence and absence of DivK. Multi-angle light scattering (MALS) was used to measure the molecular weight of purified proteins. Measured values are indicated with theoretical values shown in brackets. DivJ behaved as stable dimer under all conditions tested.
(B) Measurement of kinase activity of purified DivJ from (A) in the presence or absence of DivK.

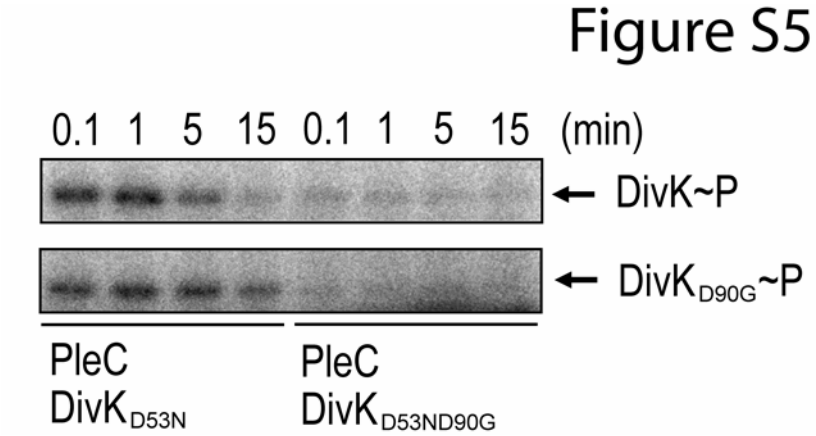

Figure S5: Phosphotransfer from PleC to DivK and DivK$_{D90G}$.
Phosphotransfer reactions with PleC (10 µM), DivK (10 µM), DivK$_{D90G}$ (10 µM), DivK$_{D53N}$ (10 µM), and DivK$_{D53ND90G}$ (10 µM). The bands corresponding to the phosphorylated proteins are indicated.

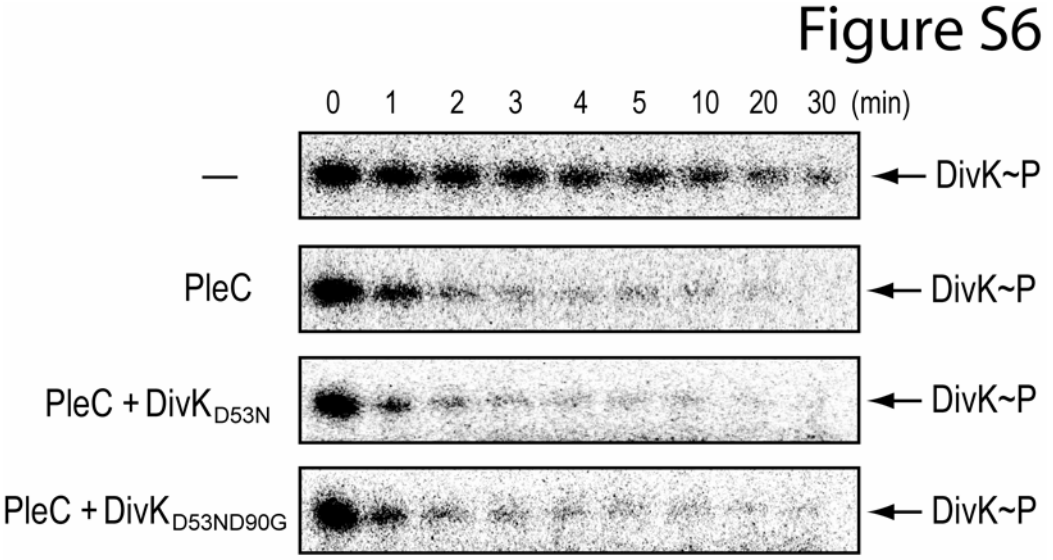

Figure S6: DivK$_{D90G}$ Does not Affect PleC Phosphatase Activity.

(A) PleC-mediated dephosphorylation of DivK. Purified DivK~P was incubated alone (top row), with PleC (second row), with DivK$_{D53N}$ and PleC (third row), or with DivK$_{D53ND90G}$ and PleC (bottom row) for the time indicated. Quantification of PleC-mediated DivK dephosphorylation is indicated in the panel below.

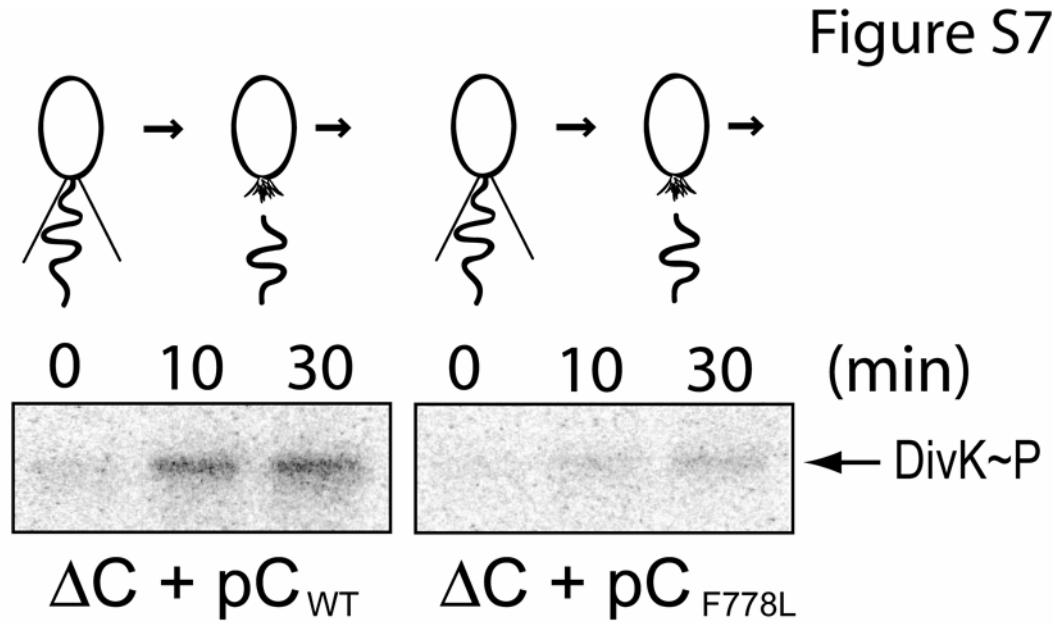

Figure S7: PleC Wild Type and PleC$_{F778L}$ Have Similar Phosphatase Activities *in Vivo*.

Levels of DivK~P were determined in synchronized swarmer cells of *ΔpleC* (ΔC) containing a plasmid copy of *pleC* wild type (pC$_{WT}$) or *pleC$_{F778L}$* (pC$_{F778L}$). Cells were released into fresh medium, pulse labeled at the indicated time points, and extracts were used for immunoprecipitation experiments with anti-DivK antibody.

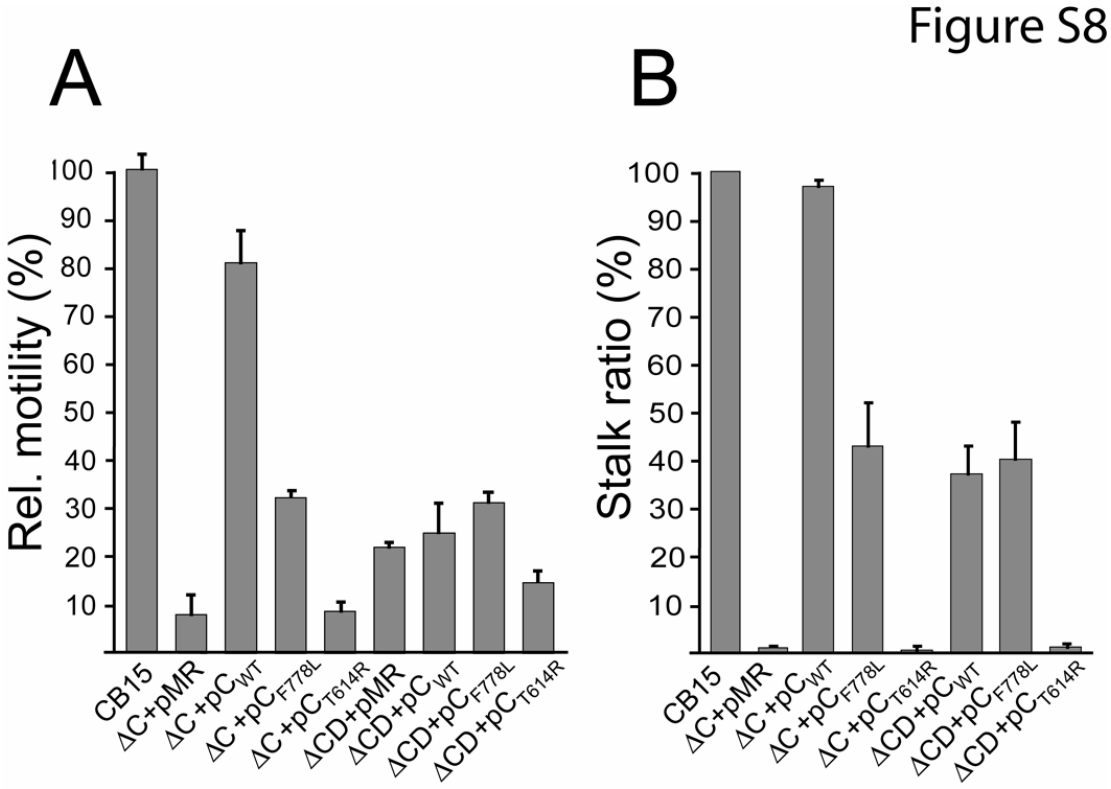

Figure S8: PleD-Dependent Pole Morphogenesis Requires the PleC Kinase.

(A) PleC kinase affects motility in a PleD-dependent manner. The relative motility of the following strains was determined by comparing colony size on semi-solid agar plates after 3 days incubation at 30°C: CB15N, *ΔpleC (ΔC)*, and *ΔpleC ΔpleD (ΔCD)*. As indicated the strains contained an empty vector (pMR) or a plasmid copy of the following *pleC* alleles: *pleC* wild type (pC$_{WT}$), *pleC$_{F778L}$* (pC$_{F778L}$), or *pleC$_{T614R}$* (pC$_{T614R}$). Error bars represent the mean +/- standard deviation.

(B) PleC kinase activity is required for PleD-dependent stalk biogenesis. The percentage of predivisional cells carrying a stalk was determined for the strains indicated by light microscopy. Strain and plasmid designations are as outlined in (A).

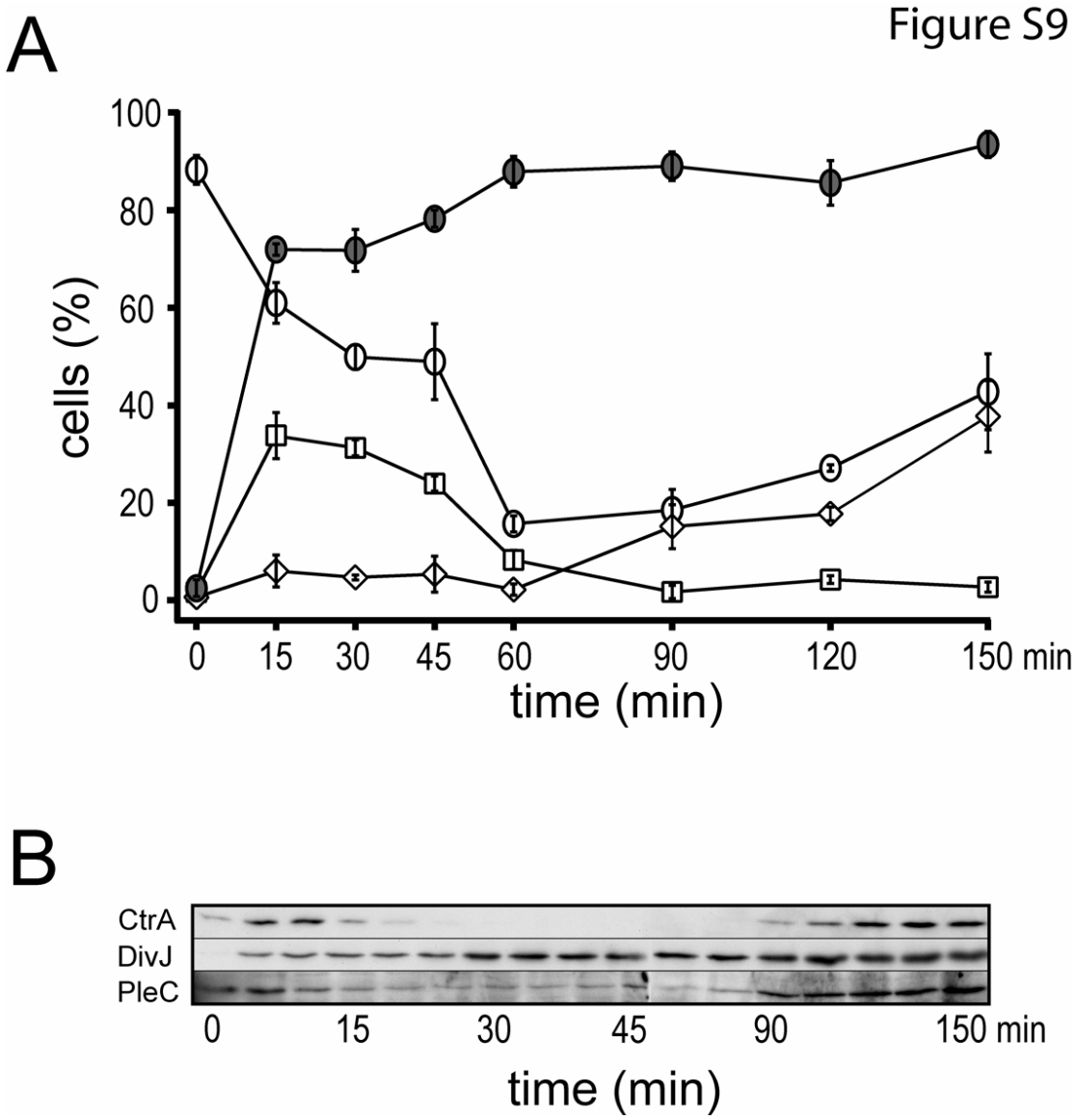

Figure S9: Polar Localization of DivJ and PleC during the *C. crescentus* Cell Cycle.

(A) Quantification of PleC-mYFP and DivJ-tDimer2 localization to the cell poles (Matroule et al., 2004; Ohta and Newton, 2003; Wheeler and Shapiro, 1999). Synchronized populations of cells were examined by epi-fluorescence microscopy at the indicated time points and scored visually. Polar foci of PleC-mYFP (open circles) and DivJ-tDimer2 (closed circles) are indicated. The numbers of cells with PleC-mYFP and DivJ-tDimer2 foci at the same (open squares) or opposite poles (open diamonds) are shown. Error bars represent the mean +/- standard deviation.

(B) Immunoblot analysis of synchronized cell populations using anti-CtrA, anti-DivJ, and anti-PleC antibodies.

Table S1: Strains and Plasmids

Strain or Plasmid	Relevant genotype or description	Reference or source
Caulobacter crescentus strains		
CB15	*C. crescentus* wild type	ATCC19089
CB15N	synchronizable variant strain of CB15	(Evinger and Agabian, 1977)
UJ730	CB15 *Δ pleD*	(Levi and Jenal, 2006)
UJ731	CB15 *ΔpleC*	(Levi and Jenal, 2006)
UJ1983	CB15N $divK_{D90G}$	(Hung and Shapiro, 2002)
UJ3165	CB15N Δ*pleC* + pC_{WT}	This study
UJ3166	CB15N Δ*pleC* + pC_{F778L}	This study
UJ3167	CB15N Δ*pleC* + pC_{T614R}	This study
UJ3168	CB15N Δ*pleC* Δ*pleD* + pC_{WT}	This study
UJ3169	CB15N Δ*pleC* Δ*pleD* + pC_{F778L}	This study
UJ3170	CB15N Δ*pleC* Δ*pleD* + pC_{T614R}	This study
UJ3190	CB15 Δ*pleC* + pC_{WT}	This study
UJ3191	CB15 Δ*pleC* and pC_{F778L}	This study
UJ3192	CB15 Δ*pleC* and pC_{T614R}	This study
UJ3234	CB15 *ΔpleC ΔpleD*	This study
UJ3528	CB15 Δ*pleC* Δ*pleD* + pC_{WT}	This study
UJ3529	CB15 Δ*pleC* Δ*pleD* + pC_{F778L}	This study
UJ3530	CB15 Δ*pleC* Δ*pleD* + pC_{T614R}	This study
UJ3572	CB15 + pK_{D53N}	This study
UJ3578	CB15 *ΔpleC* + pK_{D53N}	This study
UJ3579	CB15 *ΔpleD* + pK_{D53N}	This study
UJ3611	CB15 Δ*pleC* $divK_{D90G}$	This study
UJ3629	CB15 Δ*pleC* $divK_{D90G}$ + pC_{WT}	This study
UJ3631	CB15 Δ*pleC* $divK_{D90G}$ + pC_{T614R}	This study
UJ3905	CB15 Δ*pleC* Δ*pleD* $divK_{D90G}$ + pC_{WT}	This study
UJ4507	pBGentdivJ-tdimer2,pleC-mYFP in NA1000	(Matroule et al., 2004)
UJ4518	NA1000 *ctrA401 divK::Ω*	Thiș study
Escherichia coli strains		
BL21(DE3)	F^- *dcm ompT hsdS*(rB^-mB^-)	Stratagene
(pLysS)	*gal* λ (DE3) [pLysS CAM^r]	
BL21 RIL	F^- *ompT hsdS*(rB^-mB^-) dcm^+ Tet^r *gal*	Stratagene
(codonPlus)	*λ* (DE3) *endA* Hte [*argU ileY leuW* Cam^r]	

DH10B	F$^-$ *mcr*A Δ(*mrr*- hsd RMS- *mcr*BC) ϕ80d*lacZ*ΔM15 Δ*lac*X74 endA1 recA1 deoR Δ(*ara, leu*)7697 *araD139 galU galK nupG rpsL thi pro hsdR$^-$ hsd$^+$ recA RP4-2-Tc::Mu-Tn7*	Stratagene
S17-1	RP4-2, Tc::Mu, KM-Tn7	(Simon et al., 1983)
Plasmid		
pMR20	Tet^R low copy number vector	(Roberts et al., 1996)
pBAD	Amp^R expression plasmid	Invitrogen
pCC2	pET11; *pleD*, C-terminal His_6 tag	(Paul et al., 2004)
pET11	Amp^R expression plasmid	Stratagene
pET28	Amp^R expression plasmid	Stratagene
pET28H_6-K	DivK-His tag with thrombin site	(Matroule et al., 2004)
pJS14	pBBR1-derived medium copy number broad host range vector	J. Skerker
pC_{WT}	pJS14 carrying *pleC*	(Matroule et al., 2004)
pC_{F778L}	pJS14 carrying $pleC_{F778L}$	(Matroule et al., 2004)
pC_{T614R}	pJS14 carrying $pleC_{T614R}$	(Matroule et al., 2004)
pPA89	pMR20 carrying $divK_{D53N}$	(Aldridge et al., 2003)
pRP49	pBAD; $pleC_{489}$, N-terminal His_6 tag	(Paul et al., 2004)
pRP63	pBAD; $divJ_{296}$, N-terminal His_6 tag	(Paul et al., 2004)
pRP87	pET11; $pleD_{D53N}$, C-terminal His_6 tag	(Paul et al., 2004)
pRP111	pET11; *divK*, C-terminal His_6 tag	This study
pRP112	pET11; $divK_{D53N}$, C-terminal His_6 tag	This study
pRP122	pBAD; $pleC_{313}$, N-terminal His_6 tag	This study
pRP123	pET11; $divK_{D53N\ D90G}$	This study
pRP124	pNPT138S; $divK_{D90G}$	This study
pTRX-HIS-CC2482	$pleC_{540}$, His_6 and Trx tags	(Skerker et al., 2005)

REFERENCES:

Aldridge, P., Paul, R., Goymer, P., Rainey, P., and Jenal, U. (2003). Role of the GGDEF regulator PleD in polar development of Caulobacter crescentus. Mol Microbiol *47*, 1695-1708.

Evinger, M., and Agabian, N. (1977). Envelope-associated nucleoid from Caulobacter crescentus stalked and swarmer cells. J Bacteriol *132*, 294-301.

Hung, D. Y., and Shapiro, L. (2002). A signal transduction protein cues proteolytic events critical to Caulobacter cell cycle progression. Proc Natl Acad Sci U S A *99*, 13160-13165.

Levi, A., and Jenal, U. (2006). Holdfast formation in motile Swarmer cells optimizes surface attachment during Caulobacter crescentus development. J Bacteriol *188*, 5315-5318.

Matroule, J. Y., Lam, H., Burnette, D. T., and Jacobs-Wagner, C. (2004). Cytokinesis monitoring during development; rapid pole-to-pole shuttling of a signaling protein by localized kinase and phosphatase in Caulobacter. Cell *118*, 579-590.

Ohta, N., and Newton, A. (2003). The core dimerization domains of histidine kinases contain recognition specificity for the cognate response regulator. J Bacteriol *185*, 4424-4431.

Paul, R., Abel, S., Wassmann, P., Beck, A., Heerklotz, H., and Jenal, U. (2007). Activation of the diguanylate cyclase pleD by phosphorylation-mediated dimerization. J Biol Chem.

Paul, R., Weiser, S., Amiot, N. C., Chan, C., Schirmer, T., Giese, B., and Jenal, U. (2004). Cell cycle-dependent dynamic localization of a bacterial response regulator with a novel di-guanylate cyclase output domain. Genes Dev *18*, 715-727.

Roberts, R. C., Toochinda, C., Avedissian, M., Baldini, R. L., Gomes, S. L., and Shapiro, L. (1996). Identification of a Caulobacter crescentus operon encoding hrcA, involved in negatively regulating heat-inducible transcription, and the chaperone gene grpE. J Bacteriol *178*, 1829-1841.

Simon, R., Prieffer, U., and Puhler, A. (1983). A broad host range mobilization system for *in vivo* genetic engineering: Transposon mutagenesis in gram negative bacteria. Biotechnology *1*, 784-790.

Skerker, J. M., Prasol, M. S., Perchuk, B. S., Biondi, E. G., and Laub, M. T. (2005). Two-component signal transduction pathways regulating growth and cell cycle progression in a bacterium: a system-level analysis. PLoS Biol *3*, e334.

Wheeler, R., and Shapiro, L. (1999). Differential localization of two histidine kinases controlling bacterial cell differentiation. Molecular Cell *4*, 683- 694.

3.5 Second messenger mediated spatiotemporal control of protein degradation during the bacterial cell cycle

Anna Dürig, Marc Folcher, Sören Abel, Torsten Schwede, Nicolas Amiot, Bernd Giese, Urs Jenal

Genes and Development, manuscript submitted

Statement of my work

I contributed to this work by performing the fluorescence resonance energy transfer (FRET) based *in vivo* interaction study between PopA and RcdA (Fig. 3D).

Second messenger mediated spatiotemporal control of protein degradation during the bacterial cell cycle

Anna Dürig, Marc Folcher, Sören Abel, Torsten Schwede, Nicolas Amiot[1], Bernd Giese[1], and Urs Jenal[2]

Biozentrum, University of Basel, Klingelbergstrasse 70, 4056 Basel, Switzerland,
[1]Department of Chemistry, University of Basel, St. Johanns-Ring 19, 4056 Basel, Switzerland

[2]For correspondence: Phone: ++41 (0)61 267 2135; Fax: ++41 (0)61 267 2118; e-mail: urs.jenal@unibas.ch

Short title: c-di-GMP mediated protein degradation control

Key Words: PopA, cyclic di-GMP, CtrA, protein degradation, Caulobacter crescentus, cell cycle, polar localization, second messenger

Summary

Second messengers control a wide range of important cellular functions in eukaryotes and prokaryotes. Here we show that cyclic di-GMP, a global bacterial second messenger promotes cell cycle progression in *Caulobacter crescentus* by mediating the degradation of the replication initiation inhibitor CtrA. During the G1-to-S phase transition both CtrA and its cognate protease ClpXP dynamically localise to the old cell pole where CtrA is degraded. Sequestration of CtrA to the cell pole depends on PopA, a newly identified c-di-GMP effector protein. PopA itself dynamically localises to cell pole and directs CtrA to this subcellular site via interaction with the RcdA adaptor protein. PopA mutants that are unable to bind c-di-GMP fail to sequester to the cell pole and, as a consequence, to promote CtrA degradation. Thus, c-di-GMP facilitates CtrA degradation during the cell cycle by controlling the dynamic sequestration of the PopA recruitment factor to the cell pole. Finally, we present evidence that CtrA degradation and G1-to-S cell cycle progression rely on converging pathways responsible for substrate and protease localization to the old cell pole. This is the first report that links c-di-GMP to protein dynamics and cell cycle control in bacteria.

Introduction

Regulated proteolysis has a major impact on cellular physiology as it plays a primordial role in cell cycle control, stress response, and cell differentiation in both pro- and eukaryotes. To avoid unwanted protein destruction eukaryotic cells largely restrict proteolysis to specific cellular compartments. In bacteria several energy-dependent cytoplasmic proteases and their associated factors are responsible for the rapid degradation of a number of key cellular regulators [260, 261]. These so called self-compartmentalizing proteases select their substrates through an ATPase complex, which gates the access to the proteolytic active site. To specifically select target proteins destined for degradation bacteria have evolved a series of regulatory mechanisms, including trans-translation [262], interference of small effector molecules [263], pre-processing [264, 265], protein association [266, 267], or the use of specific targeting factors [268]. The recent observation that in *Caulobacter crescentus* the master cell cycle regulator CtrA dynamically sequesters to the old cell pole, where it is degraded by the polarly localised ClpXP protease complex, suggested that a spatial concurrence might also play a role in protein degradation control in bacteria [184, 269].

In *C. crescentus* protein degradation plays a significant role in controlling cell cycle progression [109, 270]. *Caulobacter* cells divide asymmetrically to produce two distinct daughter cells, a smaller motile swarmer cell and a larger surface adherent stalked cell. Whereas the newborn stalked cell enters S-phase and reinitiates chromosome replication immediately, the chromosome of the swarmer cell remains quiescent for an extended period, equivalent to the G1-phase of eukaryotic cells. Concurrent with the morphological transformation of the swarmer cell into a stalked cell, the replication block is suspended and cells proceed into S-phase. Differential activity of the essential response regulator CtrA is critical to control the *Caulobacter* G1-to-S phase transition. Phosphorylated CtrA, CtrA~P, blocks the initiation of replication by directly binding to five sites in the chromosomal OriC region where it apparently restricts access of replication initiation factors [106]. The activity of CtrA is redundantly controlled at the levels of expression, phosphorylation, and degradation [109, 271]. Importantly, to initiate chromosome replication activated CtrA~P is eliminated from the cell by two redundant mechanisms, temporally controlled dephosphorylation and proteolysis [109].

In vivo and *in vitro* experiments have demonstrated that the essential ClpXP protease complex degrades CtrA during G1-to-S transition [108, 272]. The observation that ClpXP rapidly degrades CtrA *in vitro* without the requirement for additional stimulatory factors

indicated that control of CtrA degradation might involve an inhibitory mechanism [272]. Moreover, recent findings suggested that cell cycle-dependent degradation of CtrA involves spatial control. Intriguingly, the ClpXP protease complex transiently sequesters to the incipient stalked cell pole during the G1-to-S transition [184]. At the same time CtrA transiently localises to the same pole where it is degraded by ClpXP (Fig. 1A) [111, 184]. Two distinct factors, which themselves sequester to the stalked cell pole, are responsible for the dynamic localization of the protease and its substrate. RcdA, a protein that interacts with CtrA *in vivo* helps to localise CtrA to the pole [184]. Similarly, polarly localised CpdR tags ClpXP to the incipient stalked cell pole [269]. CpdR is a member of the response regulator family of two-component signal transduction systems that lacks a dedicated output domain and consists of a receiver domain module with a conserved Asp51 phosphoryl acceptor residue. Phosphorylation controls CpdR localization to the cell pole and by that the cellular dynamics of ClpXP [140, 269]. The observation that phosphorylation and localization of CpdR inversely correlate during the cell cycle together with the finding that a CpdRD51A mutant almost exclusively localises to the pole, suggested that CpdR sequestration and ClpXP recruitment are negatively controlled by phosphorylation [269]. Strikingly, phosphorylation of CtrA and CdpR are catalyzed by the same cell cycle phosphorelay comprising the CckA sensor kinase and the ChpT phosphotransferase [140]. Under conditions where the CckA-ChpT pathway is active, CtrA is activated by phosphorylation and concomitantly appears to be stabilized through the phosphorylation of CdpR and delocalization of ClpXP. Inversely, CckA downregulation would prevent the phosphorylation of CtrA and CpdR and, as a consequence, would lead to ClpXP localization and CtrA degradation [140].

These studies suggested that the timing of CtrA degradation during the G1-to-S transition is intimately linked to its dynamic localization to the cell pole. But what are the molecular mechanisms that mediate RcdA and CtrA localization to this subcellular site and how is this event temporally controlled during the cell cycle? Here we propose that the second messenger c-di-GMP critically contributes to temporal and spatial control of CtrA degradation during the *C. crescentus* cell cycle. C-di-GMP has recently been recognized as ubiquitous second messenger in bacteria controlling the transition between a motile, single-cell state and a sessile, surface-attached biofilm mode in a wide range of organisms [8, 10]. Two opposing enzyme activities, diguanylate cyclase (DGC) and phosphodiesterase (PDE) control the cellular level of c-di-GMP. The DGC and PDE activities are contained within the highly conserved GGDEF and EAL domains, respectively [14, 20]. GGDEF and EAL domains are often associated with sensory input domains and it is assumed that these regulatory proteins

serve to directly couple environmental or internal stimuli to a specific cellular response through the synthesis or degradation of c-di-GMP. But how these two enzyme classes are regulated is still largely unclear. DGCs are activated through dimerisation of two GGDEF protomers [17, 186]. In addition, many DGCs are tightly controlled by product inhibition through the binding of c-di-GMP to an allosteric I-site, which is distinct from the catalytic active A-site [16, 19].

We have recently shown that *C. crescentus* pole morphogenesis during the swarmer-to-stalked cell transition is controlled by the DGC PleD [14, 47, 61]. PleD is an unorthodox member of the response regulator family of two-component signal transduction systems with two receiver domains arranged in tandem fused to a GGDEF output domain [16]. During development PleD is activated by phosphorylation and in response is sequestered to the differentiating pole [14, 186]. The observation that phosphorylation-mediated dimerisation not only leads to DGC activation but also to PleD polar localization, suggested a coupling of these two events and a spatially confinement of PleD mediated c-di-GMP signaling to the old cell pole [14, 186]. Here we have analysed the role of PopA, a PleD paralog with identical Rec1-Rec2-GGDEF domain structure, in *C. crescentus* development and cell cycle progression. Similar to PleD, PopA is sequestered to the old cell pole. But in contrast to PleD, PopA localization does not require phosphorylation but depends on c-di-GMP binding to the conserved I-site of its GGDEF output domain. We demonstrate that PopA directly interacts with RcdA and helps to recruit both RcdA and CtrA to the cell pole. Based on our data we postulate that upon c-di-GMP binding PopA dynamically sequesters to the old cell pole where it helps to recruit the machinery responsible for cell cycle-dependent degradation of CtrA. This establishes the GGDEF domain as bona fide c-di-GMP effector module and discovers a novel role for c-di-GMP in interfering with the central machinery driving cell proliferation.

Results

PopA is a structural homolog of the PleD diguanylate cyclase

In the course of the functional characterization of *C. crescentus* proteins involved in c-di-GMP turnover, we analysed open reading frame CC1842. This gene codes for a response regulator with two receiver domains and a GGDEF output domain (Fig. 1B). Because of its homology to the diguanylate cyclase PleD [14, 16, 61, 186], CC1842 was renamed *popA* (paralog of *pleD*). Based on this homology relationship, the overall fold of the receiver domains and the GGDEF domain can be expected to be conserved, and a 3-D model of the PopA structure was build using the crystal structure of PleD [16] as template (23% identity; Fig. S1). Despite the low sequence conservation, the modeled PopA structure was similar to PleD (Fig. 1C), suggesting that the overall fold of the receiver domains and the GGDEF domain is conserved. Sequence comparison of PleD and PopA revealed that the phosphoryl acceptor site (Asp55; P-site) of the first receiver domain and the I-site motif (RVED) of the GGDEF domain were conserved, while the catalytic A-site motif was degenerate (Fig. 1B).

PopA is required for cell cycle dependent degradation of CtrA

A chromosomal *popA* in-frame deletion mutant was generated and analysed for a number of morphological and cell cycle-associated markers. The mutant strain showed a significantly reduced motility on semisolid agar plates compared to wild type (data not shown), suggesting a specific defect in motor function or in timing of motility during the cell cycle. Moreover, the Δ*popA* mutant failed to degrade the cell cycle regulator CtrA upon entry into S-phase (Fig. 2A). Cell cycle-dependent degradation of the chemoreceptor McpA, another ClpX substrate [273], was not affected (Fig. 2A). Thus, PopA appears to be specifically required for CtrA degradation during the cell cycle. To test if PopA phosphorylation or the GGDEF output domain are required for CtrA degradation, we generated mutations in the conserved P- (D55N) and I-site (R357G), and in the degenerate A-site motif (E368Q) (Fig. 1C). Analysis of CtrA turnover in the $popA_{D55N}$, $popA_{R357G}$, or $popA_{E368Q}$ mutant strains revealed that CtrA was degraded normally in the P- and A-site mutants but stabilized in the I-site mutant (Fig. 2A).

To confirm that PopA interferes with CtrA stability, wild type and Δ*popA* mutant strains were engineered that expressed the *YFP-CtrARD+15* allele from the xylose-inducible promoter P_{xylX}. The YFP-CtrARD+15 fusion protein is a fluorescent CtrA derivative, which contains the minimal requirements for cell cycle-regulated proteolysis and polar sequestration [110]. Cells grown in the presence of xylose were synchronized and released into fresh

minimal medium lacking xylose. In wild-type cells both full-length CtrA and YFP-CtrARD+15 were degraded normally during the G1-to-S transition (Fig. 2B, Fig. S2). However, synthesis of the fusion protein did not resume after cells had entered S-phase, confirming that the *yfp-ctrARD+15* allele was not expressed under these conditions (Fig. 2B). In the Δ*popA* mutant the YFP-CtrARD+15 fusion protein was stabilized (Fig. 2B, Fig. S2).

Mutants that are unable to remove active CtrA during the cell cycle show a distinct G1 arrest and cell division block [109]. To test if *popA* mutants display a similar cell cycle arrest, plasmid-borne copies of *ctrA* wild-type and *ctrAD51E*, which codes for a constitutive active form of the regulator [109], were expressed from the xylose inducible promoter. While the expression of *ctrA* or *ctrAD51E* had no effect in *C. crescentus* wild-type cells, the Δ*popA* mutant showed a pronounced cell division block upon induction by xylose (Fig. 2C).

To conclude, these data suggest that PopA is required for the cell cycle-dependent degradation of the CtrA master regulator and that PopA is required to promote the G1-to-S phase transition in *C. crescentus*.

PopA is required for CtrA and RcdA sequestration to the cell pole

To analyse at which level PopA interferes with CtrA degradation we first examined the cellular position of the YFP-CtrARD+15 fusion protein in the Δ*popA* mutant. Whereas YFP-CtrARD+15 transiently localises to the cell poles in *C. crescentus* wild type cells, CtrA foci were not present in stalked or predivisional cells of the Δ*popA* mutant (Fig. 3A). Instead, diffuse fluorescence was observed in all Δ*popA* mutant cells, indicative of a stabilized CtrA fusion protein. These results indicated that PopA is involved in polar sequestration of CtrA. We then asked if PopA was required for the localization of RcdA. As shown in Fig. 3B an RcdA-GFP fusion localises to the old pole in wild type cells, but fails to sequester to the pole in the Δ*popA* mutant. Based on these results we propose that PopA is positioned upstream of RcdA in the signal transduction cascade leading to cell cycle-dependent degradation of CtrA and that PopA directs CtrA to the cell pole via the localization of RcdA.

Because RcdA interacts with CtrA and ClpX *in vivo* [184] we examined if PopA also interacts with any of these factors. For this we used the bacterial adenylate cyclase two-hybrid (BACTH) system, which is based on the interaction-mediated reconstruction of a cyclic AMP (cAMP) signaling cascade [274]. Fusions between PopA, RcdA, CpdR, CtrA, ClpX, or ClpP and two complementary fragments, T25 and T18, that constitute the catalytic domain of *Bordetella pertussis* adenylate cyclase, were generated in all possible combinations and assayed for cAMP production on maltose MacConkey agar plates. Strong signals indicating

interaction were obtained for the following protein pairs: ClpX/ClpX, ClpP/ClpP, ClpX/CpdR, and CpdR/CpdR (data not shown). This is in agreement with earlier results demonstrating ClpX-CpdR interaction by co-immunoprecipitation [269] or with ClpX and ClpP forming oligomeric complexes [275, 276]. The observation that CpdR also strongly interacts with itself suggests that this protein is able to form oligomers. In addition, we obtained a strong positive signal for the interaction between PopA and RcdA (Fig. 3C). Interaction with RcdA as measured by the two-hybrid system did not require an intact PopA I-site or A-site (Fig. 3C). Relatively weak but reproducible interaction signals were obtained for PopA/PopA. No interactions were detected between PopA and CtrA (data not shown). This result adds PopA to the protein-protein interaction map of the CtrA degradation machinery as outlined in Fig. S3.

To measure the interaction between PopA and RcdA *in vivo*, we used fluorescence resonance energy transfer (FRET), which relies on the distance-dependent transfer of energy from an excited donor fluorophore to an acceptor fluorophore [277-279]. We engineered two *C. crescentus* strains containing plasmid-born copies of either *popA-cfp* and *rcdA-yfp* or *popA-yfp* and *rcdA-cfp*. Both strains were used to perform FRET measurements by quantifying the difference of the CFP donor fluorescence before and after specific bleaching of the YFP acceptor (see experimental procedures) [279]. For both strains clear differences in CFP fluorescence intensity were measured, indicative of a direct interaction between the two partners (Fig. 3D). To conclude, we propose that PopA directly interacts with RcdA and by mediating RcdA localization to the old cell pole directs CtrA to this subcellular site during the G1-to-S transition.

PopA localises to the new and old cell pole in an RcdA- and ClpX-independent manner

The observation that PopA directly interacts with RcdA and directs this small protein to the cell pole prompted us to test if PopA itself is sequestered to the *C. crescentus* cell poles where it could act as pole specificity factor for RcdA. To observe the dynamic intracellular position of PopA, we constructed a *popA-egfp* fusion expressed from its own promoter on a low copy number plasmid. The PopA-eGfp fusion protein was fully functional as Δ*popA* mutant cells carrying a plasmid-borne *popA-egfp* allele showed a wild type motility and CtrA turnover phenotype (data not shown). As shown in Figs. 4A and S4, PopA-eGFP localises to the cell poles throughout the cell cycle. A single focus appeared at one pole of the incipient swarmer cell. Because predivisional cells show a focus at both the stalked and the flagellated pole, we presume that the focus observed in newborn swarmer cells occupies the old flagellated pole.

During the G1-to-S transition PopA-eGFP dynamically positions to the new cell pole resulting in a bipolar distribution pattern in stalked and predivisional cells (Figs. 4A, S4, movies S10). It is important to note that in stalked and predivisional cells the fluorescence intensity is different at the two cell poles with stronger foci normally marking the old stalked cell pole. After cell division PopA-eGFP asymmetrically positions to the new pole of the daughter stalked cell, while the new pole inherited by the swarmer progeny remains unoccupied during most of the G1 phase (Fig. 4A, S4).

Because polar positioning of RcdA requires both ClpX [184] and PopA (Fig. 3B) we wanted to test if PopA localization also requires one of these factors. As shown in Figs. 4B and 4C, PopA-eGFP localization was unaltered in mutants either lacking RcdA or being depleted for ClpX. Based on this we propose that PopA is at the top of the recruitment and degradation hierarchy for CtrA and that this factor is primarily responsible for the spatiotemporal behavior associated with CtrA degradation during the cell cycle.

PopA localization to the old cell pole requires an intact c-di-GMP binding site

If PopA alone is responsible for the temporal and spatial control of RcdA and CtrA upon entry into S-phase one would expect that the dynamic sequestration of the three proteins to the cell pole more or less coincides. However, PopA localises to the new pole long before RcdA and CtrA are sequestered to the same subcellular site. It is possible that PopA works in conjunction with (an) additional factor(s) responsible for temporal control of CtrA degradation. Alternatively, the cellular dynamics and specificities of PopA might be more complex and thus not apparent by analyzing its overall distribution in wild type cells. PopA is a bifunctional protein involved in motility and cell cycle-dependent degradation of CtrA and could for instance have different function-specific addresses in the cell. To test this possibility we analysed the molecular basis of PopA sequestration to the cell poles. The observation that in the *popA*$_{R357G}$ I-site mutant RcdA failed to mediate CtrA degradation even though PopA$_{R357G}$ was still able to interact with RcdA, suggested that an intact I-site might be required for polar localization of PopA rather than for the subsequent recruitment of RcdA. To test this hypothesis, low copy number plasmids containing the mutant alleles *popA*$_{D55N}$-*egfp* (P-site), *popA*$_{R357G}$-*egfp* (I-site), and *popA*$_{E368Q}$-*egfp* (A-site) were constructed and were introduced into the *C. crescentus* wild type and Δ*popA* mutant strains. In accordance with their wild type-like CtrA degradation behavior, both PopA P- and A-site mutants showed a localization pattern indistinguishable from PopA wild type (Figs. 5, S5). In contrast,

$PopA_{R357G}$-eGfp showed a characteristic unipolar localization pattern (Figs. 5, S5B). Noticeably, the PopA I-site mutant failed to localise to the stalked cell pole but was still able to sequester to the opposite pole of the cell. As a result of $PopA_{R357G}$-eGfp loss from the stalked cell pole an increased diffuse fluorescence was observed in all cells. Because of the asymmetric positioning of $PopA_{R357G}$-eGfp in predivisional cells, newborn swarmer cells inherited a fluorescent focus at the old flagellated pole. During the G1-to-S transition $PopA_{R357G}$-eGfp was rapidly lost from the old pole after 20 to 40 minutes and appeared at the opposite new pole after 40 to 60 minutes (Fig. S5B). The relatively high number of cells with no detectable polar $PopA_{R357G}$-eGfp focus at the beginning of S-phase coincides with the fading of the fluorescent signal at the old pole and the subsequent appearance of a fluorescent focus at the new pole (Fig. S5B). However, as polar signals are relatively weak at this stage of the cell cycle and can easily be missed by selecting the wrong focal plane during data acquisition, the number of cells without polar foci is most likely overestimated.

In summary, the $PopA_{R357G}$-eGfp mutant appears to specifically recognize the new pole of the cell but disappears from this site as cells undergo the G1-to-S transition at a time corresponding to RcdA and CtrA recruitment to the old pole. Based on this we propose that I-site specific binding of c-di-GMP is required for spatiotemporal control of PopA during the cell cycle and that ligand binding either sequesters PopA to the old stalked pole or retains pre-localised protein at this subcellular site during cell differentiation. In agreement with this, the C-terminal GGDEF domain is required for polar localization of PopA as both a Rec1-Rec2-eGfp and a Rec1-eGfp fusion failed to localise to the cell pole (Fig. S6, Tab. S1).

The localization pattern of $PopA_{R357G}$-eGfp suggested that an additional mechanism is required to sequester PopA to the new cell pole. Because the motility defect of the *ΔpopA* mutant is similar to the phenotype described for a *podJ* mutant [280] and because PodJ functions as a swarmer pole-specific protein localization factor [281], we next analysed if PopA localization to the new cell pole was dependent on PodJ. Similar to a PopA I-site mutant, PopA wild type showed a unipolar pattern in a Δ*podJ* mutant. But unlike $PopA_{R357G}$-eGfp, PopA-eGFP primarily localised to the pole opposite the stalk under these conditions (Fig. 5, Tab. S2). Moreover, when the I-site mutant $PopA_{R357G}$-eGfp was analysed in the Δ*podJ* mutant the polar foci were replaced by a strong diffuse fluorescence throughout the cell (Fig. 5, Tab. S2). Based on these results we conclude that PodJ is responsible for PopA recruitment to the new cell pole where it might engage in motility-specific functions. Together these data suggested that PopA has two function-specific addresses in the cell. While PodJ directs the protein to the new cell pole, binding of c-di-GMP to the PopA I-site is responsible

for PopA recruitment to or retention at the ClpXP-occupied old pole during the G1-to-S transition.

PopA lacks DGC activity but binds c-di-GMP specifically and with high affinity

The phenotype of the *popA*$_{R357G}$ mutant indicated that the conserved I-site plays an important role in temporal and spatial control of PopA. More specifically, these data suggested that PopA specifically binds c-di-GMP at the I-site and, in response, alter its dynamic cellular behavior. Because the I-site was originally identified as an allosteric binding site of the GGDEF domain that regulates diguanylate cyclase activity [16, 17, 19], we first analysed if PopA, despite its degenerate A-site, shows enzymatic activity. A hexahistidine-tagged version of PopA was purified and used for DGC *in vitro* activity assays [14, 19]. Because DGCs are active as a dimers, which are able to form spontaneously at high protein concentrations (K_d of 100 µM) [17, 186] we assayed PopA at increasing concentrations. However, PopA failed to show DGC activity even at the highest protein concentrations used (data not shown). This is in agreement with the observation that most amino acid changes in the highly conserved GGDEF signature motif abolished enzyme activity of an active DGC [18].

Next we used a UV crosslink assay [19] with radiolabeled c-di-GMP to assay ligand binding of PopA. The following proteins were purified and analysed: PopA wild type, PopA$_{E368Q}$ (A-site mutant), and PopA$_{D357G}$ (I-site mutant). While both PopA wild type and PopA$_{E368Q}$ bound c-di-GMP, ligand binding was abolished in the I-site mutant protein PopA$_{D357G}$ (Fig. 6A). Binding of radiolabeled ligand was then assayed in the presence of increasing concentrations of non-labeled c-di-GMP to determine binding affinity. As shown in Figs. 6B and 6C, PopA binds c-di-GMP with a K_d of about 2 µM. Other nucleotides like GTP or GDP were not able to chase radiolabeled c-di-GMP suggesting that binding of c-di-GMP to PopA is highly specific (data not shown). Together this suggested that PopA is a *bona fide* c-di-GMP binding protein and that it exploits the conserved I-site to modulate its own activity and cellular behavior in response to fluctuating levels of c-di-GMP.

CpdR and PopA pathways converge leading to cell cycle-dependent degradation of CtrA.

To analyse if PopA, in addition to its role in RcdA and CtrA sequestration, is also involved in the recruitment of the ClpXP protease to the cell pole, we assayed ClpX localization during the *C. crescentus* cell cycle. As reported previously [269], in *C. crescentus* wild type ClpX

localises to the old cell pole during the G1-to-S transition, coinciding with CtrA degradation (Figs. 7, 7S; note that the cell timing in Figs. 7 and 7S is identical to the experiments shown in Fig. 2A). ClpX localization, although not completely abolished, was significantly impaired in a Δ*popA* mutant (Figs. 7, 7S). Importantly, a *popA* P-site mutant (*popAD55N*) showed an equally impaired ClpX localization (Figs. 7, 7S) arguing that PopA is being phosphorylated *in vivo* and that phosphorylation of PopA, directly or indirectly, influences ClpX localization. Reduction of ClpX localization in *popA* mutants was associated with a similar reduction in the localization of the ClpXP targeting factor CpdR (Tab. 1). In contrast, localization of $CpdR_{D51A}$, a constitutively active mutant that can no longer be phosphorylated, is not reduced in *popA* mutants (Fig. 8A, B). Thus, we conclude that PopA interferes with the polar recruitment of the ClpXP protease by stimulating polar sequestration of CpdR in a phosphorylation-dependent manner.

The observation that the ClpXP protease and its substrate CtrA have distinct targeting factors raised the questions if these two polar recruitment pathways converge and if they are ultimately responsible for the timing of CtrA degradation during the G1-to-S transition. To test this we analysed CtrA stability in *popA* mutants that also carried a $cpdR_{D51A}$-YFP mutant allele. The $CpdR_{D51A}$ mutant more effectively localises to the cell pole as compared to wild type CpdR and to cause an increased CtrA turnover via a more efficient polar recruitment of the ClpXP protease [269]. In agreement with this, we find severely reduced levels of CtrA in cells expressing the $cpdR_{D51A}$ (Fig. 8C). This was due to increased degradation of CtrA, as normal CtrA levels were restored in cells co-expressing the stable variant CtrA::W (Fig. 8C). Surprisingly, while cells carrying the $cpdR_{D51A}$ allele showed a severe filamentation and bulging phenotype in a *popA* wild type background, they had a normal morphology in a Δ*popA* mutant (Fig. 8A, B). This effect was not due to reduced localization of $CpdR_{D51A}$-YFP in the *DpopA* mutant (Fig. 8B). Strikingly, in the Δ*popA* null mutant or the *popA* I-site mutant (R357G) normal CtrA levels and cell morphology was restored even when the expression of the $cpdR_{D51A}$ allele was induced (Fig. 8C).

In summary, these data provide evidence that the CpdR-ClpXP and PopA-RcdA-CtrA localization pathways converge and that CtrA degradation is mediated through the concomitant dynamic localization of these factors to the old cell pole during the G1-to-S transition.

Discussion

In *C. crescentus* G1-to-S cell cycle progression is mediated by the irreversible destruction of the master regulator CtrA. To understand how this event is regulated and to elucidate the general control mechanisms operating during the bacterial cell cycle we have examined the spatiotemporal behavior of CtrA degradation. CtrA is degraded by the ClpXP protease complex [108, 272], which dynamically positions to the old cell pole coincident with CtrA turnover [184]. The observation that CtrA itself sequesters to the same pole before being degraded suggested that the timing of CtrA degradation might be dictated by a dynamic spatial convergence of substrate and protease at this subcellular site [111, 184]. Here we present evidence that the timing of CtrA degradation is ultimately mediated by the bacterial second messenger c-di-GMP via the dynamic polar localization of a c-di-GMP specific binding protein, PopA. Our data suggest that PopA, in its c-di-GMP ligated form, is sequestered to the cell pole where it acts as polar recruitment factor for CtrA. This is the first report that links c-di-GMP to the dynamic spatiotemporal control of the bacterial cell cycle and is reminiscent of the function of eukaryotic second messengers in cell polarity and behavior [282-284].

PopA is responsible for polar recruitment of CtrA during the G1-to-S transition

CtrA localization to the cell pole is mediated by RcdA, a small stalked pole-specific protein that interacts with CtrA and ClpXP *in vivo* [184]. We show here that RcdA also interacts with PopA, a GGDEF domain protein required for CtrA degradation and RcdA localization. The strong positive signals observed with the bacterial two-hybrid system and by FRET analysis, indicated that PopA and RcdA interaction is direct. Furthermore, epistasis experiments positioned PopA upstream of RcdA. Thus, we propose that PopA directs CtrA to the cell pole via its interaction with RcdA, which in turn might play an intermediary role between CtrA and PopA (Fig. 9A). It is important to note that *in vitro* experiments have argued against the idea that RcdA enhances CtrA degradation by tethering the substrate to its protease [272]. However, RcdA could contribute to the timing of CtrA polar localization and/or confer substrate specificity to the cellular machinery that recruits proteins destined for degradation to the ClpXP tagged cell pole.

But if PopA is at the top of the cascade that determines CtrA sequestration and degradation, what controls its activity during the cell cycle? We found that PopA, like the

other components involved in CtrA degradation, dynamically localises to the *C. crescentus* cell poles. PopA localization control appears to be complex in that the protein is sequestered to both the new and the old cell poles at distinct times of the cell cycle. Remarkably, PopA localization to these two subcellular sites relies on distinct mechanisms and might serve two distinct cellular functions. PopA localization to the incipient swarmer pole requires PodJ, a cell polarity determinant that also recruits the PleC histidine kinase/phosphatase and components of the pili assembly machinery to the flagellated pole [281, 285, 286]. Upon cell division full-length PodJ, $PodJ_L$, is processed into a truncated form, $PodJ_S$, which is needed for chemotaxis of the newborn swarmer cell [280, 281, 286]. Localization of PopA to the swarmer pole requires the cytoplasmic portion of $PodJ_S$ (A. Moser and U. Jenal, unpublished). Hence, $PodJ_S$ mediated targeting of PopA to the flagellated pole might be important for the proper functioning of the flagellar motor. Although PodJ is cleared from the cell pole during the G1-to-S transition [287], PopA persists at the incipient stalked pole. This strongly suggested the existence of a second, PodJ-independent polar localization mechanism for PopA, which is specific for the incipient stalked cell pole and for the CtrA degradation pathway. In support of this, a PopA I-site mutant ($PopA_{D357G}$) was able to localise to the swarmer pole but failed to localise to the stalked cell pole independent of the presence or absence of PodJ.

Several experiments suggested that for CtrA sequestration and degradation the important functional element of the PopA GGDEF output domain is not the catalytic active A-site, but rather the conserved I-site. Firstly, PopA sequestration to the incipient stalked cell pole required an intact I-site, but not the P- or A-site. Secondly, PopA lacks the highly conserved GGDEF signature motif and biochemistry experiments failed to detect PopA DGC activity, even when high protein concentrations were used. This is consistent with the finding that the catalytic activity of DGCs requires a highly conserved GGDEF active site [17, 18], and argues that PopA is not involved in the synthesis of c-di-GMP. Thirdly, PopA is a c-di-GMP binding protein. Binding studies with PopA wild type and mutant proteins demonstrated that the protein is able to specifically bind c-di-GMP with high affinity and that an intact I-site, but not the A-site, is required for binding. The binding affinity (K_d 2 µM) is similar to the affinities determined for the allosteric I-sites of two enzymatically active DGCs [16, 17, 19]. It has been proposed that product inhibition of DGCs represents a major control element for c-di-GMP signaling establishing threshold levels of the second messenger in the cell [19]. From this it can be inferred that PopA binds c-di-GMP in a physiologically relevant concentration range [19]. The observation that an intact I-site is required for PopA sequestration to the stalked cell

pole, but not for protein-protein interaction with RcdA, argues that c-di-GMP binding specifically influences the timing of PopA sequestration to the old cell pole, rather than its interaction with downstream components.

If a transient increase of c-di-GMP during the G1-to-S transition is responsible for the timing of PopA, RcdA and CtrA localization, cell cycle control must be mediated by one or several DGCs and/or PDEs. We have recently shown that c-di-GMP levels peak during the G1-to-S transition and that the PleD diguanylate cyclase is mainly responsible for this fluctuation (R. Paul and U. Jenal, unpublished). However, PopA localization was unaltered in a *pleD* mutant. Also, PopA localization was not affected in mutants lacking any of the other 12 *C. crescentus* proteins harboring a GGDEF or EAL domain (S. Abel and U. Jenal, unpublished). This leaves the possibility that several DGCs redundantly contribute to the c-di-GMP pool required for PopA activation. It is also possible that cell cycle timing of c-di-GMP levels and PopA localization to the stalked cell pole might ultimately be determined by a c-di-GMP specific phosphodiesterase, which specifically reduces c-di-GMP levels in G1.

A possible mechanism for c-di-GMP mediated PopA localization to the cell pole

PopA and the diguanylate cyclase PleD show a similar dynamic localization to the incipient stalked cell pole. But do they also take advantage of a similar localization mechanism? PleD localization and activation during the swarmer-to-stalked cell transition requires phosphorylation-mediated dimerisation [14, 17, 186]. Based on the finding that the ability to dimerize is critical for PleD activation and polar localization we have proposed a simple model for the coupling of PleD DGC activity to its subcellular distribution [186]. The model predicts that the timing of PleD polar localization during the cell cycle is determined by phosphorylation-dependent dimerisation. Despite of its conserved phosphoryl acceptor site, PopA phosphorylation does not appear to be required for polar localization. PopA and PleD share the same Rec1-Rec2-GGDEF domain structure but are only 23% identical. Intriguingly, the amino residues that contribute to the Rec1-Rec2 interdomain interface in activated PleD dimers [17] are strictly conserved in PopA (Fig. S1). *In vivo* interaction (Fig. S3) and biochemical experiments (A. Moser and U. Jenal, unpublished) suggested that PopA can oligomerize. This raises the possibility that PopA oligomerization also influences its dynamic cellular behavior. But how would c-di-GMP binding affect PopA oligomerization? Atomic simulations of ligated and unligated PleD have suggested reduced flexibility of all three domains upon c-di-GMP binding to the I-site. Strikingly, simulations found stronger

correlations between D1 and D2 for unligated PleD, which may affect the dimerisation rate [288]. Consistent with the idea that I-site occupancy negatively influences PleD dimerisation, mutation of two residues of the Rec2 domain involved in c-di-GMP binding displayed a 20-fold higher DGC activity compared with wild-type PleD [19]. Hence, it is possible that binding of c-di-GMP to the I-site affects the oligomerization behavior of PleD and PopA in a similar manner and by that influences the dynamic positioning of these proteins during the cell cycle.

Converging localization pathways for substrate and protease mediate cell cycle-dependent degradation of CtrA

Two response regulators, CpdR and PopA, are involved in directing the protease ClpXP and its substrate CtrA to the emerging stalked cell pole. Whereas PopA is responsible for the transient localization of CtrA, CpdR controls ClpX localization. CpdR and ClpX polar recruitment depends on the phosphorylation state of CpdR [269]. In particular, in the presence of $CpdR_{D51A}$, a mutant that can no longer be phosphorylated, the proportion of cells with ClpX and CpdR at the cell pole is dramatically increased and, as a result, cellular levels of CtrA are severely reduced [269] (Fig. 8). Expression of $CpdR_{D51A}$ also results in a severe cell morphology and cell growth phenotype. The finding that cell morphology, viability, and CtrA levels are restored in *popA* mutant cells expressing $cpdR_{D51A}$ argues that this phenotype is a direct consequence of reduced levels of CtrA and possibly additional ClpXP substrates. The latter can be inferred from the observation that the effect of $cpdR_{D51A}$ is not completely abolished in cells expressing a stable CtrA variant. In contrast, the expression of a PopA I-site mutant that fails to localise to the stalked cell pole fully suppresses the $cpdR_{D51A}$ phenotype. Together this argues that the two pathways responsible for the polar localization of substrate and protease converge and together are responsible for the accurate cell cycle timing of CtrA degradation (Fig. 9A). In addition, the convergent CpdR and PopA pathways might be interlinked. We found that PopA also contributes to CpdR and ClpX localization. In *DpopA* mutants CpdR and ClpX frequently mislocalise. This effect is most pronounced during G1-to-S transition, when CtrA is being degraded. Intriguingly, a PopA mutant lacking the conserved phosphoryl acceptor site Asp55 showed the same localization defect for CdpR and ClpX arguing that this effect is somehow mediated through PopA phosphorylation. Although we failed to provide evidence for a direct interaction between PopA and CpdR, we cannot exclude that PopA is part of a macromolecular complex at the stalked cell pole thereby contributing to CpdR and ClpX localization. Alternatively, mislocalisation of CdpR and ClpX in *popA*

mutants could stem from increased phosphorylation of CpdR under these conditions. The observation that $CpdR_{D51A}$ localises normally to the stalked cell pole even when PopA is absent (Fig. 8) is in line with this hypothesis and argues against a direct involvement of PopA in CpdR localization. Thus, we propose that PopA activity and polar localization, in addition to being stimulated by c-di-GMP binding to the I-site of its output domain, is modulated negatively by phosphorylation of the first receiver domain. Such a mechanism would allow PopA to integrate distinct signals from the cell cycle via phosphorylation and c-di-GMP binding. Recently, the CckA-ChpT phosphorelay was shown to phosphorylate both CtrA and CpdR in response to cell cycle cues [140]. This elegant mechanism allows the cells to inversely control CtrA activation and degradation during the cell cycle. It is possible that the CckA-ChpT pathway controls CtrA stability not only by turning off CpdR and preventing ClpXP localization, but in parallel downregulates CtrA recruitment through the phosphorylation of PopA.

Materials and methods

Strains, plasmids, and media

The bacterial strains and plasmids used in this study are listed in Table S1. *Caulobacter crescentus* strains were either grown in peptone yeast extract (PYE), in minimal glucose media (M2G, [196], or minimal xylose media (M2X) at 30^{o}C, unless stated otherwise. Where necessary, growth medium was supplemented with D-xylose varying from 0.1-0.3%. Newborn swarmer cells (SW cells) were isolated by Ludox gradient centrifugation [179], and released into the appropriate minimal medium. Plasmids were introduced into *C. crescentus* either by conjugation or electroporation.

E. coli strains were grown in Luria Broth (LB) media. Antibiotics for selection were added to the media where necessary. The exact procedure of strain and plasmid construction is available on request.

Microscopy

For fluorescence imaging cells were placed on a microscope slide layered with a pad of 1% agarose dissolved in water or in PYE for time laps microscopy. An Olympus IX71 microscope equipped with an UPlanSApo 100x/1.40 Oil objective (Olympus, Germany) and a coolSNAP HQ (Photometrics, AZ, United States) CCD camera was used to take differential interference contrast (DIC) and fluorescence photomicrographs. For GFP fluorescence FITC filter sets (Ex 490/20 nm, Em 528/38 nm), for YFP (Ex 500/20 nm, Em 535/30 nm) and for CFP (Ex436/10,

Em 470/30 nm) were used with an exposure time of 1.0 sec. Images were processed with softWoRx v3.3.6 (Applied Precision, WA, United States) and Photoshop CS2 (Adobe, CA, United States) softwares.

Bacterial Two-Hybrid Analysis

Proteins of interest were fused in frame to the 3'end of the T25 fragment (pKT25) and to the 3' end (pUT18C) or 5' end (pUT18) of the T18 fragment of the *B. pertussis* adenylate cyclase [274]. pKT25-zip and pUT18C-zip were used as positive controls. The adenylate cyclase deficient *E. coli* strain MM337 was used to screen for positive interactions. pKT25 derivatives were transformed together with pUT18 or pUT18C derivatives into MM337 and the transformants selected on LB with ampicillin (100 ug/ml) and kanamycin (50 ug/ml). To screen for protein-protein interaction single colonies were streaked on McConkey Agar Base supplemented with maltose (1%), ampicillin (100 µg/ml) and kanamycin (50 µg/ml).

Protein Expression and Purification

Expression plasmids (pET21C, Novagen) were transformed into *E. coli* BL21 (DE3) ArcticExpress (Stratagen). The strains were grown in LB with ampicilin 100 µg/l at 17°C. Expression was induced with IPTG (0.1 mM) over night. Cells were collected by centrifugation, resuspended in cold sonication buffer SB (20 mM Tris pH 8.0, 150 mM NaCl, 10 mM $MgCl_2$, 5 mM imidazole). Cells were disrupted by sonication using a Branson Sonifier and cell debris were removed by centrifugation. The clear lysate was incubated for 1 h with 1 ml Ni-NTA agarose (Qiagen). The matrix was washed with SB containing 250 mM NaCl and proteins were eluted with SB buffer containing 50 mM and 250 mM imidazole, respectively. Proteins were dialyzed against 20 mM Tris pH 8, 150 mM NaCl, 10 mM $MgCl_2$, 1 mM DTT, 10 % glycerol and dialyzed fractions were concentrated using Amicon ultrafiltration cell. The concentrated proteins were further purified by gel filtration using a Superdex 75 PC 3.2 /30 column on Smart system (GE healthcare) equilibrated with 20 mM Tris pH 8, 250 mM NaCl, 10 mM $MgCl_2$, 1 mM DTT. The monomer fractions were collected and used for UV cross-linking assay.

Antibody Production and Immunoblots

PopA fused to a C-terminal hexa-histidine tag was purified as described above and injected into rabbits for polyclonal antibody production (Laboratoire d'Hormonologie, Marloie, Belgium). For immunoblots anti-PopA serum was diluted 1:5'000. Antibodies against CtrA and McpA were used as described [109, 289].

Fluorescence Resonance Energy Transfer

Cultures of strains UJ4329 and UJ4330 were grown in PYE supplemented with 2.5 μg/ml tetracycline and 2.5 μg/ml gentamycin until they reached an OD660 of 0.3. 5 ml of this culture were harvested by centrifugation, washed with and resuspended in 50 μl tethering buffer (10mM potassium phosphate, 0.1mM EDTA, 1 mM L-methionine, 10mM sodium lactate, pH 7). For FRET analysis the cell suspension was placed on thin agarose pads (1 % agarose in tethering buffer) on microscopy slides and allowed to immobilise for 5–10 min. The agarose pads were then covered with cover slips and were sealed with an Apiezon grease. Fluorescence of 300-500 cells was monitored in each experiment. Fluorescence signals in cyan and yellow channels were detected using two photon-counting photomultipliers (H7421-40, Hamamatsu,Bridgewater, NJ) whose outputs were converted to analog signals by ratemeters (RIS-375, Rowland Institute).

UV Cross-linking with [^{33}P] c-di-GMP

The ^{33}P-labeled c-di-GMP was enzymatically produced using [^{33}P]GTP (300 Ci/mmol) and purified as described [19]. Purified protein samples were incubated 10 min on ice in reaction buffer (25 mM Tris-HCl pH 8.0, 250 mM NaCl, 10 mM $MgCl_2$, and 5 mM β-mercaptoethanol) together with 1 μM c-di-GMP and ^{33}P-radiolabeled c-di-GMP (0.75 μCi, 6000 Ci/mmol). Samples were then UV irradiated and analysed as previously described [19]. The c-di-GMP binding constant of PopA was determined as described previously [19].

Comparative Modeling of PopA

A comparative three-dimensional model of *Caulobacter crescentus* PopA was built based on the crystal structure of the response regulator PleD in complex with c-di-GMP (PDB: 1W25; [16]. Template identification and alignment was performed by scanning the PDB database [290] for suitable template structures using a PSI-BLAST [291] sequence profile for the target based on the NCBI non-redundant protein sequence database [175]. Model coordinates were generated in Swiss-Model Workspace following visual assessment of placements of insertions and deletions in the alignment [292]. The orientation of c-di-GMP in the model was inferred from the PleD - c-di-GMP template structure complex.

Acknowledgements

We thank A. Iniesta and L. Shapiro for strains. This work was supported by Swiss National Science Foundation Fellowship 3100A0-108186 to U.J

Figure legends

Figure 1: Dynamic protein localization and CtrA degradation during the cell cycle.

(A) Schematic of CtrA, ClpXP, RcdA, and CpdR localization during the *C. crescentus* cell cycle. (B) Sequence alignment of the PleD and PopA paralogs. The amino acid sequence flanking the phosphoryl acceptor site (P-site), I-site, and A-site are shown with the conserved residues colored in red and the signature motifs boxed. (C) Comparison of the 3-D structure of the GGDEF domains of PleD (as determined by x-ray crystallography [16]) and PopA (as determined by modeling). A- and I-sites are marked and the position of a dimer of c-di-GMP bound to the I-site is indicated. In the PleD crystal structure a c-di-GMP monomer is found in the A-site [16].

Figure 2: Cell cycle dependent degradation of CtrA requires PopA.

(A) Immunoblots of synchronized cultures of *C. crescentus* wild type and *popA* mutant strains. The upper panels show immunoblots stained with anti-CtrA antibodies, immunoblots shown in the lower panels were stained with anti-McpA antibodies. (B) Synchronized swarmer cells of strains expressing *yfp-ctrARD+15* from the xylose-inducible promoter P_{xyl} were released into M2G minimal glucose medium and monitored throughout the cell cycle. Samples of *C. crescentus* wild type (upper panel) and *popA* mutant (lower panel) were analysed by immunoblots using anti-CtrA antibodies. The YFP-CtrARD+15 fusion protein and wild type CtrA are marked. (C) Morphology of *C. crescentus* wild type and Δ*popA* mutant expressing *ctrA* (left panels) or $ctrA_{D51E}$ (right panels) from the xylose inducible promoter P_{xyl}. Cells were harvested under inducing (xylose) or non-inducing (glucose) conditions and analysed by light microscopy.

Figure 3: PopA mediates polar localization of RcdA and CtrA.

(A) CtrA localization to the cell pole requires PopA. Wild-type and Δ*popA* mutant cells expressing *yfp-ctrARD+15* were analysed by DIC and fluorescence microscopy. Polar foci of Yfp-CtrARD+15 are marked by arrows and shown schematically in the right panel. (B) RcdA localization to the cell pole requires PopA. Wild type and Δ*popA* mutant cells expressing *rcdA-yfp* were analysed by DIC and fluorescence microscopy. Polar foci of RcdA-Yfp are shown schematically in the right panel. (C) PopA directly interacts with RcdA. The red color on McConkey agar base maltose plates is an indicator for protein-protein interaction. 1) pT18-zip + pT25-zip (positive control); 2) pT25-PopA + pT18-RcdA; 3) pT25-PopA + pT18; 4)

pT25-PopA$_{E368Q}$ (A-site mutant) + pT18-RcdA; 5) pT25-PopA$_{E368Q}$ (A-site mutant) + pT18; 6) pT25-PopA$_{R357G}$ (I-site mutant) + pT18-RcdA; 7) pT25-PopA$_{R357G}$ (I-site mutant) + pT18, 8) pT25 + pT18-RcdA. (D) In *vivo* FRET analysis demonstrating direct protein-protein interaction between PopA and RcdA. *C. crescentus* cells expressing *rcdA-ecfp* and *popA-eyfp* (left panel) or *popA-ecfp* and *rcdA-eyfp* (right panel) were analysed. The intensity of the CFP channel was recorded before and after YFP-specific bleaching. The increase of signal intensity of the CFP channel after specific bleaching of the YFP channel is a measure of the FRET efficiency (%).

Figure 4: PopA localises to the old and new cell poles.

(A) PopA dynamically localises to the old and new cell pole during the *C. crescentus* cell cycle. Representative time-laps experiment with *C. crescentus* wild-type expressing *popA-egfp*. DIC images (top), fluorescent images (middle), and a schematic representation (bottom) are shown. (B) RcdA is dispensable for PopA localization to the cell poles. Mixed cultures of *C. crescentus* wild type and Δ*rcdA* mutant cells expressing *popA-egfp* were analysed by DIC and fluorescence microscopy. The polar localization pattern of PopA-eGFP was indistinguishable in the two strains. (C) ClpX is dispensable for PopA localization to the cell poles. Mixed cultures of the *C. crescentus* conditional *clpX* mutant strain UJ271 expressing *popA-egfp* were analysed by DIC and fluorescence microscopy under permissive (PYEX) and restrictive conditions (PYEG). The polar localization pattern of PopA-eGFP was indistinguishable under these conditions.

Figure 5: Distinct mechanisms mediate PopA localization to the new and old pole.

C. crescentus wild type and *podJ* mutant expressing GFP fusion proteins to PopA wild type and the following PopA mutants were analysed by DIC and fluorescence microscopy: PopA$_{D55N}$ (P-site mutant), PopA$_{E368Q}$ (A-site mutant), PopA$_{R357G}$ (I-site mutant). Polar localization is indicated schematically in the panels on the right.

Figure 6: PopA specifically binds c-di-GMP at the conserved I-site of the GGDEF domain.

(A) UV crosslink experiment of purified hexahistidine-tagged PopA with [^{33}P] labeled c-di-GMP. The following proteins were used: PopA, PopA$_{E368D}$ (A-site mutant), PopA$_{R357G}$ (I-site mutant). The Coomassie blue stained gel (left) and the autoradiograph (right) are shown. (B)

UV crosslinking of purified PopA with [^{33}P] labeled c-di-GMP and increasing concentrations of non-labeled c-di-GMP (0 – 80 μM). Coomassie blue-stained gel (top panel) and Autoradiograph (bottom panel) are shown.

Figure 7: PopA is required for proper localization of ClpX to the cell pole.

Cultures of *C. crescentus* wild type and *popA* mutants expressing a *clpX-egfp* were synchronized and cells were analysed by DIC and fluorescence microscopy as they progressed through the cell cycle. At intervals, cells were scored for polar localization of ClpX. The upper panel shows the ratio of cells with a polar ClpX-GFP focus. The lower panel shows the ratio of cells with mis- or delocalised ClpX-GFP. The timing of cell cycle progression is equivalent to the experiments shown in Fig. 2A.

Figure 8: CpdR and PopA constitute two converging pathways leading to cell cycle-dependent degradation of CtrA.

Cultures of *C. crescentus DcpdR* single (A) and *DcpdRDpopA* double mutants (B) expressing *cpdR$_{D51A}$-yfp* under the control of the xylose-inducible promoter P$_{xyl}$, were grown in the presence of xylose and analysed microscopically. (C) Cultures of *C. crescentus DcpdR* single (left panels) and *DcpdRDpopA* double mutants (right panels) expressing *cpdR$_{D51A}$-yfp* under the control of the xylose-inducible promoter P$_{xyl}$, were grown in the presence (PYEX) or absence of xylose (PYEG) and analysed by immunoblots using anti-CtrA (upper panels) and anti-CC1850 (lower panels) antibodies, respectively.

Figure 9: Model for the role of PopA in cell cycle-dependent degradation of CtrA.

(A) Converging pathways involved in polar sequestration of ClpXP and its substrate CtrA. The CckA-ChpT phosphorelay inversely regulates CtrA activity and stability through the phosphorylation of CtrA and CpdR. A possible link of the CckA phosphorelay with PopA activity is indicated. Sensor histidine kinase and phosphotransfer protein are shown in blue, response regulators are highlighted green. The model proposes that cell cycle-dependent localization of PopA to the stalked cell pole involves the timed synthesis and/or hydrolysis of c-di-GMP by one or several as yet unidentified DGCs or PDEs. Upon binding of c-di-GMP PopA sequesters to the cell pole, where it recruits RcdA and CtrA (B).

Figure 1

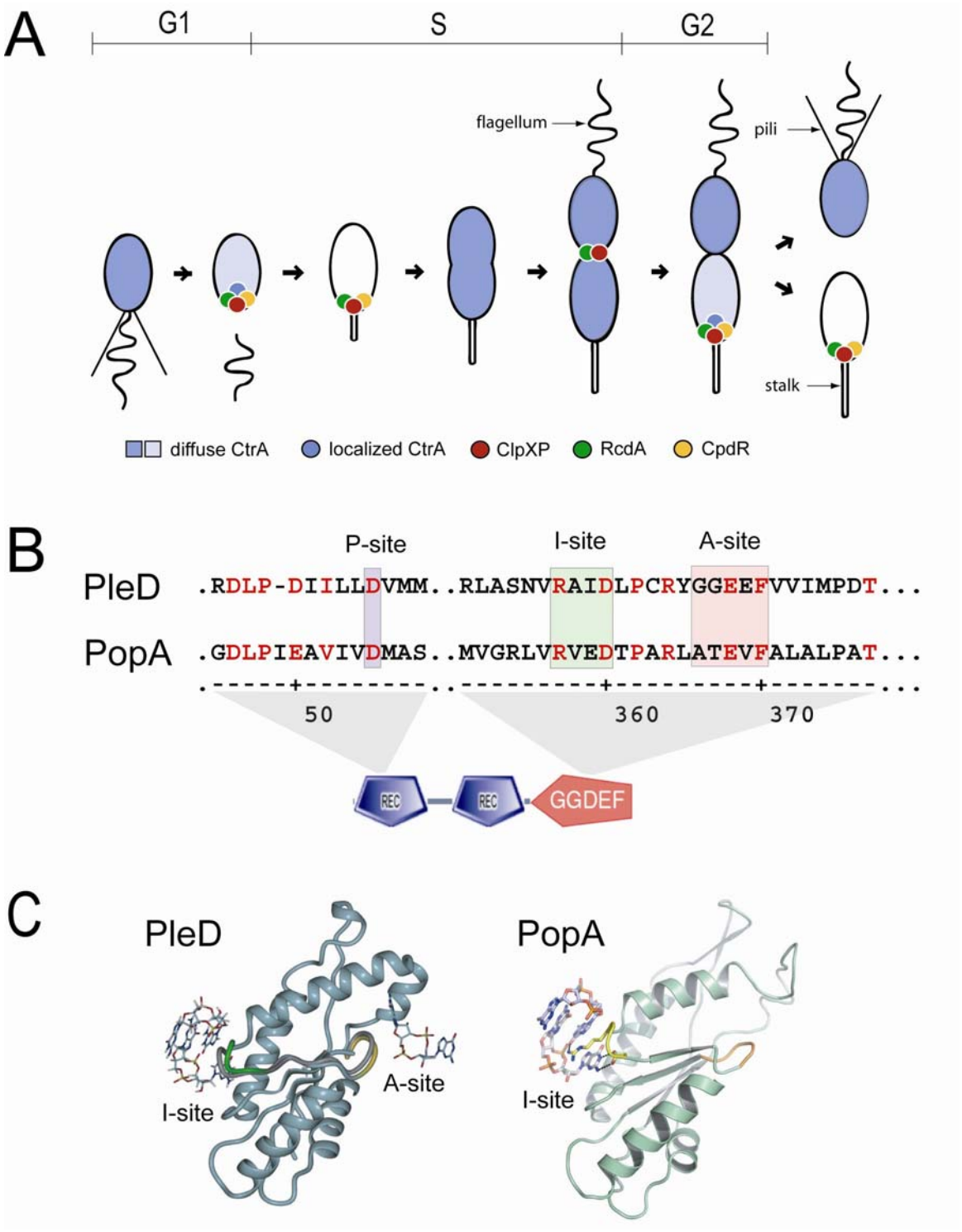
A
G1
S
G2
flagellum
pili
stalk
diffuse CtrA
localized CtrA
ClpXP
RcdA
CpdR
B
P-site
I-site
A-site
PleD .RDLP-DIILLDVMM..RLASNVRAIDLPCRYGGEEFVVIMPDT...
PopA .GDLPIEAVIVDMAS..MVGRLVRVEDTPARLATEVFALALPAT...
50
360
370
REC
REC
GGDEF
C
PleD
PopA
I-site
A-site
I-site

Figure 2

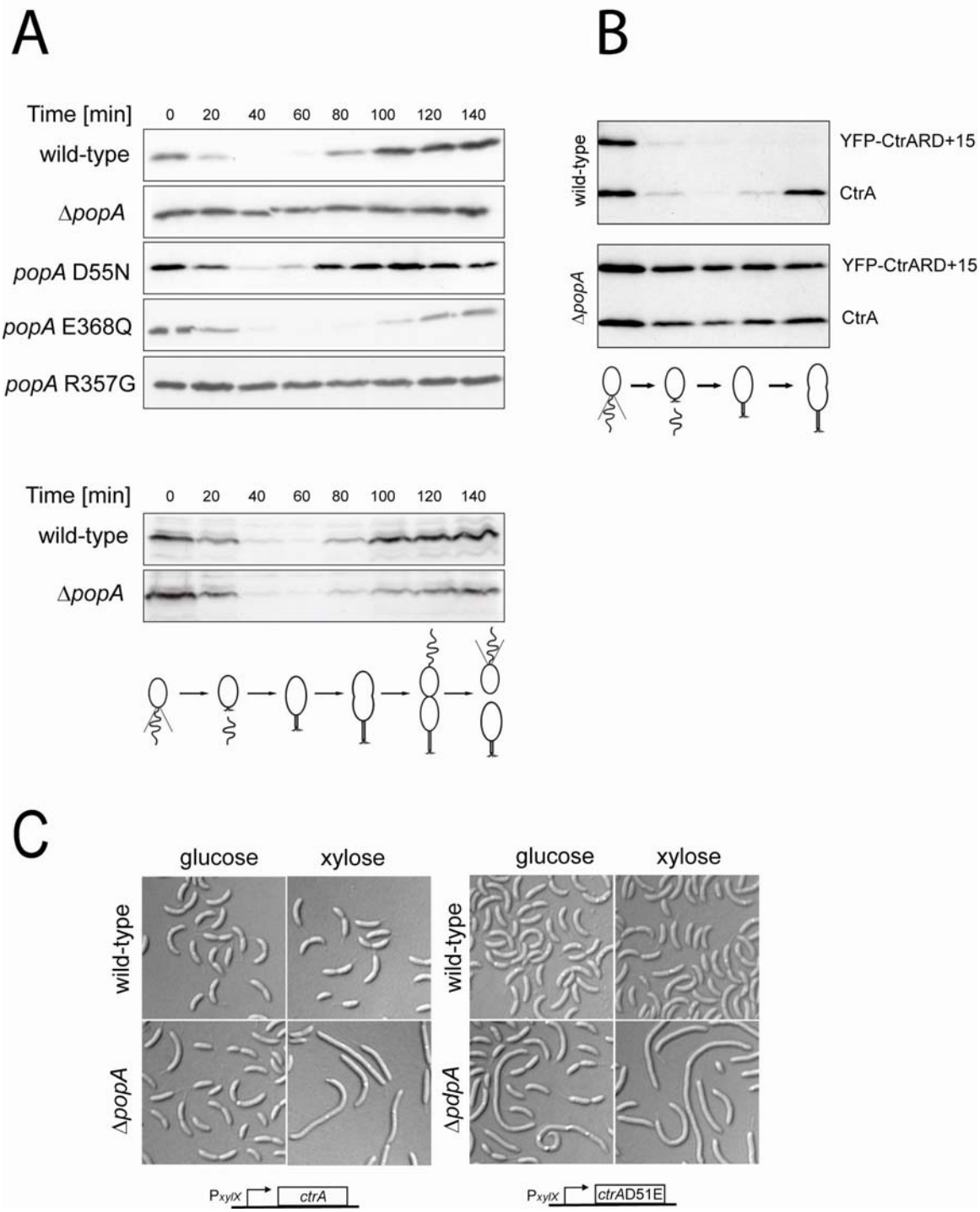
A
Time [min] 0 20 40 60 80 100 120 140
wild-type
ΔpopA
popA D55N
popA E368Q
popA R357G
Time [min] 0 20 40 60 80 100 120 140
wild-type
ΔpopA
B
wild-type
YFP-CtrARD+15
CtrA
ΔpopA
YFP-CtrARD+15
CtrA
C
glucose
xylose
glucose
xylose
wild-type
ΔpopA
wild-type
ΔpdpA
Pxyl ctrA
Pxyl ctrAD51E

Figure 3

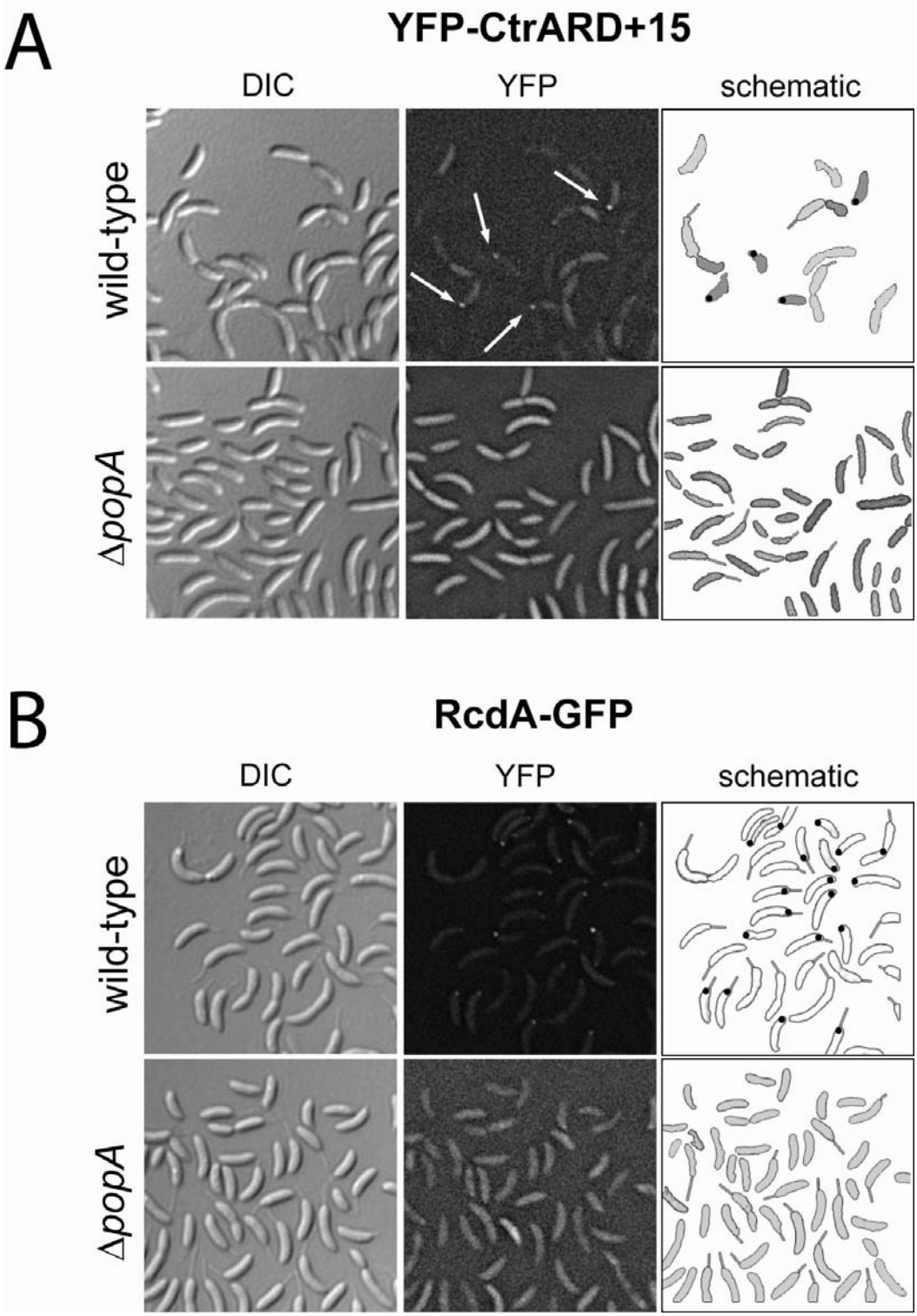
A
YFP-CtrARD+15
DIC
YFP
schematic
wild-type
ΔpopA
B
RcdA-GFP
DIC
YFP
schematic
wild-type
ΔpopA

Figure 3

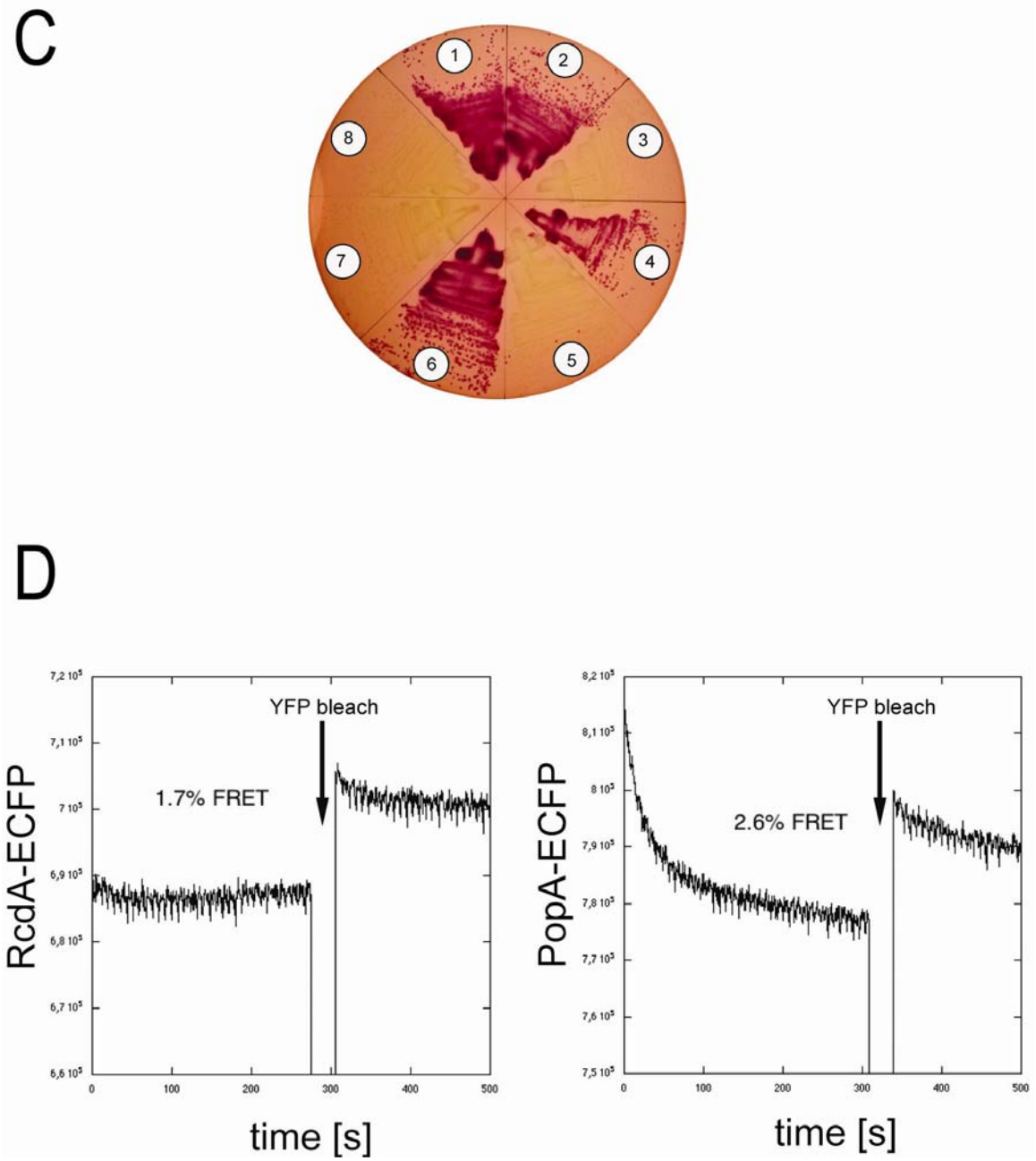
C
1
2
3
4
5
6
7
8
D
RcdA-ECFP
1.7% FRET
YFP bleach
time [s]
PopA-ECFP
2.6% FRET
YFP bleach
time [s]

Figure 4

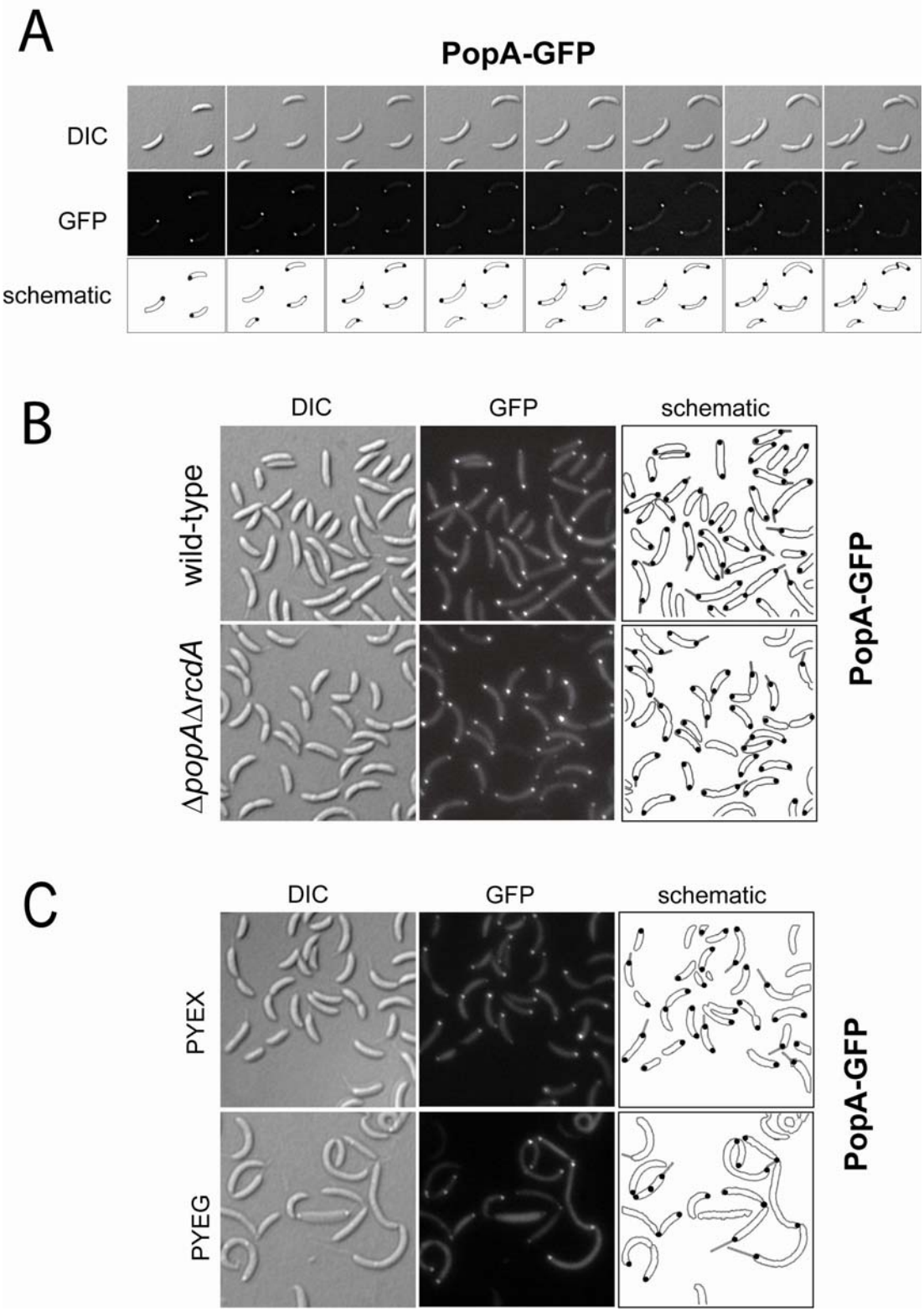
A
PopA-GFP
DIC
GFP
schematic
B
DIC
GFP
schematic
wild-type
ΔpopAΔrcdA
PopA-GFP
C
DIC
GFP
schematic
PYEX
PYEG
PopA-GFP

Figure 5

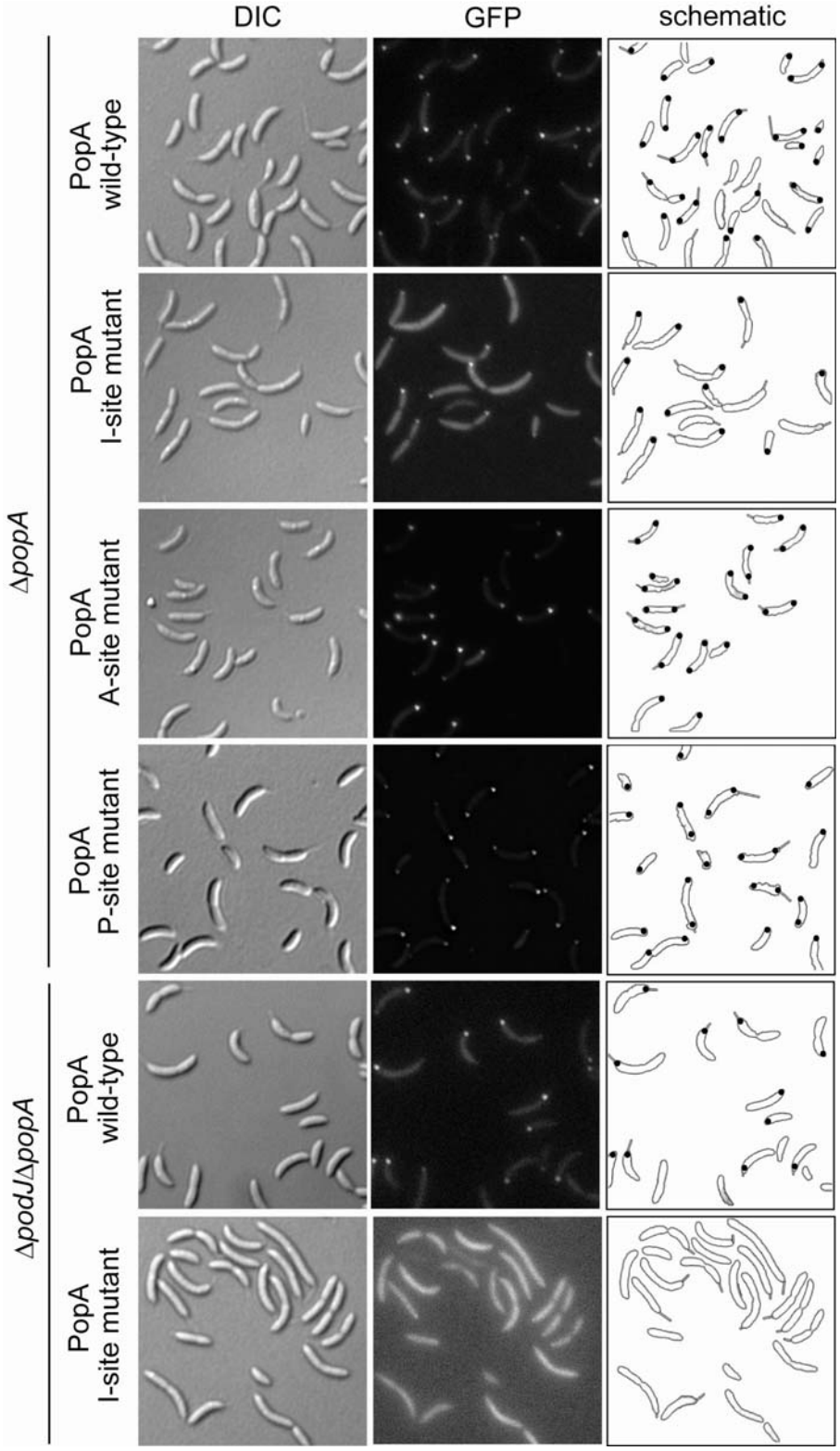
DIC
GFP
schematic
ΔpopA
PopA wild-type
PopA I-site mutant
PopA A-site mutant
PopA P-site mutant
ΔpodJΔpopA
PopA wild-type
PopA I-site mutant

Figure 6

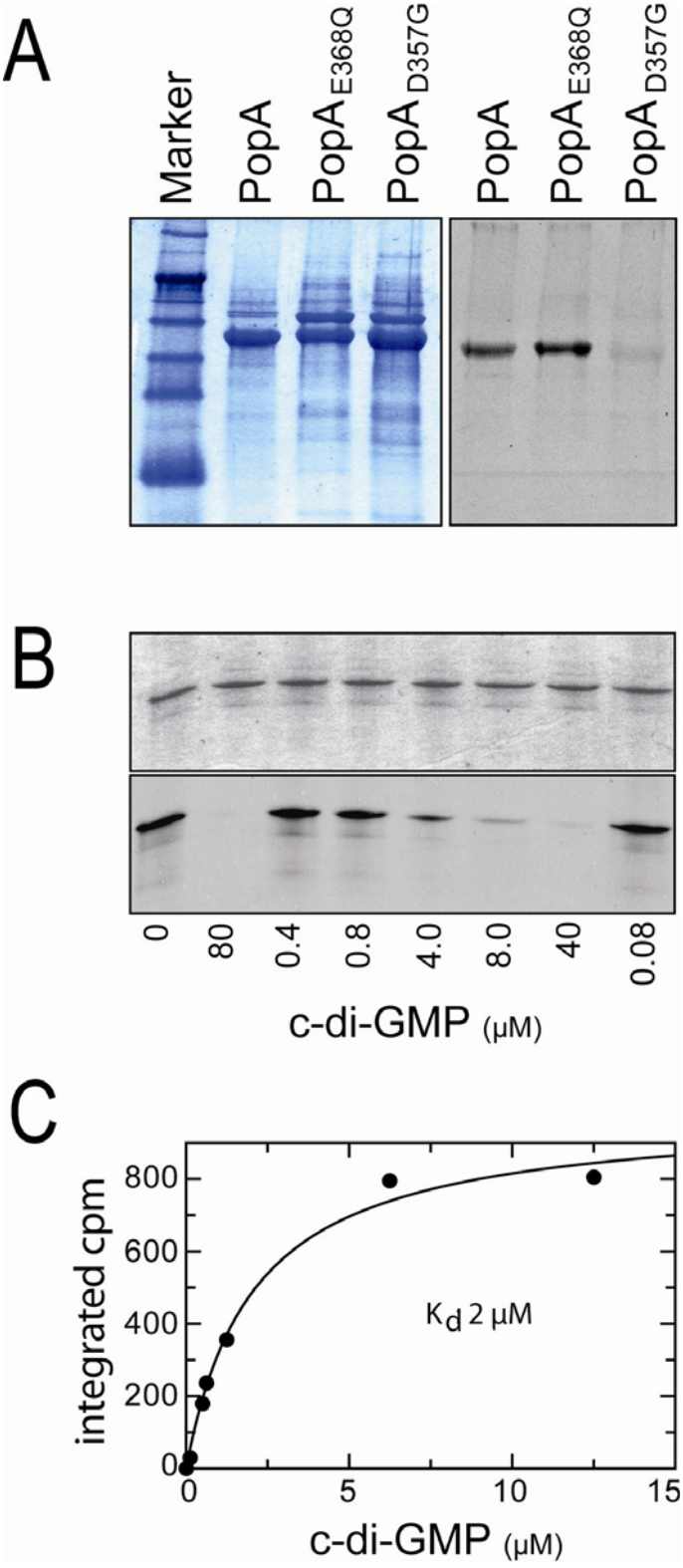
A
Marker
PopA
PopA E368Q
PopA D357G
PopA
PopA E368Q
PopA D357G
B
0
80
0.4
0.8
4.0
8.0
40
0.08
c-di-GMP (µM)
C
integrated cpm
800
600
400
200
0
0
5
10
15
Kd 2 µM
c-di-GMP (µM)

Figure 7

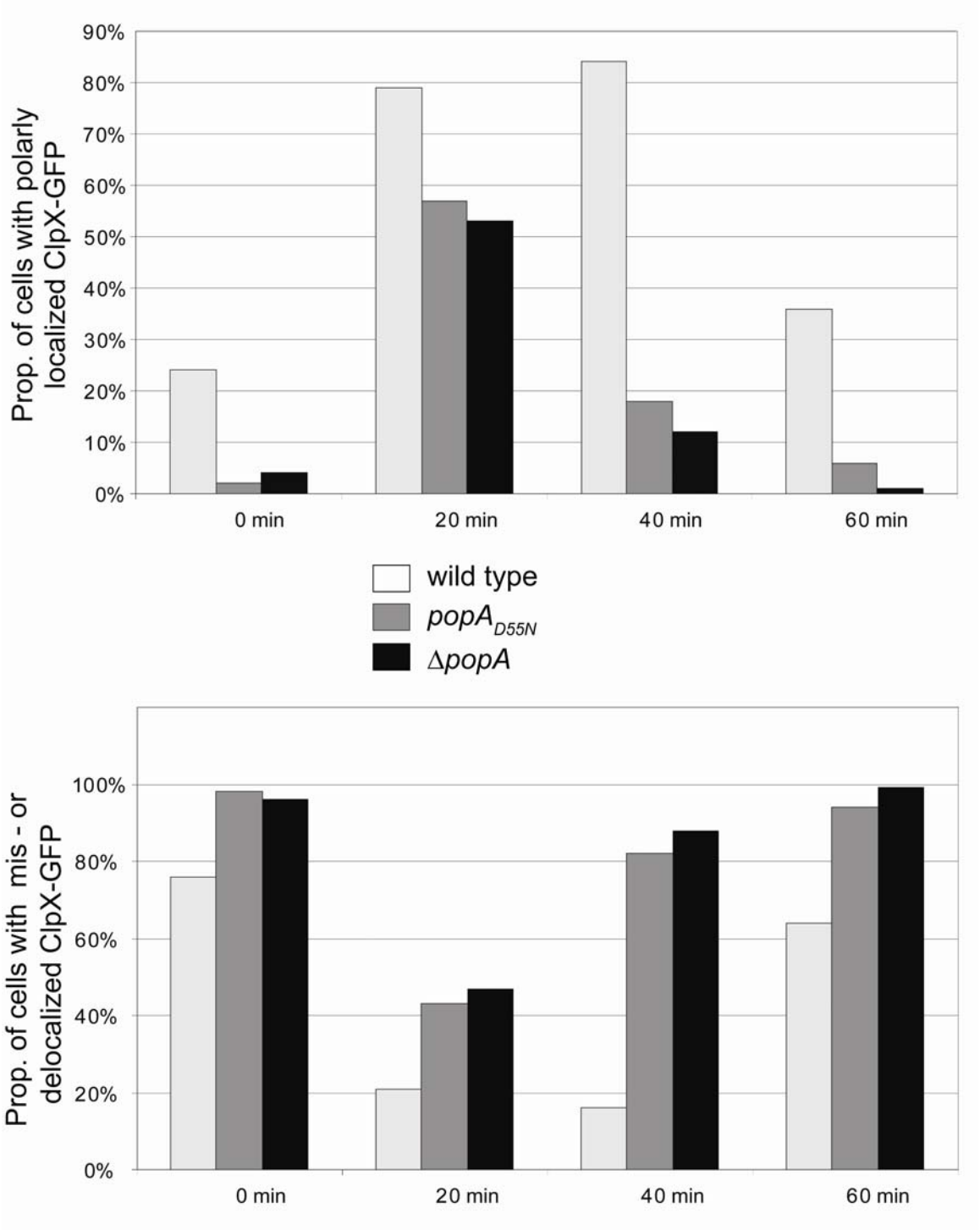
Prop. of cells with polarly localized ClpX-GFP
90%
80%
70%
60%
50%
40%
30%
20%
10%
0%
0 min
20 min
40 min
60 min
wild type
popA D55N
ΔpopA
Prop. of cells with mis - or delocalized ClpX-GFP
100%
80%
60%
40%
20%
0%
0 min
20 min
40 min
60 min

Figure 8

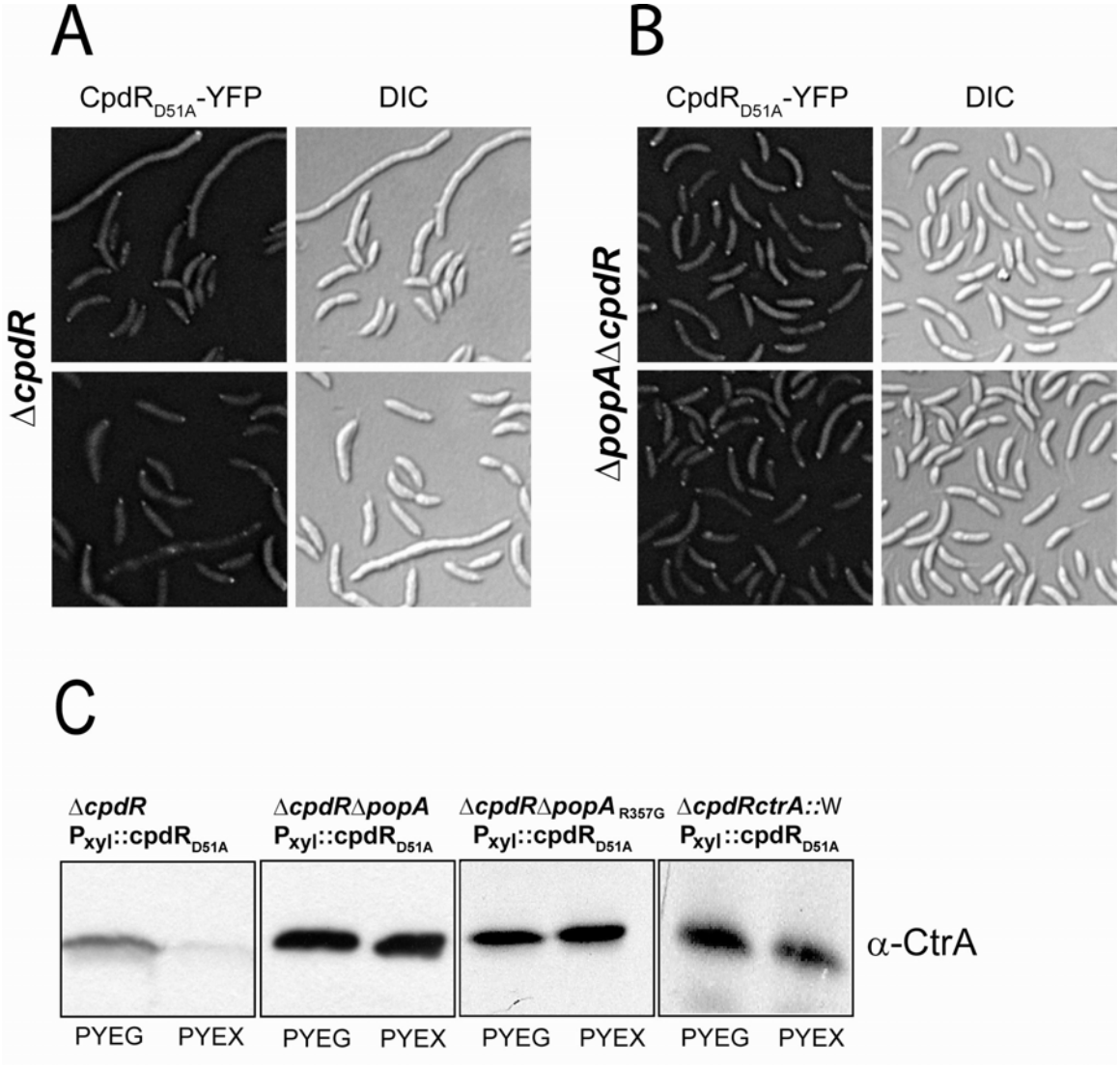
A
CpdR$_{D51A}$-YFP
DIC
Δ*cpdR*
B
CpdR$_{D51A}$-YFP
DIC
Δ*popA*Δ*cpdR*
C
Δ*cpdR*
P$_{xyl}$::cpdR$_{D51A}$
Δ*cpdR*Δ*popA*
P$_{xyl}$::cpdR$_{D51A}$
Δ*cpdR*Δ*popA*$_{R357G}$
P$_{xyl}$::cpdR$_{D51A}$
Δ*cpdRctrA::*W
P$_{xyl}$::cpdR$_{D51A}$
α-CtrA
PYEG PYEX PYEG PYEX PYEG PYEX PYEG PYEX

Figure 9

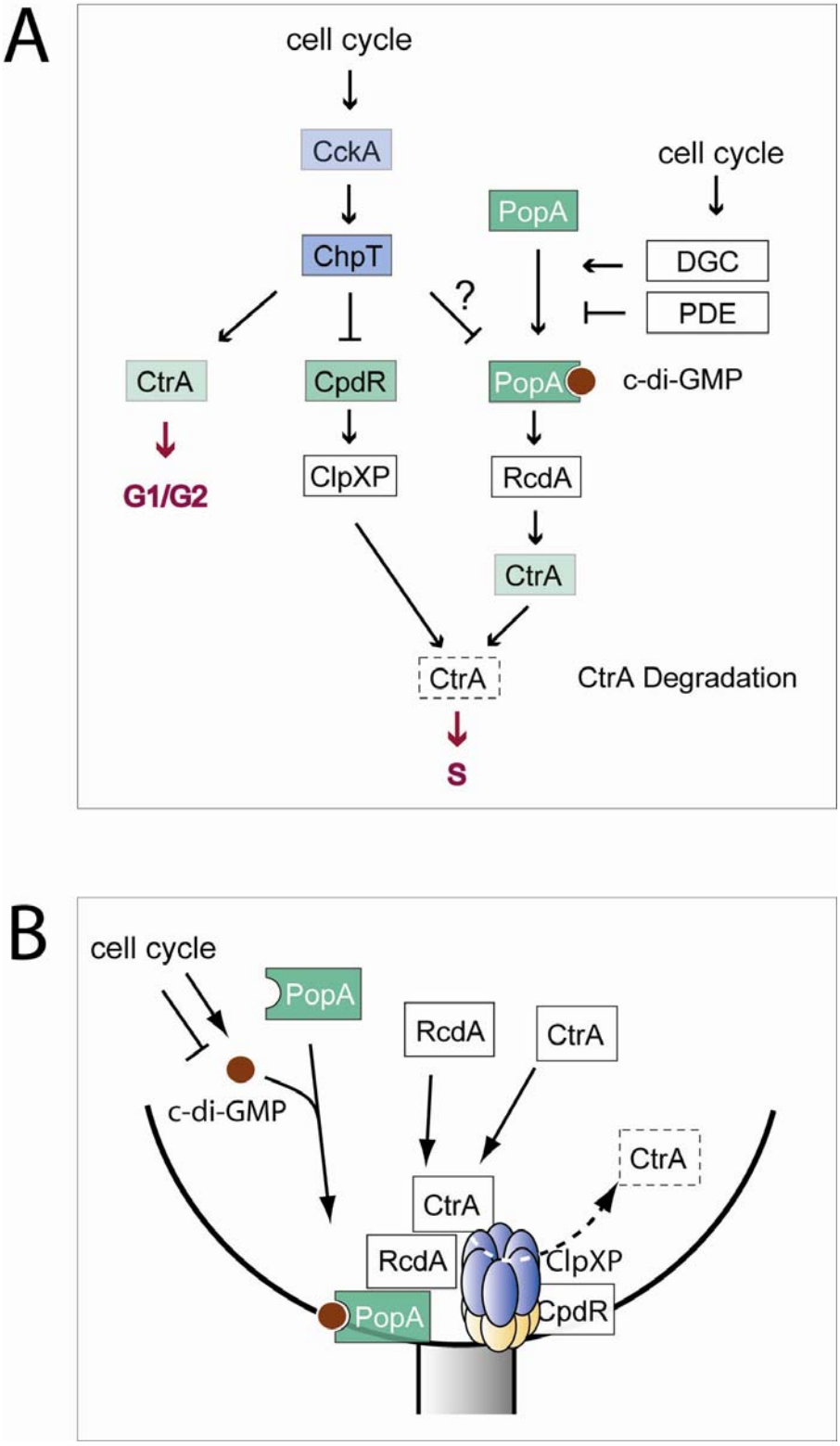
A
cell cycle
CckA
ChpT
CtrA
G1/G2
CpdR
ClpXP
?
cell cycle
PopA
DGC
PDE
PopA
c-di-GMP
RcdA
CtrA
CtrA
CtrA Degradation
S
B
cell cycle
PopA
c-di-GMP
RcdA
CtrA
CtrA
CtrA
RcdA
ClpXP
PopA
CpdR

Table 1

	CdpR-YFP localized 		CdpR-YFP delocalized 	
	Δ*cpdR*	Δ*cpdR*Δ*popA*	Δ*cpdR*	Δ*cpdR*Δ*popA*
0 min	57%	36%	43%	64%
20 min	75%	38%	25%	62%
40 min	68%	13%	32%	87%
60 min	36%	4%	64%	96%
80 min	4%	1%	96%	99%

Supplementary Material:

Figure S1: Sequence comparison of the diguanylate cyclase PleD and the c-di-GMP binding protein PopA.

A sequence alignment of PopA (Query) and PleD (Sbjct) is shown. The three domains are indicated by different colors. Conserved residues of Rec1 known to be important for intra-molecular signaling are boxed green, conserved residues of the putative dimerisation interface are boxed red, and residues important for GGDEF domain function are highlighted in purple.

Figure S2: CtrA is stabilized in a Δ*popA* mutant.

Cell cycle time lapse experiment with wild-type and Δ*popA* mutant cells expressing *yfp-ctrARD+15* from the xylose inducible promoter P_{xyl}. Cells grown in the presence of the inducer xylose were synchronized and released into fresh M2G minimal glucose medium lacking the inducer. Samples were removed at intervals and analysed by DIC and fluorescence microscopy.

Fig. S3: Protein – protein interaction map of the *C. crescentus* CtrA degradation machinery.

Arrows indicate interactions between proteins. Interactions shown by co-immunoprecipitation are in blue, interactions shown by the bacterial two-hybrid system (BACTH) are in red. Stippled arrows indicate weak interactions.

Fig. S4: Polar localization of PopA-eGFP during the *C. crescentus* cell cycle.

(A) *C. crescentus* wild-type cells expressing *popA-egfp* were synchronized and samples removed at 20 minute intervals were analysed by fluorescence microscopy. Cell cycle progression is shown schematically. (B) Statistics of PopA-eGFP localization as shown in (A). Cells with no focus, with a PopA-eGFP focus at one pole, and with a bipolar pattern were scored throughout the cell cycle as indicated.

Fig. S5: Polar localization of PopA I- and A-site mutants during the *C. crescentus* cell cycle.

C. crescentus popA mutant cells expressing either $popA_{E368Q}$-*egfp* (A) or $popA_{D357G}$-*egfp* (B) were synchronized and samples removed at 20 minute intervals were analysed by DIC and

fluorescence microscopy. The statistics of $PopA_{E368Q}$-eGFP and $PopA_{D357G}$-eGFP localization is shown underneath the microscopy panels. Cells with no focus, with a focus at one pole, and with a bipolar pattern were scored throughout the cell cycle as indicated.

Fig. S6: The GGDEF domain is required for efficient localization of PopA to the pole.

C. crescentus popA mutant cells expressing *popA-rec1-egfp* (receiver domain 1 of PopA), *popA-rec1-rec2-egfp* (receiver domains 1 and 2 of PopA), or *popA-egfp* (full-length PopA) were analysed by DIC (left) and fluorescence microscopy (middle). The localization patterns are indicated on the right.

Fig. S7: PopA is required for proper localization of ClpX to the cell pole.

Cultures of *C. crescentus* wild type and *popA* mutants expressing a *clpX-egfp* were synchronized and cells were analysed by DIC and fluorescence microscopy as they progressed through the cell cycle. Polar localization of ClpX is shown schematically in the middle panel. Progression of cells through the cell cycle is indicated on the left.
The timing of cell cycle progression is equivalent to the experiments shown in Fig. 2A.

Fig. S8: CpdR is not required for localization of PopA to the cell pole.

Cultures of *C. crescentus* wild type and *DcpdR*mutant expressing *popA-egfp* were analysed by DIC (middle) and fluorescence microscopy (left). The localization patterns are indicated on the right.

Fig. S9: PopA is required for proper CpdR localization to the cell pole.

Cultures of *C. crescentus DcpdR* (upper panels) and *DcpdRDpopA* (lower panels) mutants expressing *cpdR-yfp* were synchronized and cells were analysed by DIC and fluorescence microscopy throughout the cell cycle. The localization patterns are shown schematically.

Figure S1


Score = 77.8 bits (190), Expect = 2e-12
Identities = 105/431 (24%), Positives = 163/431 (37%), Gaps = 21/431 (4%)
Query 5 ARILIVARDDVRAGP--LAEGLDRLGWRTITAR-GPYAALAALGDLPIEAVIVDMASAGP 61
ARIL+V DD+ A L L + TA GP A A DLP + +++D+ G
Sbjct 3 ARILVV--DDIEANVRLLEAKLTAEYYEVSTAMDGPTALAMAARDLP-DIILLDVMMPGM 59
Query 62 ETQTLARRLKAAVAPRRLPVIAISEPNA------DFRSQSFDLTLSPPLHPSQAALRLES 115
+ T+ R+LK R +PV+ I+ + S + D L+ P+ R+ S
Sbjct 60 DGFTVCRKLKDDPTTRHIPVVLITALDGRGDRIQGLESGASDF-LTKPIDDVMLFARVRS 118
Query 116 LVRTAIAEEEFEIRLETFGERGRRLDLPEPLDA-PYRILAVGEPAPQFLALSNALQASGA 174
L R + +E R + G LD R+L V + Q ++ L
Sbjct 119 LTRFKLVIDELRQREASGRRMGVIAGAAARLDGLGGRVLIVDDNERQAQRVAAELGVEHR 178
Query 175 EVVGAFTAYTAFDYLHERPFDSVVLWAGDSQQEALSIAAGMRRNTRLFHIPALLYLKAES 234
V+ + P D V++ A + L A +R R +P L + +
Sbjct 179 PVIESDPEKAKISA--GGPVDLVIVNAAAKNFDGLRFTAALRSEERTRQLPVLAMVDPDD 236
Query 235 YVTMSEAFHRGVSDVASPETPEGETAMRVMELARSFRRGESIRGALEKARSSGLMDAATG 294
M +A GV+D+ S E + RV + R + +R L+ + + D TG
Sbjct 237 RGRMVKALEIGVNDILSRPIDPQELSARVKTQIQRKRYTDYLRNNLDHSLELAVTDQLTG 296
Query 295 LFTRDLFAAHLARLASAARERSRPLSICVLRV--ADKPETVWARQNGWLDRAIPQIGSMV 352
L R L L A P+S ++ + K + G D + + +
Sbjct 297 LHNRRYMTGQLDSLVKRATLGGDPVSALLIDIDFFKKINDTFGHDIG--DEVLREFALRL 354
Query 353 GRLVRVEDTPARLATEVFALALPATNQNAACAAAERIAAVIGCTAFDAGEDRAPFVCEFD 412
VR D P R E F + +P T A AERI + + F R
Sbjct 355 ASNVRAIDLPCRYGGEEFVVIMPDTALADALRIAERIRMHVSGSPFTVAHGREMLNVTIS 414
Query 413 IGVAEVQPGEG 423
IGV+ GEG
Sbjct 415 IGVS-ATAGEG 424
Rec1
Rec2
GGDEF

Figure S2

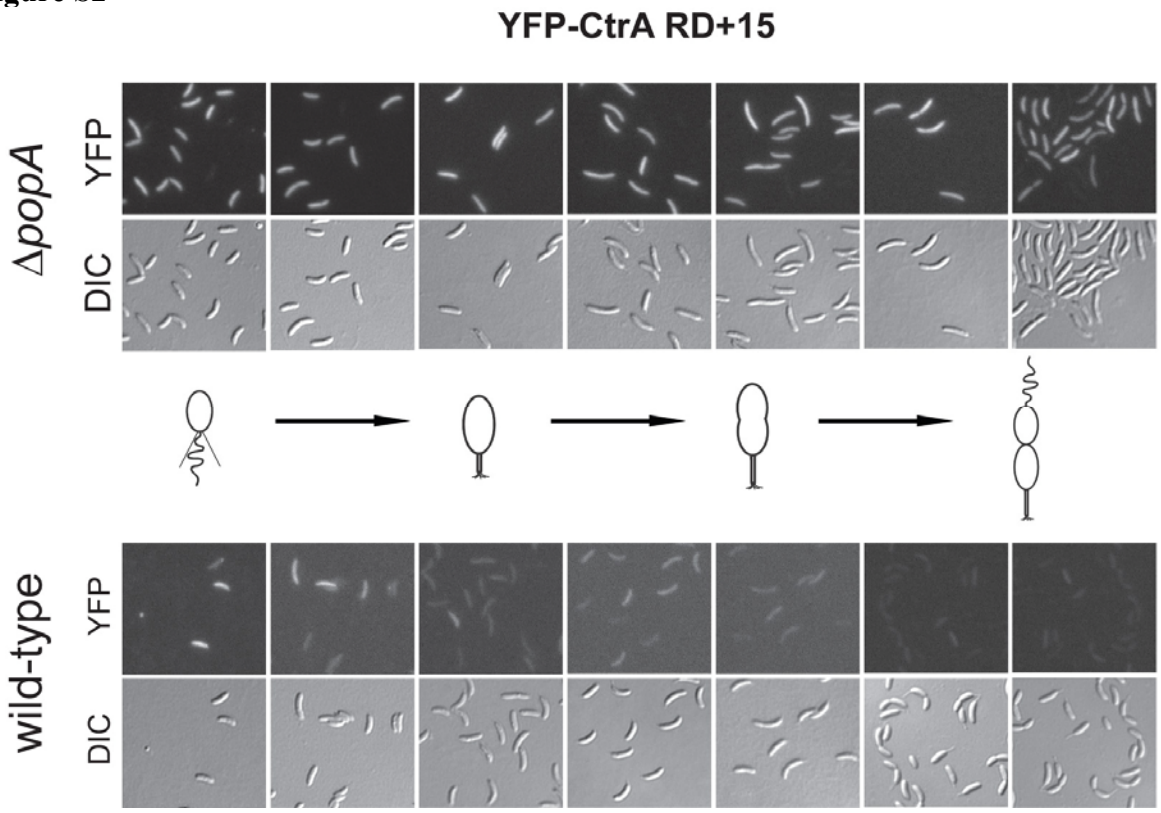

Figure S3

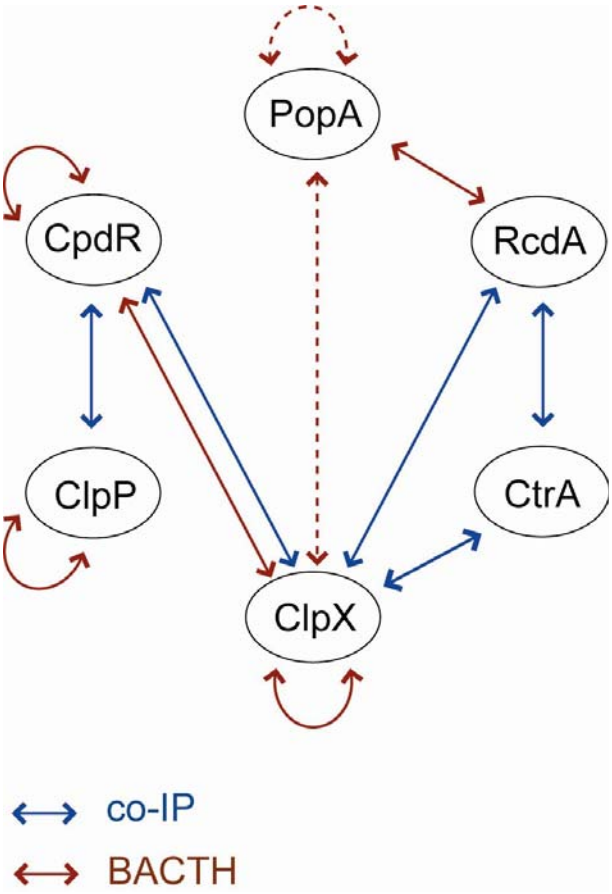

Figure S4

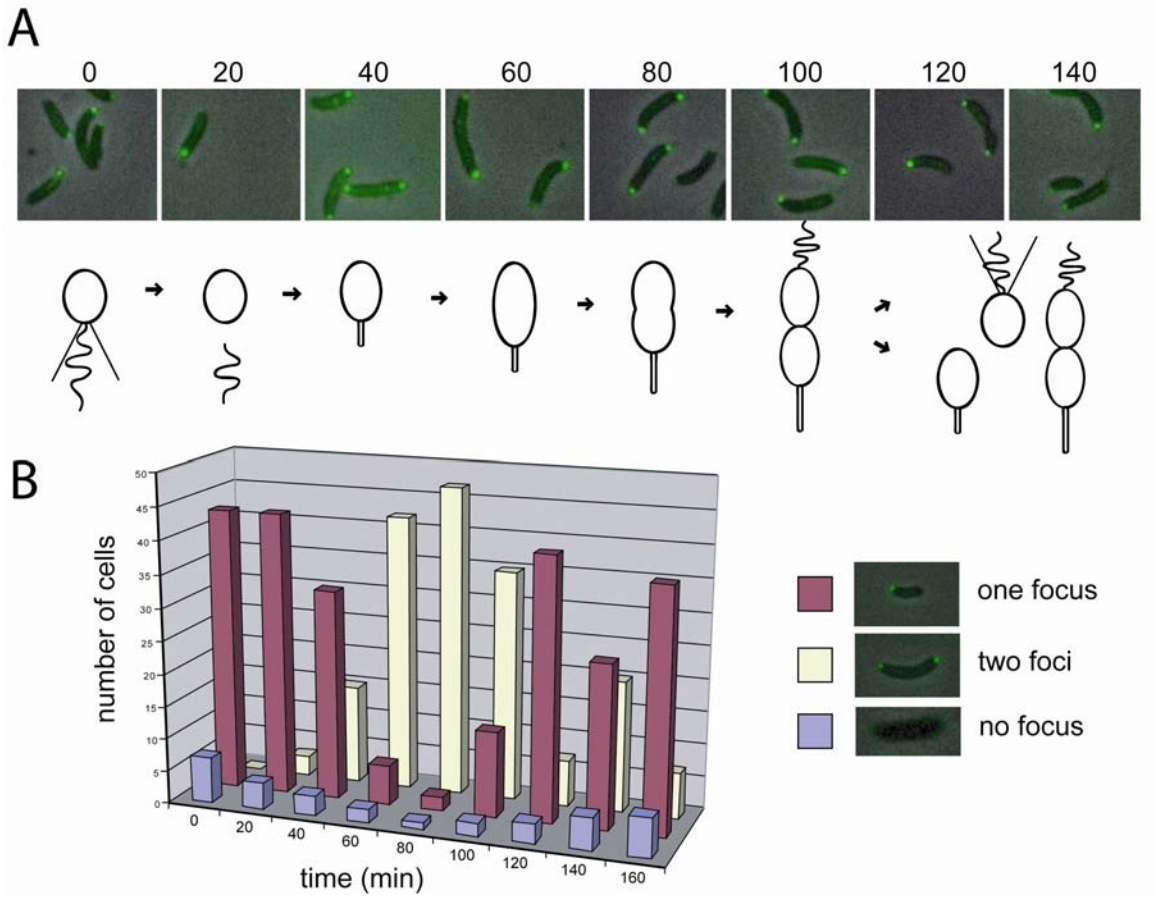
A
0
20
40
60
80
100
120
140
B
number of cells
time (min)
one focus
two foci
no focus

Figure S5

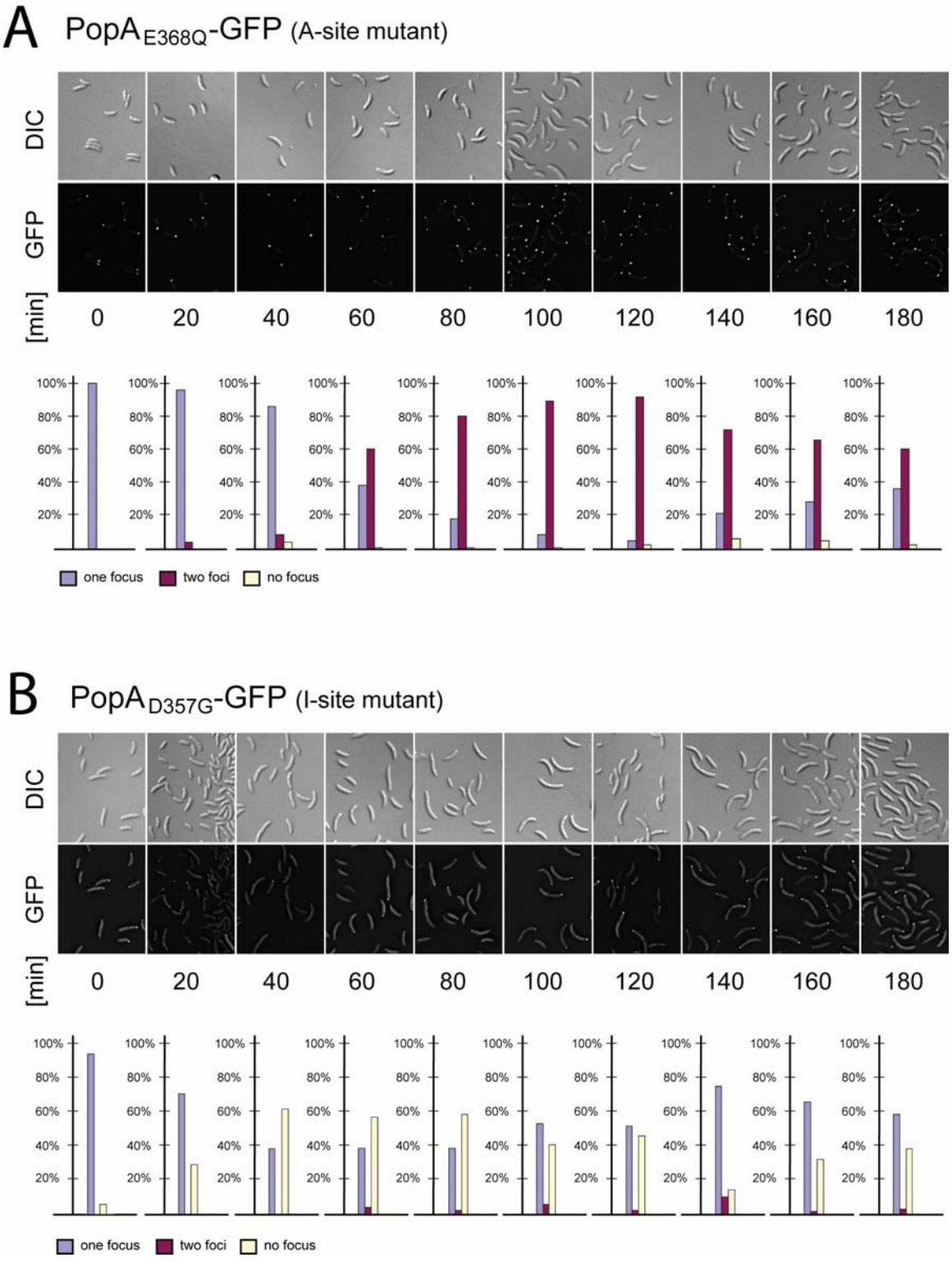
A
PopA E368Q-GFP (A-site mutant)
DIC
GFP
[min]
0
20
40
60
80
100
120
140
160
180
100%
80%
60%
40%
20%
one focus
two foci
no focus
B
PopA D357G-GFP (I-site mutant)
DIC
GFP
[min]
0
20
40
60
80
100
120
140
160
180
100%
80%
60%
40%
20%
one focus
two foci
no focus

Figure S6

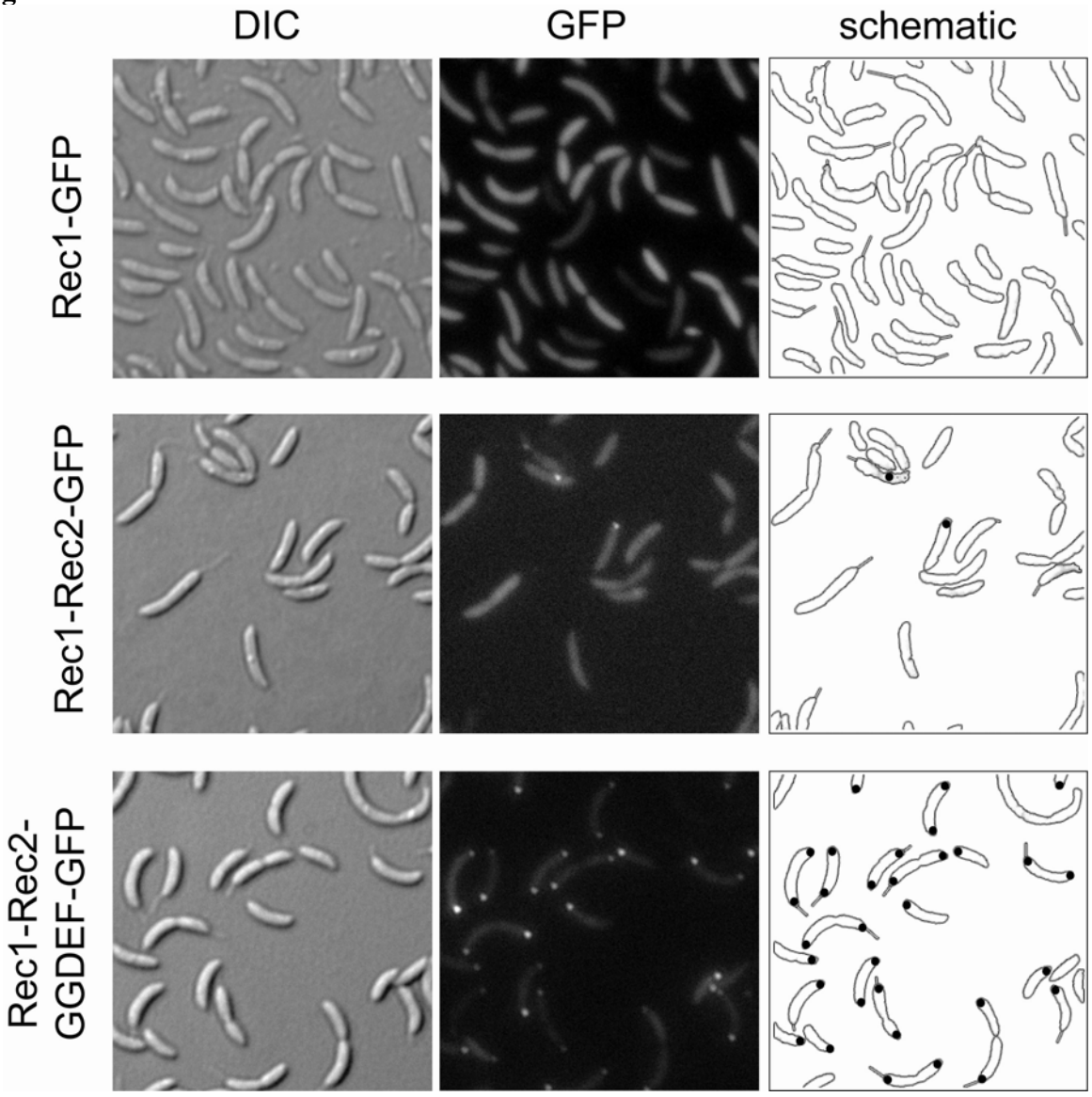

Figure S7

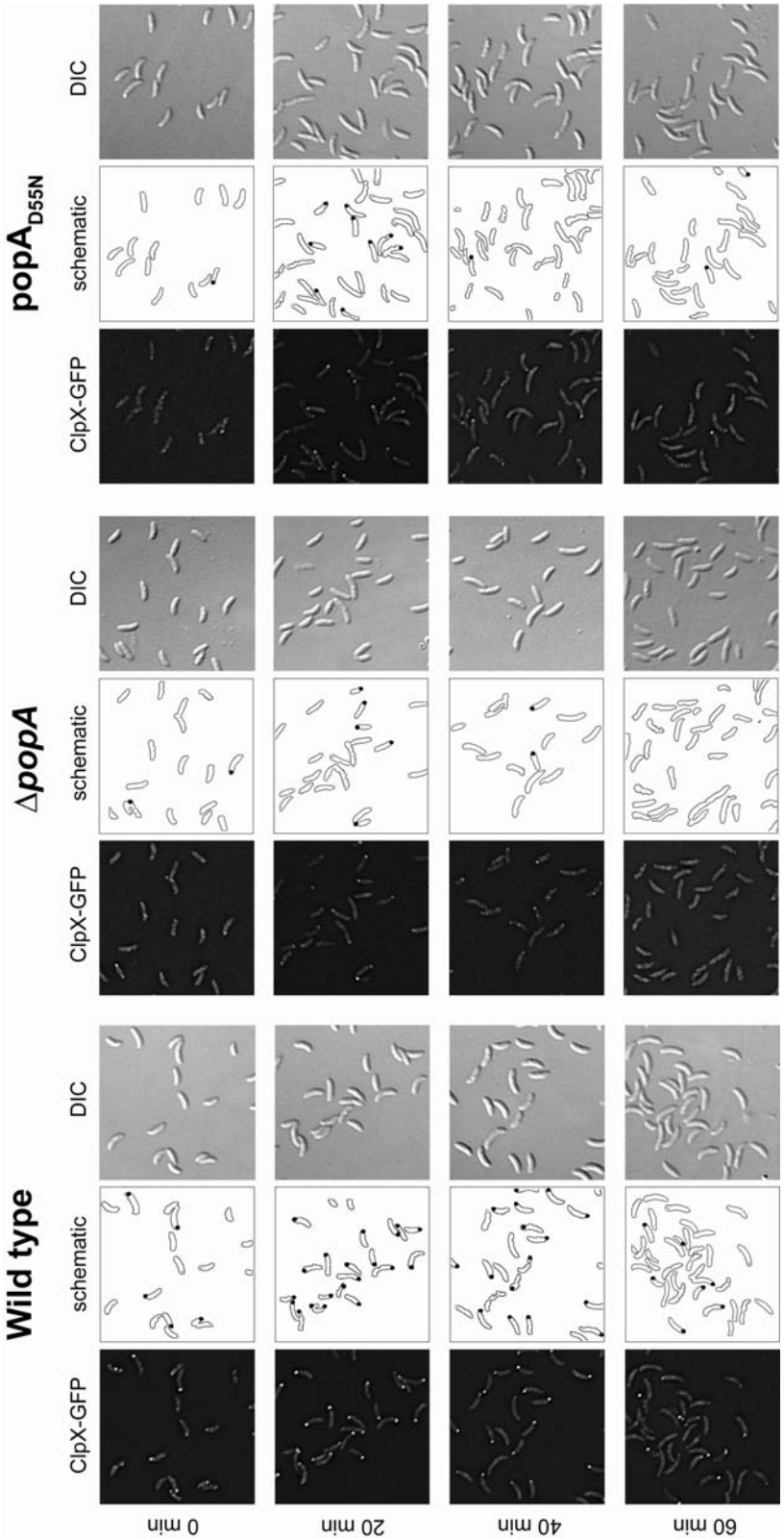
Wild type
ΔpopA
popA D55N
DIC
schematic
ClpX-GFP
0 min
20 min
40 min
60 min

Figure S8

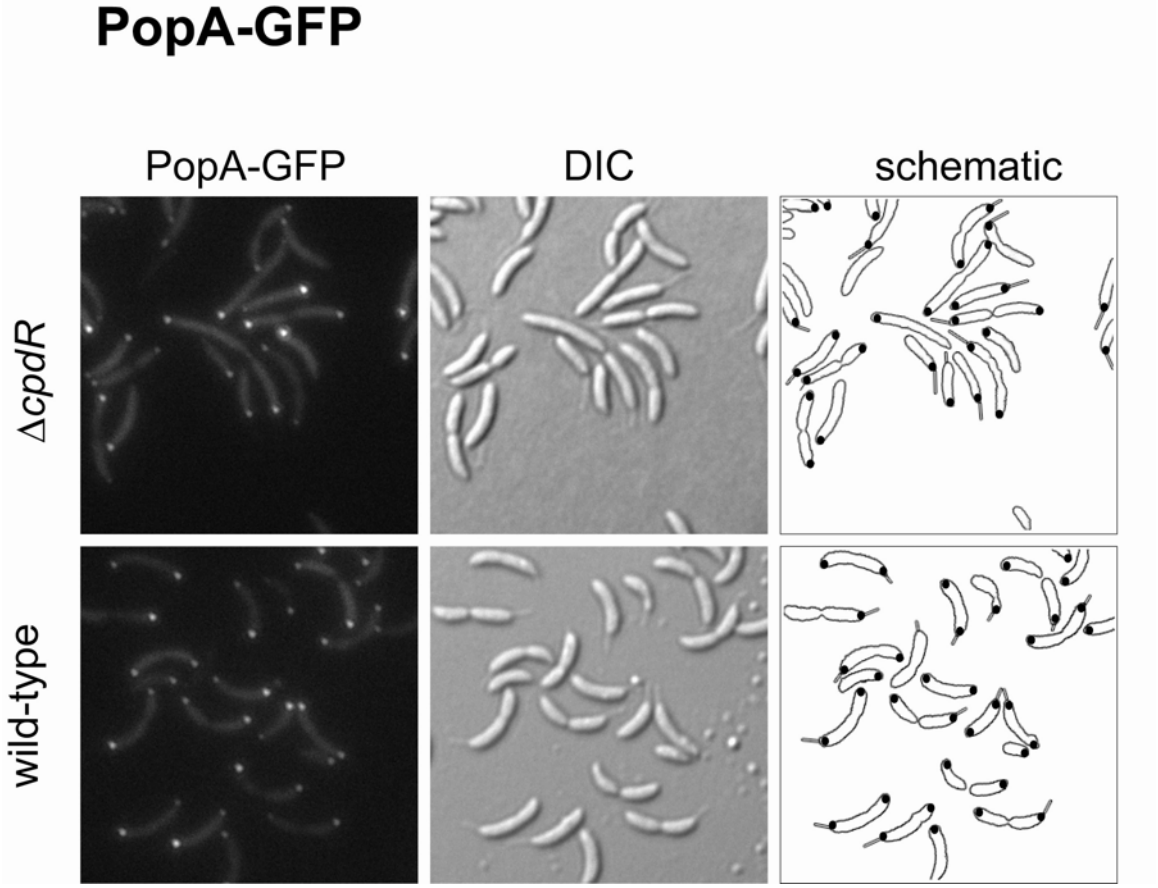

Figure S9

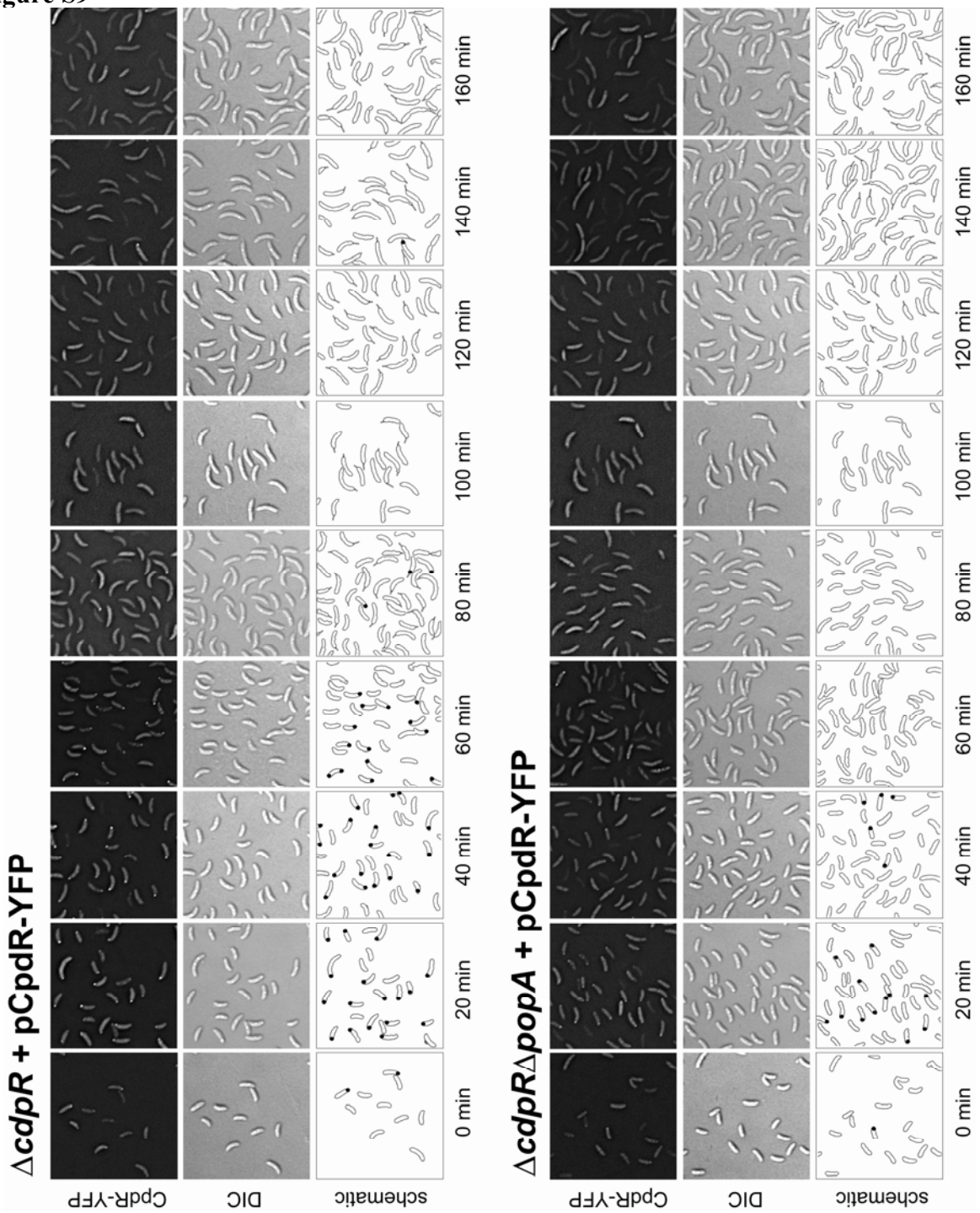
Δcdpr + pCpdR-YFP
ΔcdpRΔpopA + pCpdR-YFP
CpdR-YFP
DIC
schematic
0 min
20 min
40 min
60 min
80 min
100 min
120 min
140 min
160 min

Table S1

Strain or plasmid	Relevant genotype and description	Reference or source
C. crescentus strains		
NA1000	Synchronizable laboratory strain of CB15	[114]
UJ271	NA1000 *clpX*::Ω::pUJ168	[108]
UJ2765	NA1000 Δ*podJ* and plasmid pAD5	this study
UJ2796	NA1000 and plasmid pAD5	this study
UJ2827	NA1000 Δ*popA*	this study
UJ3125	NA1000 and plasmid pEJ146	this study
UJ3127	NA1000 Δ*popA* and plasmid pEJ146	this study
UJ3159	NA1000 Δ*popA* and plasmid pAD19	this study
UJ3563	NA1000 Δ*popA* and plasmid pAD32	this study
UJ3565	NA1000 Δ*popA* and plasmid pAD30	this study
UJ3640	NA1000 Δ*popA* Δ*podJ*	this study
UJ3665	NA1000 Δ*popA* Δ*rcdA* and plasmid pAD5	this study
UJ3666	NA1000 Δ*popA* Δ*podJ* and plasmid pAD5	this study
UJ3672	NA1000 Δ*popA* Δ*podJ* and plasmid pAD30	this study
UJ3742	NA1000 ΔpopA *rcdA*::prcdA-egfp	this study
UJ3743	NA1000 ΔpopA *xylX*::pX-clpX-egfp	this study
UJ3966	NA1000 and plasmid pID42	this study
UJ3967	NA1000 and plasmid pIDC42	this study
UJ3969	NA1000 Δ*popA* and plasmid pID42	this study
UJ3970	NA1000 Δ*popA* and plasmid pIDC42	this study
UJ3972	NA1000 *clpX*::Ω::pUJ168 and plasmid pAD5	this study
UJ4329	NA1000 and plasmids pAD105, pAD82	this study
UJ4330	NA1000 and plasmids pAD106, pAD83	this study
UJ4331	NA1000 Δ*popA* and plasmid pAD128	this study
UJ4333	NA1000 Δ*popA* and plasmid pAD130	this study
UJ4374	NA1000 Δ*cpdR* and plasmid pAD147	this study
UJ4417	NA1000 Δ*popA xylX*::pX-clpX-egfp and plasmid pAD150	this study
UJ4401	NA1000 Δ*popA* Δ*cpdR*	this study
UJ4434	NA1000 Δ*cpdR* and plasmid pcpdR-yfp	this study
UJ4435	NA1000 Δ*popA* Δ*cpdR* and plasmid pcpdR-yfp	this study
UJ4471	NA1000 Δ*popA* Δ*cpdR* and plasmid pX-cpdRD51A-yfp	this study
UJ4473	NA1000 Δ*cpdR* and plasmid pX-cpdRD51A-yfp	this study
LS4183	NA1000 *xylX*::pX-clpX-egfp	[184]
LS4191	NA1000 *rcdA*::prcdA-egfp	[184]
NA1000 Δ*cpdR*	Disruption of *cpdR* (*tet*^{R})	[173]
NA1000 Δ*podJ*	Deletion of *podJ*	[281]
***E. coli* strains**		
MM337	*E. coli* K-12 *araD139 flbB5301* ptsF25 *rbsR relA1 rpsL150* (*argF-lac*)U169 *cya*	M. Manson
DH10B	F- *mcr*A Δ(*mrr*- hsd RMS- *mcr*BC) Φ80d*lacZ*ΔM15 Δ*lac*X74 endA1 recA1 deoR Δ (*ara, leu*)7697 *araD139 galU galK nupG rpsL thi pro hsdR- hsd+ recA RP4-2-Tc*::*Mu-Tn7*	[205]
S17	RP4-2, Tc::Mu, KM-Tn7	[205]
DH5α	*supE44* Δ*lac*U169(Φ80 *lacZ*ΔM15) *hsdR17 recA1 endA1gyrA96 thi-1 relA1*	[204]
ArcticR	BL21 (DE3) arctic express strain for protein expression	Stratagene
Plasmids		
pAD5	pMR20; *popA-eGfp* under control of *popA* promoter	this study

pAD8	pNPTS138; used for clean deletion of *popA*	this study
pAD19	pMR20; *popAD55N-eGfp* under control of *popA* promoter	this study
pAD30	pMR20; *popAR357G-eGfp* under control of *popA* promoter	this study
pAD32	pMR20; *popAE368Q-eGfp* under control of *popA* promoter	this study
pAD33	pET21C; *popAR357G* C-terminal His6 tag	this study
pAD34	pET21C; *popAE368Q* C-terminal His6 tag	this study
pAD44	pUT18C; *clpX* C-terminal fused to the T18 fragment	this study
pAD45	pKT25; *clpX* C-terminal fused to the T25 fragment	this study
pAD47	pUT18C; *clpP* C-terminal fused to the T18 fragment	this study
pAD48	pKT25; *clpP* C-terminal fused to the T25 fragment	this study
pAD50	pUT18C; *rcdA* C-terminal fused to the T18 fragment	this study
pAD51	pKT25; *rcdA* C-terminal fused to the T25 fragment	this study
pAD53	pUT18C; *cpdR* C-terminal fused to the T18 fragment	this study
pAD54	pKT25; *cpdR* C-terminal fused to the T25 fragment	this study
pAD56	pUT18; *rcdA* N-terminal fused to the T18 fragment	this study
pAD58	pUT18; *clpX* N-terminal fused to the T18 fragment	this study
pAD60	pUT18; *clpP* N-terminal fused to the T18 fragment	this study
pAD62	pUT18; *cpdR* N-terminal fused to the T18 fragment	this study
pAD65	pUT18; *ctrA* N-terminal fused to the T18 fragment	this study
pAD67	pUT18; *popA* N-terminal fused to the T18 fragment	this study
pAD82	pMR20; *popA-eYfp* under control of popA promoter	this study
pAD83	pMR10; *popA-eCfp* under control of popA promoter	this study
pAD90	pKT25; *popAR357G* C-terminal fused to the T25 fragment	this study
pAD91	pKT25; *popAE368Q* C-terminal fused to the T25 fragment	this study
pAD105	pBBR-MCS-5; *rcdA-eCfp* under the control of rcdA promoter	this study
pAD106	pBBR-MCS-5; *rcdA-eYfp* under the control of rcdA promoter	this study
pAD128	pMR20; *popA-Rec1-eGfp* under the control of popA promoter	this study
pAD130	pMR20; *popA-Rec1Rec2-eGfp* under the control of popA promoter	this study
pAD140	pKT25; *ctrA* C-terminal fused to the T25 fragment	this study
pAD141	pKT25; *popA* C-terminal fused to the T25 fragment	this study
pAD142	pUT18C; *ctrA* C-terminal fused to the T18C fragment	this study
pAD143	pUT18C; *popA* C-terminal fused to the T18C fragment	this study
pAD147	pMR10; *popA-eGfp* under control of popA promoter	this study
pAD150	pMR20; *popAD55N* under the control of popA promoter, chloramphenicol cassette integrated	this study
pAD153	pMR20; *popAR357G* under the control of popA promoter,kanamycin cassette integrated	this study
pBBR1MCS-5	GentR, broad host range cloning vector	[206]
pcpdR-yfp	pMR11; *cpdR* 3' fused to eyfp with cpdR promoter	[269]
pECFP	AmpR vector for creation of *eCFP*-fusion proteins	Clontech
pEGFP	AmpR vector for creation of *eGFP*-fusion proteins	Clontech
pEJ146	pMR10-P_{xyl}::*yfp-ctrA* RD+15	[110]
pET21C	AmpR expression vector, high copy number	Novagen
pET21C::PopA	pET21C; *popA* C-terminal His6 tag	this study
pEYFP	AmpR vector for creation of *eYFP*-fusion proteins	Clontech
pID42	pJS14; P_{xyl}::*ctrA*	[109]
pIDC42	pJS14; P_{xyl}::*ctrAD51E*	[109]
pJS14	$Chlor^R$ high copy number expression vector	J. Skerker
pKT25	pSU40 derivative with T25 fragment of CyaA	[293]
pKT25-zip	pKT25 derivative with leucine zipper of GCN4	[293]
pMR10	Kan^R low copy number and broad host range vector	[259]
pMR20	TetR low copy number and broad host range vector	[259]
pNPTS138	Kan^R, suicide vector with sacB gene and oriT	D. Alley
prcdA-egfp	pXGFP4 with xylX promoter replaced with last 300 bp of rcdA	[184]

pUT18C-zip	pUT18C derivative with leucine zipper of GCN4	[293]
pUT18C	pUC19 derivative with T18 fragment of CyaA. C-terminal fusions	[293]
pUT18	pUC19 derivative with T18 fragment of CyaA. N-terminal fusions	[293]
pX-clpX-egfp	pXGFP4 with *clpX*	[184]
pX-cpdRD51A-yfp	pMR31; *cpdRD51A* 3' fused to *eyfp* with *xylX* promoter	[269]

4. Outlook

In this work we characterised a network of enzymes involved in c-di-GMP turnover that regulates the developmental transition form free-living, motile swarmer cells into sessile stalked cell of the model organism *Caulobacter crescentus*. We identified the phosphodiesterase PdeA and the di-guanylate cyclase DgcB as two important antagonistic regulatory components in this process and analysed the already known DGC PleD in more detail. As the correct timing of intertwined developmental events is important for the swarmer-to-stalked cell transition, the activity of regulatory components has to be carefully controlled. Based on the findings presented in this work, it would be of interest to investigate the regulation of the activities of PdeA and DgcB more closely. A first question would be whether PdeA is restricted to the swarmer cell compartment in the predivisional cell, which could be addressed by investigating the spatial distribution of a degradable PdeA-GFP fusion during the cell cycle. The finding that PdeA localises to the ClpXP occupied developing stalked pole concurring its degradation raises the question for the role of this localisation. Has it a regulatory function, in analogy to the PopA-RcdA-CtrA pathway? Is there a PdeA specific polar receptor or is its localisation mediated by ClpXP itself? The former may be solved by the generation of delocalised PdeA mutants and the investigation of their degradation pattern. The latter could be addressed by the examination of PdeA localisation in a Δ*cpdR* mutant, in which ClpXP is not localised to the stalked pole [269]. Additionally it would be intriguing to examine whether there is a second layer of PdeA activity control despite the proteolytic regulation. Furthermore, it is of interest to unravel the mechanisms underlying the activation of the PdeA antagonist DgcB. Is DgcB a constitutive or regulated di-guanylate cyclase and how is its activity profile during the cell cycle? What is the nature of the regulatory mechanism; oligomerisation in dependence of c-di-GMP? Are further factors involved the regulation of DgcB and can we make use of the motile suppressors in the Δ*pdeA* mutant background to identify them?

Next to the activity control of the components in this regulatory network it is also of importance to define whether, which and how further regulatory components are involved in the control of the swarmer-to-stalked cell development via c-di-GMP. It was suggested that CC0091 may act as an additional antagonist to PleD (A. Levi unpublished). Furthermore, the performed epistasis experiments argue for an unknown DGC that, in addition to DgcB, feeds in the c-di-GMP pool accessible to PdeA and is involved in the motility control. Thus, one perspective is to address the possible role of the phosphodiesterase CC0091 and the potential

di-guanylate cyclase in the regulatory network presented here to build a more comprehensive model.

In a broader perspective, it is important to define the downstream targets that are controlled by the c-di-GMP regulated by the components of the network described here. Especially the finding that the known c-di-GMP effector proteins DgrA and DgrB are not involved in the motility regulation by PdeA raises the question for the nature of additional c-di-GMP receptors. Again, the answer to this question may reside in the motile suppressors in the Δ*pdeA* mutant background. Another important question would be, whether c-di-GMP effector proteins that regulate motility also affect attachment and vice versa or whether these processes are individually regulated. A candidate c-di-GMP binding protein effecting holdfast synthesis is the glycosyltransferase CC0095, which also has to be further investigated and eventually integrated into a global model of the developmental aspects of the swarmer-to-stalked cell transition.

A major question is how different c-di-GMP mediated signalling pathways are separated from each other. The finding that the paralysis of the flagellum upon deletion of *pdeA* is not mediated via DgrA/B could provide an insight into the underlying mechanisms, if it is possible to solve the presence, activity and spatial distribution of the individual components. In the same context it would also be interesting to further investigate the role of PleD localisation, as we have shown here that despite PleD delocalisation in a Δ*cc1064* mutant background, these cells do not show the known developmental phenotypes of a Δ*pleD* mutant. This unexpected phenomenon may be addressed by generating PleD mutants that retain activity without being localised. In contrast to the PleD activity in a Δ*cc1064* strain, their activity could be directly quantified in an *in vitro* assay and allow a better interpretation of their *in vivo* phenotypes.

Finally, another major, yet widely uncharacterised problem is the nature of upstream signals. What regulates DGC and PDE activity? Are environmental or cell cycle signals responsible for the timing of the swarmer-to-stalked cell transition; or both, and how are these signals transmitted?

Despite its importance to study the localisation of PleD, the further understanding of the pleitropic phenotypes of a Δ*cc1064* mutant is of interest, as CC1064 could be part of a general mechanism used by *C. crescentus* to react to changing environmental conditions. Most important would be to assign a direct molecular function to CC1064 and investigate how this molecule is able to regulate such diverse functions like motor protein assembly, surface attachment regulation and PleD localisation.

Taken together, the suggested follow-up experiments based on the work presented here would take us a step closer to understand the spatiotemporal dynamics of the network of c-di-GMP metabolizing and effector proteins, how this integrates external and internal signals and thereby allows bacteria to decide over their further lifestyle.

5. Bibliography

1. Kolter, R. and E.P. Greenberg, *Microbial sciences: the superficial life of microbes.* Nature, 2006. **441**(7091): p. 300-2.
2. Harshey, R.M., *Bacterial motility on a surface: many ways to a common goal.* Annu Rev Microbiol, 2003. **57**: p. 249-73.
3. Pratt, L.A. and R. Kolter, *Genetic analyses of bacterial biofilm formation.* Curr Opin Microbiol, 1999. **2**(6): p. 598-603.
4. Fux, C.A., et al., *Survival strategies of infectious biofilms.* Trends Microbiol, 2005. **13**(1): p. 34-40.
5. Kolter, R., *Surfacing views of biofilm biology.* Trends Microbiol, 2005. **13**(1): p. 1-2.
6. Stewart, P.S. and M.J. Franklin, *Physiological heterogeneity in biofilms.* Nat Rev Microbiol, 2008. **6**(3): p. 199-210.
7. Jenal, U., *Cyclic di-guanosine-monophosphate comes of age: a novel secondary messenger involved in modulating cell surface structures in bacteria?* Curr Opin Microbiol, 2004. **7**(2): p. 185-91.
8. Jenal, U. and J. Malone, *Mechanisms of cyclic-di-GMP signaling in bacteria.* Annu Rev Genet, 2006. **40**: p. 385-407.
9. Romling, U. and D. Amikam, *Cyclic di-GMP as a second messenger.* Curr Opin Microbiol, 2006. **9**(2): p. 218-28.
10. Tamayo, R., J.T. Pratt, and A. Camilli, *Roles of cyclic diguanylate in the regulation of bacterial pathogenesis.* Annu Rev Microbiol, 2007. **61**: p. 131-48.
11. Cotter, P.A. and S. Stibitz, *c-di-GMP-mediated regulation of virulence and biofilm formation.* Curr Opin Microbiol, 2007. **10**(1): p. 17-23.
12. Galperin, M.Y., A.N. Nikolskaya, and E.V. Koonin, *Novel domains of the prokaryotic two-component signal transduction systems.* FEMS Microbiol Lett, 2001. **203**(1): p. 11-21.
13. Tal, R., et al., *Three cdg operons control cellular turnover of cyclic di-GMP in Acetobacter xylinum: genetic organization and occurrence of conserved domains in isoenzymes.* J Bacteriol, 1998. **180**(17): p. 4416-25.
14. Paul, R., et al., *Cell cycle-dependent dynamic localization of a bacterial response regulator with a novel di-guanylate cyclase output domain.* Genes Dev, 2004. **18**(6): p. 715-27.
15. Ryjenkov, D.A., et al., *Cyclic diguanylate is a ubiquitous signaling molecule in bacteria: insights into biochemistry of the GGDEF protein domain.* J Bacteriol, 2005. **187**(5): p. 1792-8.
16. Chan, C., et al., *Structural basis of activity and allosteric control of diguanylate cyclase.* Proc Natl Acad Sci U S A, 2004. **101**(49): p. 17084-9.
17. Wassmann, P., et al., *Structure of BeF3- -modified response regulator PleD: implications for diguanylate cyclase activation, catalysis, and feedback inhibition.* Structure, 2007. **15**(8): p. 915-27.
18. Malone, J.G., et al., *The structure-function relationship of WspR, a Pseudomonas fluorescens response regulator with a GGDEF output domain.* Microbiology, 2007. **153**(Pt 4): p. 980-94.
19. Christen, B., et al., *Allosteric control of cyclic di-GMP signaling.* J Biol Chem, 2006. **281**(42): p. 32015-24.
20. Christen, M., et al., *Identification and characterization of a cyclic di-GMP-specific phosphodiesterase and its allosteric control by GTP.* J Biol Chem, 2005. **280**(35): p. 30829-37.

21. Schmidt, A.J., D.A. Ryjenkov, and M. Gomelsky, *The ubiquitous protein domain EAL is a cyclic diguanylate-specific phosphodiesterase: enzymatically active and inactive EAL domains.* J Bacteriol, 2005. **187**(14): p. 4774-81.
22. Tamayo, R., A.D. Tischler, and A. Camilli, *The EAL domain protein VieA is a cyclic diguanylate phosphodiesterase.* J Biol Chem, 2005. **280**(39): p. 33324-30.
23. Kazmierczak, B.I., M.B. Lebron, and T.S. Murray, *Analysis of FimX, a phosphodiesterase that governs twitching motility in Pseudomonas aeruginosa.* Mol Microbiol, 2006. **60**(4): p. 1026-43.
24. Chang, A.L., et al., *Phosphodiesterase A1, a regulator of cellulose synthesis in Acetobacter xylinum, is a heme-based sensor.* Biochemistry, 2001. **40**(12): p. 3420-6.
25. Ryan, R.P., et al., *Cell-cell signaling in Xanthomonas campestris involves an HD-GYP domain protein that functions in cyclic di-GMP turnover.* Proc Natl Acad Sci U S A, 2006. **103**(17): p. 6712-7.
26. Dürig, A., et al., *Second messenger mediated spatiotemporal control of protein degradation during the bacterial cell cycle.* Cell, 2008. **manuscript ready for submission**.
27. Amikam, D. and M.Y. Galperin, *PilZ domain is part of the bacterial c-di-GMP binding protein.* Bioinformatics, 2006. **22**(1): p. 3-6.
28. Pratt, J.T., et al., *PilZ domain proteins bind cyclic diguanylate and regulate diverse processes in Vibrio cholerae.* J Biol Chem, 2007. **282**(17): p. 12860-70.
29. Ko, M. and C. Park, *Two novel flagellar components and H-NS are involved in the motor function of Escherichia coli.* J Mol Biol, 2000. **303**(3): p. 371-82.
30. Huang, B., C.B. Whitchurch, and J.S. Mattick, *FimX, a multidomain protein connecting environmental signals to twitching motility in Pseudomonas aeruginosa.* J Bacteriol, 2003. **185**(24): p. 7068-76.
31. Ross, P.A., Y; Weinhouse, H; Michaeli, D; Weinberger-Ohana, P; et al., *Control of cellulose synthesis Acetobacter xylinum. A unique guanyl oligonucleotide is the immediate activator of the cellulose synthase.* Carbohydrate Research, 1986. **149**: p. 101–117.
32. Alm, R.A., et al., *Identification of a novel gene, pilZ, essential for type 4 fimbrial biogenesis in Pseudomonas aeruginosa.* J Bacteriol, 1996. **178**(1): p. 46-53.
33. Christen, M., et al., *DgrA is a member of a new family of cyclic diguanosine monophosphate receptors and controls flagellar motor function in Caulobacter crescentus.* Proc Natl Acad Sci U S A, 2007. **104**(10): p. 4112-7.
34. Ryjenkov, D.A., et al., *The PilZ domain is a receptor for the second messenger c-di-GMP: the PilZ domain protein YcgR controls motility in enterobacteria.* J Biol Chem, 2006. **281**(41): p. 30310-4.
35. Levi, A., *Genetic Dissection of Caulobacter crescentus Surface Colonization*, in *Biocenter*. 2007, University of Basel: Basel.
36. Merighi, M., et al., *The second messenger bis-(3'-5')-cyclic-GMP and its PilZ domain-containing receptor Alg44 are required for alginate biosynthesis in Pseudomonas aeruginosa.* Mol Microbiol, 2007. **65**(4): p. 876-95.
37. Schultz, J., et al., *SMART, a simple modular architecture research tool: identification of signaling domains.* Proc Natl Acad Sci U S A, 1998. **95**(11): p. 5857-64.
38. Guvener, Z.T. and C.S. Harwood, *Subcellular location characteristics of the Pseudomonas aeruginosa GGDEF protein, WspR, indicate that it produces cyclic-di-GMP in response to growth on surfaces.* Mol Microbiol, 2007. **66**(6): p. 1459-73.
39. Ross, P.A., Y; Weinhouse, H; Michaeli, D; Weinberger-Ohana, P; et al., *An unusual guanyl oligonucleotide regulates cellulose synthesis in Acetobacter xylinum.* FEBS Lett., 1985. **186**: p. 191–196.

40. Lee, S.H., et al., *Nucleotide sequence and spatiotemporal expression of the Vibrio cholerae vieSAB genes during infection.* J Bacteriol, 1998. **180**(9): p. 2298-305.
41. Perry, R.D., M.L. Pendrak, and P. Schuetze, *Identification and cloning of a hemin storage locus involved in the pigmentation phenotype of Yersinia pestis.* J Bacteriol, 1990. **172**(10): p. 5929-37.
42. Perry, R.D., et al., *Temperature regulation of the hemin storage (Hms+) phenotype of Yersinia pestis is posttranscriptional.* J Bacteriol, 2004. **186**(6): p. 1638-47.
43. Tischler, A.D. and A. Camilli, *Cyclic diguanylate regulates Vibrio cholerae virulence gene expression.* Infect Immun, 2005. **73**(9): p. 5873-82.
44. Hisert, K.B., et al., *A glutamate-alanine-leucine (EAL) domain protein of Salmonella controls bacterial survival in mice, antioxidant defence and killing of macrophages: role of cyclic diGMP.* Mol Microbiol, 2005. **56**(5): p. 1234-45.
45. Kulasakara, H., et al., *Analysis of Pseudomonas aeruginosa diguanylate cyclases and phosphodiesterases reveals a role for bis-(3'-5')-cyclic-GMP in virulence.* Proc Natl Acad Sci U S A, 2006. **103**(8): p. 2839-44.
46. Kader, A., et al., *Hierarchical involvement of various GGDEF domain proteins in rdar morphotype development of Salmonella enterica serovar Typhimurium.* Mol Microbiol, 2006. **60**(3): p. 602-16.
47. Levi, A. and U. Jenal, *Holdfast formation in motile swarmer cells optimizes surface attachment during Caulobacter crescentus development.* J Bacteriol, 2006. **188**(14): p. 5315-8.
48. Ross, P., et al., *The cyclic diguanylic acid regulatory system of cellulose synthesis in Acetobacter xylinum. Chemical synthesis and biological activity of cyclic nucleotide dimer, trimer, and phosphothioate derivatives.* J Biol Chem, 1990. **265**(31): p. 18933-43.
49. Weber, H., et al., *Cyclic-di-GMP-mediated signalling within the sigma network of Escherichia coli.* Mol Microbiol, 2006. **62**(4): p. 1014-34.
50. Boles, B.R. and L.L. McCarter, *Vibrio parahaemolyticus scrABC, a novel operon affecting swarming and capsular polysaccharide regulation.* J Bacteriol, 2002. **184**(21): p. 5946-54.
51. Costerton, J.W., et al., *Microbial biofilms.* Annu Rev Microbiol, 1995. **49**: p. 711-45.
52. Potera, C., *Biofilms invade microbiology.* Science, 1996. **273**(5283): p. 1795-7.
53. Mah, T.F., et al., *A genetic basis for Pseudomonas aeruginosa biofilm antibiotic resistance.* Nature, 2003. **426**(6964): p. 306-10.
54. Matz, C., et al., *Biofilm formation and phenotypic variation enhance predation-driven persistence of Vibrio cholerae.* Proc Natl Acad Sci U S A, 2005. **102**(46): p. 16819-24.
55. Weitere, M., et al., *Grazing resistance of Pseudomonas aeruginosa biofilms depends on type of protective mechanism, developmental stage and protozoan feeding mode.* Environ Microbiol, 2005. **7**(10): p. 1593-601.
56. Stoodley, P., et al., *Biofilms as complex differentiated communities.* Annu Rev Microbiol, 2002. **56**: p. 187-209.
57. O'Toole, G., H.B. Kaplan, and R. Kolter, *Biofilm formation as microbial development.* Annu Rev Microbiol, 2000. **54**: p. 49-79.
58. Watnick, P. and R. Kolter, *Biofilm, city of microbes.* J Bacteriol, 2000. **182**(10): p. 2675-9.
59. Donlan, R.M., *Biofilms: microbial life on surfaces.* Emerg Infect Dis, 2002. **8**(9): p. 881-90.
60. Sutherland, I., *Biofilm exopolysaccharides: a strong and sticky framework.* Microbiology, 2001. **147**(Pt 1): p. 3-9.

61. Aldridge, P., et al., *Role of the GGDEF regulator PleD in polar development of Caulobacter crescentus.* Mol Microbiol, 2003. **47**(6): p. 1695-708.
62. Bobrov, A.G., O. Kirillina, and R.D. Perry, *The phosphodiesterase activity of the HmsP EAL domain is required for negative regulation of biofilm formation in Yersinia pestis.* FEMS Microbiol Lett, 2005. **247**(2): p. 123-30.
63. Bomchil, N., P. Watnick, and R. Kolter, *Identification and characterization of a Vibrio cholerae gene, mbaA, involved in maintenance of biofilm architecture.* J Bacteriol, 2003. **185**(4): p. 1384-90.
64. Choy, W.K., et al., *MorA defines a new class of regulators affecting flagellar development and biofilm formation in diverse Pseudomonas species.* J Bacteriol, 2004. **186**(21): p. 7221-8.
65. Drenkard, E. and F.M. Ausubel, *Pseudomonas biofilm formation and antibiotic resistance are linked to phenotypic variation.* Nature, 2002. **416**(6882): p. 740-3.
66. Enos-Berlage, J.L., et al., *Genetic determinants of biofilm development of opaque and translucent Vibrio parahaemolyticus.* Mol Microbiol, 2005. **55**(4): p. 1160-82.
67. Garcia, B., et al., *Role of the GGDEF protein family in Salmonella cellulose biosynthesis and biofilm formation.* Mol Microbiol, 2004. **54**(1): p. 264-77.
68. Goymer, P., et al., *Adaptive divergence in experimental populations of Pseudomonas fluorescens. II. Role of the GGDEF regulator WspR in evolution and development of the wrinkly spreader phenotype.* Genetics, 2006. **173**(2): p. 515-26.
69. Guvener, Z.T. and L.L. McCarter, *Multiple regulators control capsular polysaccharide production in Vibrio parahaemolyticus.* J Bacteriol, 2003. **185**(18): p. 5431-41.
70. Kirillina, O., et al., *HmsP, a putative phosphodiesterase, and HmsT, a putative diguanylate cyclase, control Hms-dependent biofilm formation in Yersinia pestis.* Mol Microbiol, 2004. **54**(1): p. 75-88.
71. Simm, R., et al., *GGDEF and EAL domains inversely regulate cyclic di-GMP levels and transition from sessility to motility.* Mol Microbiol, 2004. **53**(4): p. 1123-34.
72. Tischler, A.D. and A. Camilli, *Cyclic diguanylate (c-di-GMP) regulates Vibrio cholerae biofilm formation.* Mol Microbiol, 2004. **53**(3): p. 857-69.
73. Gjermansen, M., et al., *Characterization of starvation-induced dispersion in Pseudomonas putida biofilms.* Environ Microbiol, 2005. **7**(6): p. 894-906.
74. Ude, S., et al., *Biofilm formation and cellulose expression among diverse environmental Pseudomonas isolates.* Environ Microbiol, 2006. **8**(11): p. 1997-2011.
75. Spiers, A.J., et al., *Adaptive divergence in experimental populations of Pseudomonas fluorescens. I. Genetic and phenotypic bases of wrinkly spreader fitness.* Genetics, 2002. **161**(1): p. 33-46.
76. Spiers, A.J., et al., *Biofilm formation at the air-liquid interface by the Pseudomonas fluorescens SBW25 wrinkly spreader requires an acetylated form of cellulose.* Mol Microbiol, 2003. **50**(1): p. 15-27.
77. Simm, R., et al., *Phenotypic convergence mediated by GGDEF-domain-containing proteins.* J Bacteriol, 2005. **187**(19): p. 6816-23.
78. Johnson, M.R., et al., *Population density-dependent regulation of exopolysaccharide formation in the hyperthermophilic bacterium Thermotoga maritima.* Mol Microbiol, 2005. **55**(3): p. 664-74.
79. Rashid, M.H., et al., *Identification of genes involved in the switch between the smooth and rugose phenotypes of Vibrio cholerae.* FEMS Microbiol Lett, 2003. **227**(1): p. 113-9.
80. Kovacikova, G., W. Lin, and K. Skorupski, *Dual regulation of genes involved in acetoin biosynthesis and motility/biofilm formation by the virulence activator AphA*

and the acetate-responsive LysR-type regulator AlsR in Vibrio cholerae. Mol Microbiol, 2005. **57**(2): p. 420-33.
81. Beyhan, S., et al., *Transcriptome and phenotypic responses of Vibrio cholerae to increased cyclic di-GMP level.* J Bacteriol, 2006. **188**(10): p. 3600-13.
82. Casper-Lindley, C. and F.H. Yildiz, *VpsT is a transcriptional regulator required for expression of vps biosynthesis genes and the development of rugose colonial morphology in Vibrio cholerae O1 El Tor.* J Bacteriol, 2004. **186**(5): p. 1574-8.
83. Yildiz, F.H., N.A. Dolganov, and G.K. Schoolnik, *VpsR, a Member of the Response Regulators of the Two-Component Regulatory Systems, Is Required for Expression of vps Biosynthesis Genes and EPS(ETr)-Associated Phenotypes in Vibrio cholerae O1 El Tor.* J Bacteriol, 2001. **183**(5): p. 1716-26.
84. Bantinaki, E., et al., *Adaptive divergence in experimental populations of Pseudomonas fluorescens. III. Mutational origins of wrinkly spreader diversity.* Genetics, 2007. **176**(1): p. 441-53.
85. D'Argenio, D.A., et al., *Autolysis and autoaggregation in Pseudomonas aeruginosa colony morphology mutants.* J Bacteriol, 2002. **184**(23): p. 6481-9.
86. Hickman, J.W., D.F. Tifrea, and C.S. Harwood, *A chemosensory system that regulates biofilm formation through modulation of cyclic diguanylate levels.* Proc Natl Acad Sci U S A, 2005. **102**(40): p. 14422-7.
87. Friedman, L. and R. Kolter, *Two genetic loci produce distinct carbohydrate-rich structural components of the Pseudomonas aeruginosa biofilm matrix.* J Bacteriol, 2004. **186**(14): p. 4457-65.
88. Jackson, K.D., et al., *Identification of psl, a locus encoding a potential exopolysaccharide that is essential for Pseudomonas aeruginosa PAO1 biofilm formation.* J Bacteriol, 2004. **186**(14): p. 4466-75.
89. Furukawa, S., S.L. Kuchma, and G.A. O'Toole, *Keeping their options open: acute versus persistent infections.* J Bacteriol, 2006. **188**(4): p. 1211-7.
90. Lee, V.T., et al., *A cyclic-di-GMP receptor required for bacterial exopolysaccharide production.* Mol Microbiol, 2007. **65**(6): p. 1474-84.
91. Merz, A.J., M. So, and M.P. Sheetz, *Pilus retraction powers bacterial twitching motility.* Nature, 2000. **407**(6800): p. 98-102.
92. Mattick, J.S., *Type IV Pili and Twitching Motility.* Annu. Rev. Microbiol., 2002. **56**: p. 289–314.
93. McCarter, L., *The multiple identities of Vibrio parahaemolyticus.* J Mol Microbiol Biotechnol, 1999. **1**(1): p. 51-7.
94. Wolfe, A.J. and K.L. Visick, *Get the message out: cyclic-Di-GMP regulates multiple levels of flagellum-based motility.* J Bacteriol, 2008. **190**(2): p. 463-75.
95. Merino, S., J.G. Shaw, and J.M. Tomas, *Bacterial lateral flagella: an inducible flagella system.* FEMS Microbiol Lett, 2006. **263**(2): p. 127-35.
96. Kim, Y.K. and L.L. McCarter, *ScrG, a GGDEF-EAL protein, participates in regulating swarming and sticking in Vibrio parahaemolyticus.* J Bacteriol, 2007. **189**(11): p. 4094-107.
97. Mendez-Ortiz, M.M., et al., *Genome-wide transcriptional profile of Escherichia coli in response to high levels of the second messenger 3',5'-cyclic diguanylic acid.* J Biol Chem, 2006. **281**(12): p. 8090-9.
98. Frye, J., et al., *Identification of new flagellar genes of Salmonella enterica serovar Typhimurium.* J Bacteriol, 2006. **188**(6): p. 2233-43.
99. Poindexter, J.S. and J.G. Hagenzieker, *Constriction and septation during cell division in caulobacters.* Can J Microbiol, 1981. **27**(7): p. 704-19.
100. Poindexter, J.S., *Biological Properties and Classification of the Caulobacter Group.* Bacteriol Rev, 1964. **28**: p. 231-95.

101. Jacobs-Wagner, C., *Regulatory proteins with a sense of direction: cell cycle signalling network in Caulobacter.* Mol Microbiol, 2004. **51**(1): p. 7-13.
102. Degnen, S.T. and A. Newton, *Dependence of cell division on the completion of chromosome replication in Caulobacter.* J Bacteriol, 1972. **110**(3): p. 852-6.
103. Marczynski, G.T., A. Dingwall, and L. Shapiro, *Plasmid and chromosomal DNA replication and partitioning during the Caulobacter crescentus cell cycle.* J Mol Biol, 1990. **212**(4): p. 709-22.
104. Brun, Y.V. and R. Janakiraman, *The dimorphic life cycle of Caulobacter and stalked bacteria.*, in *Prokaryotic development*, Y.V.a.S. Brun, L.J., Editor. 2000, ASM Press: Washington, DC. p. 297-317.
105. Skerker, J.M. and L. Shapiro, *Identification and cell cycle control of a novel pilus system in Caulobacter crescentus.* Embo J, 2000. **19**(13): p. 3223-34.
106. Quon, K.C., et al., *Negative control of bacterial DNA replication by a cell cycle regulatory protein that binds at the chromosome origin.* Proc Natl Acad Sci U S A, 1998. **95**(1): p. 120-5.
107. Laub, M.T., et al., *Global analysis of the genetic network controlling a bacterial cell cycle.* Science, 2000. **290**(5499): p. 2144-8.
108. Jenal, U. and T. Fuchs, *An essential protease involved in bacterial cell-cycle control.* Embo J, 1998. **17**(19): p. 5658-69.
109. Domian, I.J., K.C. Quon, and L. Shapiro, *Cell type-specific phosphorylation and proteolysis of a transcriptional regulator controls the G1-to-S transition in a bacterial cell cycle.* Cell, 1997. **90**(3): p. 415-24.
110. Ryan, K.R., E.M. Judd, and L. Shapiro, *The CtrA response regulator essential for Caulobacter crescentus cell-cycle progression requires a bipartite degradation signal for temporally controlled proteolysis.* J Mol Biol, 2002. **324**(3): p. 443-55.
111. Ryan, K.R., S. Huntwork, and L. Shapiro, *Recruitment of a cytoplasmic response regulator to the cell pole is linked to its cell cycle-regulated proteolysis.* Proc Natl Acad Sci U S A, 2004. **101**(19): p. 7415-20.
112. Alley, M.R., J.R. Maddock, and L. Shapiro, *Polar localization of a bacterial chemoreceptor.* Genes Dev, 1992. **6**(5): p. 825-36.
113. Merker, R.I. and J. Smit, *Characterization of the Adhesive Holdfast of Marine and Freshwater Caulobacters.* Appl Environ Microbiol, 1988. **54**(8): p. 2078-2085.
114. Evinger, M. and N. Agabian, *Envelope-associated nucleoid from Caulobacter crescentus stalked and swarmer cells.* J Bacteriol, 1977. **132**(1): p. 294-301.
115. Stallmeyer, M.J., et al., *Image reconstruction of the flagellar basal body of Caulobacter crescentus.* J Mol Biol, 1989. **205**(3): p. 511-8.
116. Trachtenberg, S. and D.J. DeRosier, *Three-dimensional reconstruction of the flagellar filament of Caulobacter crescentus. A flagellin lacking the outer domain and its amino acid sequence lacking an internal segment.* J Mol Biol, 1988. **202**(4): p. 787-808.
117. Wagenknecht, T., et al., *Three-dimensional reconstruction of the flagellar hook from Caulobacter crescentus.* J Mol Biol, 1981. **151**(3): p. 439-65.
118. Kojima, S. and D.F. Blair, *The bacterial flagellar motor: structure and function of a complex molecular machine.* Int Rev Cytol, 2004. **233**: p. 93-134.
119. Lagenaur, C. and N. Agabian, *Caulobacter flagellins.* J Bacteriol, 1977. **132**(2): p. 731-3.
120. Macnab, R.M., *Genetics and biogenesis of bacterial flagella.* Annu Rev Genet, 1992. **26**: p. 131-58.
121. Aldridge, P. and K.T. Hughes, *Regulation of flagellar assembly.* Current Opinion in Microbiology, 2002. **5**: p. 160–65.

122. Newton, A., et al., *Genetic switching in the flagellar gene hierarchy of Caulobacter requires negative as well as positive regulation of transcription.* Proc Natl Acad Sci U S A, 1989. **86**(17): p. 6651-5.
123. Ramakrishnan, G., J.L. Zhao, and A. Newton, *Multiple structural proteins are required for both transcriptional activation and negative autoregulation of Caulobacter crescentus flagellar genes.* J Bacteriol, 1994. **176**(24): p. 7587-600.
124. Komeda, Y., *Transcriptional control of flagellar genes in Escherichia coli K-12.* J Bacteriol, 1986. **168**(3): p. 1315-8.
125. Kutsukake, K., Y. Ohya, and T. Iino, *Transcriptional analysis of the flagellar regulon of Salmonella typhimurium.* J Bacteriol, 1990. **172**(2): p. 741-7.
126. Wu, J. and A. Newton, *Regulation of the Caulobacter flagellar gene hierarchy; not just for motility.* Mol Microbiol, 1997. **24**(2): p. 233-9.
127. Kalir, S., et al., *Ordering genes in a flagella pathway by analysis of expression kinetics from living bacteria.* Science, 2001. **292**(5524): p. 2080-3.
128. Quon, K.C., G.T. Marczynski, and L. Shapiro, *Cell cycle control by an essential bacterial two-component signal transduction protein.* Cell, 1996. **84**(1): p. 83-93.
129. Reisenauer, A., K. Quon, and L. Shapiro, *The CtrA response regulator mediates temporal control of gene expression during the Caulobacter cell cycle.* J Bacteriol, 1999. **181**(8): p. 2430-9.
130. Gober, J.W. and M.V. Marques, *Regulation of cellular differentiation in Caulobacter crescentus.* Microbiol Rev, 1995. **59**(1): p. 31-47.
131. Ramakrishnan, G. and A. Newton, *FlbD of Caulobacter crescentus is a homologue of the NtrC (NRI) protein and activates sigma 54-dependent flagellar gene promoters.* Proc Natl Acad Sci U S A, 1990. **87**(6): p. 2369-73.
132. Wingrove, J.A., E.K. Mangan, and J.W. Gober, *Spatial and temporal phosphorylation of a transcriptional activator regulates pole-specific gene expression in Caulobacter.* Genes Dev, 1993. **7**(10): p. 1979-92.
133. Brun, Y.V. and L. Shapiro, *A temporally controlled sigma-factor is required for polar morphogenesis and normal cell division in Caulobacter.* Genes Dev, 1992. **6**(12A): p. 2395-408.
134. Anderson, D.K., et al., *Regulation of the Caulobacter crescentus rpoN gene and function of the purified sigma 54 in flagellar gene transcription.* Mol Gen Genet, 1995. **246**(6): p. 697-706.
135. Xu, H., A. Dingwall, and L. Shapiro, *Negative transcriptional regulation in the Caulobacter flagellar hierarchy.* Proc Natl Acad Sci U S A, 1989. **86**(17): p. 6656-60.
136. Minnich, S.A. and A. Newton, *Promoter mapping and cell cycle regulation of flagellin gene transcription in Caulobacter crescentus.* Proc Natl Acad Sci U S A, 1987. **84**(5): p. 1142-6.
137. Mangan, E.K., et al., *FlbT couples flagellum assembly to gene expression in Caulobacter crescentus.* J Bacteriol, 1999. **181**(19): p. 6160-70.
138. Anderson, P.E. and J.W. Gober, *FlbT, the post-transcriptional regulator of flagellin synthesis in Caulobacter crescentus, interacts with the 5' untranslated region of flagellin mRNA.* Mol Microbiol, 2000. **38**(1): p. 41-52.
139. Muir, R.E. and J.W. Gober, *Mutations in FlbD that relieve the dependency on flagellum assembly alter the temporal and spatial pattern of developmental transcription in Caulobacter crescentus.* Molecular Microbiology, 2002. **43**(3): p. 597-615.
140. Biondi, E.G., et al., *Regulation of the bacterial cell cycle by an integrated genetic circuit.* Nature, 2006. **444**(7121): p. 899-904.
141. Laub, M.T., et al., *Genes directly controlled by CtrA, a master regulator of the Caulobacter cell cycle.* Proc Natl Acad Sci U S A, 2002. **99**(7): p. 4632-7.

142. Gober, J.W., et al., *Identification of cis and trans-elements involved in the timed control of a Caulobacter flagellar gene.* J Mol Biol, 1991. **217**(2): p. 247-57.
143. Gober, J.W. and L. Shapiro, *A developmentally regulated Caulobacter flagellar promoter is activated by 3' enhancer and IHF binding elements.* Mol Biol Cell, 1992. **3**(8): p. 913-26.
144. Wingrove, J.A. and J.W. Gober, *Identification of an asymmetrically localized sensor histidine kinase responsible for temporally and spatially regulated transcription.* Science, 1996. **274**(5287): p. 597-601.
145. Muir, R.E. and J.W. Gober, *Regulation of late flagellar gene transcription and cell division by flagellum assembly in Caulobacter crescentus.* Mol Microbiol, 2001. **41**(1): p. 117-30.
146. Ueno, T., K. Oosawa, and S. Aizawa, *M ring, S ring and proximal rod of the flagellar basal body of Salmonella typhimurium are composed of subunits of a single protein, FliF.* J Mol Biol, 1992. **227**(3): p. 672-7.
147. Magariyama, Y., et al., *Very fast flagellar rotation.* Nature, 1994. **371**(6500): p. 752.
148. Blair, D.F. and H.C. Berg, *The MotA protein of E. coli is a proton-conducting component of the flagellar motor.* Cell, 1990. **60**(3): p. 439-49.
149. Blair, D.F., D.Y. Kim, and H.C. Berg, *Mutant MotB proteins in Escherichia coli.* J Bacteriol, 1991. **173**(13): p. 4049-55.
150. Blair, D.F. and H.C. Berg, *Mutations in the MotA protein of Escherichia coli reveal domains critical for proton conduction.* J Mol Biol, 1991. **221**(4): p. 1433-42.
151. Blair, D.F., *Flagellar movement driven by proton translocation.* FEBS Lett, 2003. **545**(1): p. 86-95.
152. Stolz, B. and H.C. Berg, *Evidence for interactions between MotA and MotB, torque-generating elements of the flagellar motor of Escherichia coli.* J Bacteriol, 1991. **173**(21): p. 7033-7.
153. Wilson, M.L. and R.M. Macnab, *Co-overproduction and localization of the Escherichia coli motility proteins motA and motB.* J Bacteriol, 1990. **172**(7): p. 3932-9.
154. Braun, T.F. and D.F. Blair, *Targeted disulfide cross-linking of the MotB protein of Escherichia coli: evidence for two H(+) channels in the stator Complex.* Biochemistry, 2001. **40**(43): p. 13051-9.
155. Sato, K. and M. Homma, *Functional reconstitution of the Na(+)-driven polar flagellar motor component of Vibrio alginolyticus.* J Biol Chem, 2000. **275**(8): p. 5718-22.
156. Zhou, J., et al., *Function of protonatable residues in the flagellar motor of Escherichia coli: a critical role for Asp 32 of MotB.* J Bacteriol, 1998. **180**(10): p. 2729-35.
157. Zhou, J., S.A. Lloyd, and D.F. Blair, *Electrostatic interactions between rotor and stator in the bacterial flagellar motor.* Proc Natl Acad Sci U S A, 1998. **95**(11): p. 6436-41.
158. Chun, S.Y. and J.S. Parkinson, *Bacterial motility: membrane topology of the Escherichia coli MotB protein.* Science, 1988. **239**(4837): p. 276-8.
159. De Mot, R. and J. Vanderleyden, *The C-terminal sequence conservation between OmpA-related outer membrane proteins and MotB suggests a common function in both gram-positive and gram-negative bacteria, possibly in the interaction of these domains with peptidoglycan.* Mol Microbiol, 1994. **12**(2): p. 333-4.
160. Garza, A.G., et al., *Mutations in motB suppressible by changes in stator or rotor components of the bacterial flagellar motor.* J Mol Biol, 1996. **258**(2): p. 270-85.
161. Khan, I.H., T.S. Reese, and S. Khan, *The cytoplasmic component of the bacterial flagellar motor.* Proc Natl Acad Sci U S A, 1992. **89**(13): p. 5956-60.

162. Muramoto, K. and R.M. Macnab, *Deletion analysis of MotA and MotB, components of the force-generating unit in the flagellar motor of Salmonella.* Mol Microbiol, 1998. **29**(5): p. 1191-202.
163. Blair, D.F. and H.C. Berg, *Restoration of torque in defective flagellar motors.* Science, 1988. **242**(4886): p. 1678-81.
164. Reid, S.W., et al., *The maximum number of torque-generating units in the flagellar motor of Escherichia coli is at least 11.* Proc Natl Acad Sci U S A, 2006. **103**(21): p. 8066-71.
165. Block, S.M. and H.C. Berg, *Successive incorporation of force-generating units in the bacterial rotary motor.* Nature, 1984. **309**(5967): p. 470-2.
166. Yuan, J. and H.C. Berg, *Resurrection of the flagellar rotary motor near zero load.* Proc Natl Acad Sci U S A, 2008. **105**(4): p. 1182-5.
167. Dean, G.E., et al., *Gene sequence and predicted amino acid sequence of the motA protein, a membrane-associated protein required for flagellar rotation in Escherichia coli.* J Bacteriol, 1984. **159**(3): p. 991-9.
168. Enomoto, M., *Genetic Studies of Paralyzed Mutants in Salmonella. II. Mapping of Three mot Loci by Linkage Analysis.* Genetics, 1966. **54**(5): p. 1069-1076.
169. Enomoto, M., *Genetic studies of paralyzed mutant in Salmonella. I. Genetic fine structure of the mot loci in Salmonella typhimurium.* Genetics, 1966. **54**(3): p. 715-26.
170. Aldridge, P. and U. Jenal, *Cell cycle-dependent degradation of a flagellar motor component requires a novel-type response regulator.* Mol Microbiol, 1999. **32**(2): p. 379-91.
171. Sommer, J.M. and A. Newton, *Turning off flagellum rotation requires the pleiotropic gene pleD: pleA, pleC, and pleD define two morphogenic pathways in Caulobacter crescentus.* J Bacteriol, 1989. **171**(1): p. 392-401.
172. Sommer, J.M. and A. Newton, *Pseudoreversion analysis indicates a direct role of cell division genes in polar morphogenesis and differentiation in Caulobacter crescentus.* Genetics, 1991. **129**(3): p. 623-30.
173. Skerker, J.M., et al., *Two-component signal transduction pathways regulating growth and cell cycle progression in a bacterium: a system-level analysis.* PLoS Biol, 2005. **3**(10): p. e334.
174. Hecht, G.B. and A. Newton, *Identification of a novel response regulator required for the swarmer-to-stalked-cell transition in Caulobacter crescentus.* J Bacteriol, 1995. **177**(21): p. 6223-9.
175. Wheeler, R.T. and L. Shapiro, *Differential localization of two histidine kinases controlling bacterial cell differentiation.* Mol Cell, 1999. **4**(5): p. 683-94.
176. Matroule, J.Y., et al., *Cytokinesis monitoring during development; rapid pole-to-pole shuttling of a signaling protein by localized kinase and phosphatase in Caulobacter.* Cell, 2004. **118**(5): p. 579-90.
177. Jacobs, C., D. Hung, and L. Shapiro, *Dynamic localization of a cytoplasmic signal transduction response regulator controls morphogenesis during the Caulobacter cell cycle.* Proc Natl Acad Sci U S A, 2001. **98**(7): p. 4095-100.
178. Grunenfelder, B., et al., *Identification of the protease and the turnover signal responsible for cell cycle-dependent degradation of the Caulobacter FliF motor protein.* J Bacteriol, 2004. **186**(15): p. 4960-71.
179. Jenal, U. and L. Shapiro, *Cell cycle-controlled proteolysis of a flagellar motor protein that is asymmetrically distributed in the Caulobacter predivisional cell.* Embo J, 1996. **15**(10): p. 2393-406.
180. Burton, G.J., G.B. Hecht, and A. Newton, *Roles of the histidine protein kinase pleC in Caulobacter crescentus motility and chemotaxis.* J Bacteriol, 1997. **179**(18): p. 5849-53.

181. Zogaj, X., et al., *The multicellular morphotypes of Salmonella typhimurium and Escherichia coli produce cellulose as the second component of the extracellular matrix.* Mol Microbiol, 2001. **39**(6): p. 1452-63.
182. Zogaj, X., et al., *Production of cellulose and curli fimbriae by members of the family Enterobacteriaceae isolated from the human gastrointestinal tract.* Infect Immun, 2003. **71**(7): p. 4151-8.
183. Huitema, E., et al., *Bacterial birth scar proteins mark future flagellum assembly site.* Cell, 2006. **124**(5): p. 1025-37.
184. McGrath, P.T., et al., *A dynamically localized protease complex and a polar specificity factor control a cell cycle master regulator.* Cell, 2006. **124**(3): p. 535-47.
185. Dürig, A., *Second messenger mediated spatiotemporal control of cell cycle and development* in *Biocenter*. 2008, University of Basel: Basel.
186. Paul, R., et al., *Activation of the diguanylate cyclase PleD by phosphorylation-mediated dimerization.* J Biol Chem, 2007. **282**(40): p. 29170-7.
187. Paul, R., et al., *Allosteric Regulation of Histidine Kinases by Their Cognate Response Regulator Determines Cell Fate.* Cell, 2008. **in press**.
188. Jenal, U., J. White, and L. Shapiro, *Caulobacter flagellar function, but not assembly, requires FliL, a non-polarly localized membrane protein present in all cell types.* J Mol Biol, 1994. **243**(2): p. 227-44.
189. Gottesman, S., et al., *ClpX, an alternative subunit for the ATP-dependent Clp protease of Escherichia coli. Sequence and in vivo activities.* J Biol Chem, 1993. **268**(30): p. 22618-26.
190. Potocka, I., et al., *Degradation of a Caulobacter soluble cytoplasmic chemoreceptor is ClpX dependent.* J Bacteriol, 2002. **184**(23): p. 6635-41.
191. Gorbatyuk, B. and G.T. Marczynski, *Regulated degradation of chromosome replication proteins DnaA and CtrA in Caulobacter crescentus.* Mol Microbiol, 2005. **55**(4): p. 1233-45.
192. Bodenmiller, D., E. Toh, and Y.V. Brun, *Development of surface adhesion in Caulobacter crescentus.* J Bacteriol, 2004. **186**(5): p. 1438-47.
193. Christen, M., *Mechanisms of Cyclic-di-GMP Signaling*, in *Biocenter*. 2007, University of Basel: Basel.
194. Wiederkehr, I., *Methodology for the analysis of in vivo levels of cyclic-di-GMP in Caulobacter crescentus*, in *Biocenter*. 2007, University of Basel: Basel.
195. Cohen, C., Parry, D. A. D. , *Alpha-helical coiled coils - a widespread motif in proteins.* Trends Biochem. Sci., 1986. **11**: p. 245-48.
196. Ely, B., *Genetics of Caulobacter crescentus.* Methods Enzymol, 1991. **204**: p. 372-84.
197. Sambrook, J., E.F. Fritsch, and T. Maniatis, *Molecular cloning. A laboratory manual.* 1989, New York: Cold Spring Harbor Laboratory Press.
198. Abramoff, M.D., Magelhaes, P.J., Ram, S.J., *Image Processing with ImageJ.* Biophotonics International, 2004. **11**(7): p. 36-42.
199. O'Toole, G.A. and R. Kolter, *Initiation of biofilm formation in Pseudomonas fluorescens WCS365 proceeds via multiple, convergent signalling pathways: a genetic analysis.* Mol Microbiol, 1998. **28**(3): p. 449-61.
200. West, L., D. Yang, and C. Stephens, *Use of the Caulobacter crescentus genome sequence to develop a method for systematic genetic mapping.* J Bacteriol, 2002. **184**(8): p. 2155-66.
201. Chenna, R., et al., *Multiple sequence alignment with the Clustal series of programs.* Nucleic Acids Res, 2003. **31**(13): p. 3497-500.
202. Fischer, B., et al., *The FtsH protease is involved in development, stress response and heat shock control in Caulobacter crescentus.* Mol Microbiol, 2002. **44**(2): p. 461-78.

203. Wright, R., et al., *Caulobacter Lon protease has a critical role in cell-cycle control of DNA methylation.* Genes Dev, 1996. **10**(12): p. 1532-42.
204. Hanahan, D., *Studies on transformation of Escherichia coli with plasmids.* J Mol Biol, 1983. **166**(4): p. 557-80.
205. Simon, R., U. Prieffer, and A. Puhler, *A broad host range mobilization system for in vivo genetic engineering: Transposon mutagenesis in gram negative bacteria.* Biotechnology, 1983. **1**: p. 784-90.
206. Kovach, M.E., et al., *Four new derivatives of the broad-host-range cloning vector pBBR1MCS, carrying different antibiotic-resistance cassettes.* Gene, 1995. **166**(1): p. 175-6.
207. Larsen, S.H., et al., *Change in direction of flagellar rotation is the basis of the chemotactic response in Escherichia coli.* Nature, 1974. **249**(452): p. 74-7.
208. Manson, M.D., et al., *A protonmotive force drives bacterial flagella.* Proc Natl Acad Sci U S A, 1977. **74**(7): p. 3060-4.
209. Brun, Y.V., G. Marczynski, and L. Shapiro, *The expression of asymmetry during Caulobacter cell differentiation.* Annu Rev Biochem, 1994. **63**: p. 419-50.
210. Ridgway, H.G., M. Silverman, and M.I. Simon, *Localization of proteins controlling motility and chemotaxis in Escherichia coli.* J Bacteriol, 1977. **132**(2): p. 657-65.
211. Khan, S., M. Dapice, and T.S. Reese, *Effects of mot gene expression on the structure of the flagellar motor.* J Mol Biol, 1988. **202**(3): p. 575-84.
212. Zhou, J., R.T. Fazzio, and D.F. Blair, *Membrane topology of the MotA protein of Escherichia coli.* J Mol Biol, 1995. **251**(2): p. 237-42.
213. Zhou, J. and D.F. Blair, *Residues of the cytoplasmic domain of MotA essential for torque generation in the bacterial flagellar motor.* J Mol Biol, 1997. **273**(2): p. 428-39.
214. Garza, A.G., et al., *Extragenic suppression of motA missense mutations of Escherichia coli.* J Bacteriol, 1996. **178**(21): p. 6116-22.
215. Garza, A.G., et al., *Motility protein interactions in the bacterial flagellar motor.* Proc Natl Acad Sci U S A, 1995. **92**(6): p. 1970-4.
216. Sharp, L.L., J. Zhou, and D.F. Blair, *Features of MotA proton channel structure revealed by tryptophan-scanning mutagenesis.* Proc Natl Acad Sci U S A, 1995. **92**(17): p. 7946-50.
217. Sharp, L.L., J. Zhou, and D.F. Blair, *Tryptophan-scanning mutagenesis of MotB, an integral membrane protein essential for flagellar rotation in Escherichia coli.* Biochemistry, 1995. **34**(28): p. 9166-71.
218. Leake, M.C., et al., *Stoichiometry and turnover in single, functioning membrane protein complexes.* Nature, 2006. **443**(7109): p. 355-8.
219. Van Way, S.M., et al., *Mot protein assembly into the bacterial flagellum: a model based on mutational analysis of the motB gene.* J Mol Biol, 2000. **297**(1): p. 7-24.
220. Hosking, E.R., et al., *The Escherichia coli MotAB proton channel unplugged.* J Mol Biol, 2006. **364**(5): p. 921-37.
221. Inoue, T., et al., *Genome-wide screening of genes required for swarming motility in Escherichia coli K-12.* J Bacteriol, 2007. **189**(3): p. 950-7.
222. McAuley, K.E., et al., *Structural details of an interaction between cardiolipin and an integral membrane protein.* Proc Natl Acad Sci U S A, 1999. **96**(26): p. 14706-11.
223. Bogdanov, M., P.N. Heacock, and W. Dowhan, *A polytopic membrane protein displays a reversible topology dependent on membrane lipid composition.* Embo J, 2002. **21**(9): p. 2107-16.
224. Williamson, I.M., et al., *The potassium channel KcsA and its interaction with the lipid bilayer.* Cell Mol Life Sci, 2003. **60**(8): p. 1581-90.

225. Zhang, W., et al., *Reversible topological organization within a polytopic membrane protein is governed by a change in membrane phospholipid composition.* J Biol Chem, 2003. **278**(50): p. 50128-35.
226. Zhang, W., et al., *Phospholipids as determinants of membrane protein topology. Phosphatidylethanolamine is required for the proper topological organization of the gamma-aminobutyric acid permease (GabP) of Escherichia coli.* J Biol Chem, 2005. **280**(28): p. 26032-8.
227. Denich, T.J., et al., *Effect of selected environmental and physico-chemical factors on bacterial cytoplasmic membranes.* J Microbiol Methods, 2003. **52**(2): p. 149-82.
228. Chintalapati, S., M.D. Kiran, and S. Shivaji, *Role of membrane lipid fatty acids in cold adaptation.* Cell Mol Biol (Noisy-le-grand), 2004. **50**(5): p. 631-42.
229. Chattopadhyay, M.K., *Mechanism of bacterial adaptation to low temperature.* J Biosci, 2006. **31**(1): p. 157-65.
230. Zhang, Y.M. and C.O. Rock, *Membrane lipid homeostasis in bacteria.* Nat Rev Microbiol, 2008. **6**(3): p. 222-33.
231. Atkins, P.W., *Physical Chemistry*. 5 ed. 1994, Oxford: Oxford University Press.
232. Kawagishi, I., et al., *The sodium-driven polar flagellar motor of marine Vibrio as the mechanosensor that regulates lateral flagellar expression.* Mol Microbiol, 1996. **20**(4): p. 693-9.
233. Wang, Q., et al., *Sensing wetness: a new role for the bacterial flagellum.* Embo J, 2005. **24**(11): p. 2034-42.
234. Lauriano, C.M., et al., *The sodium-driven flagellar motor controls exopolysaccharide expression in Vibrio cholerae.* J Bacteriol, 2004. **186**(15): p. 4864-74.
235. Cronan, J.E. and P.R. Vagelos, *Metabolism and function of the membrane phospholipids of Escherichia coli.* Biochim Biophys Acta, 1972. **265**(1): p. 25-60.
236. Haest, C.W., et al., *The effect of lipid phase transitions on the architecture of bacterial membranes.* Biochim Biophys Acta, 1974. **356**(1): p. 17-26.
237. Sinensky, M., *Homeoviscous adaptation--a homeostatic process that regulates the viscosity of membrane lipids in Escherichia coli.* Proc Natl Acad Sci U S A, 1974. **71**(2): p. 522-5.
238. McElhaney, R.N. and K.A. Souza, *The relationship between environmental temperature, cell growth and the fluidity and physical state of the membrane lipids in Bacillus stearothermophilus.* Biochim Biophys Acta, 1976. **443**(3): p. 348-59.
239. Russell, N.J., et al., *Membranes as a target for stress adaptation.* Int J Food Microbiol, 1995. **28**(2): p. 255-61.
240. Russell, N.J., *Psychrophilic bacteria--molecular adaptations of membrane lipids.* Comp Biochem Physiol A Physiol, 1997. **118**(3): p. 489-93.
241. Russell, N.J. and N. Fukunaga, *A comparison of thermal adaptation of membrane lipids in psychrophilic and thermophilic*
bacteria. FEMS Microbiol. Rev., 1990. **75**: p. 171-82.
242. Fishov, I. and C.L. Woldringh, *Visualization of membrane domains in Escherichia coli.* Mol Microbiol, 1999. **32**(6): p. 1166-72.
243. Mileykovskaya, E. and W. Dowhan, *Visualization of phospholipid domains in Escherichia coli by using the cardiolipin-specific fluorescent dye 10-N-nonyl acridine orange.* J Bacteriol, 2000. **182**(4): p. 1172-5.
244. Kawai, F., et al., *Cardiolipin domains in Bacillus subtilis marburg membranes.* J Bacteriol, 2004. **186**(5): p. 1475-83.
245. Helms, V., *Attraction within the membrane. Forces behind transmembrane protein folding and supramolecular complex assembly.* EMBO Rep, 2002. **3**(12): p. 1133-8.
246. Lee, A.G., *How lipids and proteins interact in a membrane: a molecular approach.* Mol Biosyst, 2005. **1**(3): p. 203-12.

247. Lam, H., J.Y. Matroule, and C. Jacobs-Wagner, *The asymmetric spatial distribution of bacterial signal transduction proteins coordinates cell cycle events.* Dev Cell, 2003. **5**(1): p. 149-59.
248. Miller, F., *Glycopeptides of human immunoglobulins. 3. The use and preparation of specific glycosidases.* Immunochemistry, 1972. **9**(3): p. 217-28.
249. Tusnady, G.E. and I. Simon, *The HMMTOP transmembrane topology prediction server.* Bioinformatics, 2001. **17**(9): p. 849-50.
250. Cserzo, M., et al., *Prediction of transmembrane alpha-helices in prokaryotic membrane proteins: the dense alignment surface method.* Protein Eng, 1997. **10**(6): p. 673-6.
251. Hirokawa, T., S. Boon-Chieng, and S. Mitaku, *SOSUI: classification and secondary structure prediction system for membrane proteins.* Bioinformatics, 1998. **14**(4): p. 378-9.
252. Mitaku, S., et al., *Proportion of membrane proteins in proteomes of 15 single-cell organisms analyzed by the SOSUI prediction system.* Biophys Chem, 1999. **82**(2-3): p. 165-71.
253. Mitaku, S., T. Hirokawa, and T. Tsuji, *Amphiphilicity index of polar amino acids as an aid in the characterization of amino acid preference at membrane-water interfaces.* Bioinformatics, 2002. **18**(4): p. 608-16.
254. Sonnhammer, E.L., G. von Heijne, and A. Krogh, *A hidden Markov model for predicting transmembrane helices in protein sequences.* Proc Int Conf Intell Syst Mol Biol, 1998. **6**: p. 175-82.
255. Krogh, A., et al., *Predicting transmembrane protein topology with a hidden Markov model: application to complete genomes.* J Mol Biol, 2001. **305**(3): p. 567-80.
256. Hofmann K., S.W., *TMbase - A database of membrane spanning proteins segments.* Biol. Chem. Hoppe-Seyler, 1993. **374**: p. 166.
257. Mohr, C.D., U. Jenal, and L. Shapiro, *Flagellar assembly in Caulobacter crescentus: a basal body P-ring null mutation affects stability of the L-ring protein.* J Bacteriol, 1996. **178**(3): p. 675-82.
258. de Lorenzo, V., et al., *Mini-Tn5 transposon derivatives for insertion mutagenesis, promoter probing, and chromosomal insertion of cloned DNA in gram-negative eubacteria.* J Bacteriol, 1990. **172**(11): p. 6568-72.
259. Roberts, R.C., et al., *Identification of a Caulobacter crescentus operon encoding hrcA, involved in negatively regulating heat-inducible transcription, and the chaperone gene grpE.* J Bacteriol, 1996. **178**(7): p. 1829-41.
260. Gottesman, S., *Proteolysis in bacterial regulatory circuits.* Annu Rev Cell Dev Biol, 2003. **19**: p. 565-87.
261. Jenal, U. and R. Hengge-Aronis, *Regulation by proteolysis in bacterial cells.* Curr Opin Microbiol, 2003. **6**: p. 163-172.
262. Keiler, K.C., P.R. Waller, and R.T. Sauer, *Role of a peptide tagging system in degradation of proteins synthesized from damaged messenger RNA.* Science, 1996. **271**(5251): p. 990-3.
263. Zhu, J. and S.C. Winans, *The quorum-sensing transcriptional regulator TraR requires its cognate signaling ligand for protein folding, protease resistance, and dimerization.* Proc Natl Acad Sci U S A, 2001. **98**(4): p. 1507-12.
264. Alba, B.M., et al., *DegS and YaeL participate sequentially in the cleavage of RseA to activate the sigma(E)-dependent extracytoplasmic stress response.* Genes Dev, 2002. **16**(16): p. 2156-68.
265. Kanehara, K., K. Ito, and Y. Akiyama, *YaeL (EcfE) activates the sigma(E) pathway of stress response through a site-2 cleavage of anti-sigma(E), RseA.* Genes Dev, 2002. **16**(16): p. 2147-55.

266. Gonzalez, M., et al., *Subunit-specific degradation of the UmuD/D' heterodimer by the ClpXP protease: the role of trans recognition in UmuD' stability.* Embo J, 2000. **19**(19): p. 5251-8.
267. Johansson, J. and B.E. Uhlin, *Differential protease-mediated turnover of H-NS and StpA revealed by a mutation altering protein stability and stationary-phase survival of Escherichia coli.* Proc Natl Acad Sci U S A, 1999. **96**(19): p. 10776-81.
268. Turgay, K., et al., *Competence in Bacillus subtilis is controlled by regulated proteolysis of a transcription factor.* EMBO J, 1998. **17**(22): p. 6730-6738.
269. Iniesta, A.A., et al., *A phospho-signaling pathway controls the localization and activity of a protease complex critical for bacterial cell cycle progression.* Proc Natl Acad Sci U S A, 2006. **103**(29): p. 10935-40.
270. Grünenfelder, B., et al., *Proteomic analysis of the bacterial cell cycle.* Proc Natl Acad Sci U S A, 2001. **98**(8): p. 4681-4686.
271. Domian, I.J., A. Reisenauer, and L. Shapiro, *Feedback control of a master bacterial cell-cycle regulator.* Proc Natl Acad Sci USA, 1999. **96**(12): p. 6648-53.
272. Chien, P., et al., *Direct and adaptor-mediated substrate recognition by an essential AAA+ protease.* Proc Natl Acad Sci U S A, 2007. **104**(16): p. 6590-5.
273. Tsai, J.W. and M.R. Alley, *Proteolysis of the Caulobacter McpA chemoreceptor is cell cycle regulated by a ClpX-dependent pathway.* J Bacteriol, 2001. **183**(17): p. 5001-7.
274. Karimova, G., et al., *A bacterial two-hybrid system based on a reconstituted signal transduction pathway.* Proc Natl Acad Sci U S A, 1998. **95**(10): p. 5752-6.
275. Wang, J., J.A. Hartling, and J.M. Flanagan, *Crystal structure determination of Escherichia coli ClpP starting from an EM-derived mask.* J Struct Biol, 1998. **124**(2-3): p. 151-63.
276. Kim, Y.R., et al., *Characterization and pathogenic significance of Vibrio vulnificus antigens preferentially expressed in septicemic patients.* Infect Immun, 2003. **71**(10): p. 5461-71.
277. Miyawaki, A. and R.Y. Tsien, *Monitoring protein conformations and interactions by fluorescence resonance energy transfer between mutants of green fluorescent protein.* Methods Enzymol, 2000. **327**: p. 472-500.
278. Selvin, P.R., *The renaissance of fluorescence resonance energy transfer.* Nat Struct Biol, 2000. **7**(9): p. 730-4.
279. Sourjik, V. and H.C. Berg, *Receptor sensitivity in bacterial chemotaxis.* Proc Natl Acad Sci U S A, 2002. **99**(1): p. 123-7.
280. Wang, S.P., et al., *A histidine protein kinase is involved in polar organelle development in Caulobacter crescentus.* Proc Natl Acad Sci USA, 1993. **90**(2): p. 630-4.
281. Viollier, P.H., N. Sternheim, and L. Shapiro, *Identification of a localization factor for the polar positioning of bacterial structural and regulatory proteins.* Proc Natl Acad Sci U S A, 2002. **99**(21): p. 13831-6.
282. Janetopoulos, C., et al., *Temporal and spatial regulation of phosphoinositide signaling mediates cytokinesis.* Dev Cell, 2005. **8**(4): p. 467-77.
283. Evans, J.H. and J.J. Falke, *Ca2+ influx is an essential component of the positive-feedback loop that maintains leading-edge structure and activity in macrophages.* Proc Natl Acad Sci U S A, 2007. **104**(41): p. 16176-81.
284. Insall, R. and N. Andrew, *Chemotaxis in Dictyostelium: how to walk straight using parallel pathways.* Curr Opin Microbiol, 2007. **10**(6): p. 578-81.
285. Hinz, A.J., et al., *The Caulobacter crescentus polar organelle development protein PodJ is differentially localized and is required for polar targeting of the PleC development regulator.* Mol Microbiol, 2003. **47**(4): p. 929-41.

286. Lawler, M.L., et al., *Dissection of functional domains of the polar localization factor PodJ in Caulobacter crescentus.* Mol Microbiol, 2006. **59**(1): p. 301-16.
287. Chen, J.C., et al., *Cytokinesis signals truncation of the PodJ polarity factor by a cell cycle-regulated protease.* Embo J, 2006. **25**(2): p. 377-86.
288. Schmid, F.F. and M. Meuwly, *All-atom simulations of structures and energetics of c-di-GMP-bound and free PleD.* J Mol Biol, 2007. **374**(5): p. 1270-85.
289. Tsai, J.W. and M.R. Alley, *Proteolysis of the McpA chemoreceptor does not require the Caulobacter major chemotaxis operon.* J Bacteriol, 2000. **182**(2): p. 504-7.
290. Berman, H.M., et al., *The Protein Data Bank.* Nucleic Acids Res, 2000. **28**(1): p. 235-42.
291. Altschul, S.F., et al., *Gapped BLAST and PSI-BLAST: a new generation of protein database search programs.* Nucleic Acids Res, 1997. **25**(17): p. 3389-402.
292. Schwede, T., et al., *SWISS-MODEL: An automated protein homology-modeling server.* Nucleic Acids Res, 2003. **31**(13): p. 3381-5.
293. Karimova, G., A. Ullmann, and D. Ladant, *Protein-protein interaction between Bacillus stearothermophilus tyrosyl-tRNA synthetase subdomains revealed by a bacterial two-hybrid system.* J Mol Microbiol Biotechnol, 2001. **3**(1): p. 73-82.

6. Acknowledgements

First of all, I would like to thank my supervisor Professor Urs Jenal for the opportunity to work in his group on such an interesting topic, the inspiring scientific atmosphere with lots of freedom for own thoughts and ideas, his advice and - last but not least - for making sure I could concentrate on science instead of finance during the last time. I also want to thank the members of my PhD committee, Professor Tilman Schirmer and Professor Christoph Dehio, for their scientific advice.

I would like to thank Dr. Anna Dürig for her companionship and friendship during the last four years, joined fights with the microscope and lunch breaks in the hospital park (when it still existed). I am especially grateful to Dr. Alex Böhm for his advice, fruitful scientific discussions, the good collaboration, and for reading and correcting the manuscript. Dr. Jacob Malone helped me a lot by proof-reading and correcting the thesis and eliminating one-to-one translated German phrases. He also accompanied me to great movies whose quality is widely underestimated by most other people. I am very grateful to Fabienne Hamburger and her extraordinary cloning abilities as well as for her funny cutting remarks. Also, I would like to thank Professor Thomas Egli for letting me perform chemostat experiments in his lab and Marc Folcher for his help and knowledge about biochemistry.

I really enjoyed the nice and friendly atmosphere in the lab and I would like to thank all former and current members of our group: Alain, (f)Alex, Annina, Assaf, Dominique, Flora, Irene, Jenny, Lucy, Martha, Micael, Ralf, Samuel, Sharif, Sue, Thierry, Tina, Wanda.

I am indebted to my friends and family, especially my parents for their support, understanding and untiring encouragement, as well as Dr. Björn Titz for not only being a good friend, but also for inspiring discussions.

Finally, I would like to thank Pia Schulz zur Wiesch for all the love and support during the last years. Especially during the writing process of this thesis she has been a constant source of inspiration and motivation, without which I would have never managed to complete this project the way it is now.

7. Curriculum vitae

Personal data

Name	Sören Abel
Birth	May 29th, 1978 in Kiel, Germany
Nationality	German
Civil status	single/no children

Education

01.06.2008 –	Postdoctoral researcher at the Biozentrum of the University of Basel, Switzerland in the group of Prof. Dr. Urs Jenal
04/2004 – 05/2008	Doctoral thesis "Analysis of the c-di-GMP mediated cell fate determination in *Caulobacter crescentus*" at the Biozentrum of the University of Basel, Switzerland in the group of Prof. Dr. Urs Jenal
09/2003 – 10/2003	Practical training in real-time at the biochemical institute of the Christian-Albrechts-University Kiel, Germany in the group of Prof. Dr. Rose John under the supervision of Dr. Andreas Ludwig
10/2002 – 07/2003	Diploma thesis, "Klonierung, Expression und Charakterisierung der proteolytischen Regulation des transmembranen CXC-Chemokins CXCL16" at the biochemical institute of the Christian-Albrechts-University Kiel, Germany in the group of Prof. Dr. Rose John under the supervision of Dr. Andreas Ludwig
10/1998 – 07/2003	Studies in biochemistry and molecular biology at the Christian-Albrechts-University Kiel, Germany
08/1988 – 05/1997	High School, Heinrich-Heine-Gymnasium Heikendorf, Germany
08/1984 – 08/1988	Elementary School, Grund- und Hauptschule Heikendorf, Germany

Teaching experience

01/2008 –	Supervision of the Master thesis of Micael Nicollier "The development and cell cycle of a c-di-GMP depleted *Caulobacter crescentus*" at the Biozentrum of the University of Basel, Switzerland in the group of Prof. Dr. Urs Jenal

04/2004 – 03/2008	Assistant at annual practical courses in microbiology for students of biology at the Biozentrum of the University of Basel, Switzerland
10/2002 – 02/2003	Assistant at a practical course in biochemistry for students of medicine at the biochemical institute of the Christian-Albrechts-University Kiel, Germany

Scholarship and awards

14.10.2004	Poster prize at the "Biozentrumssymposium"
01.09.2002 – 14.09.2002	Summer school "Protein Evolution" of the "Studienstiftung des Deutsche Volkes" under the supervision of Prof Dr. A. Lupas and Dr. R. Russell
01.02.2002 – 30.07.2003	Scholarship of the "Studienstiftung des Deutschen Volkes"
03/1997	16th rank at the german "VIII. Internationalen Bioolympiade"

Publication record

01.01.2009	Duerig A, **Abel S**, Folcher M, Nicollier M, Schwede T, Amiot N, Giese B, Jenal U. Second messenger-mediated spatiotemporal control of protein degradation regulates bacterial cell cycle progression. *GENES & DEVELOPMENT*, 23:93–104.
02.05.2008	Paul R, Jaeger T*, **Abel S***, Wiederkehr I, Folcher M, Biondi EG, Laub MT, Jenal U. Allosteric Regulation of Histidine Kinases by Their Cognate Response Regulator Determines Cell Fate. *CELL*, 133:452–61.
19.07.2007	Paul R, **Abel S**, Wassmann P, Beck A, Heerklotz H, Jenal U. Activation of the diguanylate cyclase PleD by phosphorylation-mediated dimerization. *J BIOL CHEM*. 2007, 282(40):29170-7.
15.05.2004	**Abel S***, Hundhausen C*, Mentlein R, Schulte A, Berkhout TA, Broadway N, Hartmann D, Sedlacek R, Dietrich S, Muetze B, Schuster B, Kallen KJ, Saftig P, Rose-John S, Ludwig A. The transmembrane CXC-chemokine ligand 16 is induced by IFN-gamma and TNF-alpha and shed by the activity of the disintegrin-like metalloproteinase ADAM10. *J IMMUNOL*, 2004, 172(10):6362-72.

* authors contributed equally

During my PhD studies I attended courses by the following lecturers:
A G Rolink, C Arrieumerlou, C Dehio, D Bumann, G Cornelis, J Pieters, M Dürrenberger, T Hohn, U A Meyer, U Jenal, W Gehrig

Ich erkläre, dass ich die Dissertation „Analysis of the c-di-GMP mediated cell fate determination in *Caulobacter crescentus*“ nur mit der darin angegebenen Hilfe verfasst und bei keiner anderen Universität und keiner anderen Fakultät der Universität Basel eingereicht habe.

Basel, den 01.05.08

Sören Abel